GEORGE S. WISE FACULTY OF LIFE SCIENCES
GRADUATE SCHOOL

Thesis submitted

Doctor of Philosophy degree

"Systems Biology approach for Stress Resistance and Yield Traits in Crops"

by

Zechariah Haber

This research was performed in the School of Plant Sciences

Under the supervision of

Dr. Nir Sade

April 2024

Contents

1. Acknowledgments and dedication 2

2. Abstract 4

3. Introduction 6

4. Material, methods and results as an article collection 9

4.1 The effect of circular soil biosolarization treatment on the physiology, metabolomics, and microbiome of tomato plants under certain abiotic stresses 9

4.2 The Alteration of Tomato Chloroplast Vesiculation Positively Affects Whole-Plant Source–Sink Relations and Fruit Metabolism under Stress Conditions 23

4.3 Is CRISPR/Cas9-based multi-trait enhancement of wheat forthcoming? 43

4.4 Network analysis and machine learning identify important control points in metabolic pathway associated with abiotic stress in the bread wheat pan-genome collection. 53

5. Discussion 99

6. References 101

1. Acknowledgments and dedication

“For He Loved The Soil” (2 Chronicles 26:10).

This doctoral thesis is dedicated to the memory of our beloved son, husband, father, and brother, Zechariah Haber OB”M. His love of nature, Israel and humanity led him to pursue a doctorate at Tel Aviv University on increasing wheat production despite adverse climate change. Zechariah focused on researching the genetic profile of wild wheat variants in Israel which uniquely thrive in all of Israel’s diverse climates and whether those features can be transferred to bread wheat. He moved to Israel with his family at the age of 8 from the United States and died at the age of 32, defending the State of Israel, when he was on the verge of finishing this thesis. In addition to pursuing his doctorate, Zechariah was a devoted husband to Talia and a father of three young children, Sdayel Elisheva, Yosef Yerachem Shevet and Nachaliel Tzvi. From a young age, Zechariah was a brilliant student who was deeply connected to nature and to science, as well as to people of all ages and backgrounds. Our hope is that his work will serve to further scientific advances that will help ensure food is widely available to all and that Israel continues to grow and prosper and to serve as a beacon of scientific progress. May Zechariah’s memory be a blessing. He is sorely missed.

Aharon and Miriam, Talia, Sdayel, Shevet and Nachaliel, Netanel, Noam and Yisrael

This Thesis is dedicated to the beloved memory of my Ph.D student Zechariah Haber OB”M who died defending the State of Israel.

Zechariah was my first Ph.D student. which is a fateful decision for a new and young researcher like me. I remember when we met for the first time on the lawn of the Faculty of Agriculture. I met a young man who within a minute I realized that this is the person I want with me. It was immediately possible to recognize his love for science and the Land of Israel. And for Zechariah part, he was so enthusiastic about the possibility of working on Israeli wild wheat plants that so represent who he was. An Israeli! There are several parameters by which a good student can be defined. The level of independence, ability to think outside the box, precision and perseverance, love of science, ability to express himself and more. Zechariah not only answered all of these perfectly, but also added his own parameters of love of the Land of Israel, helping all his peers at any hour and at any time. It is enough to look at everything he have achieved in his too short scientific life and realize that Zechariah was a special person with rare

personal abilities. Because of Zechariah modesty, his amazing family, only now after his death receives the confirmation that in science as in everything else Zechariah was elite. And on his way to doing great things. I promise that Zechariah 's scientific legacy and contribution to agricultural science, which he loved so much, will not be forgotten and will continue to be immortalized in this thesis.

Nir Sade

The Wheat Still Grows Again

Lyrics: *Dorit Tzameret*

Translation: Elli Sacks

“The fields spill out below, as far as earth meets sky,
Beneath the olive trees and Mount Gilboa.
At eve, the valley’s splendor hits your eye,
The likes of which you’ve never seen before.
It’s not the same old house now, it’s not the same old valley,
You’re gone and never can return again.
The path, the boulevard, a skyward eagle tarries…
And yet the wheat still grows again.
And from the bitter earth, the asphodels still bloom,
A boy upon the grass, next to his puppy lies.
The nights descend upon a well-lit room,
On those within, and thoughts locked up inside.
It’s not the same old house now, it’s not the same old valley,
You’re gone and never can return again.
The path, the boulevard, a skyward eagle tarries…
And yet the wheat still grows again.
And everything that was, perhaps will ever be,
The rising and the setting of the sun…
And songs are always sung, but can they speak
The vastness of the loss and all the love.
It is the same old house now, yes it’s the same old valley,
But you — they never can return again.
And can it be, how can it be, that through Time’s endless tally…
Somehow the wheat still grows again.”

2. Abstract

One major focus in agriculture today is enhancing crop productivity, specifically under intensifying environmental stress. Stress resistance was originally introduced by selecting the fittest plants. Modern improvements included breeding, genetic transformation and genomic editing, yet these had a marginal impact on the discovery of genes and factors important to stress resistance. Recently, Omics have allowed to generate relatively cheap high-throughput biological data, yet their Achilles' heel is the inability to manually process the quantity of data. Therefore, many are turning to statistics and computational biology to bridge the gap and this combination is also known as "Systems Biology".

In subsequent chapters, we apply in both wheat (*Triticum aestivum)* and tomato (*Solanum lycopersicum*) crop plants a system biology approach utilizing wide physiological, biochemical, metabolomic and microbiomic diverse measurements under control, drought, salinity and nitrogen deficiency stress conditions. In order to decipher these data, as well as specifically elucidate the data in its metabolic context, we employed computational biology techniques, such as correlation network analysis and machine learning and identify novel metabolic pathways and target genes involved in the crops' response to stress. Moreover, the discovery of these novel genes is validated in planta through genetic engineering techniques, including Clustered Regularly Interspaced Short Palindromic Repeats (CRISPR) and virus-induced gene silencing (VIGS).

We explored circular soil biosolarization (CSBS) by using tomato pomace residues and studied its impact on tomato crops under high salinity and nitrogen deficiency. The results showed that CSBS enhanced plant growth, yield, and physiological performance compared to standard soil solarization, especially under abiotic stress. CSBS also altered the soil microbiome and plant metabolome, positively affecting tomato health.

We further explored chloroplast stabilization (source capacity) as a trait to increase the ability of tomato source leaves to both maintain a high photo-assimilation rate and to prolong the overall duration of the assimilation thus effecting fruit metabolism. Knockout of the chloroplast vesiculation (CV) gene under stress led to more efficient use of carbon and nitrogen and to higher yields. Detailed metabolic and transcriptomic network combined with machine learning approach analysis of fruits revealed that the l-glutamine and l-arginine biosynthesis pathways

are associated with stress-response conditions and also identified putative novel genes involved in tomato fruit quality under stress.

Additionally, we explored wheat pan-genome collection affect by drought and salinity and used multi-omics (integrating data from physiolomes, metabolomes, transcriptomes, and microbiomes) and advanced analytical techniques like network analysis and machine learning, to identify specific pathways and genes involved in stress response. These include two pathways (indole-3-acetic acid inactivation VIII and L-carnitine biosynthesis) and their related genes and physiological aspects. Experimental silencing of certain genes confirmed their roles in plant physiology and stress response.

Finally, we discuss the application of CRISPR technologies in genome editing, particularly in complicated crops as wheat. We highlight the importance of trait multiplexing in crops, considering the redundancy of genomes and genes and the challenges of generating stable transgenic plant lines. We provide examples of successful manipulation of various wheat traits using CRISPR/Cas9, such as yield, biofortification, stress tolerance, and resistance to biotic stresses. The focus shifts towards the potential creation of a multi-stress tolerant wheat cultivar, addressing climate change impacts. The review suggests enhancing local landraces with specific stress tolerances rather than pursuing a general 'super wheat,' as a more sustainable solution for improving crop yields under diverse environmental conditions

3. Introduction

In the past twenty years, Omics (including genomics, transcriptomics, proteomics, metabolomics and microbiomics) technologies have developed, allowing to generate relatively cheap high-throughput data (Joyce and Palsson, 2006; Ivanova et al., 2019), which hopefully contain genes or other factors, apparent in their importance to the tested conditions, e.g. for plant stress resistance (Bagati et al., 2018). The first plant (*Arabidopsis thaliana*) genome was completely sequenced and analyzed already by 2000 (AGI, 2000). However, crop plants sequencing usually with much more complicated genomes has been hampered. For example, the common wheat genome (e.g, high polyploidy, large size and genetic repetitiveness), was fully sequenced only in 2012 (Brenchley et al., 2012), significantly annotated in 2014 (IWGSC, 2014) and fully annotated in 2018 (IWGSC, 2018). Recently, 15 cultivars were sequenced, assembled and annotated, in order to increase the variation of genomic data available for wheat cultivar research and improvement (Walkowiak et al., 2020). It is therefore expected to have an outburst of wheat and other crops Omics data, which will supposedly point towards definite factors associated with stress resistance (Shah et al., 2018; Goel et al., 2020; Alotaibi et al., 2021).

Yet, one major setback to the Omics revolution is the inability to manually process the quantity of data (Berger et al., 2013). Many computational and statistical tools are being implemented to solve this problem, including bioinformatic databases (Berger et al., 2013), Principal Component Analysis (PCA; Gastinel, 2012), computer programming tools (e.g. for Bioconductor packages in R, see http://www.bioconductor.org), machine learning (van Dijk et al., 2021) and network analysis (Toubiana et al., 2013), with some examples of combinations (Toubiana et al., 2019; Toubiana et al., 2020). This integration of Omics, together with computational tools, is often called "Systems Biology (Shah et al., 2017).

System biology approaches offer comprehensive and integrated methods for studying complex biological systems in plant science. By employing multi-omics techniques such as genomics, transcriptomics, proteomics, metabolomics, and microbiomics, along with computational modeling and data analysis, system biology aims to understand the intricate networks and interactions within plants. This holistic approach enables researchers to explore various biological processes, including growth, development, metabolism, and response to environmental stresses, at a systems level (Kumar et al.,2015)

“System biology” approach in crop stress resistance research, has rarely been used. This is mainly due to the fact that extracting meaningful biological insights from vast data requires appropriate analytical tools (Misra et al., 2019). Correlation-based network analysis (CNA) has emerged as a powerful tool in systems biology, enabling the integration of heterogeneous data into coherent datasets and this has been recently highlighting in the context of plant metabolism under stress (Toubiana et al., 2019). It is indeed an ideal tool to analyze and highlight the differences of metabolic behavior between plants grown under controlled conditions and plants exposed to abiotic or biotic stress (e.g., Hochberg et al, 2013; Toubiana et al; 2020a, Toubiana et al, 2020b). In a correlation network (CN), nodes represent metabolites and the edges between them the significant correlation coefficients (r). Setting the correlation coefficient threshold is a non-trivial task. A recent study has shown the correlation coefficient thresholds must be set dynamically determined by the network topology of the system of study (Toubiana and Maruenda, 2021). Only by doing so the resulting CN captures the relevant biological information.

The reconstruction of metabolic pathways involves a complex process utilizing a constraint-based bottom-up approach. This typically involves gene annotation, computational derivation, and manual curation, relying on knowledge of compound stoichiometry, thermodynamic data, cellular compartmentalization, and other factors. Due to its complexity, metabolic pathways are often predicted computationally rather than through extensive experimental evidence (Monk et al.,2014). The process follows specific steps starting with known biochemistry, genomics, and physiology, then applying physico-chemical constraints, predicting flux distributions, and determining meaningful physiological states (Fiehn et al.,2011). These pathways, whether fully validated or not, are cataloged in databases like PlantCyc, BioCyc, and KEGG (Toubiana et al.,2019a). In addition to the constraint-based approach, metabolite networks utilize high-throughput metabolite profiles to study coordinated metabolite behavior without prior knowledge. Metabolite profiles are correlated using mathematically defined similarity measures, which are then represented in network form with nodes representing metabolites and links indicating correlation coefficients (Toubiana et al.,2019a; Toubiana et al.,2019b). Machine learning (ML) encompasses a set of methods enabling computers to learn from available data without explicit programming and can be harnessed to improve high-throughput data. ML approach can be used to map existing metabolic pathways onto the metabolite correlation networks followed by the computation of a set of network properties for

each pathway to derive an ML model. The resulting ML model can then use to predict the existence of yet unidentified pathways and functional genes based on the mapping of pathways onto the correlation networks and computation of the same set of network properties (Toubiana et al.,2020a; Toubiana et al.,2020b).

When using ML combined with CN to predict metabolic pathways, it is also necessary to experimentally validate those pathways and genes as a part of the "system biology" holistic approach. This usually include the use of reverse genetics for experimental validation. Firstly, it allows researchers to directly target specific genes or genetic pathways identified through predictive analyses, thereby providing a focused approach to testing hypotheses. Secondly, reverse genetics enables the precise manipulation of genetic material, such as gene knockout (Virus Induced gene silencing (VIGS) and Clustered Regularly Interspaced Short Palindromic Repeats (CRISPR)) or overexpression, to observe the resulting phenotypic changes (Lu et al.,2003; Feng et al., 2014). Those methodologies provide direct evidence linking genotype to phenotype, helping to confirm the function of predicted genes. (Ben Amar et al.,2016)

In the following sections, we utilize a systems biology approach to investigate wheat (*Triticum aestivum*) and tomato (*Solanum lycopersicum*) crop plants under various stress conditions including control, drought, salinity, and nitrogen deficiency. We integrate a wide range of physiological, biochemical, metabolomic, and microbiomic measurements to analyze the data. To interpret these findings within the metabolic framework, we employ computational biology methods such as correlation network analysis and machine learning. This enables us to identify new metabolic pathways and target genes associated with the plants' response to stress. Furthermore, we validate the discovery of these novel genes through genetic engineering techniques like Clustered Regularly Interspaced Short Palindromic Repeats (CRISPR) and virus-induced gene silencing (VIGS) in planta.

4. Material, methods and results as an article collection

Sub- chapter 4.1

Results presented in this sub-chapter has been published in the journal “Frontiers in Plant Science”

Title: The effect of circular soil biosolarization treatment on the physiology, metabolomics, and microbiome of tomato plants under certain abiotic stresses

frontiers | Frontiers in Plant Science

TYPE Original Research
PUBLISHED 08 November 2022
DOI 10.3389/fpls.2022.1009956

OPEN ACCESS

EDITED BY
Suresh Kumar,
Indian Agricultural Research Institute (ICAR), India

REVIEWED BY
Willem Desmedt,
Ghent University, Belgium
Ojas Natarajan,
University of South Florida, United States

*CORRESPONDENCE
Yigal Achmon
yigal.achmon@gtiit.edu.cn
Nir Sade
nirsa@tauex.tau.ac.il

SPECIALTY SECTION
This article was submitted to Plant Biotechnology, a section of the journal Frontiers in Plant Science

RECEIVED 02 August 2022
ACCEPTED 14 October 2022
PUBLISHED 08 November 2022

CITATION
Haber Z, Wilhelmi MdMR, Fernández-Bayo JD, Harrold DR, Stapleton JJ, Toubiana D, VanderGheynst JS, Blumwald E, Simmons CW, Sade N and Achmon Y (2022) The effect of circular soil biosolarization treatment on the physiology, metabolomics, and microbiome of tomato plants under certain abiotic stresses.
Front. Plant Sci. 13:1009956.
doi: 10.3389/fpls.2022.1009956

The effect of circular soil biosolarization treatment on the physiology, metabolomics, and microbiome of tomato plants under certain abiotic stresses

Zechariah Haber[1], María del Mar Rubio Wilhelmi[2], Jesus D. Fernández-Bayo[3], Duff R. Harrold[3], James J. Stapleton[4], David Toubiana[1], Jean S. VanderGheynst[5], Eduardo Blumwald[2], Christopher W. Simmons[3], Nir Sade[1]* and Yigal Achmon[6,7,8]*

[1]School of Plant Sciences and Food Security, Tel Aviv University, Tel Aviv, Israel, [2]Department of Plant Sciences, University of California, Davis, CA, United States, [3]Department of Food Science and Technology, University of California, Davis, CA, United States, [4]Statewide Integrated Pest Management Program, University of California Kearney Agricultural Research and Extension Center, Parlier, CA, United States, [5]College of Engineering, University of Massachusetts Dartmouth, Dartmouth, MA, United States, [6]Biotechnology and Food Engineering, Guangdong Technion - Israel Institute of Technology, Shantou, Guangdong, China, [7]Faculty of Biotechnology and Food Engineering, Technion - Israel Institute of Technology, Haifa, Israel, [8]Guangdong Provincial Key Laboratory of Materials and Technologies for Energy Conversion, Guangdong Technion - Israel Institute of Technology, Shantou, Guangdong, China

Soil biosolarization (SBS) is an alternative technique for soil pest control to standard techniques such as soil fumigation and soil solarization (SS). By using both solar heating and fermentation of organic amendments, faster and more effective control of soilborne pathogens can be achieved. A circular economy may be created by using the residues of a given crop as organic amendments to biosolarize fields that produce that crop, which is termed circular soil biosolarization (CSBS). In this study, CSBS was employed by biosolarizing soil with amended tomato pomace (TP) residues and examining its impact on tomato cropping under conditions of abiotic stresses, specifically high salinity and nitrogen deficiency. The results showed that in the absence of abiotic stress, CSBS can benefit plant physiological performance, growth and yield relative to SS. Moreover, CSBS significantly mitigated the impacts of abiotic stress conditions. The results also showed that CSBS impacted the soil microbiome and plant metabolome. *Mycoplana* and *Kaistobacter* genera were found to be positively correlated with benefits to tomato plants health under abiotic stress conditions. Conversely, the relative abundance of the orders RB41, MND1, and the family Ellin6075 and were negatively correlated with tomato plants health. Moreover, several metabolites were significantly affected in plants grown in SS- and CSBS-treated soils under abiotic stress conditions. The metabolite xylonic acid isomer was found to be significantly negatively correlated with tomato

plants health performance across all treatments. These findings improve understanding of the interactions between CSBS, soil ecology, and crop physiology under abiotic stress conditions.

KEYWORDS

rhizosphere microbiome, plant metabolome, abiotic stress, sustainable agriculture, organic waste management, soil solarization, anaerobic soil disinfestation, circular economy

Introduction

As the anthropogenic burden on agricultural systems keeps increasing, the need for new sustainable agricultural techniques increases as well. The massive use of modern disruptive techniques in agriculture such as chemical fertilization, fertigation, excessive irrigation, use of chemical pesticides and others is causing both biotic stresses (invasive species, resistant pathogens) and abiotic stresses (soil salinity, heavy metal pollution, nitrogen deficiency, soil erosion and more (Sade et al., 2018; Goswami and Suresh, 2020)) in the soil and on crops. Soils salinity is a rapidly growing global problem (Sade et al., 2020) that necessitates sustainable solutions to increase crop growth in harsh conditions for the maintaining of global food security. Looking for alternative nitrogen sources is also an important mission as chemical fertilizers are a major environmental problem (Savci, 2012). One of the techniques that is being used to mitigate these problems is soil solarization (SS). SS was established as an alternative to chemical soil fumigation to treat a broad spectrum of soil borne pathogens (DeVay and Katan, 1991). SS is done by placing a clear plastic cover over the crop rows ahead of crop planting. The idea behind the technique is to use the resulting heat caused by the greenhouse effect to elevate the soil temperature to a level that can kill a large share of the soil borne pathogens and weeds (Stapleton, 2000). Although SS is a sustainable and environmentally friendly technique that is currently being used around the world (mainly for growing strawberries and other high value crops (Chamorro et al., 2015; Katan, 2015; Oldfield et al., 2017)) it has several pitfalls that prevent it from becoming more popular among farmers. The pitfalls are coming from its passive nature, as it is completely dependent on the available solar radiation, which demands a long duration of treatment and has a limited ability to control soil-borne pathogens beneath the soil surface (Achmon et al., 2017). To overcome these problems a modification of SS is being studied and implemented in the form of soil biosolarization (SBS). In SBS, besides the covering with transparent plastic sheets, additional organic matter (OM) is added to the soil to accelerate the pathogens' inactivation process by adding biological and chemical pressures on them (Achmon et al., 2017; Hestmark et al., 2019; Achmon et al., 2020). Recent studies done on circular SBS (CSBS, a variety of the SBS technique in which the amendments to the soil are the output residues of the same crop that is established after the SBS treatment thereby using the "closing the loop" concept) together with industrial tomato pomace (TP) residues (e.g. the waste residues of the tomato processing industry) showed promising results in terms of inactivation of weeds and pathogens (Achmon et al., 2016; Achmon et al., 2017) and also in terms of tomato crop growth and health (Achmon et al., 2018). Additionally, more emphasis was given in recent studies to the impact that SBS has on the soil microbial population (e.g. soil microbiome) (Fernández-Bayo et al., 2019; Achmon et al., 2020; Shea et al., 2022). In these studies it was observed that SBS can alter the soil microbiome, mainly due to the combination of elevated quantity of organic matter, higher temperature and anaerobic conditions that serve as natural selective forces for an adaptive microbial community (Achmon et al., 2020). Yet, the impact that these changes in the microbiome have on the consecutive crop is still unknown. At the same time it is observed that the microbiome under SBS treatment also have impacts on the soil chemical composition by addition of products from the microbial metabolism such as volatile fatty acids (VFAs) and other organic compounds (Hestmark et al., 2019; Fernandez-Bayo et al., 2020; Liang et al., 2022). These compounds in turn serve both as selective forces and pathogens' suppressors, but on the other hand can also have some phytotoxic effect on the consecutive crop growth (Achmon et al., 2016; Achmon et al., 2018). SBS and CSBS have also the advantage over standard SS in that they can be used as an additional venue to valorize organic wastes such as food waste (Spang et al., 2019; Liang et al., 2022) and agricultural waste (Fernández-Bayo et al., 2017; Hestmark et al., 2019; Fernandez-Bayo et al., 2020). While SBS looks as a promising sustainable agricultural technique that can have multiple advantages, the impact on consecutive crop plants and its ability to mitigate the adverse effect of abiotic stress are still unknown. In this study the impact of CSBS with TP on consecutive tomato crop under salinity and nitrogen deficiency abiotic stresses was investigated. The study was aimed to elucidate the complex interaction

between the soil microbiome of the CSBS treatment and the tomato plants metabolome (e.g. the collection of primary metabolites of the plant) under abiotic stressors compared to the SS traditional treatment.

Materials and methods

CSBS field experiment

Mesocosms (3.8 L plastic soil growth bags) were prepared using soil collected from the field site (UC Davis Plant Pathology Research Farm (Davis, CA, USA; 38.521028, –121.760755; elevation 18.5 m above sea level)). The field soil was sandy clay loam (47%, 27% and 26% of sand, silt and clay, respectively), the OM content was 2.64% and the field capacity was 21.90% (wet basis). More details about the history of this field can be found elsewhere (Fernández-Bayo et al., 2018; Randall et al., 2020). Dry topsoil was collected from the upper 0–15 cm of the soil in the field site and transferred for further preparations. The soil was sieved (~2 mm) to give unified and homogeneous material. Details about soil amendments characterization and preparation can be found elsewhere (Achmon et al., 2016; Achmon et al., 2017). Briefly, TP was collected from a commercial processing facility during the 2016 harvest season (more details can be found here (Achmon et al., 2018; Achmon et al., 2019)). The TP was sun dried after collection and then stored under ambient conditions. The dried TP was processed in a laboratory blender to reduce the particle size to less than 1 mm to make it unified. Soil was placed inside the mesocosms to achieve 2.5% TP in the soil (on a dry weight basis), a concentration level that was previously shown to be optimal for the CSBS process (Achmon et al., 2018). Non-amended soil was used for SS treatments. Mesocosms containing amended or non-amended soil were transferred to the field site. Mesocosms were constructed by loading soil into 3.8 L plastic soil growth bags (New England Hydroponics, Southampton, MA). The weight of the mesocosms after filling with soil was adjusted to 10 kg (on a dry weight basis) for all systems. All the systems were wetted with distilled water and brought to the field water holding capacity. The mesocosms were laid in pre-dug holes in the field. The field was divided into six plots to give enough material for the greenhouse study and the plots were prepared as previously described (Achmon et al., 2017). Soil treatment was initiated on August 20, 2016 by covering the plot with 0.7 mil, transparent, low density polyethylene film ('Huskey Film Sheeting'; Poly-America, Inc., Grand Prairie, TX). The experiment lasted 8 days in accordance with previous results (Achmon et al., 2018), after which the plastic film was removed from the field site. The experiment was conducted in proximity (same time and same field site) to other SBS experiments and the data for the treatment temperatures can be found elsewhere (Fernández-Bayo et al., 2018). The mesocosms were left in the field to aerate for additional 15 days to allow for remediation of any residual phytotoxic conditions. After 15 days the mesocosms were transferred to the greenhouse for the growth experiment.

Greenhouse tomato growth study

Pots (2.37 L) were prepared with the treated soil and were each filled with 6 kg of treated soil for the tomato growth experiment. The pots were assigned randomly to the abiotic stress treatments and were placed on two steel screens metal tables in the greenhouse. The fertigation system was placed prior to transplanting the tomato seedlings the tomato transplants inside the soil. Tomato (cv. SUN6366, Nunhems USA, Inc., Parma, ID) transplants were grown in germination trays in a commercial potting soil mixture (Hastie's Capitol Sand and Gravel; 25% screened topsoil, 5% lava fines and sand, and 70% mixture in equal parts of forest humus, composted fir, and compost from horse manure and wheat straw). Approximately 2 weeks after germination (BBCH stage 2 digit code 11 or 3 digit code 101), seedlings of approximately the same size were transplanted into pots containing the field soils. The seedlings were transplanted in the soil directly after the field treatment including the aeration stage (at the same day the soil was transported to the greenhouse).

Pots were fertigated twice daily with 300 mL of water containing 143 mg/L N (delivered as 136 mg/L NO_3 -N and 7 mg/L NH_4 -N), 63 mg/L P (delivered as H_2PO_4), 199 mg/L K^+, 125 mg/L Ca^{2+}, 49 mg/L Mg2+, 65 mg/L S (delivered as SO_4^{-2}), 2 mg/L Fe^{3+}, 0.097 mg/L Cu^{2+}, 0.633 mg/L Mn^{2+}, 0.055 mg/L Mo^{6+}, and 0.097 mg/L Zn^{2+}. The stress conditions were created as follows: Nitrogen deficiency stress was created by lowering the amount of fertigated nitrogen to 30 mg vs the normal 143 mg (the additional nitrogen coming from the TP was calculated (Achmon et al., 2019) as less than a one dose of 40mg to the samples and hence was considered negligible(. The high salinity stress was created by adding salt as 100 mmol NaCl (A non-lethal concentration stimulates a long term response to salinity and a physiological penalty that was previously used in a relevant study (Zhang and Blumwald, 2001)) to the fertigation regime. Salinity treatments started at 4 weeks after transplanting and continued until harvest. The plants were grown for three and a half months from September 13, 2016 until December 2, 2016 in a semi-controlled greenhouse maintained between 18°C and 28°C and at 50–70% relative humidity with ambient light conditions. The plants were monitored for plant diseases, presence of weeds and fruit ripening.

Tomato plants analyses

Tomatoes were harvested in a similar way as that of (Achmon et al., 2018) with several modifications. The fruits were picked and counted. The fruits and the plant biomass were

weighed (the biomass was dried in oven at 50°C and weighted to determine the dry weight, fruits were weighted on a wet basis). The harvest index was calculated as the proportion of the total fruit weight divided by the sum of the vegetation fresh weight and the total fruit weight. The °Brix was determined using a digital refractometer (PR-100, ATAGO USA, Inc., Bellevue, WA). Measurements of photosynthesis and stomatal conductance were made on fully expanded leaves of plants in proximity to the harvest. Leaves were chosen by leaf number. The 5th leaf (fully expanded) was chosen and a single leaflet per plant was measured. A Li-6400 portable gas-exchange system (LI-COR) was used to measure gas exchange, photosynthesis and stomatal conductance similar to a previous study (Achmon et al., 2018).

DNA sequencing and tomato metabolomics

The soil microbiome DNA samples were taken from the soil at the harvest from the rhizosphere area of all the treated plants. The DNA was extracted as previously done (Achmon et al., 2020). Briefly, DNA purification was performed using a PowerSoil DNA Isolation Kit (MO BIO Laboratories Inc., Carlsbad, CA). The V4-V5 regions of the 16S rRNAgene were amplified and sequenced using the MiSeqplatform (Illumina Inc., San Diego, CA) in paired-end mode (2 × 300bp read format) with the v3 reagent kit and a qPCR library quantification kit (KAPA Biosystems, Wilmington, MA) was used to determine the concentration of V4 and V5 amplicons capable of being sequenced ahead of loading into the MiSeq system. The complete DNA sequencing procedure was done according to the Joint Genome Institute (Walnut Creek, CA 94598, USA Project ID: 1145678) protocol as described in (Achmon et al., 2020). Metabolomic analysis was done on leaves samples taken from the same leaves that were used for the physiological analysis (described above) All leaflets (including periole/midrib) were sampled and immediately frozen in liquid nitrogen followed by grinding to fine powder. Equal amounts of ground frozen powder were submitted to the West Coast Metabolomics Center (University of California, Davis), extracted, measured, and analyzed by gas chromatography–mass spectrometry (MS) (Gerstel CIS4–with a dual MPS Injector/Agilent 6,890 GC-Pegasus III TOF MS) as described before (Weckwerth et al., 2004)). Processes for the integrated extraction, identification, and quantification of metabolites were performed according to Fiehn et al. (2008). For the extraction, the solvent was prepared by mixing isopropanol/acetonitrile/water at the volume ratio 3:3:2 and degassing the mixture by directing a gentle stream of nitrogen through the solvent for 5 min. The solvent (cooled at −20°C) was added to the ground tissue (1-ml solvent/20-mg tissue), vortexed, and shaken for 5 min for metabolite's extraction. After centrifugation at 12,800 g for 2 min, the supernatant was concentrated to dryness. The residue was resuspended in 0.5-ml 50% aqueous acetonitrile and centrifuged at 12,800 g for 2 min. The supernatant was then concentrated to dryness in a vacuum concentrator, and the dried extracts were stored at −80°C until use. Untargeted metabolomic analysis was used. The signals were normalized by classic sum normalization i.e. normalization to a sum of intensities in a sample, only that here on the sum was defined as restricted to only identified metabolites to avoid normalizing to peaks that may or may not be possibly related to non-biological compounds (such as phthalates or other laboratory contaminants). This was done with the sum of all peak heights of the annotated detected metabolites as suggested by Fiehn et al. (2008). The equation used in this calculations was (for metabolite i of sample j) metabolite ij, normalized = metabolite ij, raw/mTIC j * mTIC average.

Data analysis

The microbiome data were initially quantified using QIIME1 (Caporaso et al., 2010). Briefly, the centralized rolling quality control system and the iTagger computational pipeline (Tremblay et al., 2015) for sequence trimming was used. Clustering operational taxonomic units (OTUs) were used based on 97% sequence identity, and taxonomic assignment with SILVA version 119 (Quast et al., 2012). Subsequently, the data were rarefied for diversity analysis (phylum abundance and alpha, beta and gamma diversity) using the 'phyloseq' R package. For quantitative analysis, the microbiome count table was normalized using Variance Stabilizing Transformation of the 'DESeq2' R package. The physiological and metabolomic parameters were individually compared between solarized and biosolarized treatments using the permuted Brunner Munzel test (*via* the 'brunnermunzel' R package). Heatmaps were prepared using the 'circlize' and 'ComplexHeatmap' R packages, and the boxplots were prepared using the 'ggpubr' R package. The raw data of this study can be found in the Supplementary Materials.

Results and discussion

CSBS impact on tomato plants health under abiotic stress

This study was designed (as shown in Figure 1) to explore the effects of a short time CSBS with TP residues on the health of tomato plants (including a deep look into the metabolome of the plants' leaves) and of the soil microbiome under abiotic stress of nitrogen deficiency and high salinity. The study was designed to compare the CSBS with traditional SS. Previous studies (Achmon et al., 2017; Achmon et al., 2018) showed that CSBS and SBS can be effective in terms of inactivation of weeds and

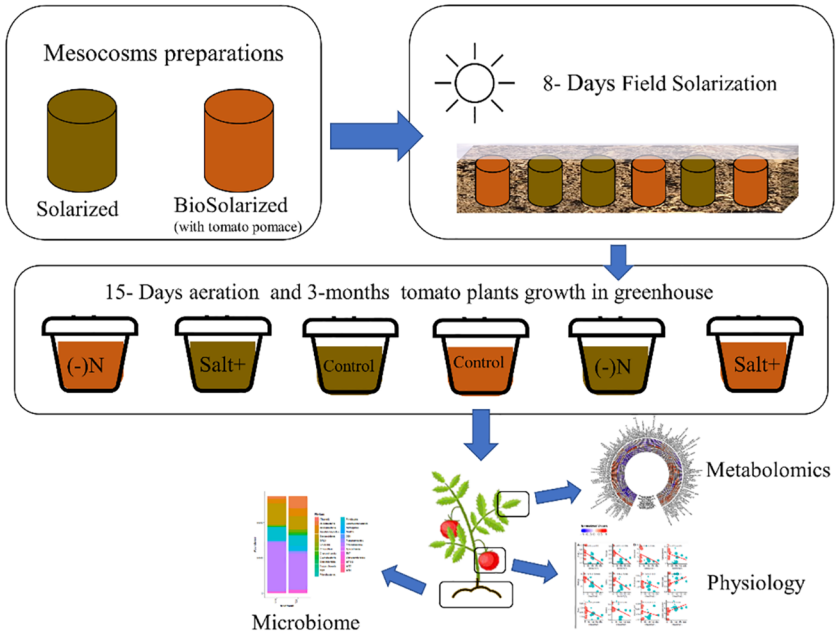

FIGURE 1
Schematic illustration of the experimental design. Starting by preparing the mesocosms for soil solarization (soil without tomato pomace) and soil biosolarization (with 2.5 w/w tomato pomace). Conducting an 8 days field solarization treatment of the mesocosms. Transferring the treated soil into a controlled greenhouse and transplanting tomato plants under different stress conditions: control – without any stress, salt – adding excess salinity to the soil and Nitrogen deficiency – lower amount of nitrogen in the fertilization regime. After 3-months the plant were harvested and tested for their physiological characteristics (including fruit quality and yield) and leaves' metabolomics. Additionally the soil was taken for a microbiome analysis.

pests even after a short treatment of less than two weeks (whereas SS usually lasts at least one month or more (Achmon et al., 2017)). Yet, the impact of SBS and CSBS under abiotic causes of stress such as soil salinity, drought and lack of sufficient soil nitrogen has not been previously explored. In this study the treatment of 8 days solarization was done in field conditions prior to the use of the soil as potting soil in the greenhouse study. This was done to mimic the solarization treatment in an optimal way while at the same time enabling a specific look per plant per treatment in the greenhouse. In a previous study it was found that a 12 days remediation of the soil can be too short and can cause some lingering residual phytotoxicity in the soil (Achmon et al., 2018). To avoid phytotoxicity all samples were given a 15 days remediation period. After the remediation period the tomato plants were grown in different conditions of salinity and nitrogen deficiency (as described above in the methods section) for a period of three months until the harvest. The results indicate that CSBS was superior ($P<0.05$) to SBS in this study in terms of total yield, fruit numbers, plant weight, and plant health (carbon dioxide assimilation, water transpiration) under both abiotic stresses and the control (no stress) treatments (Figure 2). Interestingly, the total BRIX per plant (representing the total potentially sugar content a plant can produce, an important parameter for processing tomatoes; (Gur et al., 2011) was higher in all CSBS treatments as compared to SS. These findings support several studies that showed that SBS can have an advantage in plant health and crop yield in addition to its effect against weeds and pathogens (Domínguez et al., 2014; Chamorro et al., 2015; García-Raya et al., 2019). However, this is the first study that showed a beneficial effect of CSBS in conditions of abiotic stresses. It is noteworthy to note that the effect under salinity conditions was such that CSBS did as well as, and even better than, the control SS treatment (Figure 2). To better understand the alleviation of CSBS effects in abiotic stresses an examination of the plant leaves metabolome and soil microbiome was done.

CSBS impact on tomato plants metabolome under abiotic stress

The analysis of the metabolites of the leaves of the tomato plants was done in close proximity to the harvest to reflect the plant health at the same conditions as those of the tomato plants' fruits and the soil microbiome. The metabolomic analysis showed significant differences in the control treatment between the CSBS and the SS in terms of inulotriose, xylonic acid, sulfuric acid and fucose (Figure 3A).

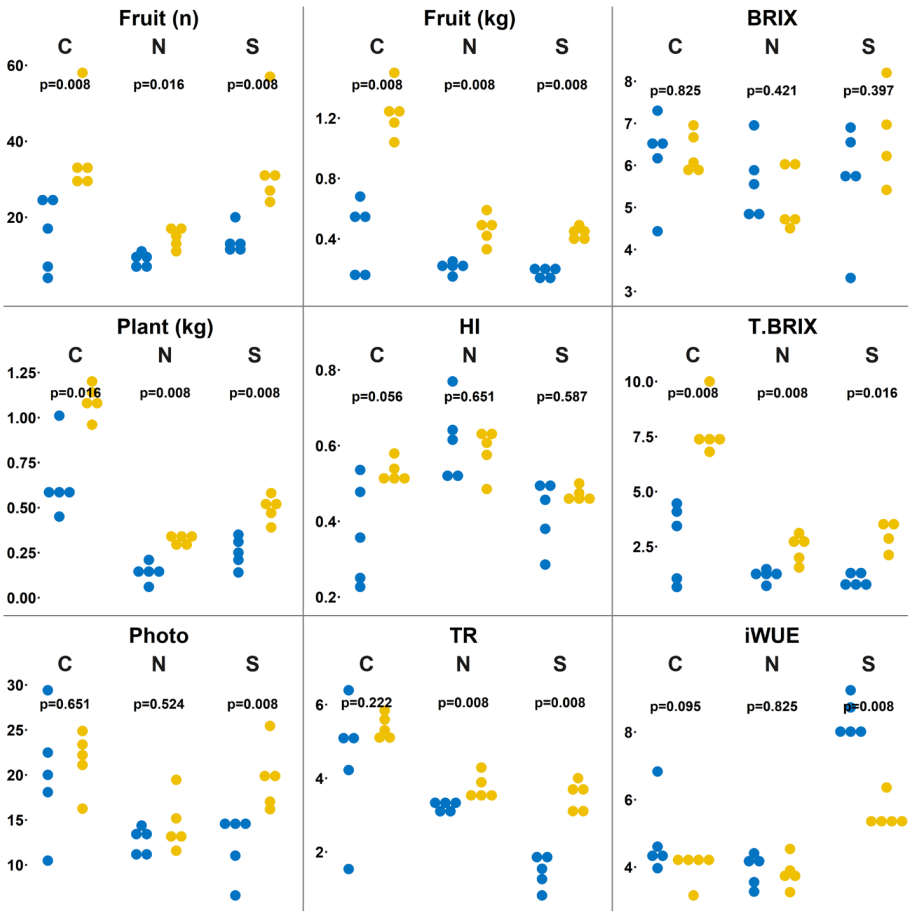

FIGURE 2
Physiological comparison between solarized and biosolarized pretreated plants. Boxplots of number of fruit (n), plant fresh biomass (kg), fruit weight (kg), harvest index in proportion of fruit weight out of total weight (HI), sugar content (BRIX), Total sugar content as the product of fruit weight and sugar content (T.BRIX), Leaf gas exchange analysis as carbon dioxide assimilated (Photo), transpiration as water transpired over time and space (Tr), instantaneous water use efficiency (iWUE) comparing solarized (SOL) and biosolarized (BIO) pretreated plants under well-watered (C), nitrogen-deprived (N) and salinity-treated (S) (n=4-5) plants. Significance was tested using the permuted Brunner Munzel test, presenting the p-values.

These sugars and acids have roles in important cellular processes such as the biosynthesis of starch and other energy storing molecules (Preiser et al., 2020), and in stress tolerance (Carrasco-Gil et al., 2021) and they might be connected to defending mechanisms against fungal attacks (Bashir et al., 2016). In samples of nitrogen deficiency the differences in metabolites were also mainly in sugars. The significant differences ($P<0.05$) were found in lactose, putrescine, arabitol, maltose, isobutene glycol, arabitol, galactonic acid and erythrose (Figure 3B). Putrescine was previously recognized as a metabolite with a role in stress responses in different types of abiotic stresses in tomato such as chilling tolerance (Song et al., 2014), drought (Farzane et al., 2020), and also nitrogen deficiency (González-Hernández et al., 2022). Some of the sugars identified as present in cases of significant difference in nitrogen deficiency conditions between CSBS and SS are associated with ripening processes in tomato fruits (Badejo et al., 2012). In the salinity stress test the two metabolites that showed significant differences between the three treatments were quinic acid, glycerol-3-galactoside and hydroxylamine (Figure 3C). Quinic acid was previously associated with salinity stress in tomato plants (Kwon et al., 2019; Moles et al., 2019) and other plants (LI et al., 2021), but the exact mechanism of its association with the stress is unclear. Glycerol-3-galactoside and hydroxylamine were not been known previously to be related to salinity stress in tomato plants, but hydroxylamine as it is an important metabolite in nitrogen cycles in the plant (Yao et al., 2022) it can be hypothesized that its role in stress can be connected with protein synthesis in the plants. The metabolomic results in

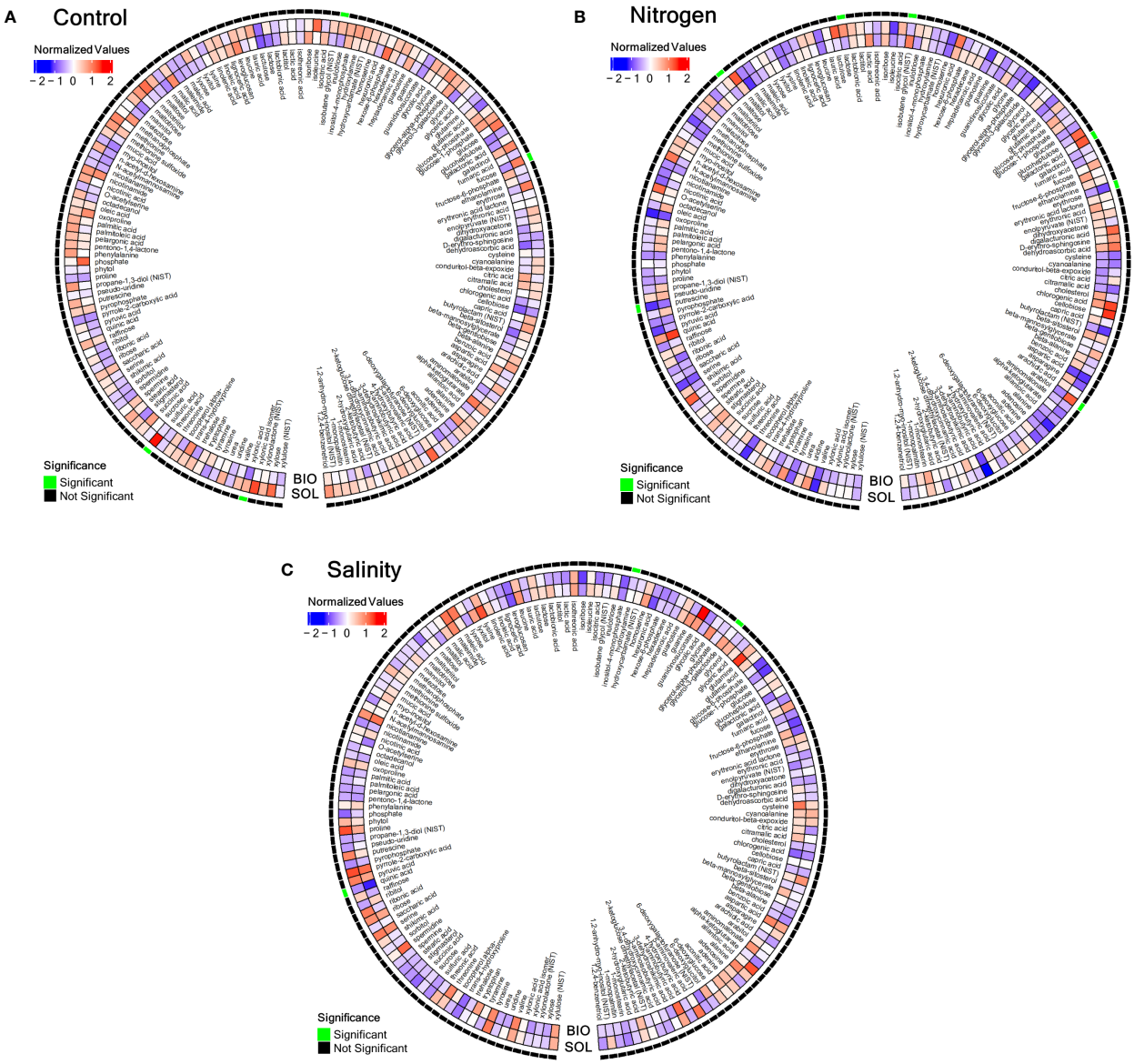

FIGURE 3
Metabolomic comparison between solarized and biosolarized pre-treated **(A)** control-treated plants, **(B)** nitrogen-deprived plants, **(C)** salinity-treated plants. A heatmap comparing the standardized averages of metabolite counts in salinity-treated solarized (SOL) and biosolarized (BIO) plants (n=5). Each metabolite value was standardized as the standard deviation from the average metabolite value of all plants (n=30), and the values were averaged for solarized and biosolarized treatments and were shown in the red-white-blue scale (blue denotes low values and red denotes high values), while significance (p<=0.05) was tested between the two groups (n=5) using the permuted Brunner Munzel test (significance was denoted by an outer green box, while insignificance was denoted by an outer black box). values), while significance (p<=0.05) was tested between the two groups (n=5) using the T-Test (significance was denoted by an outer green box, while insignificance was denoted by an outer black box).

this study indicate that CSBS can have a specific impact on the plants metabolism. It is also important to note that in both the control group and the nitrogen deficiency group the main differences were mostly noted on sugars. This result should be further explored in future studies. Additionally, it is important to mention that some metabolites such as volatile organic compounds were not within the focus of this study. These metabolites can also have a significant contribution to the observed results and should be investigated in a future study as well. In this study the assumption was that the impact on the plants metabolism will be associated with changes of the microbial population (e.g. microbiome) in the soil rhizosphere. To elucidate these changes the soil rhizosphere at the time of harvest was taken for DNA sequencing.

CSBS impact on the soil microbiome under abiotic stress

Several recent studies of SBS showed the impact this agricultural technique has on the soil microbiome (Achmon et al., 2017; Achmon et al., 2020; Fernandez-Bayo et al., 2020; Randall et al., 2020). Across all these studies, SBS was able to alter the soil microbiome significantly. Our results showed, as the previously mentioned studies suggested, that CSBS had a different impact on the soil microbiome than the SS treatment (Figure 4). CSBS elevated the abundance of Firmicutes, similar to the trend that was shown in other recent studies (Achmon et al., 2020; Shea et al., 2022) (Figure 4A). This might suggest that the soil conditions developing in SBS are more anaerobic than those in SS treatment, a finding that was also previously reported (Achmon et al., 2018). Changes in the abundance of Proteobacteria and Bacteroidetes were also noticeable and in a same trend in a similar CSBS (Achmon et al., 2020). Interestingly, the diversity was significantly lower in the CSBS than in the SS (Figure 4B) and also the richness (Figure 4D), which can be expected as the CSBS treatment applies additional natural selection forces because of the high volatile organic compounds produced which are mainly volatile fatty acids (Hestmark et al., 2019; Fernandez-Bayo et al., 2020; Liang et al., 2022).

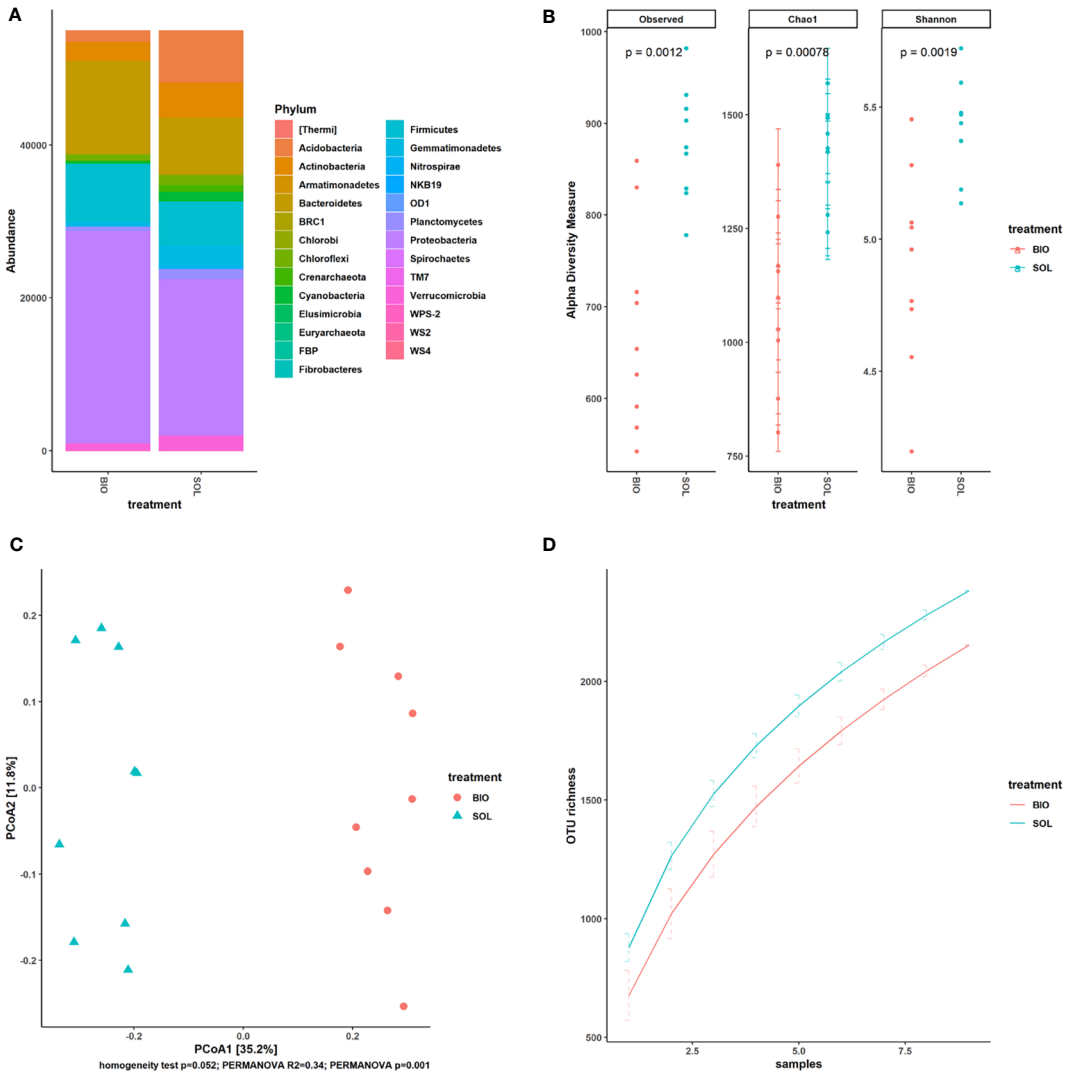

FIGURE 4
Microbiome diversity comparison between solarized and biosolarized pretreated plants. OTU counts of solarized (SOL) and biosolarized (BIO) plants (n=18) were rarefied. **(A)** comparison of the abundance of taxa by phylum (n=9). **(B)** Alpha diversity analysis using observed species, Chao1 and Shannon indices together with p-values (significance was tested using an unequal-variance Mann-Whitney U test). **(C)** Beta diversity analysis with Principal Coordinates Analysis (PCoA) using Bray-Curtis dissimilarity. Significance was tested *via* PERMANOVA. **(D)** Gamma diversity analysis using geocluster accumulation curves for mean OTU richness from a random sampling of geoclusters ± SD.

Relationships between microbiome metabolome and plant physiology in CSBS done under abiotic stress

This study is the first to date to correlate between the microbiome of CSBS/SS (or SBS) and tomato plants metabolome and physiology. The leaves were chosen as the metabolomic focus of this study in order to try to examine the correlations between the soil microbiome below the ground, that is directly impacted by the soil treatments and the abiotic stresses, and the above ground plant growth which is indirectly impacted by the soil treatments and the abiotic stresses. The result of this correlation is shown in Figure 5. The approach in this study was to take the array of data (e.g. metabolites+OTUs+physiology) of all the tests together and to try to sieve out the most significant one. This approach was taken since no specific prior knowledge about this system is available and to avoid imposing biased knowledge on the data. Figures 5A, B show the results of the total correlations between the leaf's metabolites and physiological characters of the tomato plants under the different conditions and the different OTUs of the soil microbiome. The results showed many positive and negative correlations (Figure 5A) most of which were significant (5B). To get more insight from the data, an additional filtration process was imposed to get the most significant OTUs and plant characteristics. The filtration process that was chosen was characteristics and OTUs combination which has an above 80% significant P values combined with R>0.5 or R<-0.5. Figures 5C, D present the results of the filtration process for the 30 OTUs and plant characteristics that were filtered from the

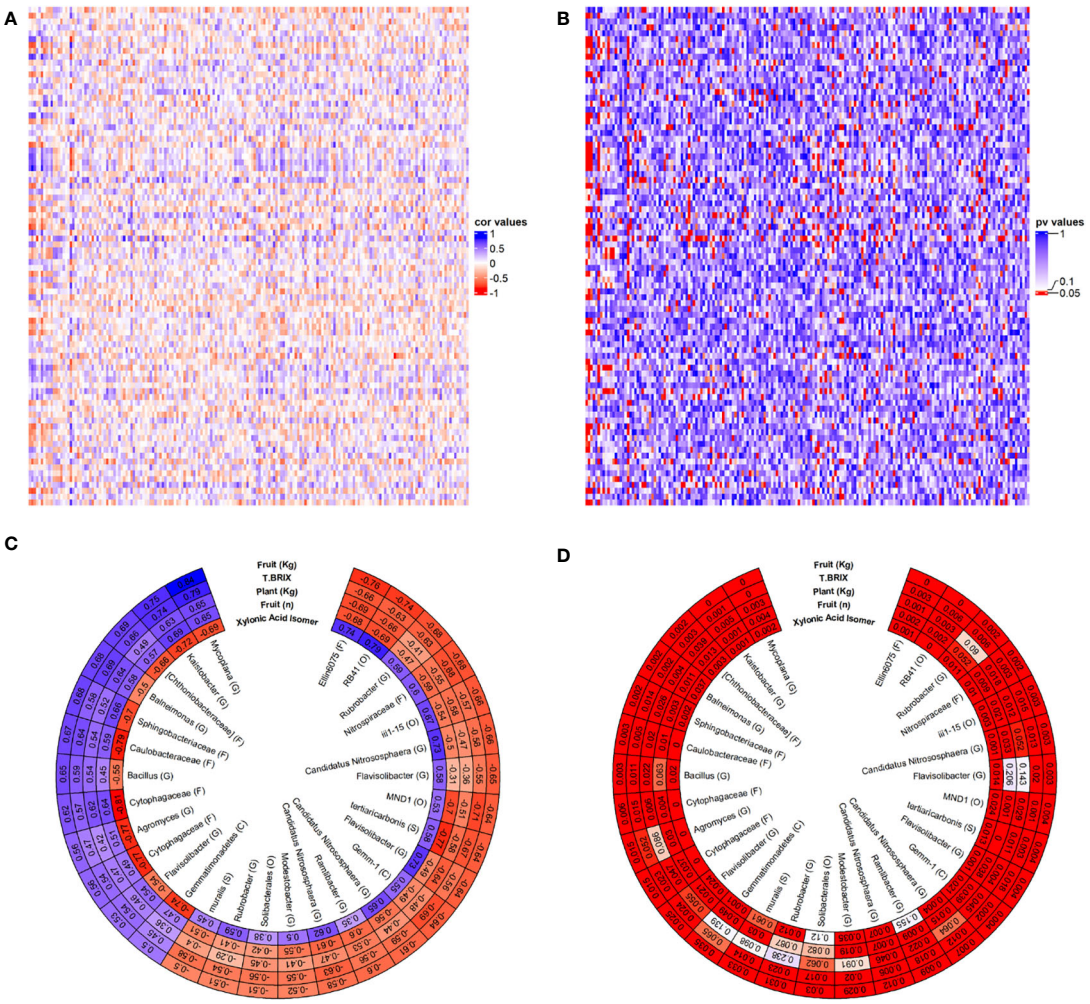

FIGURE 5
Correlations between the microbiome and between physiological and metabolomic measurements. OTU count data were normalized using Variance Stabilizing Transformation and OTUs with missing data (NAs) were filtered out. **(A, B)** Each OTU was correlated (Spearman) with each physiological measurement and metabolite and correlation values **(A)** and p-values **(B)** are presented. **(C, D)** The most highly correlated OTUs and metabolomic and physiological measurements were manually sifted and the correlation values **(C)** and p-values **(D)** are presented.

cut-off. Interestingly, only one metabolite and four tomato plants physiological characteristics were filtered in. The metabolite that showed a significant correlation with these OTUs was xylonic acid isomer. The xylonic acid isomer was positively correlated with R>0.7 with the OTUs of: Ellin6075, RB41, *Candidatus Nitrososphaera* and *Flavisolibacter*. The OTUs with a negative correlation of R<-0.7 to the Xylonic Acid isomer were: *Kaistobacter*, Sphingobacteriaceae, Caulobacteraceae, Cytophagaceae, *Agromyces*, Cytophagaceae and Gemmatimonadetes. Although xylonic Acid is not known to be directly connected with SBS or with abiotic stress it is a degradation product that is derived from xylem and is produced by microbial metabolism (Zhang et al., 2017; Trichez et al., 2022). The OTUs in this study are not known to be associated with xylonic acid metabolisms and additional studying is needed to try to understand the rule xylonic acid may play in SBS systems. It is worth noting that the Acidobacteria RB41 which had the highest positive correlation with the xylonic acid isomer, was found to have a key role in control over soil carbon cycle (Stone et al., 2021). The main interesting finding about the xylonic acid isomer is the fact that it is the exact mirror image of the wanted physiological characteristics in the tomato plants. This might suggest that the xylonic acid isomer can be used as a negative indicator for the success of SBS. Unlike the leaf's metabolites, four physiological characteristics (fruit weight, total Brix, plant weight and fruit number) were all filtered in by the cut off, with highly significant correlations with 30 relevant OTUs (Figures 5C, D). It is important to note that all these characteristics showed significant differences between SS and SBS treatments (Figure 2) and they were shown here again by using a non-supervised statistical tool. The fruit weight was highly correlated positively (R>0.7) with *Mycoplana* and *Kaistobacter* and was negatively correlated with Ellin6075 and RB41 (R<-0.7). *Mycoplana* was reported to have some role in bioremediation of soils (Cao et al., 2018; Wolf et al., 2019) and is showing an elevated abundance in these studies, which may indicate its potential in bio degradation of organic material such done in the case of SBS. More importantly, some of the *Mycoplana* species were found to be growth promoting bacteria found in wheat in nutrient-poor Calcisol and have some antifungal activity in plant diseases (Legrand et al., 2019). These attributes might explain the positive correlation *Mycoplana* has between the fruit weights and number, total brix and plant weight (Figure 5C) in this study. Additionally, it was found *Mycoplana* has a role in salt stress plant growth (Egamberdieva et al., 2018), suggesting that salt stress in this study can also cause the elevated abundance of *Mycoplana*. Similar trend as that found in *Mycoplana* was also found in *Kaistobacter* which was also found to be a potential disease suppressing bacteria in plants (Liu et al., 2016). *Kaistobacter* species are also involved in the soil bioremediation process (Gao et al., 2021; Lin et al., 2021). This might suggest that bacteria species that are adapting fast to harsh contaminated environments might also adapt fast to "organic" contaminations such as the one in SBS. These findings is suggesting that SBS might has also the potential to be effective in solving cases of other soil stressors such as heavy metals' contamination, but this was not within the focus of this research and should be tested in a future study. While *Mycoplana* and *Kaistobacter* can have the potential to serve as positive indicators for the SBS process success on tomato plants consecutive growth. Ellin6075 and RB41might serve as negative indicators for SBS as they were negatively correlated with all the plant's four physiological characteristics described above. The Ellin6075 bacterial family was previously found to be correlated with the soil's location and with using a no-till practice (Yin et al., 2017), but we have found no indication in the current literature for any role in soil stresses. As Ellin6075 bacterial family has some role in organic matter decomposing (Ye et al., 2016) and it is might be worth to focus on this family in future SBS microbiome studies. The RB41 bacterial order has previously shown an elevated abundance in soil under stress, including a salinity stress (Wang et al., 2019). It might be the case that the RB41 bacterial order changes of abundance is more related to the stress conditions than to the SBS treatment, but this should be further explored in the future. Except of Ellin6075 and RB41OTUs the OTUs of MND1 and *tertiaricarbonis* also showed highly negative correlation with the plants' four physiological characteristics. The MND1 bacterial order was also found in several studies that were looking at contaminated soils (Shen et al., 2018; Wang et al., 2020) suggesting that this order can be fast adapted to harsh conditions in the soil and is maybe an indication for the existence of abiotic stress. *Tertiaricarbonis* species negative correlation in this study with fruit weights and number, total brix and plant weight is interesting as it is not known to be related to soil stress or as a negative indication for soil conditions or for plant growth. *Tertiaricarbonis* is usually coming from aquatic systems (Chen et al., 2018; Brand et al., 2019) and is worth an additional study to see if it has a role in SBS systems. The result of the correlation between the microbiome and the plant characteristics in this study suggest that the soil microbiome has a significant impact on the plant growth performance in tomato CSBS treatments.

Conclusions

This is the first study that looked at the impact SBS has on consecutive plant crops under abiotic stress conditions. The results showed that CSBS with TP can alleviate the damaging effect of abiotic stresses in cases of high salinity and nitrogen deficiency compared to the traditional SS technique. The impact on soil

microbiome and plant metabolome is also significant in CSBS and can partially explain the advantage that CSBS has compared to SS. The results suggest that several OTUs have important role in CSBS performance in tomato growth. *Mycoplana* and *Kaistobacter* genera showed potential to serve as positive indicators for successful CSBS and on the contrary Ellin6075, RB41, MND1 and *tertiaricarbonis* might serve as negative indictors. Additionally, xylonic acid isomer metabolite in the plant leaf was highly correlated with poor plant agriculture performance in this study and should gain more attention in future SBS research. This study is an important step towards the implementation of SBS techniques as a broad group of soil treatments that can be used to mitigate a wide variety of agricultural problems and doing so by creating additional solutions of getting rid of organic waste residues. As this is the first time SBS was tested as a solution for growing plants under abiotic stress, further studies should be done with different stressors and different organic amendments as well as large scale field experiments to explore the full potential this of treatment and the microbiome landscape involved in this response.

Data availability statement

The data presented in the study are deposited in the DOE Joint Genome Institute repository, accession number 1145680. https://genome.jgi.doe.gov/portal/Soiandcoitagspl5_FD/Soiandcoitagspl5_FD.info.html.

Author contributions

YA and NS conceived of the presented idea. ZH, DT performed the computational analysis on microbiome and metabolomics, MMRW and NS conducted the greenhouse experiments, JF-B, DH and YA conducted the field experiments, ZH, JJS, JV, EB, CS, NS and YA wrote the manuscript. All authors contributed to the article and approved the submitted version.

Funding

This study was partially supported by a grant from the National Institute of Occupational Safety and Health (grant agreement number U54 OH007550) and California Department of Pesticide Regulation (grant agreement number 14-PML-R004). YA is partially support by the Guangdong Provincial Key Laboratory of Materials and Technologies for Energy Conversion, by the 2021 Guangdong Special Fund for Science and Technology, Multi-effect valorization of tea waste by soil biosolarization and restoration of farmland soil ecosystem (#STKJ2021128) and Special funds for higher education development of Guangdong Province. ZH was partially supported by a scholarship from The ADAMA Center for Novel Delivery Systems in Crop Protection, Tel Aviv University.

Conflict of interest

The authors declare that the research was conducted in the absence of any commercial or financial relationships that could be construed as a potential conflict of interest.

Publisher's note

All claims expressed in this article are solely those of the authors and do not necessarily represent those of their affiliated organizations, or those of the publisher, the editors and the reviewers. Any product that may be evaluated in this article, or claim that may be made by its manufacturer, is not guaranteed or endorsed by the publisher.

Supplementary material

The Supplementary Material for this article can be found online at: https://www.frontiersin.org/articles/10.3389/fpls.2022.1009956/full#supplementary-material

References

Achmon, Y., Claypool, J. T., Fernández-Bayo, J. D., Hernandez, K., McCurry, D. G., Harrold, D. R., et al. (2020). Structural changes in bacterial and fungal soil microbiome components during biosolarization as related to volatile fatty acid accumulation. *Appl. Soil Ecol.* 153. doi: 10.1016/j.apsoil.2020.103602

Achmon, Y., Claypool, J. T., Pace, S., Simmons, B. A., Singer, S. W., and Simmons, C. W. (2019). Assessment of biogas production and microbial ecology in a high solid anaerobic digestion of major California food processing residues. *Bioresour. Technol. Rep.* 5, 1–11. doi: 10.1016/j.biteb.2018.11.007

Achmon, Y., Fernández-Bayo, J. D., Hernandez, K., McCurry, D. G., Harrold, D. R., Su, J., et al. (2017). Weed seed inactivation in soil mesocosms *via* biosolarization with mature compost and tomato processing waste amendments. *Pest Manage. Sci.* 73, 862–873. doi: 10.1002/ps.4354

Achmon, Y., Harrold, D. R., Claypool, J. T., Stapleton, J. J., VanderGheynst, J. S., and Simmons, C. W. (2016). Assessment of tomato and wine processing solid wastes as soil amendments for biosolarization. *Waste. Manag.* 48, 156–164. doi: 10.1016/j.wasman.2015.10.022

Achmon, Y., Sade, N., Wilhelmi, M., del, M. R., Fernández-Bayo, J. D., Harrold, D. R., et al. (2018). Effects of short-term biosolarization using mature compost and industrial tomato waste amendments on the generation and persistence of biocidal soil conditions and subsequent tomato growth. *J. Agric. Food Chem.* 66, 5451–5461. doi: 10.1021/acs.jafc.8b00424

Badejo, A. A., Wada, K., Gao, Y., Maruta, T., Sawa, Y., Shigeoka, S., et al. (2012). Translocation and the alternative d-galacturonate pathway contribute to increasing the ascorbate level in ripening tomato fruits together with the d-

mannose/L-galactose pathway. *J. Exp. Bot.* 63, 229–239. doi: 10.1093/jxb/err275

Bashir, Z., Shafique, S., Ahmad, A., Shafique, S., Yasin, N. A., Ashraf, Y., et al. (2016). Tomato plant proteins actively responding to fungal applications and their role in cell physiology. *Front. Physiol.* 7, 257. doi: 10.3389/fphys.2016.00257

Brand, V. R., Crosby, L. D., and Criddle, C. S. (2019). Niche differentiation among three closely related competibacteraceae clades at a full-scale activated sludge wastewater treatment plant and putative linkages to process performance. *Appl. Environ. Microbiol.* 85, e02301–e02318. doi: 10.1128/AEM.02301-18

Cao, B., Zhang, Y., Wang, Z., Li, M., Yang, F., Jiang, D., et al. (2018). Insight into the variation of bacterial structure in atrazine-contaminated soil regulating by potential phytoremediator: Pennisetum americanum (L.) k. schum. *Front. Microbiol.* 9, 864. doi: 10.3389/fmicb.2018.00864

Caporaso, J. G., Kuczynski, J., Stombaugh, J., Bittinger, K., Bushman, F. D., Costello, E. K., et al. (2010). QIIME allows analysis of high-throughput community sequencing data. *Nat. Methods* 7, 335–336. doi: 10.1038/nmeth.f.303

Carrasco-Gil, S., Allende-Montalbán, R., Hernández-Apaolaza, L., and Lucena, J. J. (2021). Application of seaweed organic components increases tolerance to fe deficiency in tomato plants. *Agronomy* 11, 507. doi: 10.3390/agronomy11030507

Chamorro, M., Miranda, L., Domínguez, P., Medina, J. J., Soria, C., Romero, F., et al. (2015). Evaluation of biosolarization for the control of charcoal rot disease (Macrophomina phaseolina) in strawberry. *Crop Prot.* 67, 279–286. doi: 10.1016/j.cropro.2014.10.021

Chen, W.-M., Chen, Y.-L., Li, Y.-S., and Sheu, S.-Y. (2018). Aquincola amnicola sp. nov., isolated from a freshwater river. *Arch. Microbiol.* 200, 811–817. doi: 10.1007/s00203-018-1492-4

DeVay, J. E., and Katan, J. (1991). Mechanisms of pathogen control in solarized soils. *Soil Solarization.* Boca Raton: CRC Press, 87–101.

Domínguez, P., Miranda, L., Soria, C., de los Santos, B., Chamorro, M., Romero, F., et al. (2014). Soil biosolarization for sustainable strawberry production. *Agron. Sustain. Dev.* 34, 821–829. doi: 10.1007/s13593-014-0211-z

Egamberdieva, D., Davranov, K., and Wirth, S. (2018). *"Soil salinity and microbes: Diversity, ecology, and biotechnological potential BT - extremophiles in Eurasian ecosystems: Ecology, diversity, and applications,"*. Eds. D. Egamberdieva, N.-K. Birkeland, H. Panosyan and W.-J. Li (Singapore: Springer Singapore), 317–332. doi: 10.1007/978-981-13-0329-6_11

Farzane, A., Nemati, H., Shoor, M., and Ansari, H. (2020). Antioxidant enzyme and plant productivity changes in field-grown tomato under drought stress conditions using exogenous putrescine. *J. Plant Physiol. Breed.* 10, 29–40.

Fernández-Bayo, J. D., Achmon, Y., Harrold, D. R., McCurry, D. G., Hernandez, K., Dahlquist-Willard, R. M., et al. (2017). Assessment of two solid anaerobic digestate soil amendments for effects on soil quality and biosolarization efficacy. *J. Agric. Food Chem.* 65, 3434–3442. doi: 10.1021/acs.jafc.6b04816

Fernández-Bayo, J. D., Hestmark, K. V., Claypool, J. T., Harrold, D. R., Randall, T. E., Achmon, Y., et al. (2019). The initial soil microbiota impacts the potential for lignocellulose degradation during soil solarization. *J. Appl. Microbiol.* 126, 1729–1741. doi: 10.1111/jam.14258

Fernández-Bayo, J. D., Randall, T. E., Harrold, D. R., Achmon, Y., Hestmark, K. V., Su, J., et al. (2018). Effect of management of organic wastes on inactivation of brassica nigra and fusarium oxysporum f. sp. lactucae using soil biosolarization. *Pest Manage. Sci.* 74, 1892–1902.doi: 10.1002/ps.4891

Fernandez-Bayo, J. D., Shea, E. A., Parr, A. E., Achmon, Y., Stapleton, J. J., VanderGheynst, J. S., et al. (2020). Almond processing residues as a source of organic acid biopesticides during biosolarization. *Waste. Manage.* 101, 74–82. doi: 10.1016/j.wasman.2019.09.028

Fiehn, O., Wohlgemuth, G., Scholz, M., Kind, T., Lee, D. Y., Lu, Y., et al. (2008). Quality control for plant metabolomics: reporting MSI-compliant studies. *Plant J.* 53, 691–704. doi: 10.1111/j.1365-313X.2007.03387.x

Gao, T.-P., Wan, Z.-D., Liu, X.-X., Fu, J.-W., Chang, G.-H., Sun, H.-L., et al. (2021). Effects of heavy metals on bacterial community structure in the rhizosphere of salsola collina and bulk soil in the jinchuan mining area. *Geomicrob. J.* 38, 620–630. doi: 10.1080/01490451.2021.1914784

García-Raya, P., Ruiz-Olmos, C., Marín-Guirao, J. I., Asensio-Grima, C., Tello-Marquina, J. C., and de Cara-García, M. (2019). Greenhouse soil biosolarization with tomato plant debris as a unique fertilizer for tomato crops. *Int. J. Environ. Res. Public Health* 16, 279. doi: 10.3390/ijerph16020279

González-Hernández, A. I., Scalschi, L., Troncho, P., García-Agustín, P., and Camañes, G. (2022). Putrescine biosynthetic pathways modulate root growth differently in tomato seedlings grown under different n sources. *J. Plant Physiol.* 268, 153560. doi: 10.1016/j.jplph.2021.153560

Goswami, M., and Suresh, D. (2020). Plant growth-promoting rhizobacteria–alleviators of abiotic stresses in soil: a review. *Pedosphere* 30, 40–61. doi: 10.1016/S1002-0160(19)60839-8

Gur, A., Semel, Y., Osorio, S., Friedmann, M., Seekh, S., Ghareeb, B., et al. (2011). Yield quantitative trait loci from wild tomato are predominately expressed by the shoot. *Theor. Appl. Genet.* 122, 405–420. doi: 10.1007/s00122-010-1456-9

Hestmark, K. V., Fernández-Bayo, J. D., Harrold, D. R., Randall, T. E., Achmon, Y., Stapleton, J. J., et al. (2019). Compost induces the accumulation of biopesticidal organic acids during soil biosolarization. *Resour. Conserv. Recycl.* 143, 27–35. doi: 10.1016/j.resconrec.2018.12.009

Katan, J. (2015). Soil solarization: the idea, the research and its development. *Phytoparasitica* 43, 1–4. doi: 10.1007/s12600-014-0419-0

Kwon, M. C., Kim, Y. X., Lee, S., Jung, E. S., Singh, D., Sung, J., et al. (2019). Comparative metabolomics unravel the effect of magnesium oversupply on tomato fruit quality and associated plant metabolism. *Metabolites* 9, 231. doi: 10.3390/metabo9100231

Legrand, F., Chen, W., Cobo-Díaz, J. F., Picot, A., and Le, F. G. (2019). Co-Occurrence analysis reveal that biotic and abiotic factors influence soil fungistasis against fusarium graminearum. *FEMS Microbiol. Ecol.* 95, fiz056. doi: 10.1093/femsec/fiz056

Liang, Y., Li, Y., Lin, Y., Liu, X., Zou, Y., Yu, P., et al. (2022). Assessment of using solid residues of fish for treating soil by the biosolarization technique as an alternative to soil fumigation. *J. Clean. Prod.* 357, 131886. doi: 10.1016/j.jclepro.2022.131886

Lin, H., Liu, C., Li, B., and Dong, Y. (2021). Trifolium repens l. regulated phytoremediation of heavy metal contaminated soil by promoting soil enzyme activities and beneficial rhizosphere associated microorganisms. *J. Hazard. Mater.* 402, 123829. doi: 10.1016/j.jhazmat.2020.123829

Liu, X., Zhang, S., Jiang, Q., Bai, Y., Shen, G., Li, S., et al. (2016). Using community analysis to explore bacterial indicators for disease suppression of tobacco bacterial wilt. *Sci. Rep.* 6, 36773. doi: 10.1038/srep36773

LI, P., Yang, X., Wang, H., Ting, P. A. N., Yang, J., Wang, Y., et al. (2021). Metabolic responses to combined water deficit and salt stress in maize primary roots. *J. Integr. Agric.* 20, 109–119. doi: 10.1016/S2095-3119(20)63242-7

Moles, T. M., de Brito Francisco, R., Mariotti, L., Pompeiano, A., Lupini, A., Incrocci, L., et al. (2019). Salinity in autumn-winter season and fruit quality of tomato landraces. *Front. Plant Sci.* 10, 1078. doi: 10.3389/fpls.2019.01078

Oldfield, T. L., Achmon, Y., Perano, K. M., Dahlquist-Willard, R. M., VanderGheynst, J. S., Stapleton, J. J., et al. (2017). A life cycle assessment of biosolarization as a valorization pathway for tomato pomace utilization in California. *J. Clean. Prod.* 141, 146–156. doi: 10.1016/j.jclepro.2016.09.051

Preiser, A. L., Banerjee, A., Weise, S. E., Renna, L., Brandizzi, F., and Sharkey, T. D. (2020). Phosphoglucoisomerase is an important regulatory enzyme in partitioning carbon out of the Calvin-Benson cycle. *Front. Plant Sci.* 11, 580726. doi: 10.3389/fpls.2020.580726

Quast, C., Pruesse, E., Yilmaz, P., Gerken, J., Schweer, T., Yarza, P., et al. (2012). The SILVA ribosomal RNA gene database project: improved data processing and web-based tools. *Nucleic Acids Res.* 41, D590–D596. doi: 10.1093/nar/gks1219

Randall, T. E., Fernandez-Bayo, J. D., Harrold, D. R., Achmon, Y., Hestmark, K. V., Gordon, T. R., et al. (2020). Changes of fusarium oxysporum f. sp. lactucae levels and soil microbial community during soil biosolarization using chitin as soil amendment. *PloS One* 15, e0232662. doi: 10.1371/journal.pone.0232662

Sade, N., del Mar Rubio-Wilhelmi, M., Umnajkitikorn, K., and Blumwald, E. (2018). Stress-induced senescence and plant tolerance to abiotic stress. *J. Exp. Bot.* 69, 845–853. doi: 10.1093/jxb/erx235

Sade, N., Weng, F., Tajima, H., Zeron, Y., Zhang, L., Rubio Wilhelmi, M., et al. (2020). A cytoplasmic receptor-like kinase contributes to salinity tolerance. *Plants* 9, 1383. doi: 10.3390/plants9101383

Savci, S. (2012). Investigation of effect of chemical fertilizers on environment. *Apcbee. Proc.* 1, 287–292. doi: 10.1016/j.apcbee.2012.03.047

Shea, E. A., Fernández-Bayo, J. D., Hodson, A. K., Parr, A. E., Lopez, E., Achmon, Y., et al. (2022). Biosolarization restructures soil bacterial communities and decreases parasitic nematode populations. *Appl. Soil Ecol.* 172, 104343. doi: 10.1016/j.apsoil.2021.104343

Shen, Y., Ji, Y., Li, C., Luo, P., Wang, W., Zhang, Y., et al. (2018). Effects of phytoremediation treatment on bacterial community structure and diversity in different petroleum-contaminated soils. *Int. J. Environ. Res. Public Health* 15, 2168. doi: 10.3390/ijerph15102168

Song, Y., Diao, Q., and Qi, H. (2014). Putrescine enhances chilling tolerance of tomato (Lycopersicon esculentum mill.) through modulating antioxidant systems. *Acta Physiol. Plant* 36, 3013–3027. doi: 10.1007/s11738-014-1672-z

Spang, E. S., Moreno, L. C., Pace, S. A., Achmon, Y., Donis-Gonzalez, I., Gosliner, W. A., et al. (2019). Food loss and waste: measurement, drivers, and solutions. *Annu. Rev. Environ. Resour.* 44, 117–156. doi: 10.1146/annurev-environ-101718-033228

Stapleton, J. J. (2000). Soil solarization in various agricultural production systems. *Crop Prot.* 19, 837–841. doi: 10.1016/S0261-2194(00)00111-3

Stone, B. W., Li, J., Koch, B. J., Blazewicz, S. J., Dijkstra, P., Hayer, M., et al. (2021). Nutrients cause consolidation of soil carbon flux to small proportion of bacterial community. *Nat. Commun.* 12, 1–9. doi: 10.1038/s41467-021-23676-x

Tremblay, J., Singh, K., Fern, A., Kirton, E. S., He, S., Woyke, T., et al. (2015). Primer and platform effects on 16S rRNA tag sequencing. *Front. Microbiol.* 6, 771. doi: 10.3389/fmicb.2015.00771

Trichez, D., Carneiro, C. V. G. C., Braga, M., and Almeida, J. R. M. (2022). Recent progress in the microbial production of xylonic acid. *World J. Microbiol. Biotechnol.* 38, 1–15. doi: 10.1007/s11274-022-03313-5

Wang, M., Chen, S., Chen, L., and Wang, D. (2019). Responses of soil microbial communities and their network interactions to saline-alkaline stress in cd-contaminated soils. *Environ. pollut.* 252, 1609–1621. doi: 10.1016/j.envpol.2019.06.082

Wang, Q., Zheng, R., Sun, X., Jiang, Z., Yang, F., Lu, Q., et al. (2020). Effects of comamonas testosteroni on PAHs degradation and bacterial community structure in leymus chinensis rhizosphere soil. *Sheng. wu. gong. cheng. xue. bao=. Chin. J. Biotechnol.* 36, 2657–2673. doi: 10.13345/j.cjb.200381

Weckwerth, W., Wenzel, K., and Fiehn, O. (2004). Process for the integrated extraction, identification and quantification of metabolites, proteins and RNA to reveal their co-regulation in biochemical networks. *Proteomics* 4, 78–83. doi: 10.1002/pmic.200200500

Wolf, D. C., Cryder, Z., and Gan, J. (2019). Soil bacterial community dynamics following surfactant addition and bioaugmentation in pyrene-contaminated soils. *Chemosphere* 231, 93–102. doi: 10.1016/j.chemosphere.2019.05.145

Yao, R., Li, H., Yang, J., Wang, X., Xie, W., and Zhang, X. (2022). Ammonia monooxygenase activity connects nitrification rate with dominant edaphic properties under salinity stress in coastal fluvo-aquic soil. *J. Soil Sci. Plant Nutr.*, 1–12. doi: 10.1007/s42729-022-00867-z

Ye, J., Zhang, R., Nielsen, S., Joseph, S. D., Huang, D., and Thomas, T. (2016). A combination of biochar–mineral complexes and compost improves soil bacterial processes, soil quality, and plant properties. *Front. Microbiol.* 7, 372. doi: 10.3389/fmicb.2016.00372

Yin, C., Mueth, N., Hulbert, S., Schlatter, D., Paulitz, T. C., Schroeder, K., et al. (2017). Bacterial communities on wheat grown under long-term conventional tillage and no-till in the pacific Northwest of the united states. *Phytobiomes* 1, 83–90. doi: 10.1094/PBIOMES-09-16-0008-R

Zhang, H.-X., and Blumwald, E. (2001). Transgenic salt-tolerant tomato plants accumulate salt in foliage but not in fruit. *Nat. Biotechnol.* 19, 765–768. doi: 10.1038/90824

Zhang, H., Han, X., Wei, C., and Bao, J. (2017). Oxidative production of xylonic acid using xylose in distillation stillage of cellulosic ethanol fermentation broth by gluconobacter oxydans. *Bioresour. Technol.* 224, 573–580. doi: 10.1016/j.biortech.2016.11.039

Sub- chapter 4.2

Results presented in this sub-chapter has been published in the journal “Plant and Cell Physiology”

Title: The Alteration of Tomato Chloroplast Vesiculation Positively Affects Whole-Plant Source–Sink Relations and Fruit Metabolism under Stress Conditions

PCP
PLANT & CELL PHYSIOLOGY

Regular Paper

The Alteration of Tomato Chloroplast Vesiculation Positively Affects Whole-Plant Source–Sink Relations and Fruit Metabolism under Stress Conditions

Yoav Ahouvi[1,†], Zechariah Haber[1,†], Yair Yehoshua Zach[1], Leah Rosental[2], David Toubiana[1], Davinder Sharma[1], Saleh Alseekh[3,4], Hiromi Tajima[5], Alisdair R. Fernie[3,4], Yariv Brotman[2], Eduardo Blumwald[5] and Nir Sade[1,*]

[1]School of Plant Sciences and Food Security, Tel Aviv University, P.O.B. 39040, 55 Haim Levanon St., Tel Aviv 6139001, Israel
[2]Department of Life Sciences, Ben-Gurion University of the Negev, P.O.B. 653, 1 David Ben Gurion Blvd., Beer-Sheva 8410501, Israel
[3]Department of Root Biology and Symbiosis, Max Planck Institute of Molecular Plant Physiology, 1 Am Mühlenberg, Golm, Potsdam 14476, Germany
[4]Department of Plant Metabolomics, Center for Plant Systems Biology and Biotechnology, 139 Ruski Blvd., Plovdiv 4000, Bulgaria
[5]Department of Plant Sciences, University of California, 1 Shields Ave., Davis, CA 95616, USA
[†]Equal contribution.

*Corresponding author: E-mail, nirsa@tauex.tau.ac.il

(Received 22 April 2022; Accepted 23 September 2022)

Changes in climate conditions can negatively affect the productivity of crop plants. They can induce chloroplast degradation (senescence), which leads to decreased source capacity, as well as decreased whole-plant carbon/nitrogen assimilation and allocation. The importance, contribution and mechanisms of action regulating source-tissue capacity under stress conditions in tomato (*Solanum lycopersicum*) are not well understood. We hypothesized that delaying chloroplast degradation by altering the activity of the tomato chloroplast vesiculation (CV) under stress would lead to more efficient use of carbon and nitrogen and to higher yields. Tomato CV is upregulated under stress conditions. Specific induction of CV in leaves at the fruit development stage resulted in stress-induced senescence and negatively affected fruit yield, without any positive effects on fruit quality. Clustered Regularly Interspaced Short Palindromic Repeats/CRISPR-associated protein 9 (CRISPR/CAS9) knock-out CV plants, generated using a near-isogenic tomato line with enhanced sink capacity, exhibited stress tolerance at both the vegetative and the reproductive stages, leading to enhanced fruit quantity, quality and harvest index. Detailed metabolic and transcriptomic network analysis of sink tissue revealed that the L-glutamine and L-arginine biosynthesis pathways are associated with stress-response conditions and also identified putative novel genes involved in tomato fruit quality under stress. Our results are the first to demonstrate the feasibility of delayed stress-induced senescence as a stress-tolerance trait in a fleshy fruit crop, to highlight the involvement of the CV pathway in the regulation of source strength under stress and to identify genes and metabolic pathways involved in increased tomato sink capacity under stress conditions.

Keywords: Chloroplast vesiculation • Correlation network analysis • Sink capacity • Source–sink relations • Source capacity • Stress-induced senescence

Introduction

An inherent gap exists between maximal theoretical crop productivity under ideal conditions and actual environment-dependent yield. Closing this gap is a major milestone on the path toward nutritional sustainability. Salinity and water deficit are two factors that contribute greatly to the yield gap: they induce premature senescence in photosynthetic source tissues and reduce plant growth and the number of sink organs by disrupting the movement of assimilated compounds) Munne-Bosch and Alegre 2004). It has been suggested that enhancing photosynthetic capabilities, in order to enhance source capacity, is one of the most important strategies that should be utilized in efforts to meet future global dietary needs under climate change conditions (Zhu et al. 2010, Long et al. 2015).

Climate change negatively affects tomato productivity by modifying the plant source–sink relationships. Therefore, the development of strategies by which tomato plants could maintain both strong source (e.g. photo-assimilation) and sink (e.g. remobilization) capacities, with a delay in stress-induced senescence under water stress and/or irrigation with brackish water (i.e. a water source that is somewhat salty), is highly desirable.

A well-established strategy for enhancing source capacity involves the stay-green trait (Gregersen et al. 2013, Thomas and Ougham 2014). The stay-green trait reflects impaired or delayed chlorophyll degradation. There are two main types of

Plant Cell Physiol. 63(12): 2008–2026 (2022) doi:https://doi.org/10.1093/pcp/pcac133, Advance Access publication on 26 September 2022, available online at https://academic.oup.com/pcp

stay-greens: cosmetic, in which pigment catabolism is the primary lesion, and functional, in which the entire senescence syndrome is delayed or slowed down (Thomas and Howarth 2000). In *Arabidopsis*, there are several characterized pathways that are involved in the degradation of chloroplast proteins such as senescence-associated vacuoles, autophagy and chloroplast vesiculation (CV) (Xie et al. 2015) with autophagy, which have a clear role in stimulating nutrient remobilization upon senescence (Havé et al. 2016, Michaeli et al. 2016). Several studies, mainly in cereals, suggested that breeding for delayed senescence by delaying chloroplast degradation (i.e. the stay-green trait) can improve source capacity throughout stress episodes and improve yield (Gregersen et al. 2013). Chloroplast stabilization increases the ability of source leaves to maintain a high photoassimilation rate and prolongs the overall duration of that assimilation. With regard to the chloroplast degradation pathways (Xie et al. 2015), the CV was shown to be directly involved in stress-induced senescence and to enhance source strength (Wang and Blumwald 2014, Sade et al. 2018b). CV has been previously characterized in *Arabidopsis* and rice, where it was shown to be associated with the chloroplast and involved in the thylakoid membrane and stroma proteins' inactivation by the protein–protein interaction (Wang and Blumwald 2014, Sade et al. 2018b). Consequently, the downregulation of CV in *Arabidopsis* and rice regulated source fitness under stress by delaying chloroplast degradation and enhancing productivity (Wang and Blumwald 2014). Recently, it was demonstrated that delayed senescence (induced by the manipulation of transcription factors) can enhance source capacity, as well as fruit quality and yield, in tomato (Lira et al. 2017, Ma et al. 2018, 2019).

The optimal utilization of enhanced source capacity [i.e. carbon (C) and nitrogen (N) assimilation] requires an effective remobilization of photoassimilates to the sink (i.e. sink capacity). This is of particular importance in fleshy fruits such as tomato, where photoassimilates influence the levels of soluble sugars in the fruit. One established strategy to increase the sink capacity for photoassimilates in tomato is the alteration of fruit cell-wall invertase. The rationale behind this strategy is that the hydrolysis of translocated sucrose at the point of unloading in the fruit sink would increase the translocation gradient from source to sink, increasing the net import of sucrose into the fruits, resulting in higher levels of soluble sugars. A near-isogenic line of tomato, derived from a cross between *Solanum lycopersicum* M82-domesticated tomato and *Solanum pennellii* wild-type (WT) tomato (Eshed and Zamir 1995), with an introgression of fruit-specific cell-wall invertase, exhibited elevated fruit-soluble sugars and sink capacity without any yield effects under optimal conditions (IL9-2-5; Fridman et al. 2004). The major underlying factor leading to increased fruit sugar in IL9-2-5 was an increase in the capacity to take up sucrose unloaded from the phloem (Baxter et al. 2005). Thus, a combination of enhanced source capacity due to the stay-green trait (e.g. CV downregulation) and enhanced sink capacity due to the enhanced loading of sugar into the fruit (e.g. IL9-2-5) can result in improved source–sink interactions, leading to higher tomato yields and improved yield quality under stress conditions.

C and N compounds (represented as metabolites) are assimilated by the plant at the source tissues and are mobilized to the sink tissues. The metabolism of tomato fruits has been widely studied, and several pathways, such as the trichloroacetic acid (TCA) cycle and ethylene metabolism, have been extensively characterized) Nunes-Nesi et al. 2011, Quinet et al. 2019). Abiotic stress affects the primary and secondary metabolism of tomato fruits with negative effects on fruit size and, depending on the stress and its severity, with positive effects on fruit quality (Quinet et al. 2019). Nevertheless, the question of whether and how enhanced source capacity affects sink metabolism in tomato has not yet been fully answered.

CV is conserved within the plant kingdom, with tomato possessing a single *CV* gene (Solyc08G067630). Here, we used a gene-editing technology in a near-isogenic tomato line (IL) of enhanced sink fitness (IL9-2-5, as the genetic background) to study the effect of a stable *cv*-knockout on the quantity and quality of tomatoes grown under abiotic stress. Additionally, we used a parallel approach by which an inducible promoter was utilized to study the effect of the induction of *CV* expression at the reproductive stage on fruit development and quality. We also performed an in-depth analysis of sink-tissue metabolites and transcriptomic data under prolonged abiotic stress and used a machine learning approach to identify unique and novel putative metabolic pathways and genes associated with tomato fruit quality.

Results

Effect of the expression of the *Arabidopsis thaliana CV* gene in tomato

Since the *A. thaliana CV* gene has been well characterized as a stress-induced senescence gene (Wang and Blumwald 2014), a dexamethasone (DEX)-induced *CV* from *A. thaliana* was inserted into the M82 line of tomato. *Arabidopsis thaliana CV* (*AtCV*) expression in the transgenic lines was tested following 4 h of treatment with DEX, and strong gene expression was confirmed (**Fig. 1A**). We used two lines of M82 that contain *AtCV*-inducible genes (L1 and L2). Leaves were sampled from 4- to 5-week-old plants and placed in control solution [H_2O and dimethyl sulfoxide (DMSO)] and in DEX-containing solution for 72 h (**Fig. 1B**). A significant decrease in chlorophyll content (**Fig. 1B**, **C**) was seen when the tissue was placed in the DEX solution, with a considerably more pronounced chlorophyll content decrease in lines L1 and L2 than in the WT.

To further evaluate the effect of *CV*-induced senescence in tomato at the reproductive stage, WT and transgenic plants were grown throughout the entire life cycle until fruit could be harvested. At the early fruit development stage (i.e. a stage by which fruits are at the growth stage and are already active sinks, and nutrient remobilization is active), leaves close to the fruits

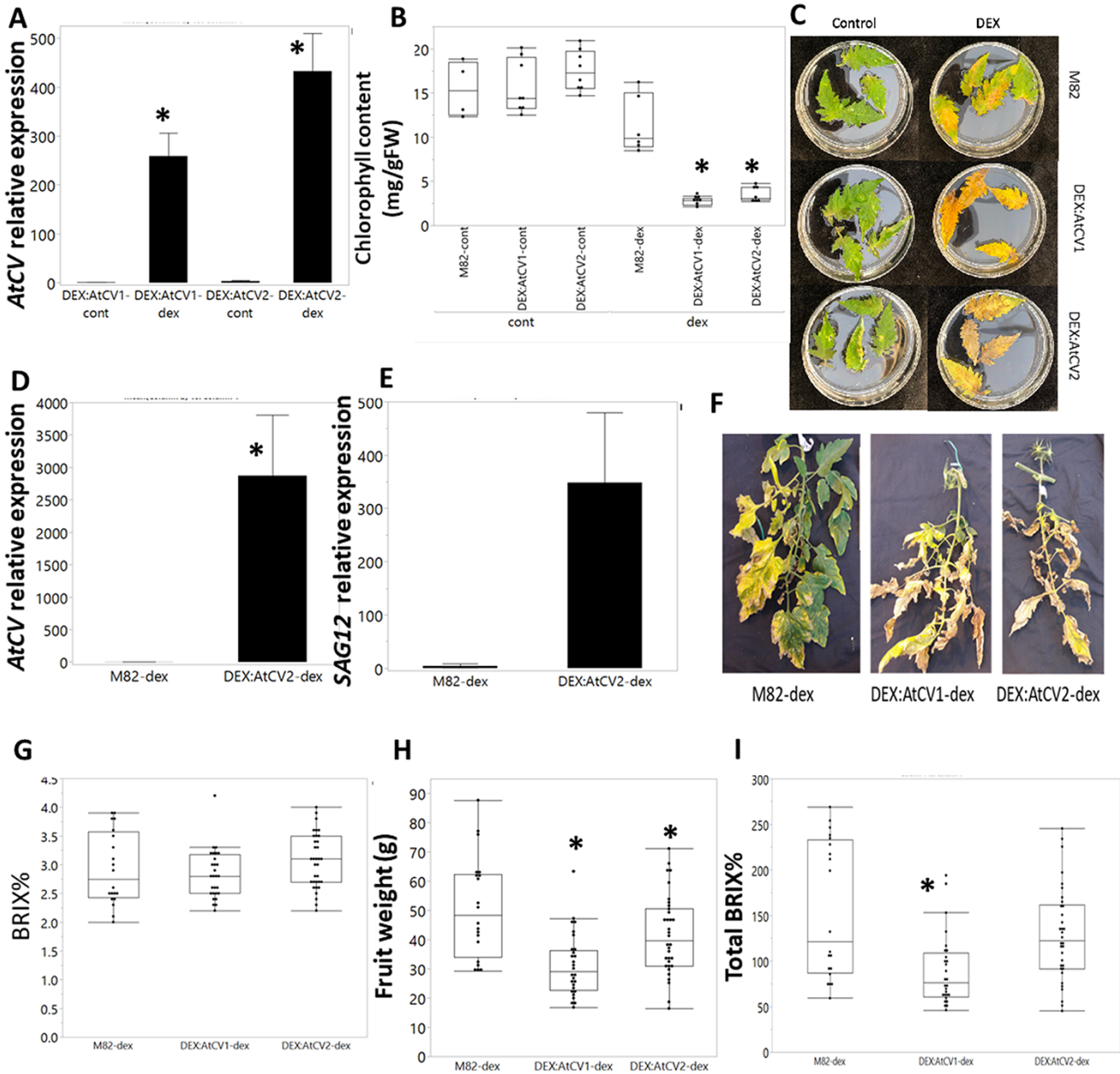

Fig. 1 Phenotypic examination of the effect of expressing *A. thaliana CV* gene in tomatoes. Different phenotypic measurements, taken on tomato lines containing *AtCV* gene fused to a DEX-induced promotor, and WT tomatoes (M82) are presented. 'Cont' stands for control, which were dipped in H_2O and DMSO, and 'DEX' stands for plants that were dipped in DEX solution (50 μM). (A) CV relative expression before treating with DEX and 4 h later. (B) Detached leaves were left floating in DEX solution and were examined for chlorophyll content. (C) Representative detached leaves after DEX solution. (D, E) Relative expression levels of AtCV and SAG12 at the end of the experiment are presented. One leaf from four plants of each group was taken for analysis ($N = 4$). (F) Representative leaves of the lines at fruit harvest time point. (G–I) Brix% levels, average individual fruit weight and product (multiplication) of fruits of WT and DEX:CV-induced plants are presented. Error bars represent the mean ± SE. The boxes represent the interquartile range, the line represents the median and the black dots are all the measurements taken. Asterisk represents significant differences between genotypes and WT ($P < 0.05$, Dunnet's test).

of each plant were routinely dipped in DEX solution to promote *AtCV* expression. *CV* expression in leaves was measured at harvest and found to be significantly higher in the *DEX::CV* line than in the WT (**Fig. 1D**). The expression of *Senescence-Associated Gene 12* (*SAG12*), which encodes a senescence-specific cysteine protease *SAG12* (Gan and Amazino 1995), was also measured and was found to be significantly higher in *DEX::CV* (**Fig. 1E**). DEX treatments additionally enhanced the senescence of the leaves of the transgenic lines, as compared to the DEX-treated WT (**Fig. 1F**).

Yield potential was measured upon treatment with DEX until fruit maturity, in terms of fruit Brix, average individual

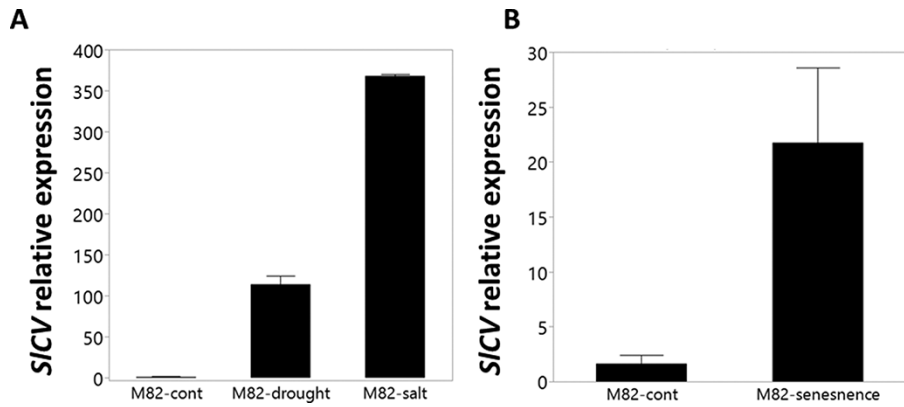

Fig. 2 Tomato CV (SlCV) expression under stress conditions. Three-week-old M82 tomato plants were either well irrigated ('cont', $N = 3$) or exposed to drought (1 week no irrigation—'drought', $N = 3$) or salt (1 week 200 mM NaCl—'salt', $N = 3$). (B) Tomato CV (SlCV) expression in senescence. Leaf samples were taken from a young and viable, well-irrigated plant, 6 weeks old ('cont', $N = 4$) and from an old plant at the end of its reproduction cycle, 12 weeks old ('senescence', $N = 4$). Error bars represent the mean ± SE. Asterisk represents significant differences between genotypes and WT ($P < 0.05$).

fruit weight and total Brix (**Fig. 1G, I**). There was no significant difference between the fruit Brix levels of the WT and *DEX:CV* plants (**Fig. 1G**), although fruit weight was significantly lower among the *DEX::CV* lines (**Fig. 1H**). The product of the multiplication of the average Brix by the fruit weight of each plant (representing total Brix potential) was generally lower in the transgenic lines than in the WT (**Fig. 1I**).

Overall, the results indicate that treating *DEX::CV* lines with DEX caused increased *CV* expression and promoted senescence. As a consequence, the yield was negatively affected without any beneficial effect on fruit Brix.

SlCV expression in tomato during senescence and under stress

We hypothesized that reinforcing the source tissue during abiotic stress, by knocking-out *CV*, could provide a means to generate tomato plants that are able to tolerate stressful, senescence-promoting environments. As a first step to test this hypothesis, we examined the expression of the endogenous tomato *CV* gene under different stress conditions in WT tomato plants. Relative expression of *CV* was examined in leaf samples from 3-week-old well-irrigated WT tomato plants, plants that were exposed to water-deficit stress (1 week without irrigation) or exposed to salt stress (1 week of treatment with 150 mM NaCl). WT tomato plants that were exposed to water-deficit stress or salt treatment exhibited significantly greater *CV* expression, as compared to the well-irrigated plants (**Fig. 2A**).

CV expression in leaves was also examined during the different growth-cycle stages of the plant. The expression of *CV* increased over the course of the plant life cycle, with relatively high expression in leaves of plants at the late fruit stage as compared to the early flowering stage (**Fig. 2B**). These experiments supported the notion that *Solanum lycopersicum CV* (*SlCV*) displayed an expression pattern that was closely related to stress-induced senescence.

Subcellular localization of SlCV protein

To further characterize the tomato CV protein, assessment of its subcellular localization was carried out (Sade et al. 2018b). We used transient agroinfiltration in tobacco leaves, and CV targeting was achieved by using a CV-yellow fluorescent protein (YFP) fusion protein. We found that CV co-localized with the chloroplast, showing a vesicle type pattern that might represent a CV-containing vesicle (CCV) or a CCV aggregation (**Fig. 3**), which was consistent with CV localization using transient expression in *Arabidopsis* and rice (Wang and Blumwald 2014, Sade et al. 2018b).

The effect of tomato *SlCV* expression in *Arabidopsis thaliana*

To assess the possible role of *SlCV* in chloroplast degradation, *SlCV* was expressed under the control of a DEX-inducible promotor in *Arabidopsis*, and two independent transgenic mutants were generated. The mutants were grown and *SlCV* expression was induced with DEX as described in Materials and Methods. quantitative PCR (qPCR) of T_2 generation plants showed that *SlCV* expression increased only in DEX-treated plants (**Fig. 4A**). In these plants, growth was inhibited, chlorophyll levels decreased (**Fig. 4B**) and plant senescence was induced (**Fig. 4C**). This indicated an occurrence of a *CV*-enhanced stress-induced senescence that resulted in a decline of leaf source capacity. WT plants were unaffected by the DEX treatment.

Generation and molecular characterization of CRISPR/Cas9-CV mutants

We used the CRISPR/Cas9 methodology to generate functional knockouts of *SlCV* in IL9-2-5 tomato plants. IL9-2-5 is characterized by an apoplastic invertase with a relatively high affinity for sucrose and relatively high levels of soluble hexoses in the fruit, leading to increased fruit Brix of plants grown

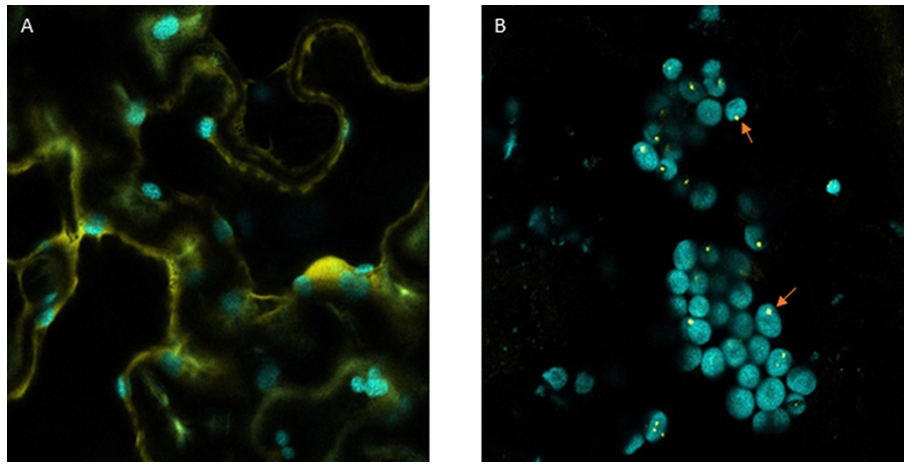

Fig. 3 Tomato CV (SlCV) protein subcellular localization in tobacco using transient agroinfiltration. (A) Free YFP (yellow signal), autofluorescence of chloroplasts (cyan signal). (B) CV-YFP. CV is co-localized with the cell chloroplast (arrows).

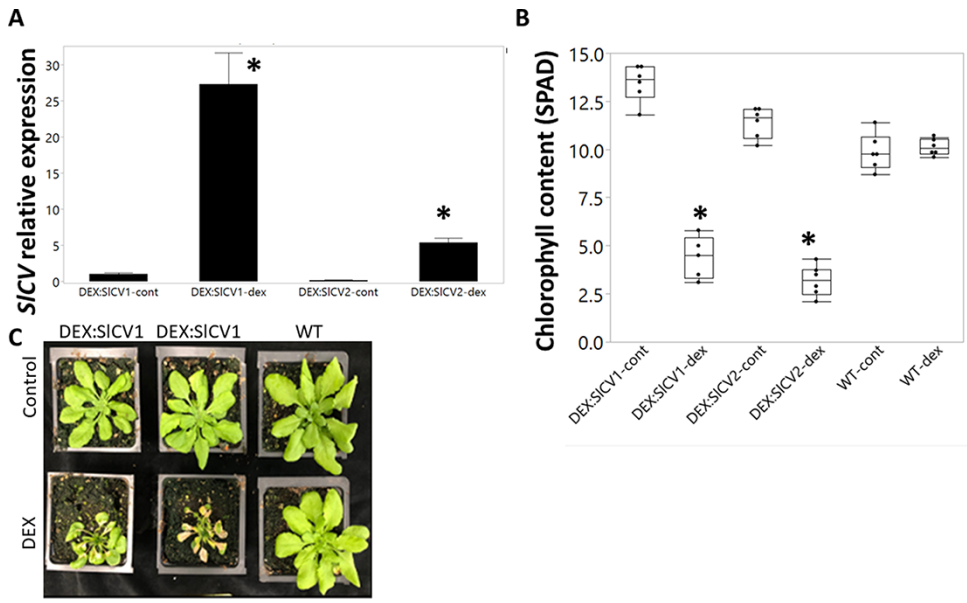

Fig. 4 The effect of tomato CV (SlCV) in *A. thaliana*. Inducing the expression of SlCV in *A. thaliana* inhibits growth and promotes senescence. (A) Phenotypic response in the plants. (B) Control group ('control') and the treatment group ('DEX') were sprayed daily with DEX (50 μM) to induce CV expression. Chlorophyll concentration was measured by SPAD reading. (C) Leaf samples were taken for measuring the relative expression of CV using qPCR. Error bars represent the mean ± SE. The boxes represent the interquartile range, the line represents the median and the black dots are all the measurements taken. Asterisk represents significant differences between genotypes within treatment ($P < 0.05$, *t*-test).

under well-watered conditions and a relatively high sink capacity (Fridman et al. 2002, 2004, Zanor et al. 2009). Because stress-induced senescence had a strong effect on C allocation (Rankenberg et al. 2021), we used a sink-enhanced line as the genetic background (**Supplementary Fig. S1**), based on the assumption that this property might contribute to mitigate the effects of stress and allow for the maintenance of a strong sink and, possibly, a more stable source under abiotic stress.

Screening and selection were performed in seeds of T_0 plants and involved a few steps aimed at the isolation of a Cas9-free homozygous mutant with the *CV* deletion. T_0 plants were characterized for the guide RNA (gRNA) region, and two mutants were found in the gRNA1 region in exon1 (**Supplementary Table S1**). T_1 plants were characterized for mutation homozygosity and scanned for the absence of the transgene cassette. Two homozygous Cas9-free mutants were found, and T_2 seeds were harvested from those mutants.

The two mutants were identified and used for the rest of this study, hereafter named CRISPR-1 and CRISPR-2 (**Fig. 6B**, **C**), both harboring a 2-bp and 4-bp deletion and resulting in a frameshift mutation and stop codon, respectively, as well as a

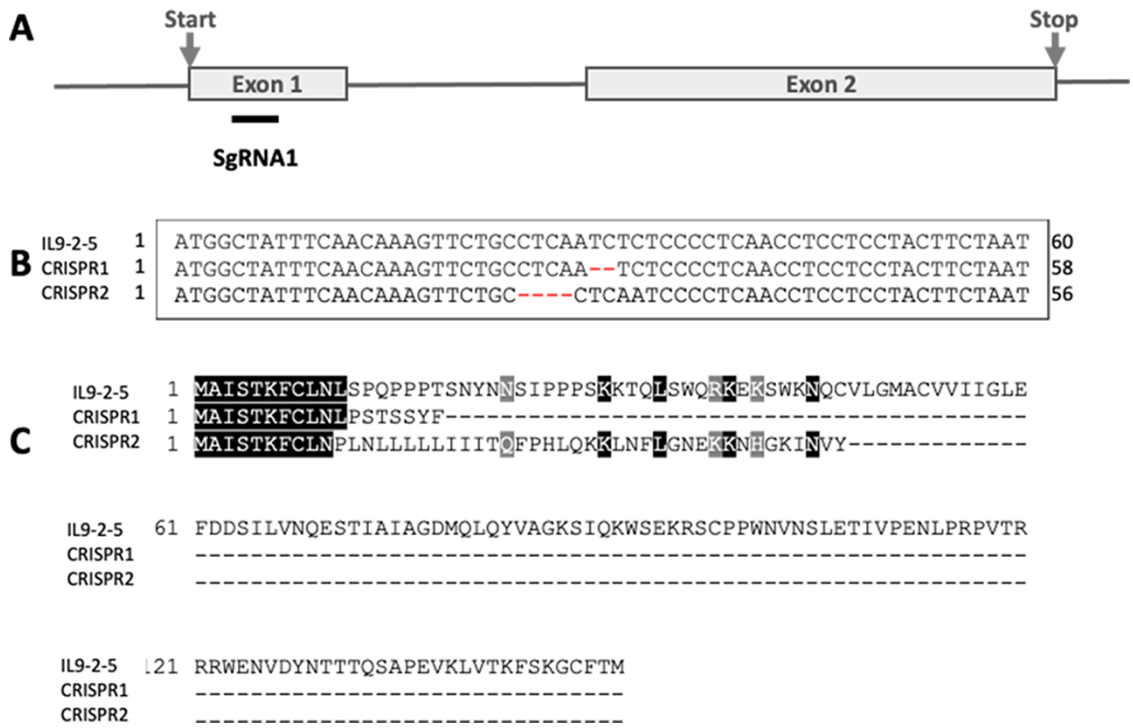

Fig. 5 The generation of CV tomato knockout lines using CRISPR/CAS9. (A) Schematic representation of the SlCV locus with exons indicated in gray. The sites targeted by sgRNA1 are indicated. (B) Nucleotide sequences of the cv mutants (CRISPR 1 and CRISPR2) and the parental sequence. The regions deleted are highlighted in dashed lines. (C) The predicted amino acid sequences of the mutant alleles. The mutations generated frameshifts that resulted in missense mutations and early stop codons.

non-functional CV protein. The low Cutting Frequency Determination off-target score, according to CRISPOR (Concordet and Haeussler 2018), suggested that the sgRNA1 did not target any gene other than *CV* (**Supplementary Fig. S2**). This computational prediction was validated using PCR and sequencing, further confirming that there were no off-target genes of the sgRNA1 (**Supplementary Fig. S2**).

Phenotypic characterization of responses to salinity and water-deficit stress at the vegetative stage in *cv*-knockout plants

The physiological effects of knocking-out *CV* were examined in tomato plants with an IL9-2-5 background at the vegetative stage. Two homozygous *cv*-knockout mutants' plants and non-transgenic plants were grown in 1-l pots in a semi-controlled greenhouse and were divided into three different treatment groups: a control group, a water-deficit stress-treated group and a salt-treated group. At ∼30 d after germination, the water-deficit stress-treated group was subjected to continuous water-deficit stress by limiting irrigation to maintain a steady, relatively low soil water content. At the same time, the salt-treated group was subjected to salinity stress by gradually increasing the salinity level in the irrigation solution, in 25 mM increments every other day over a period of 10 d, to a final concentration of 150 mM NaCl. All measurements were taken using fully expanded 4th–5th leaves.

For almost all the measured parameters, the *cv*-knockout plants were more resistant to the stress conditions. The rates of CO_2 fixation in the mutants (**Fig. 6A**) were similar to IL9-2-5 under well-watered conditions but were higher in the mutants under salinity and water-deficit stress. No differences were observed in the transpiration of the mutants under the different conditions (**Fig. 6B**), indicating that stress tolerance was not achieved through the impairment of evapotranspiration. The chlorophyll contents of the mutants, measured using a single-photon avalanche diode (SPAD), did not deviate significantly from those of IL9-2-5 plants under well-watered conditions. However, under water-deficit stress or salt stress, the chlorophyll contents of the mutants were significantly higher than those of IL9-2-5 (**Fig. 6C**). Photochemical quantum efficiency, as measured by measurement ratio of the maximum potential quantum efficiency of Photosystem II if all capable reaction centers were open (F_v/F_m), was higher in the mutants than in the IL9-2-5 line under water-deficit stress and salt stress (**Fig. 6D**). We examined whether knocking-out *CV* affected the whole-plant evapotranspiration rate, using a PlantDietch system, a multi-sensor physiological phenotyping gravimetric-based platform (Dalal et al. 2020). The results indicated that knocking-out *CV* did not alter the rate of transpiration under

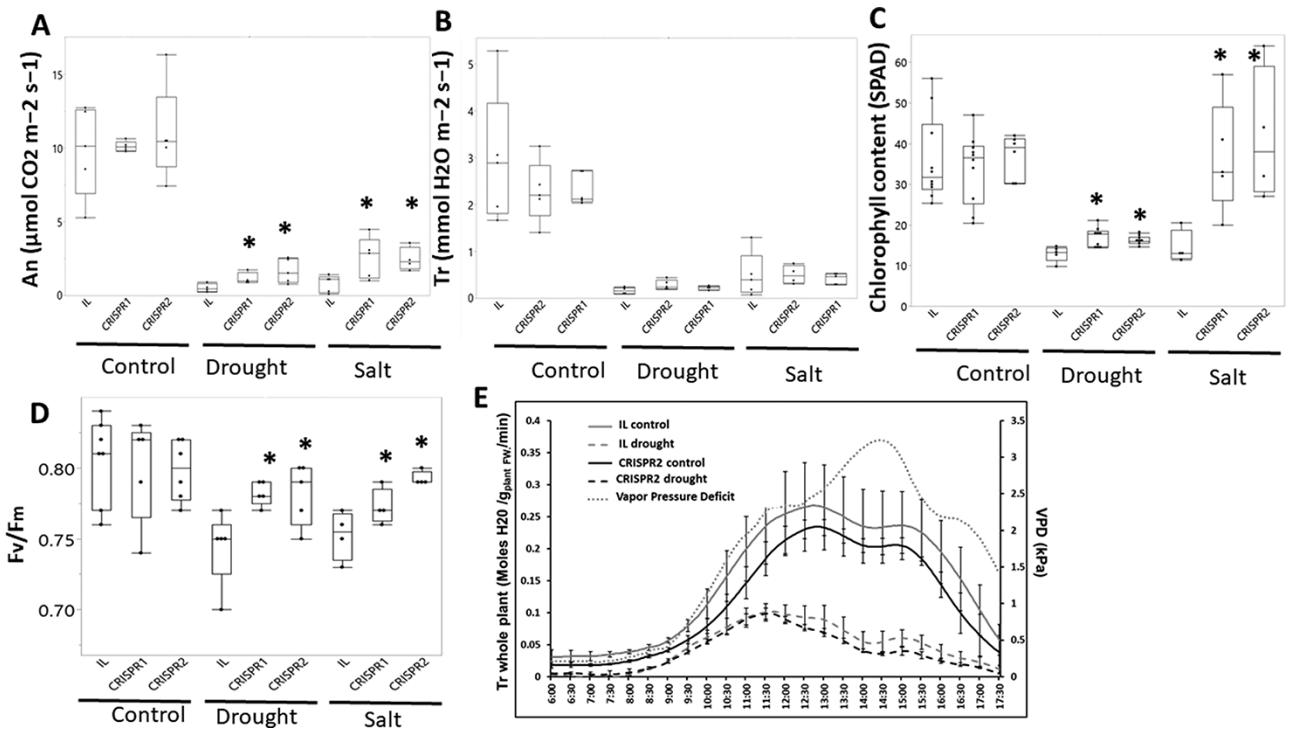

Fig. 6 Phenotypic characterization of salinity- and drought-stress responses in the vegetative stage of CRISPR lines. (A) Leaf rate of CO_2 fixation (An) and (B) leaf transpiration rate (Tr). (C) Chlorophyll concentration in leaves. (D) Maximum potential quantum efficiency of Photosystem II (F_v/F_m). (E) Whole plant daily transpiration rate at control and drought of IL and CRISPR2 genotypes (mean ± SE; $N = 3$). The boxes represent the interquartile range, the line represents the median and the black dots are all the measurements taken. Asterisk represent significant differences between genotypes and IL within a treatment ($P < 0.05$, Dunnet's test).

well-watered or water-deficit conditions (**Fig. 6E**). These results correlated well with the leaf transpiration rate measurements (**Fig. 6B**).

Yield response of *cv-crispr* plants to salinity and water-deficit stress

We assessed whether the enhancement of source capacity of the *cv*-knockout plants affected plant yield under stress conditions. Water-deficit stress was applied by limiting irrigation, maintaining a steady, relatively low soil water content; salinity stress was applied by irrigating with a 150-mM NaCl solution. Treatments were applied once plants had their first visible inflorescence and were kept constant until the end of the experiment (**Fig. 7A**). All genotypes were affected by the given stress conditions, leading to a strong decrease in production as compared to the control treatment. Whereas under the control treatment, fruit yield of *cv*-knockout plants was similar to that of IL9-2-5, *cv*-knockout tomato plants produced higher total yields under salt and water-deficit stress. In the abiotic-stress treatments, average fruit Brix was higher among fruit harvested from *cv*-knockout mutants (**Fig. 7B**). In order to assess plant productivity in relation to the total soluble sugars allocated to the fruit, we measured Brix for each plant separately. While total Brix did not differ significantly between the *cv*-knockout and IL9-2-5 in the control treatment, under salt and drought stress, Brix levels were significantly higher in the *cv*-knockout mutants than in IL9-2-5 (**Fig. 7C**).

The harvest index (HI, i.e. a measure of reproductive efficiency) was significantly higher in *cv*-knockout mutants than in IL9-2-5 under salinity and water-deficit stress (**Fig. 7D**). Finally, while all plants in the control group looked healthy, when subjected to drought and salinity stress, the CRISPR mutants were greener and senescence was less pronounced (**Fig. 7E**).

Resource allocation under salt and water-deficit stress conditions at the vegetative growth stage of *cv-crispr* plants

At the early stages of plant development, the roots act as the main sink (Aguirrezabal et al. 1994), so that they can later support the plant's need for water and nutrients. We assessed resource allocations in *cv*-knockout plants grown under water-deficit stress and salt stress. The higher photosynthesis and N-use efficiency (NUE) in *cv*-knockout plants were confirmed by the higher CO_2 assimilation capacity and better N assimilation and utilization in the *cv*-knockout plants (**Fig. 8A**, **B**). The allocation of N to the root was measured to determine whether the lack of CV was associated with enhanced N allocation to the plant sink organs of the plant. Under water-deficit stress, but not salt stress, the N allocation to the sink was significantly higher among *cv*-knockout plants, as compared to

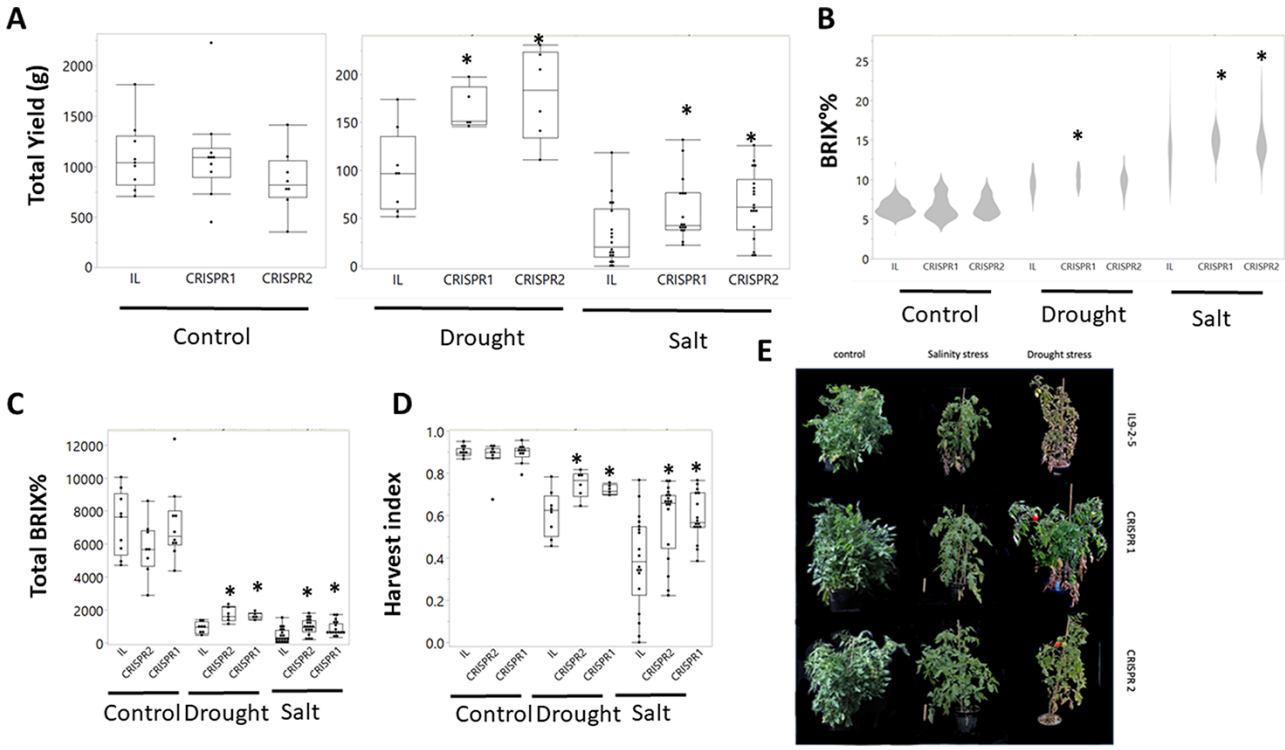

Fig. 7 The effect of knocking-out CV on yield under salinity and drought stresses. (A) Total fruit weight (yield) harvested from each plant. (B) Average Brix% of fruit from each line measured at full fruit maturity (red). (C) Total Brix%, multiply the average Brix% of each individual plant by its total fruit mass. (D) HI. (E) Represented pictures of plants at harvest. The boxes represent the interquartile range, the line represents the median and the black dots are all the measurements taken. Asterisk represents significant differences between genotypes and IL within treatment ($P < 0.05$, Dunnet's test).

the IL9-2-5 control line (**Fig. 8C**). In both salt stress and water-deficit stress, the biomass allocation (measured as the ratio of root dry weight to whole-plant dry weight) was enhanced in *cv*-knockout plants (**Fig. 8D**). These results indicated an enhanced source capacity of CRISPR mutants under stress (**Fig. 8A**, **B**, and shown as HI in **Fig. 7**) and provide evidence for an enhanced sink capacity (**Fig. 8C**, **D**, and shown as Brix in **Fig. 7**). No apparent effect was observed under well-watered growth conditions, as CO_2 assimilation capacity and biomass allocation did not differ between the genotypes (**Supplementary Fig. S3**).

Correlation network analysis combined with machine learning predicted that L-glutamine and L-arginine biosynthesis metabolic pathways are important for sinks (tomato fruits) under stress-induced senescence conditions

In an effort to assess unique metabolic pathways associated with the source–sink stress-induced senescence response in tomato, metabolite profiles were generated using a gas chromatography–mass spectrometry (GC-MS) platform for sink tissues (fruit) under all tested conditions (**Supplementary Table SIII**), and a correlation-based network was constructed from the dataset to further elucidate the relationships between the different metabolites and stress-induced metabolic pathways (Toubiana et al. 2013, **Fig. 9A**).

We used correlation-based network analysis combined with machine learning techniques to identify unique metabolic pathways associated with stress conditions in tomato fruits (Toubiana et al. 2019). Correlation-based networks were constructed for control, water-deficit stress-treated and salinity-treated plants. Nodes and edges in the networks represented compounds and significant correlation coefficients, respectively. The control network was composed of 71 nodes and 1,082 edges [including 820 positive and 262 negative edges; the positive edges/negative edges ratio (p_e/n_e) = 3.13]. The drought (water-deficit stress) network was composed of 71 nodes and 714 edges (605 positive and 109 negative edges; $p_e/n_e = 5.55$), and the salinity network was composed of 71 nodes and 543 edges (497 positive and 46 negative edges; $p_e/n_e = 10.8$).

For each correlation-based network, a machine learning model was generated, employing the extreme gradient boost algorithm (Friedman 2001). Performance evaluation of the machine learning models showed area under the curve (AUC) values of the receiving operating characteristic curve of 0.932 for the control correlation-based network model, 0.967 for the water-deficit stress correlation-based network model and 0.943 for the salinity-stress correlation-based network model.

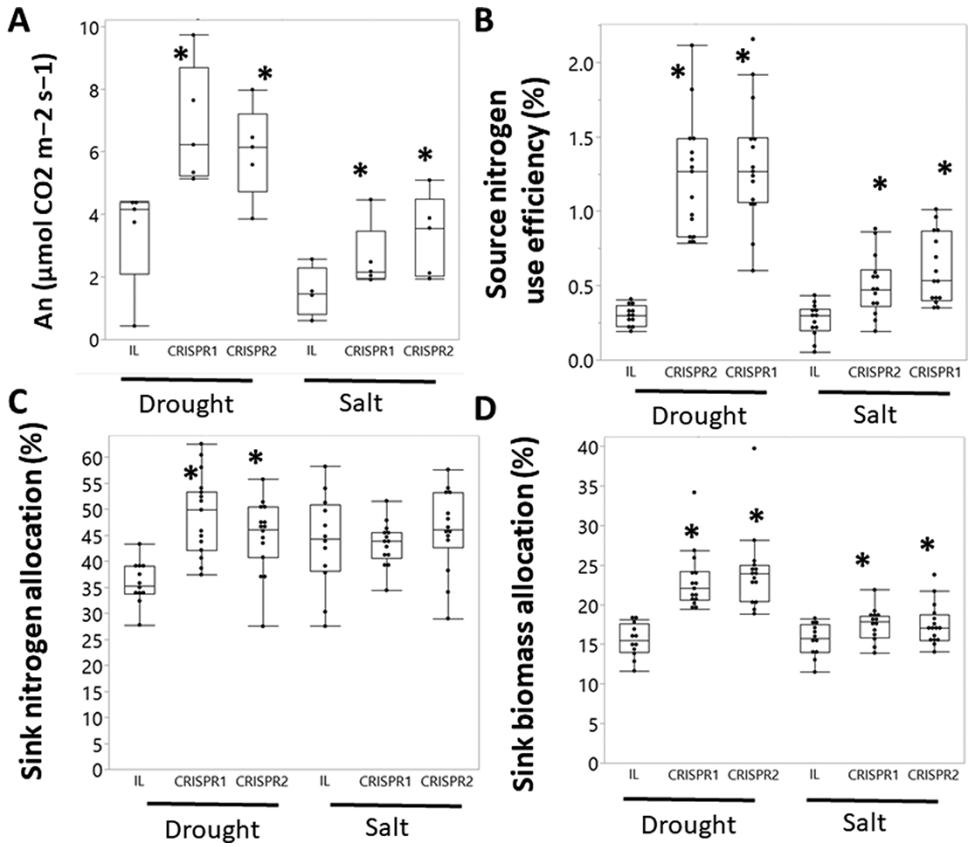

Fig. 8 Resource allocation under salinity- and drought-stress conditions at the vegetative stage in CRISPR lines. (A) Source (leaves) rate of CO_2 fixation. (B) Source (leaves) NUE . (C, D) Sink (root) N and biomass allocation. The boxes represent the interquartile range, the line represents the median and the black dots are all the measurements taken. Asterisk represents significant differences between genotypes and IL within treatment ($P < 0.05$, Dunnet's test).

The confusion matrices of the models demonstrated accuracy rates of 0.882, 0.895 and 0.882 for the control, water-deficit and salinity treatments, respectively (**Fig. 9B**). The cross-validated models were then used to predict the activity of four different stress-specific metabolic pathways (**Fig. 9C**, **Supplementary Table SIVb**) gathered from the PlantCyc repository (Schlapfer et al. 2017) at a prediction threshold value of >0.5. Sensitivity analysis was applied to validate the prediction values of the metabolic pathways. The analysis suggested the specific activity of several metabolic pathways under stress (**Fig. 9C**).

Weighted gene co-expression network analysis highlighted fruit genes associated with enhanced sink capacity and fruit quality under stress-induced senescence conditions

To identify genes associated with our predicted metabolic pathways, we generated transcriptomic data for all samples under stress (**Supplementary Table SV**). To associate the metabolic and gene expression data and to integrate the data with the unique metabolic pathway analysis, we applied a weighted gene co-expression network analysis (WGCNA) together with a genetic algorithm for optimization of the WGCNA (Toubiana et al. 2020). Specifically, we tackled two metabolic pathways (L-arginine biosynthesis and L-glutamine biosynthesis) that were predicted in stress-treated (both stresses) plants, but not in control-treated plants. Next, we took the metabolomic data of the metabolites associated with the respective pathways and took the PC1 (using PCA) as the correlational representation of the respective pathway. We then performed WGCNA using the PC1 data as the response variable to detect the highly correlated gene modules. Next, from those genes, we took only those which were differentially expressed (DE) between the IL and CRISPR mutants.

The L-arginine biosynthesis-enriched pathway under stress (**Fig. 9**) was further explored with regard to WGCNA. The turquoise module containing 2,054 genes was chosen for in-depth analysis (**Supplementary Fig. S4**, **Supplementary Table SVII**). Eight genes whose expression was significantly correlated ($R^2 = 0.54$, $P = 3.00E-05$) with the L-arginine biosynthesis-enriched pathway were DE in the CRISPR and IL mutants, with one gene upregulated and seven downregulated in the CRISPR mutants (**Fig. 10A**, **Supplementary Table SVI**). Interestingly, seven genes were enriched in mature fruit versus leaves in M82, according to available databases (eFP browser; http://bar.

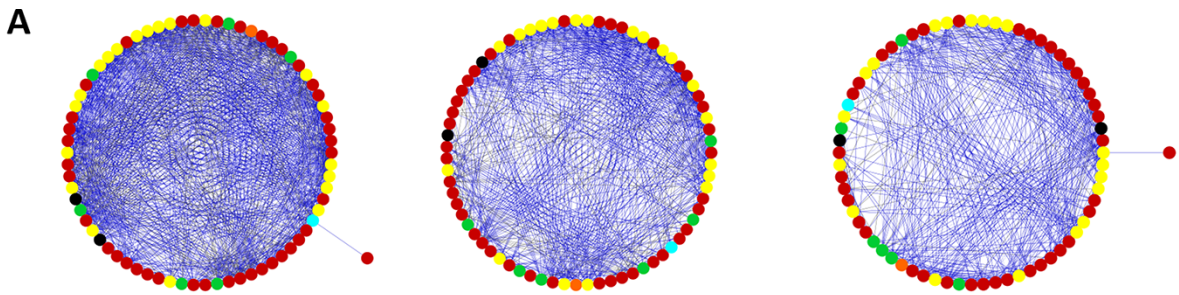

B

CON

	POS	NEG
POS	33	4
NEG	5	34

DRO

	POS	NEG
POS	36	6
NEG	2	32

SAL

	POS	NEG
POS	36	7
NEG	2	31

C

PRED				SENS			METABOLITES
	CON	DRO	SAL	CON	DRO	SAL	
L-GLUTAMINE BIOSYNTHESIS III	0.23	0.75	0.78	0.28	0.78	0.59	citric acid, aconitic acid, glutamic acid, pyruvic acid, adenosine-5-monophosphate, glutamine, alpha-ketoglutarate
L-ARGININE BIOSYNTHESIS II (ACETYL CYCLE)	0.23	0.82	0.89	0.19	0.79	0.89	glutamic acid, N-acetylornithine, citrulline, ornithine, aspartic acid, fumaric acid, glutamine, arginine, alpha-ketoglutarate, adenosine-5-monophosphate
PROANTHOCYANIDINS BIOSYNTHESIS FROM FLAVANOLS	0.09	0.68	0.78	0.10	0.61	0.69	glucose, alpha-ketoglutarate, succinic acid
REDUCTIVE TCA CYCLE I	0.34	0.75	0.93	0.31	0.72	0.92	aconitic acid, citric acid, malic acid, fumaric acid, succinic acid, pyruvic acid, adenosine-5-monophosphate, alpha-ketoglutarate

Fig. 9 Correlation-based networks of fruits in the different treatments. In order to conduct statistically robust network analyses, it is advantageous using many heterogeneous samples so as to increase the noise in data, which sifts out relatively less significant results. Therefore, all the control-, drought- and salinity-treated plants (IL, CRISPR1 and CRISPR2 together) were consolidated into the three treatment groups, respectively (e.g. control group consisted of control-treated IL, CRISPR1 and CRISPR2 plants). For each treatment, correlation network analysis was performed, by constructing a network containing all threshold passing correlations between metabolites. Pearson's correlation coefficients (r) of $r \geq 0.36$, 0.4 and 0.53 (for the control, drought and salinity networks, respectively) and q-values of $q \leq 0.05$ were applied as the thresholds to detect significant correlations, while spurious correlations were removed. (A) Cytoscape network visualization of the metabolic networks. Metabolites are displayed as elliptical nodes and color-coded according to the compound classification. Positive and negative correlations are given (CON, control; DRO, drought; SAL, salinity). (B) Confusion matrices of fruits machine learning models (ML) in the different conditions (CON, control; DRO, drought; SAL, salinity). POS, positive instances (i.e. predicted) and NEG, negative instances (i.e. not predicted). The higher the congruity between predicted and actual classification (i.e. the percentage of actual positive and negative incidences that were, respectively, predicted by the machine learning model as such), the better the machine learning model. (C) Significant stress-specific metabolic pathway prediction tables for fruits. The network analysis was done according to Toubiana et al. (2019), and the prediction values and sensitivity values, along with a list of the associated metabolites for each pathway, are presented. Prediction values represent the probability ($0 \leq P \leq 1$) of the metabolic pathway occurring in plants of the respective network. Sensitivity values represent the percentage of positive predictions using different machine learning models, which are based off of 100 random subsampling (80%) of pathways [e.g. 70 out of 100 models using random subsampling of pathways gave a positive prediction value (>0.5); this results in a sensitivity value of 0.7]. Tables in (B, C) were prepared via the 'gt' and 'gtExtras' R packages.

utoronto.ca/efp_tomato/cgi-bin/efpWeb.cgi). Among these, Solyc01g107870.3 (polyadenylate RNA-binding protein 8), Solyc05g010140.3 [proline-rich, extensin-like receptor-like kinases 9/10 (PERKs)] and Solyc07g008840.3 [Rab Small GTPase family protein (SlRabGAP2a)] were downregulated, whereas Solyc10g012070.4 (BYPASS1) was upregulated in the CRISPR mutants.

A further WGCNA of the L-glutamine biosynthesis-enriched pathway under stress marked the red module with 838 genes as a candidate for in-depth analysis (**Supplementary Fig. S4**, **Supplementary Table SVII**). Six genes were significantly correlated with the L-glutamine biosynthesis-enriched pathway ($R^2 = 0.62$, $P = 1.00E\text{-}06$) and were DE in the CRISPR mutants (**Fig. 10B**, **Supplementary Table SVI**); two genes were upregulated and four were downregulated in the CRISPR mutants. Interestingly, three genes were enriched in mature fruit versus leaves in the M82 line, according to the databases (eFP browser; http://bar.utoronto.ca/efp_tomato/cgi-bin/efpWeb.cgi). Among the six, Solyc06g063070.3 [jasmonate and ethylene response factor 1 (JERF)], Solyc12g005860.2 (aconitate hydratase 3) and Solyc01g108020.3 (thioredoxin M-type 3) were downregulated, whereas Solyc03g117180.3 (a putative chloroplast receptor-like protein kinase) was upregulated in the CRISPR mutants.

Discussion

We characterized the effects of altered *CV* expression in tomato in order to investigate the effects of inducible senescence at the reproductive stage on tomato source–sink relations. The induction of *CV* led to a significant decrease in potential yield; fruit weight was lower, Brix levels were unchanged and SAG12

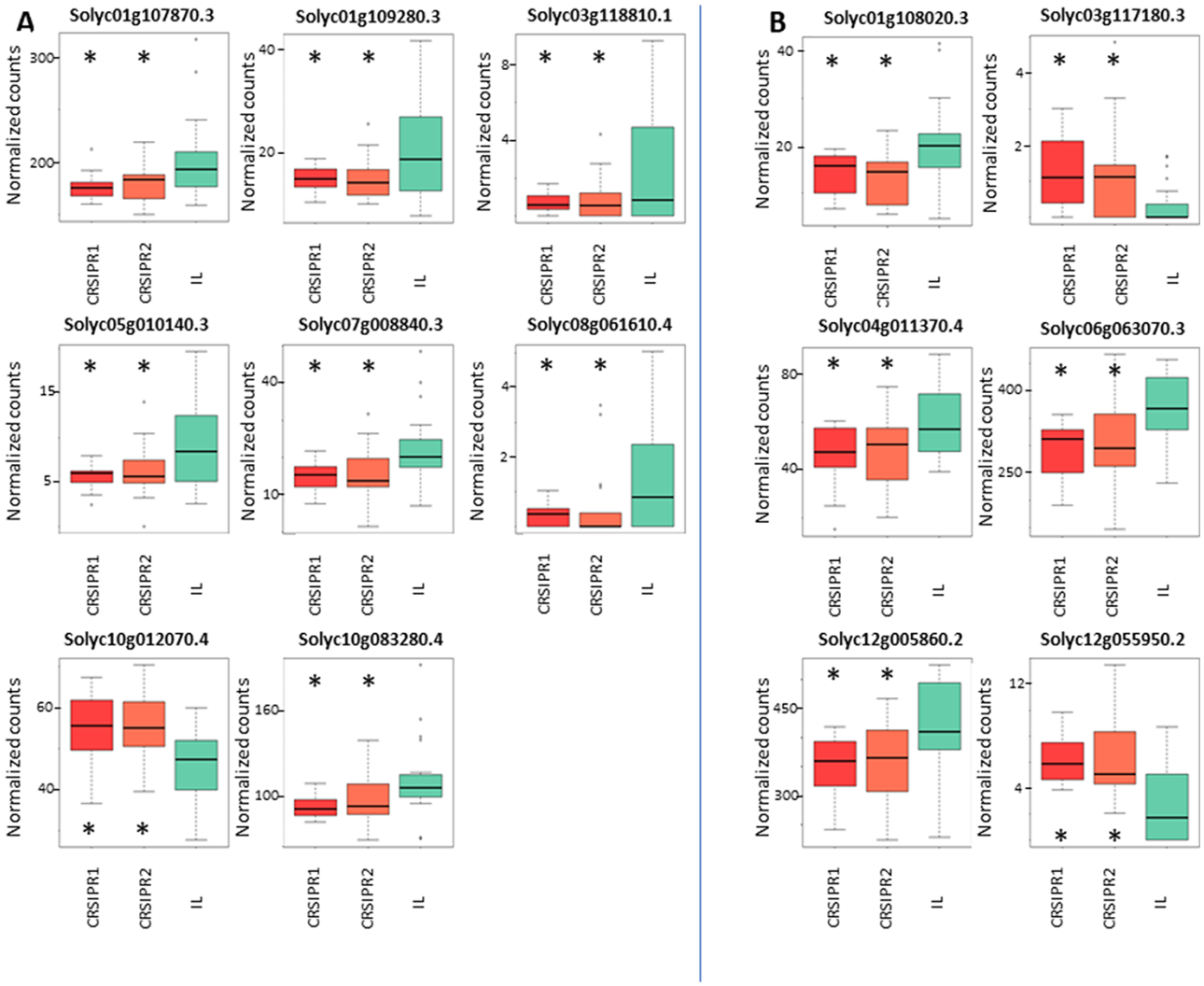

Fig. 10 Genes associated with enhanced sink capacity in CRISPR lines. (A) Boxplot illustration and description of significantly associated genes of module turquoise (**Supplementary Fig. S4**) in the L-arginine biosynthesis metabolic pathway and (B) boxplot illustration and description of significantly associated genes of module red (**Supplementary Fig. S4**) with the L-glutamine biosynthesis metabolic pathway. Values are the mean ± SD ($N > 15$; $P \leq 0.05$ according to Dunnet's test).

levels (a known senescence marker) were significantly higher (**Fig. 1**). Thus, the induction of stress-like senescence at the fruit developmental stage in tomato (at high sink capacity) did not contribute to a better sink capacity or to an improved assimilate transport but resulted in reduced productivity, probably due to the strong decrease in source capacity. These results contrasted with those previously reported in cereals (Distelfeld et al. 2014).

Our results led us to conclude that the knockout of *SlCV* in tomato might be a viable approach for enhancing tomato yield and yield quality under stress conditions. The expression patterns (**Fig. 2**), subcellular localization (**Fig. 3**) and ectopic expression (**Fig. 4**) of tomato *CV* were all consistent with this notion, as well as a recent publication showing that this approach is viable for dark-induced senescence as well (Yu et al. 2022). Interestingly, our results do not support a strong involvement of SlCV in non-stress-induced senescence, as was also shown most recently in tomato (Yu et al. 2022), rice (Sade et al. 2018b) and Arabdiopsis (Wang and Blumwald 2014); this could be either due to pathway redundancy or relatively low induction. In contrast, recent studies on tomato have shown the involvement of different Transcription Factors (TFs) (e.g. napthylphthalamic acid and ORE) in developmental senescence and that the downregulation of those TFs resulted in increased yield, fruit Brix and HI (Lira et al. 2017, Ma et al. 2018). As compared to previous studies, which used the downregulation of *CV* expression (Wang and Blumwald 2014, Sade et al. 2018b), we generated tomato *cv*-knockout plants using the CRISPR/Cas9 approach (**Fig. 5**). Our results demonstrate that its use could benefit existing breeding programs for the development of stress-resistant tomato plants.

Does chloroplast degradation contribute to tomato yield traits under stress conditions?

The timing of leaf senescence is a major determinant of crop yield and quality. If senescence occurs too early, the plant's overall capacity for assimilating CO_2 could be reduced (Wingler et al. 2006, Sade et al. 2018a). On the other hand, if senescence is inhibited, senescence-induced nutrient recycling, important for the development of reproductive tissues (Himelblau and Amasino 2001), is inhibited. Thus, plasticity in leaf senescence timing would be crucial for maximal yield production.

We found that under water-deficit or salt stress, delaying senescence is a better strategy for tomato, as *cv*-knockout plants displayed better photosynthetic capacity, resulting in improved source capacity (**Figs. 6–7**), which supported the plant productive stage. These results are in agreement with previous observations in tomato plants, all showing that delayed senescence is a viable strategy for enhanced yield and even sugar remobilization in tomato (Lira et al. 2017, Ma et al. 2018, 2019). Furthermore, very recently it was demonstrated that the knockout of CV in tomato leads to maintained source capacity and photosynthesis and to delayed chloroplast degradation under dark-induced senescence (Yu et al. 2022), further corroborating the involvement of tomato CV in stress-induced senescence. Why does the enhanced activity of SlCV (and other TFs, e.g. SlNAP2; Ma et al. 2018) not lead to better fruit sugar content and remobilization? We can only speculate that in tomato, at the fruit development and ripening stage (the stage we tested in our experimental design), the plants were source-limited (Li et al. 2015), and therefore activation of stress-induced senescence and decreasing source activity did not result in an advantageous phenotype. Additionally, a recent study that tested source-to-sink remobilization under stress showed that under stress, the main tomato sugar exporter *Solanum lycopersicum* SUCROSE TRANSPORTER1 (SlSUT1) (Osorio et al. 2014) was not upregulated and remobilization decreased (using C13 assays), which can support the hypothesis that, in tomato, delayed stress-induced senescence, and not senescence activation, is beneficial for fruits (Xu et al. 2018).

Under stress, *cv*-knockout plants displayed greater yield, with higher soluble sugar content per fruit and per plant. Regarding N assimilation and utilization, based on their behavior in rice (Sade et al. 2018b), it might be expected that assimilation in leaves would be beneficial in *cv*-knockout plants. However, N assimilation and utilization in leaves were not quantified at this stage, and we focused on photosynthesis, sugar and yield as parameters for quantification of source and sink efficiency, as was recently shown for other tomato plants with altered senescence (Lira et al. 2017, Ma et al. 2018). HI, representing the plant resource allocation capacity and source–sink relations, was also higher among *cv*-knockout plants (**Fig. 7**). Although *cv*-knockout plants performed relatively better, as compared to WT plants, all genotypes were strongly affected by the severe stress given. Future research examining their performance under mild stress and under field conditions will add knowledge regarding the full potential of this strategy for breeding purposes.

Source–sink relations: resource allocation in tomato under abiotic stress

Under stress, tomato plants alter their leaf-to-root relationships. Moles et al. (2018) found that water deficit triggered cross-talk between plant organs and that source–sink relationships differed among tomato cultivars. Our results indicated that under abiotic stress, IL9-2-5 tomato plants have lower NUE in their leaves than *cv*-knockout tomato plants (**Fig. 8**). Source's NUE and sink's N allocation are good indicators of the plant's resource capabilities, particularly under conditions of abiotic stress (Ploschuk et al. 2005). Without a functional CV, the plant sources produced more source mass per unit of N, which further strengthens our conclusion regarding tomato *CV* and source capacity under stress conditions (**Fig. 6**). As for the sinks, root biomass and N allocation were significantly higher among *cv*-knockout mutants than IL9-2-5 under stress (**Fig. 8**).

Higher sink-to-source biomass ratios in plants that maintain a strong source contribute to the development of bigger sink organs, which rely on the supply of sucrose. In contrast, the higher ratio of sink-to-source N content within plants that maintain a stronger source is somewhat counterintuitive. Leaf senescence, during which chloroplasts disassemble, is an essential process for recycling N from leaves to the sink organs of the plant and is an important factor for grain quality in cereals (Distelfeld et al. 2014). However, our results support the notion that, in tomato, preventing or delaying source leaves from undergoing stress senescence seems useful (Lira et al. 2017, Ma et al. 2018, 2019), whereas inducing *CV* expression at the reproductive stage has no beneficial effect on quality (**Fig. 1**). Our results are also in agreement with the recent observation that *CV*-downregulated rice plants exhibited enhanced sink capacity and seed quality (Umnajkitikorn et al. 2020).

Metabolic pathways and genes associated with sink capacity under stress

We used WGCNA combined with machine learning techniques to identify unique and specific metabolic pathways associated with stress conditions in tomato fruits (Toubiana et al. 2019). This approach takes advantage of the fact that metabolic pathways shape the topology of a correlation network. By mapping known metabolic pathways into the correlation-based network and learning their topological conformation, it is possible to generate a machine learning model to predict the activity of metabolic pathways (Toubiana et al. 2019). We identified L-glutamine and L-arginine biosynthesis as associated with the response of ripe tomato fruits to stress (**Fig. 9**). Interestingly, both biochemical pathways have been associated with senescence processes in leaves (Couturier et al. 2010, Liebsch et al. 2022). L-Arginine is a precursor of nitric oxide and of polyamines via the ornithine-biosynthesis pathway and has been shown to be involved in the alleviation of oxidative damage in tomato leaves under stress via a non-nitric-oxide-dependent pathway (Nasibi et al. 2011). Polyamines have also been shown to enhance tomato fruit metabolic content (Mehta et al. 2002).

The transcriptomics data (via WGCNA) showed a number of genes putatively associated with L-arginine-associated fruit response to stress conditions (**Fig. 10A**). Among these, an RNA-binding protein polyadenylate-binding protein 8 (PAB8 Solyc01g107870.3) plays a role in protein stability (Rissland 2017). Interestingly, *Arabidopsis pab8* mutants exhibited altered vegetative and reproductive growth (and particularly in the transition between the two; Gallie 2017). Next, a cell-wall regulator extensin-like receptor-like kinases 9/10 (PERK, Solyc05g010140.3), which was downregulated in the CRISPR mutants, is among a family of extensins in tomato, which are strongly relevant to fruit ripening (Ding et al. 2020). These have been suggested to be related to water stress response in *Arabidopsis* (Yoshiba et al. 2001) and have been shown to be negative regulators of the growth and pigmentation of *Arabidopsis* seedlings (Humphrey et al. 2015). Furthermore, a Rab Small GTPase family protein (SlRabGAP2a, Solyc07g008840.3), regulating cellular trafficking, was downregulated in the CRISPR mutants. Rab Small GTPases have been shown to function as molecular switches in the presence of abiotic stress, specifically salt stress (Madrid-Espinoza et al. 2019), and tomato SlRab11 has been shown to control fruit development through cell-wall modification (Lunn et al. 2013, Tripathy et al. 2021). Most recently, *Arabidopsis* Ran-GTP, a member of the Small GTPases family, has been shown to promote leaf senescence (Pham et al. 2022). Also, an ortholog to BYPASS1 (Solyc10g012070.4), an understudied gene that plays an important role in the regulation of *Arabidopsis* growth (via an inhibitor of a carotenoid-derived signaling compound; Van Norman and Sieburth 2007, Arthikala et al. 2018), and whose functionality was affected by cold stress (Zhang et al. 2020), was upregulated in our CRISPR fruits.

Our results also indicated the involvement of L-glutamine biosynthesis under stress conditions (**Fig. 10**). Interestingly, this pathway lies at the junction of C and N metabolism via the TCA cycle and GLUTAMINE SYNTHETASE/GLUTAMINE OXOGLUTARATE AMINOTRANSFERASE (GS/GOGAT) cycles and has been shown to be involved in the plant stress response (Reguera et al. 2013, Tahjib-Ul-Arif et al. 2021) and to be associated with *CV* (Sade et al. 2018b, Umnajkitikorn et al. 2020). The C–N balance and partitioning in the plant and their relationships with fruit nutritional values and yield under stress are not fully understood. Using transcriptomic data, together with our machine learning approach, we were able to compile a short list of putative genes that might be related to L-glutamine–associated fruit sink capacity under stress conditions (**Fig. 10B**) and that were significantly DE between the IL and CRISPR1-CRISPR2 mutants.

Among these genes were the *JERF1* (Solyc06g063070.3). The ethylene response factor (*ERF*) genes are a large family of transcription factors with important functions in the transcriptional regulation of a variety of biological processes associated with growth and development, as well as responses to various types of abiotic and biotic stress (Lorenzo et al. 2003, Licausi et al. 2013). *ERF*s also play a significant role in the regulation of fruit ripening and metabolism (Severo et al. 2015, Quinet et al. 2019). Second, an Aconitate hydratase (Solyc12g005860.2) was downregulated in the CRISPR mutants' fruits. Aconitate hydratases are enzymes that catalyze the isomerization of citrate to isocitrate via cis-aconitate, involved in tomato fruit sugar content and yield (Carrari et al. 2003) and associated with senescence in wheat (Gregersen and Holm 2007). Aconitate hydratases also play a role in regulating resistance to oxidative stress and cell death in *Arabidopsis* and *Nicotiana benthamiana* (Moeder et al. 2007). Next, thioredoxin M-type 3 (orthologous to AtGAT1; Solyc01g108020.3), a chloroplast protein similar to prokaryotic thioredoxin, was also altered in the CRISPR plants. GAT1 has been shown to mediate C–N interactions via glutamate-derived γ-aminobutyric acid metabolism in *Arabidopsis* (Batushansky et al. 2015), a metabolite that is important in stress response (Bouché and Fromm 2004). Furthermore, GAT1 has also been shown to be involved in the redox regulation of callose deposition and symplastic permeability in *Arabidopsis* (Benitez-Alfonso et al. 2009). Interestingly, arginine and glutamine synthesis pathways are interconnected via many metabolic intermediates and possible genes (https://www.genome.jp/kegg-bin/show_pathway?map00220). Indeed, most of the gene modules in our dataset are shared by both pathways (e.g. turquoise and red; **Supplementary Table SVII**, **Supplementary Fig. S4**), indicating shared candidate genes.

Even though the majority of these genes might not be discernibly related to L-arginine and L-glutamine biosynthesis per se (as hypothetically the tomato L-arginine synthetase and an L-glutamine synthetase would be), the advantage of the analysis used in this research allows us to circumvent addressing the more apparent and basic metabolic and transcriptomic data (e.g. comparing L-arginine levels and L-arginine synthetase expression levels between mutants) and rely on already known databases and correlational methods to uncover genes that are otherwise unknown to be related to the addressed pathways, or alternatively too far away biochemically to be noticeably related (and as in many cases, the direct metabolic and transcriptomic factors do not correlate significantly with the questioned phenomenon, e.g. the difference between the IL and CRISPR mutants). Therefore, we have not directly tested the discussed pathways, regarding the difference between the IL and CRISPR mutants and regarding stress response and source–sink relations via senescence, and mainly used their associated metabolomic data to find highly correlated expressed genes, while also assuming their specific importance under drought and salinity stress due to the correlation network analysis. Collectively, these genes may function as regulators of sink capacity under stress, and their importance via the biosynthesis of L-arginine and L-glutamine in fruits under stress conditions merits further investigation.

Conclusion and future perspectives

The use of delayed stress-induced senescence as a stress-tolerance trait and biotechnological approach for enhancing

crop photosynthesis has been suggested (Rivero et al. 2007, Sade et al. 2018a). Our results indicate that the lack of a functional CV contributes to the maintenance of source capacity in tomato under stress-induced senescence. The alteration of gene expression in the mature fruits of *cv*-knockout plants suggests a specific, yet undetermined, role for *CV* in fleshy fruits (and possibly other non-photosynthetic tissues as CV is upregulated under stress in root tissue; **Supplementary Fig. S5**) and merits further research. The abundancy of available cultivated tomato mutants offers an invaluable opportunity to identify naturally occurring variants of *CV* (and other delayed stress-induced senescence-associated genes) that might result in different abiotic stress-resistant mutants.

Data mining analysis and phylogenetic representation of the tomato *CV* throughout the *Solanum* genus revealed no apparent variability among commercial varieties, while some variability was seen among wild tomato species (although without any apparent variability in the conserved domain of *CV*; **Supplementary Fig. S6**). This observation raises the possibility of using wild tomato alleles as genetic material for integrating delayed senescence stress-tolerance traits into commercial crop mutants in breeding programs.

Materials and Methods

Plant material

Mutants examined. *Solanum lycopersicum* cv. M82 and IL9-2-5 (Fridman et al. 2002) were used in this research as control mutants and as the genetic background for transgenic mutants. Transgenic mutants of *S. lycopersicum*, specifically transgenic CRISPR-made BRIX9-2-5 mutants (referred to as CRISPR-1 and CRISPR-2 throughout this work) and transgenic tomato plants DEX:CV (DEX:AtCV-1 and DEX:AtCV-2), were characterized using PCR and were used throughout this research as well (NPTII for CRISPR plants and BiAlaphos Resistance gene for DEX:CV plants; primers are listed in **Supplementary Table S1**). Two independent T_2 homozygous mutants were used in all experiments.

Arabidopsis thaliana WT (ecotype Columbia-0) was used as a control line and for the generation of two separate DEX::SlCV mutants (DEX:SlCV-1 and DEX:SlCV-2) using the floral-dip method (Clough and Bent 1998). Transgenic plants were selected with glufosinate.

Growth conditions

A tomato experiment was conducted in a semi-controlled greenhouse in which the air temperature was kept at 20–26°C. The plants were exposed to sunlight, with no artificial light used. Tomato seeds were sown in nursery trays. Once seedlings had developed one to two true leaves, they were transplanted into 3-l pots. Irrigation was applied using a drip-irrigation system that included Galcon 6104-DC4 irrigation controllers, set to provide well-watered (i.e. control) and limited-irrigation (i.e. drought) conditions. Saline irrigation was applied every other day by hand. Fertilizer was applied using a proportional injector TEFEN MixRit 2.5 Manual, pumping a 4-2-8 liquid fertilizer (or by Deshen Gat, Kiryat Gat, Israel Inc.) at a quantity of 2 ml l^{-1}.

Arabidopsis thaliana plants were grown in a controlled growth room kept at 23°C with a light regime of 8/16 h day/night at 100 μmol photons m^{-2} s^{-1}.

Treatments

Salinity stress was applied as saline irrigation. To prevent osmotic shock, salinity was gradually increased for a period of 5 d, from 50 to 75 mM, and then 100 mM, then 125 mM and finally, 150 mM NaCl, which was the concentration used for the rest of the experiment. Standard table salt was used.

Drought stress was applied by deficit irrigation to the soil. Soil-moisture probe measurements (EC-5; Decagon, METER Group, Pullman, WA, USA) were taken to verify soil parameters. For vegetative-stress experiments, drought stress was applied by restricting irrigation (soil volumetric water content: 10.7 ± 0.9%) in comparison to the control group (soil volumetric water content: 78.3 ± 1.3%). For yield experiments, drought stress was applied by restricting irrigation (control volumetric soil content: 53 ± 0.7%; drought-stress volumetric soil content: 14 ± 0.7%) until harvest. Fruits were harvested when completely ripe. For the vegetative experiments, stress treatments were applied to tomato plants that had five or six fully developed true leaves. For the yield experiments, stress treatments were applied as soon as the first inflorescence had emerged. As for the well-watered treatment, the maximum amount of water that could be held by the soil in the containers was measured and this amount was applied daily, split between two separate watering events each day, and the volume of water applied per plant was increased over the course of the growing period.

To conduct the experiment involving the transgenic tomato mutants DEX:SlCV-1 and DEX:SlCV-2, when plants reached approximately 40 d olds and flower buds had appeared, we pruned each plant so that only two sets of one leaf and one flower-bud cluster remained. DEX:CV was induced by dipping each leaf into a 50-μM DEX solution for approximately 30 s once every 3 d at noon. DEX treatments were applied when buds had developed into fruits (two fruits per bud) and at the early green fruit stage continuing until full fruit ripening. M82 control plants were also dipped in 50-μM DEX throughout the study.

Physiological measurements

Measurements of gas exchange and photosynthesis. Stomatal conductance, transpiration rates and CO_2 assimilation were measured with a portable gas exchange LI-6400XT (LI-COR, Lincoln, NE, USA). Photosynthesis was induced at 1,200 μmol photons m^{-2} s^{-1} with 10% blue light. CO_2 surrounding the leaf was set at 400 μmol mol^{-1} CO_2, and temperature was set at 25°C. Measurements were snapshots, and the device was left to stabilize (i.e. stabilization of the A_N and E curve) for 90 s prior to each measurement.

Chlorophyll fluorescence and content

Chlorophyll content was measured using a SPAD chlorophyll-content meter (CCM-200 plus Chlorophyll Content Meter; Opti-Sciences, Hudson, NH, USA). Chlorophyll content was measured in the third or fourth leaf (counting down from the apical meristem). Each measurement was calculated as the approximate average of three measurements of a single leaf, avoiding the main vascular system of the leaf.

Chlorophyll fluorescence was measured as F_v/F_m (measuring the ratio between the fluorescent state of a pre-photosynthetic, dark-adapted leaf, F_0, and the maximum number of reaction centers to have been reduced or closed by a saturating light source, F_m). Using FluorPen FP 100 (Photon Systems Instruments, Drásov, Czechia), a period of dark adaptation (10 min, using the clips of the meter) was followed by the test itself. For the detached-leaf experiment, chlorophyll content was measured using an acetone-based extraction, as described in Wang and Blumwald (2014).

Yield analysis: preparation, total yield, Brix and HI

Preparation. In the yield experiment, tomato fruits were harvested when they had ripened to a full-red state, at which point they were firm to the touch and completely red. Tomatoes were harvested between 11:00 and 15:00. Pedicels and sepals were removed.

Total yield. Each fruit was weighed using a digital scale (BE10002; Biobase, Karnataka, India). The total fruit mass that was harvested from each plant was

calculated and recorded as 'total yield per plant'. The average total yield per plant was calculated for each line and treatment (e.g. CRIPSR-1, drought).

Brix. Brix, the total content of soluble sugars in ripe fruit (as grams of sucrose in 100 g of solution; Brix%) and a common indicator used for processing tomato fruit quality, was measured using a Brix meter refractometer (HI96801 Refractometer for Sucrose Measurements; Hanna Instruments, Woonsocket, RI, USA). To measure the fruit Brix, each fruit was cut in half using a clean sharp scalpel, and pericarp liquids were squeezed into the refractometer sample well and prism. Between each measurement, the sample well was thoroughly cleaned using Kimtech-Science™ Kimwipes™. Each fruit was measured three times, and those values were averaged. The average Brix level of all the fruits harvested from each line was calculated.

Harvest index. HI is calculated as the ratio of the total fruit weight of a plant to the weight of its shoot dry matter. At the end of the experiment, each tomato plant was harvested, oven-dried (at 65°C for 72–96 h) and then weighed. The average HI was calculated for each group of plants.

Whole-plant transpiration

Whole-plant daily transpiration rates were determined using lysimeters, as described in detail by Dalal et al. (2020). Briefly, individual IL9-2-5 and CRISPR2 tomato plants were planted in 3.9-l pots and grown under controlled conditions. Each pot was placed on a temperature-compensated load cell with a digital output and was sealed to prevent any evaporation from the surface of the growth medium. The output of the load cells was monitored every 10 s, and the average readings over 3-min periods were collected in a data-logger for further analysis. Whole-plant transpiration rate was calculated as a numerical derivative of the load-cell output following a data-smoothing process. Each plant's daily transpiration rate was normalized to its weight. For the drought experiments, irrigation was gradually reduced, and soil moisture was monitored using soil-moisture probes (EC-5; Decagon, METER Group, WA, USA).

Cellular localization

Agroinfiltration. Tobacco (*N. benthamiana*) leaves were infiltrated with recombinant *Agrobacterium* strain (GV3101) using a syringe (2 ml) without a needle. Leaves were superficially wounded with a needle to improve infiltration. Three leaves were agro-infiltrated at a time, and the infiltration procedure was performed twice. The agro-infiltrated leaves were photographed 36–48 h after infiltration.

Fluorescent imaging. Fluorescence microscopy was performed using a Zeiss LSM 780 inverted confocal laser scanning microscope (Carl Zeiss, Oberkochen, Germany). The transformed leaves were photographed using excitation/emission wavelengths for YFP (514 nm/527–572 nm) and chlorophyll (633 nm/650–720 nm). Image analysis and signal quantification were performed using the measurement function of ZEISS Efficient Navigation lite 2012 software (Carl Zeiss, Oberkochen, Germany).

Constructs

Solyc CV-CRISPR construct. The tomato *CV-CRISPR* construct was generated through GoldenGate assembly into pTRNAS_220d (Cermak et al. 2017). The three target sites: SolycCVt1, GAGGTTGAGGGGAGAGATTG; SolycCVt2, GAAAGTACGATCGCGATCGC and SolycCVt3, CTCCGGCGAGTCACCGGCCT, were chosen. Primers used to assemble gRNA were designed through the website http://crispr-multiplex.cbs.umn.edu//assembly.php (**Supplementary Table SI**). The multiplex gRNA cassette was assembled into a pMOD_B2103 module B plasmid with Csy4 as a splicing system (Cermak et al. 2017). Hence, the pMOD_A0501 that contained a P2A fusion of Csy4 ribonuclease and Cas9 was used as a module A plasmid (Cermak et al. 2017). Using tissue-culture methods, the construct was introduced into an IL9-2-5 tomato line, a *S. lycopersicum* line that carries a 9 cM introgression from the wild species, *S. pennelli* (Baxter et al. 2005). SolycCVt1 (gRNA1) generated a mutation at exon 1 as predicted (see Results). Two more gRNAs targeted exon 2 (SolycCVt2 and SolycCVt3) and did not generate any mutation.

Dex:SolycCV-3xFlag construct. The SolycCV coding region was flanked by a gateway attB1 sequence at the 5′ end and a linker sequence at the 3′ end and was PCR-amplified with M82 tomato complementary DNA (cDNA) used as a template. The 3xFlag and Arabidopsis HSP terminator fusion were synthesized (Genewiz, South Plainfield, NJ, USA) and used as a template for a nesting PCR with the SolycCV amplicon, with the primer-flanking linker sequence at the 5′ end and with the gateway attB2 sequence at the 3′ end. Nesting PCR was performed using the two PCR amplicons as templates, as well as the attB1 and attB2 primers that were used in the first round of PCR. The resulting amplicon was cloned into pDONR207 by a attB attP DNA site recombination reaction (Invitrogen, Waltham, MA, USA). This entry clone and the destination vector, pBAV154 (Vinatzer et al. 2006), harboring the Dex induction system, were recombined in an attL attR DNA site recombination (LR) reaction (Invitrogen). A floral-dip method (Clough and Bent 1998) was used to introduce the construct into a Col *A. thaliana* ecotype.

35S:SlCV:YFP construct. To exclude 3xFlag and the stop codon from the entry clone of SolycCV-3xFlag and keep the attL1 and attL2 sequences, two independent PCR reactions were performed with the pDONR 207-F: the SlCVwoStop-R primers used in one reaction and the SlCVwoStop-B2-F and the pDONR 207-R used in the other reaction, with the SolycCV-3xFlag entry clone used as the template for both reactions. The produced amplicons were used as a template for the second round of PCR with the pDONR 207-F and pDONR 207-R primers. The LR reaction was then used to directly recombine the new amplicon with the pEarleyGate101 (Earley et al. 2006), harboring the 35S promoter and the C-terminal-tagging YFP.

Fruit metabolomics

We analyzed the metabolites present in fully ripe fruit. The pericarp of each fruit was dissected, excluding seeds, epidermis, placental tissue and columella. Extracted pericarp was kept in designated opaque, plastic 10-ml tubes. The pericarp tissue was then lyophilized (−49.8°C/9 Pa, ∼36 h) and crushed into powder. To measure the concentrations of the different metabolites, equal amounts of the crushed sample were extracted using methyl-*tert*-butyl ether as a solvent (Giavalisco et al. 2011). Samples were subjected to GC-MS analysis using an Agilent 7683 series auto-sampler (Agilent Technologies, Santa Clara, CA, USA), coupled to an Agilent 6890 gas chromatograph-Leco Pegasus two time-of-flight mass spectrometer (Wu et al. 2016).

RNA extraction, cDNA synthesis, qPCR and RNAseq

RNA was extracted from leaves or fruits using the Total RNA Mini Kit (Plant) from Geneaid (New Taipei, Taiwan). The success of the extraction and the integrity of the RNA were validated using NanoDrop (MaestroNano, New Taipei, Taiwan) and gel electrophoresis.

cDNA strands were synthesized using a designated kit (qScript cDNA Synthesis Kit; QuantaBio, Beverly, MA, USA) and PCR (SimpliAmp™ Thermal Cycler; ThermoFisher Scientific, Waltham, MA, USA), according to the manufacturer's instructions. Quantitative PCR was performed using the PikoReal 96 Real-Time PCR System (Thermo Scientific, MA, USA) and qPCRBIO SyGreen Blue Mix Hi-ROX kit by PCR Biosystems (London, UK). The different sets of primers used for the amplification of the target genes are listed in **Supplementary Table SII**. Analysis of the relative gene expression was performed according to the comparative cycle threshold ($2^{-\Delta\Delta CT}$) method (Livak and Schmittgen 2001) and calibrated using transcript values relative to the endogenous tomato ACTIN. RNAseq libraries were prepared, sequenced and analyzed using

the 'TranSeq' 3′-end sequencing methodology, as fully described in Tzfadia et al. (2018).

N content

Plants were grown in a semi-controlled greenhouse in sandy soil pre-saturated with water and fertilization and were irrigated 200 ml d^{-1}. At 30 d post-germination, the plants were divided into two treatment groups: a salinity-stress group subjected to saline irrigation (gradually increased to 150 mM NaCl) and a drought-stress group, for which irrigation was limited and a steady, low irrigation of 50 ml d^{-1} (approximately 25% of normal irrigation) was given. Treatments were given for 18 d, and the plants exhibited obvious symptoms of stress at harvest. Additionally, more plants were grown under similar conditions with non-stress conditions and were irrigated 200 ml d^{-1} until harvest. The N content of each sample was determined by combustion, according to the Dumas method, using 5 mg of powder and an elemental analyzer (FlashSmart™ Elemental Analyzer; Thermo Fisher, MA, USA). At harvest, the shoots and roots were separated, and the roots were thoroughly cleaned of debris. The samples were then dried in an oven (70°C, 96 h) and crushed using a standard kitchen electric blender. Source (leaf) NUE was calculated as shoot plant dry weight divided by shoot N content. Sink (root) N content and biomass allocation reflect the proportion of the whole-plant N content or dry weight that is accounted for by the sink N content or sink dry weight.

Identification of metabolic pathways within correlation-based networks

Relative quantities of metabolites were used to construct correlation-based networks essentially as described in Toubiana et al. (2013). In brief, correlation coefficients, based on the Pearson product moments, were computed between any two metabolites of the dataset. Next, correlation-based networks were generated, in which each node represented a metabolite and the edges between the nodes represented the corresponding correlation coefficients. Threshold analysis of the correlation coefficients was applied in a recursive manner to test various network features, as described in Toubiana and Maruenda (2021), such that only correlations/edges with a q-value ≤ 0.05 and $|r| \geq 0.36$ (control), 0.4 (drought) and 0.53 (salinity) were retained in the network. The clustering of nodes in the network was performed using the walktrap community-detecting algorithm.

Next, correlation-based network analysis was combined with machine learning techniques to predict metabolic pathways in correlation-based networks (Toubiana et al. 2019). For the training set, 37 metabolic pathways that are common to all plant species listed in PlantCyc (Schlapfer et al. 2017) were used as the positive instances, while metabolic pathways not found in plants and random sets of metabolites were used as the negative instances. The pathways in the training set were then mapped onto the correlation-based network, such that the nodes corresponded to the metabolites in the pathways. Subsequently, a set of network properties was computed for each pathway (Toubiana et al. 2019) and those sets were then fed into the machine learning classifier (XGboost) as features to generate a statistically robust machine learning model. The model was run with 10× cross-validation. Finally, a test set composed of metabolic pathways from PlantCyc but not overlapping with the training set was predicted using the machine learning model. Sensitivity analysis was performed to validate the predictions of test set pathways. Only pathways that were positively predicted in both the original prediction (>0.6) and the sensitivity analysis (>0.6) were considered to have been validly predicted. Pathways that were predicted for both stress conditions, but not for the control conditions, were used for further analysis. The number of edges and nodes were extracted using the 'igraph' R package. The AUC values were extracted using the 'xgboost' R package. The confusion matrices and their accuracies [representing the percentage of the matches between the actual classification and the predicted classification (POS/POS + NEG/NEG) out of all classifications (POS/POS + POS/NEG + NEG/POS + NEG/NEG)] were extracted using the 'caret' R package.

Using WGCNA to identify the correlation between metabolites and network modules

WGCNA was applied to normalized gene expression values, with samples from all experiments combined, essentially as described in Langfelder and Horvath (2008). In brief, correlation coefficients, based on the Pearson product moment, were computed between any two genes of the dataset. Next, a correlation-based network was generated, in which each node represented a gene and the edges between the nodes represented the corresponding correlation coefficient. To achieve a scale-free network topology, the power function was used, determining the exponent ($\beta = 5$) for the correlation coefficients. The resulting topological overlap matrix was then used for hierarchical topological overlap mapping to identify modules of highly connected genes. This was done using the automated mode supplied by the WGCNA package. Next, module eigengenes were computed in order to correlate them with the metabolites. Modules that included highly significant correlations with metabolites of interest were identified. Within the module of interest, the most significant genes among the different genotypes were used to detect potential candidate genes for further research.

Statistical analysis

The JMP Pro 15 software was used for statistical analysis. Details of the analyses are provided in the figure legends.

Supplementary Data

Supplementary data are available at *PCP* online.

Data Availability

Sequence data from this article can be found in the Tomato Genomics Network data library under the following accession number: CV (Solyc08G067630). All data supporting the findings of this study are available within the paper and the **Supplementary data.**

Funding

Israel Ministry of Agriculture (01025767 to N.S. and Y.B.); European Union's Horizon 2020 Research and Innovation Programme for PlantaSYST project (SGA-CSA no. 664621 and no. 739582 under FPA no. 664620 to S.A. and A.R.F.); ADAMA Center for Novel Delivery Systems in Crop Protection, Tel Aviv University to Z.H.

Author Contributions

Y.A. participated in the investigation, data curation, formal analysis, methodology, validation, visualization and writing—original draft; Z.H. participated in the investigation, formal analysis, visualization, data curation, methodology, validation, software and writing—original draft; Y.Y.Z. participated in the investigation and formal analysis; L.R. participated in the investigation, formal analysis and visualization; D.S. participated in the data curation and methodology; D.T. participated in the software and methodology; S.A. participated in the formal analysis and methodology; H.T. participated in the data curation and methodology; Y.B. participated in the funding acquisition, methodology and writing—review and editing; E.B. participated

in the methodology and writing—review and editing; A.R.F. participated in the methodology and writing—review and editing and N.S. participated in the conceptualization, formal analysis, methodology, validation, supervision, project administration, funding acquisition, visualization, writing—original draft and writing—review and editing.

Disclosures

The authors have no conflicts of interest to declare.

References

Aguirrezabal, L.A.N., Deleens, E. and Tardieu, F. (1994) Root elongation rate is accounted for by intercepted PPFD and source-sink relations in-field and laboratory-grown sunflower. *Plant Cell Environ.* 17: 443–450.

Arthikala, M.K., Nanjareddy, K. and Lara, M. (2018) In BPS1 downregulated roots, the bypass1 signal disrupts the induction of cortical cell divisions in bean-rhizobium symbiosis. *Genes* 9: 11.

Batushansky, A., Kirma, M., Grillich, N., Pharn, P.A., Rentsch, D., Galili, G., et al. (2015) The transporter GAT1 plays an important role in GABA-mediated carbon-nitrogen interactions in *Arabidopsis*. *Front. Plant Sci.* 6: 785.

Baxter, C.J., Sabar, M., Quick, W.P. and Sweetlove, L.J. (2005) Comparison of changes in fruit gene expression in tomato introgression lines provides evidence of genome-wide transcriptional changes and reveals links to mapped QTLs and described traits. *J. Exp. Bot.* 56: 1591–1604.

Benitez-Alfonso, Y., Cilia, M., Roman, A.S., Thomas, C., Maule, A., Hearn, S., et al. (2009) Control of *Arabidopsis* meristem development by thioredoxin-dependent regulation of intercellular transport. *Proc. Natl. Acad. Sci. USA* 106: 3615–3620.

Bouche, N. and Fromm, H. (2004) GABA in plants: just a metabolite? *Trends Plant Sci.* 9: 110–115.

Carrari, F., Nunes-Nesi, A., Gibon, Y., Lytovchenko, A., Loureiro, M.E. and Fernie, A.R. (2003) Reduced expression of aconitase results in an enhanced rate of photosynthesis and marked shifts in carbon partitioning in illuminated leaves of wild species tomato. *Plant Physiol.* 133: 1322–1335.

Cermak, T., Curtin, S.J., Gil-Humanes, J., Cegan, R., Kono, T.J.Y., Konecna, E., et al. (2017) A multipurpose toolkit to enable advanced genome engineering in plants. *Plant Cell* 29: 1196–1217.

Chen, T., Zhang, W., Yang, G., Chen, J.H., Chen, B.X., Sun, R., et al. (2020) TRANSTHYRETIN-LIKE and BYPASS1-LIKE co-regulate growth and cold tolerance in *Arabidopsis*. *BMC Plant Biol.* 20: 1–11.

Clough, S.J. and Bent, A.F. (1998) Floral dip: a simplified method for *Agrobacterium*-mediated transformation of *Arabidopsis thaliana*. *Plant J.* 16: 735–743.

Concordet, J.P. and Haeussler, M. (2018) CRISPOR: intuitive guide selection for CRISPR/Cas9 genome editing experiments and screens. *Nucleic Acids Res.* 46: W242–W245.

Couturier, J., Doidy, J., Guinet, F., Wipf, D., Blaudez, D. and Chalot, M. (2010) Glutamine, arginine and the amino acid transporter Pt-CAT11 play important roles during senescence in poplar. *Ann. Bot.* 105: 1159–1169.

Dalal, A., Shenhar, I., Bourstein, R., Mayo, A., Grunwald, Y., Averbuch, N., et al. (2020) A telemetric, gravimetric platform for real-time physiological phenotyping of plant environment interactions. *J. Vis. Exp.* 162: e61280.

Ding, Q., Yang, X., Pi, Y., Li, Z., Xue, J., Chen, H., et al. (2020) Genome-wide identification and expression analysis of extensin genes in tomato. *Genomics* 112: 4348–4360.

Distelfeld, A., Avni, R. and Fischer, A.M. (2014) Senescence, nutrient remobilization, and yield in wheat and barley. *J. Exp. Bot.* 65: 3783–3798.

Earley, K.W., Haag, J.R., Pontes, O., Opper, K., Juehne, T., Song, K.M., et al. (2006) Gateway-compatible vectors for plant functional genomics and proteomics. *Plant J.* 45: 616–629.

Eshed, Y. and Zamir, D. (1995) An introgression line population of *Lycopersicon pennellii* in the cultivated tomato enables the identification and fine mapping of yield-associated QTL. *Genetics* 141: 1147–1162.

Fridman, E., Carrari, F., Liu, Y., Fernie, A.R. and Zamir, D. (2004) Zooming in on a quantitative trait for tomato yield using interspecific introgressions. *Science* 305: 1786–1789.

Fridman, E., Liu, Y., Carmel-Goren, L., Gur, A., Shoresh, M., Pleban, T., et al. (2002) Two tightly linked QTLs modify tomato sugar content via different physiological pathways. *Mol. Gen. Genom.* 266: 821–826.

Friedman, J.H. (2001) Greedy function approximation: a gradient boosting machine. *Ann. Stat.* 29: 1189–1232.

Gallie, D.R. (2017) Class II members of the poly(A) binding protein family exhibit distinct functions during *Arabidopsis* growth and development. *Translation* 5:e1295129.

Gan, S. and Amasino, R.M. (1995) Inhibition of leaf senescence by autoregulated production of cytokinin. *Science* 270: 1966–1967.

Giavalisco, P., Li, Y., Matthes, A., Eckhardt, A., Hubberten, H.M., Hesse, H., et al. (2011) Elemental formula annotation of polar and lipophilic metabolites using C-13, N-15 and S-34 isotope labelling, in combination with high-resolution mass spectrometry. *Plant J.* 68: 364–376.

Gregersen, P.L. and Holm, P.B. (2007) Transcriptome analysis of senescence in the flag leaf of wheat (*Triticum aestivum* L.). *Plant Biotechnol. J.* 5: 192–206.

Gregersen, P.L., Culetic, A., Boschian, L. and Krupinska, K. (2013) Plant senescence and crop productivity. *Plant Mol. Biol.* 82: 603–622.

Havé, M., Marmagne, A., Chardon, F. and Masclaux-Daubresse, C. (2016) Nitrogen remobilisation during leaf senescence: lessons from *Arabidopsis* to crops. *J. Exp. Bot.* 68: 2513–2529.

Himelblau, E. and Amasino, R.M. (2001) Nutrients mobilized from leaves of *Arabidopsis thaliana* during leaf senescence. *J. Plant Physiol.* 158: 1317–1323.

Humphrey, T.V., Haasen, K.E., Aldea-Brydges, M.G., Sun, H., Zayed, Y., Indriolo, E., et al. (2015) PERK-KIPK-KCBP signalling negatively regulates root growth in *Arabidopsis thaliana*. *J. Exp. Bot.* 66: 71–83.

Langfelder, P. and Horvath, S. (2008) WGCNA: an R package for weighted correlation network analysis. *BMC Bioinform.* 9: 559.

Li, T., Heuvelink, E. and Marcelis, L.F. (2015) Quantifying the source–sink balance and carbohydrate content in three tomato cultivars. *Front Plant Sci.* 6: 416.

Licausi, F., Ohme-Takagi, M. and Perata, P. (2013) APETALA/ethylene responsive factor (AP2/ERF) transcription factors: mediators of stress responses and developmental programs. *New Phytol.* 199: 639–649.

Liebsch, D., Juvany, M., Li, Z., Wang, H.L., Ziolkowska, A., Chrobok, D., et al. (2022) Metabolic control of arginine and ornithine levels paces the progression of leaf senescence. *Plant Physiol.* 189: 1943–1960.

Lira, B.S., Gramegna, G., Trench, B.A., Alves, F.R.R., Silva, E.M., Silva, G.F.F., et al. (2017) Manipulation of a senescence-associated gene improves fleshy fruit yield. *Plant Physiol.* 175: 77–91.

Livak, K.J. and Schmittgen, T.D. (2001) Analysis of relative gene expression data using real-time quantitative PCR and the 2(T)(-delta delta C) method. *Methods* 25: 402–408.

Long, S.P., Marshall-Colon, A. and Zhu, X.G. (2015) Meeting the global food demand of the future by engineering crop photosynthesis and yield potential. *Cell* 161: 56–66.

Lorenzo, O., Piqueras, R., Sanchez-Serrano, J.J. and Solano, R. (2003) ETHYLENE RESPONSE FACTOR1 integrates signals from ethylene and jasmonate pathways in plant defense. *Plant Cell* 15: 165–178.

Lunn, D., Phan, T.D., Tucker, G.A. and Lycett, G.W. (2013) Cell wall composition of tomato fruit changes during development and inhibition of vesicle trafficking is associated with reduced pectin levels and reduced softening. *Plant Physio. Biochem.* 66: 91–97.

Ma, X.M., Balazadeh, S. and Mueller-Roeber, B. (2019) Tomato fruit ripening factor NOR controls leaf senescence. *J. Exp. Bot.* 70: 2727–2740.

Ma, X.M., Zhang, Y.J., Tureckova, V., Xue, G.P., Fernie, A.R., Mueller-Roeber, B., et al. (2018) The NAC transcription factor SlNAP2 regulates leaf senescence and fruit yield in tomato. *Plant Physiol.* 177: 1286–1302.

Madrid-Espinoza, J., Salinas-Cornejo, J. and Ruiz-Lara, S. (2019) The Rab-GAP gene family in tomato (*Solanum lycopersicum*) and wild relatives: identification, interaction networks, and transcriptional analysis during plant development and in response to salt stress. *Genes* 10: 638.

Mehta, R.A., Cassol, T., Li, N., Ali, N., Handa, A.K. and Mattoo, A.K. (2002) Engineered polyamine accumulation in tomato enhances phytonutrient content, juice quality, and vine life. *Nat. Biotechnol.* 20: 613–618.

Michaeli, S., Galili, G., Genschik, P., Fernie, A.R. and Avin-Wittenberg, T. (2016) Autophagy in plants—what's new on the menu?. *Trends Plant Sci.* 21: 134–144.

Moeder, W., Del Pozo, O., Navarre, D.A., Martin, G.B. and Klessig, D.F. (2007) Aconitase plays a role in regulating resistance to oxidative stress and cell death in *Arabidopsis* and *Nicotiana benthamiana*. *Plant Mol. Biol.* 63: 273–287.

Moles, T.M., Mariotti, L., De Pedro, L.F., Guglielminetti, L., Picciarelli, P. and Scartazza, A. (2018) Drought induced changes of leaf-to-root relationships in two tomato genotypes. *Plant Physio. Biochem.* 128: 24–31.

Munne-Bosch, S. and Alegre, L. (2004) Die and let live: leaf senescence contributes to plant survival under drought stress. *Funct. Plant Biol.* 31: 203–216.

Nasibi, F., Yaghoobi, M.M. and Kalantari, K.M. (2011) Effect of exogenous arginine on alleviation of oxidative damage in tomato plant underwater stress. *J. Plant Interact.* 6: 291–296.

Nunes-Nesi, A., Araujo, W.L. and Fernie, A.R. (2011) Targeting mitochondrial metabolism and machinery as a means to enhance photosynthesis. *Plant Physiol.* 155: 101–107.

Osorio, S., Ruan, Y.L. and Fernie, A.R. (2014) An update on source-to-sink carbon partitioning in tomato. *Front Plant Sci.* 5: 516.

Pham, G., Shin, D.M., Kim, Y. and Kim, S.H. (2022) Ran-GTP/-GDP-dependent nuclear accumulation of NONEXPRESSOR OF PATHOGENESIS-RELATED GENES1 and TGACG-BINDING FACTOR2 controls salicylic acid-induced leaf senescence. *Plant Physiol.* 189: 1774–1793.

Ploschuk, E.L., Slafer, G.A. and Ravetta, D.A. (2005) Reproductive allocation of biomass and nitrogen in annual and perennial *Lesquerella* crops. *Ann. Bot.* 96: 127–135.

Quinet, M., Angosto, T., Yuste-Lisbona, F.J., Blanchard-Gros, R., Bigot, S., Martinez, J.P., et al. (2019) Tomato fruit development and metabolism. *Front Plant Sci.* 10: 1554.

Rankenberg, T., Geldhof, B., van Veen, H., Holsteens, K., Van de Poel, B. and Sasidharan, R. (2021) Age-dependent abiotic stress resilience in plants. *Trends Plant Sci.* 26: 692–705.

Reguera, M., Peleg, Z., Abdel-Tawab, Y.M., Tumimbang, E.B., Delatorre, C.A. and Blumwald, E. (2013) Stress-induced cytokinin synthesis increases drought tolerance through the coordinated regulation of carbon and nitrogen assimilation in rice. *Plant Physiol.* 163: 1609–1622.

Rissland, O.S. (2017) The organization and regulation of mRNA-protein complexes. *Wiley Interdiscip. Rev. RNA* 8: e1369.

Rivero, R.M., Kojima, M., Gepstein, A., Sakakibara, H., Mittler, R., Gepstein, S., et al. (2007) Delayed leaf senescence induces extreme drought tolerance in a flowering plant. *Proc. Natl. Acad. Sci. USA* 104: 19631–19636.

Sade, N., Rubio-Wilhelmi, M.D., Umnajkitikorn, K. and Blumwald, E. (2018a) Stress-induced senescence and plant tolerance to abiotic stress. *J. Exp. Bot.* 69: 845–853.

Sade, N., Umnajkitikorn, K., Wilhelmi, M.D.R., Wright, M., Wang, S.H. and Blumwald, E. (2018b) Delaying chloroplast turnover increases water-deficit stress tolerance through the enhancement of nitrogen assimilation in rice. *J. Exp. Bot.* 69: 867–878.

Schlapfer, P., Zhang, P.F., Wang, C.A., Kim, T., Banf, M., Chae, L., et al. (2017) Genome-wide prediction of metabolic enzymes, pathways, and gene clusters in plants. *Plant Physiol.* 173: 2041–2059.

Severo, J., Tiecher, A., Pirrello, J., Regad, F., Latche, A., Pech, J.C., et al. (2015) UV-C radiation modifies the ripening and accumulation of ethylene response factor (ERF) transcripts in tomato fruit. *Postharvest Biol. Technol.* 102: 9–16.

Tahjib-Ul-Arif, M., Zahan, M.I., Karim, M.M., Imran, S., Hunter, C.T., Islam, M.S., et al. (2021) Citric acid-mediated abiotic stress tolerance in plants. *Int. J. Mol. Sci.* 22: 7235.

Thomas, H. and Howarth, C.J. (2000) Five ways to stay green. *J. Exp. Bot.* 51: 329–337.

Thomas, H. and Ougham, H. (2014) The stay-green trait. *J. Exp. Bot.* 65: 3889–3900.

Toubiana, D. and Maruenda, H. (2021) Guidelines for correlation coefficient threshold settings in metabolite correlation networks exemplified on a potato association panel. *BMC Bioinform.* 22: 116.

Toubiana, D., Fernie, A.R., Nikoloski, Z. and Fait, A. (2013) Network analysis: tackling complex data to study plant metabolism. *Trends Biotechnol.* 31: 29–36.

Toubiana, D., Puzis, R., Wen, L.L., Sikron, N., Kurmanbayeva, A., Soltabayeva, A., et al. (2019) Combined network analysis and machine learning allows the prediction of metabolic pathways from tomato metabolomics data. *Commun. Biol.* 2: 214.

Toubiana, D., Sade, N., Liu, L.F., Wilhelmi, M.D.R., Brotman, Y., Luzarowska, U., et al. (2020) Correlation-based network analysis combined with machine learning techniques highlight the role of the GABA shunt in *Brachypodium sylvaticum* freezing tolerance. *Sci. Rep.* 10:

Tripathy, M.K., Deswal, R. and Sopory, S.K. (2021) Plant RABs: role in development and in abiotic and biotic stress responses. *Curr. Genomics* 22: 26–40.

Tzfadia, O., Bocobza, S., Defoort, J., Almekias-Siegl, E., Panda, S., Levy, M., et al. (2018) The 'TranSeq' 3′-end sequencing method for high-throughput transcriptomics and gene space refinement in plant genomes. *Plant J.* 96: 223–232.

Umnajkitikorn, K., Sade, N., Wilhelmi, M.D.R., Gilbert, M.E. and Blumwald, E. (2020) Silencing of OsCV (chloroplast vesiculation) maintained photorespiration and N assimilation in rice plants grown under elevated CO_2. *Plant Cell Environ.* 43: 920–933.

Van Norman, J.M. and Sieburth, L.E. (2007) Dissecting the biosynthetic pathway for the bypass1 root-derived signal. *Plant J.* 49: 619–628.

Vinatzer, B.A., Teitzel, G.M., Lee, M.W., Jelenska, J., Hotton, S., Fairfax, K., et al. (2006) The type III effector repertoire of *Pseudomonas syringae* pv. syringae B728a and its role in survival and disease on host and non-host plants. *Mol. Microbiol.* 62: 26–44.

Wang, S.H. and Blumwald, E. (2014) Stress-induced chloroplast degradation in *Arabidopsis* is regulated via a process independent of autophagy and senescence-associated vacuoles. *Plant Cell* 26: 4875–4888.

Wingler, A., Purdy, S., MacLean, J.A. and Pourtau, N. (2006) The role of sugars in integrating environmental signals during the regulation of leaf senescence. *J. Exp. Bot.* 57: 391–399.

Wu, S., Alseekh, S., Cuadros-Inostroza, A., Fusari, C.M., Mutwil, M., Kooke, R., et al. (2016) Combined use of genome-wide association data

and correlation networks unravels key regulators of primary metabolism in *Arabidopsis thaliana*. *PLoS Genet.* 12: e1006363.

Xie, Q., Michaeli, S., Peled-Zehavi, N. and Galili, G. (2015) Chloroplast degradation: one organelle, multiple degradation pathways. *Trends Plant Sci.* 20: 264–265.

Xu, Q.Y., Chen, S.Y., Ren, Y.J., Chen, S.L. and Liesche, J. (2018) Regulation of sucrose transporters and phloem loading in response to environmental cues. *Plant Physiol.* 176: 930–945.

Yoshiba, Y., Aoki, C., Iuchi, S., Nanjo, T., Seki, M., Sekigushi, F., et al. (2001) Characterization of four extension genes in *Arabidopsis thaliana* by differential gene expression under stress and non-stress conditions. *DNA Res.* 8: 115–122.

Yu, J.C., Lu, J.Z., Cui, X.Y., Guo, L., Wang, Z.J., Liu, Y.D., et al. (2022) Melatonin mediates reactive oxygen species homeostasis via SlCV to regulate leaf senescence in tomato plants. *J. Pineal Res.* 73. 10.1111/jpi.12810.

Zanor, M.I., Osorio, S., Nunes-Nesi, A., Carrari, F., Lohse, M., Usadel, B., et al. (2009) RNA interference of LIN5 in tomato confirms its role in controlling Brix content, uncovers the influence of sugars on the levels of fruit hormones, and demonstrates the importance of sucrose cleavage for normal fruit development and fertility. *Plant Physiol.* 150: 1204–1218.

Zhu, X.G., Long, S.P. and Ort, D.R. (2010) Improving photosynthetic efficiency for greater yield. *Annu. Rev. Plant Biol.* 61: 235–261.

Sub- chapter 4.3

Results presented in this sub-chapter has been published in the journal “Plant Science”

Title: Is CRISPR/Cas9-based multi-trait enhancement of wheat forthcoming?

Plant Science 341 (2024) 112021

Contents lists available at ScienceDirect

Plant Science

journal homepage: www.elsevier.com/locate/plantsci

Is CRISPR/Cas9-based multi-trait enhancement of wheat forthcoming?☆

Zechariah Haber [a], Davinder Sharma [a], K.S. Vijai Selvaraj [b], Nir Sade [a,*]

[a] School of Plant Sciences and Food Security, Tel Aviv University, Tel Aviv 69978, Israel
[b] Vegetable Research Station, Tamil Nadu Agricultural University, Palur 607102, Tamil Nadu, India

ARTICLE INFO

Keywords:
CRISPR/Cas9
Wheat (*Triticum aestivum*)
Stress tolerance
Multiplexing
Yield

ABSTRACT

Clustered Regularly Interspaced Short Palindromic Repeats (CRISPR) technologies have been implemented in recent years in the genome editing of eukaryotes, including plants. The original system of knocking out a single gene by causing a double-strand break (DSB), followed by non-homologous end joining (NHEJ) or Homology-directed repair (HDR) has undergone many adaptations. These adaptations include employing CRISPR/Cas9 to upregulate gene expression or to cause specific small changes to the DNA sequence of the gene-of-interest. In plants, multiplexing, *i.e.*, inducing multiple changes by CRISPR/Cas9, is extremely relevant due to the redundancy of many plant genes, and the time- and labor-consuming generation of stable transgenic plant lines *via* crossing. Here we discuss relevant examples of various traits, such as yield, biofortification, gluten content, abiotic stress tolerance, and biotic stress resistance, which have been successfully manipulated using CRISPR/Cas9 in plants. While existing studies have primarily focused on proving the impact of CRISPR/Cas9 on a single trait, there is a growing interest among researchers in creating a multi-stress tolerant wheat cultivar 'super wheat', to commercially and sustainably enhance wheat yields under climate change. Due to the complexity of the technical difficulties in generating multi-target CRISPR/Cas9 lines and of the interactions between stress responses, we propose enhancing already commercial local landraces with higher yield traits along with stress tolerances specific to the respective localities, instead of generating a general 'super wheat'. We hope this will serve as the sustainable solution to commercially enhancing crop yields under both stable and challenging environmental conditions.

1. Introduction

Clustered Regularly Interspaced Short Palindromic Repeats (CRISPR) technologies have been a hot topic in the past decade, ever since the concept of genetic engineering in eukaryotes using the bacterial CRISPR/Cas9 system was introduced (Cong et al., 2013; Mali et al., 2013; Jinek et al., 2013; Doudna and Charpentier, 2014). Briefly, many bacteria and archaea maintain a viral "database" containing spacer DNA (each spacer is a unique sequence from a specific virus) interspersed with short palindromic repetitive sequences. CRISPR-associated (Cas) proteins will bind replicas of the different spacers, and upon a viral attack onto the bacterial host cell, the protein with the spacer corresponding to the invading virus DNA will target it and cleave it (Horvath and Barrangou, 2010).

Since then, CRISPR/Cas9 systems have been introduced into the theoretical and applicative research of various organisms, including humans, animals and plants, and have successfully altered phenotypes in a desirable manner, efficiently targeting site-specific sequences. Many reviews have been conducted recently, regarding CRISPR/Cas9 systems in general (*e.g.*, Liu et al. 2022; Wang and Doudna, 2023), in plants (Zhang et al., 2019b; Cardi et al., 2023) and even specifically in bread wheat (Kumar et al., 2019; Li et al., 2021a) and the main trends are as follows.

First, the original system has been tweaked many times over, including by changing the guide RNA into single guide RNA (sgRNA; Jinek et al., 2012) and finetuning the Cas9 and Cas12a proteins (Zhang et al., 2019b). Second, non-homologous end joining (NHEJ) and Homology-directed repair (HDR) following a double-strand break (DSB) are two parallel options to generate changes in DNA *via* the CRISPR/-Cas9 system. Both have significant advantages and disadvantages. For instance, NHEJ is the default DNA repair pathway, operating swiftly and actively throughout the cell cycle in both replication-active and -inactive cells, HDR presents a significantly lower risk of undesirable alterations to the resulting DNA sequence, such as insertions, deletions and

☆ This paper is dedicated to the memory of Zechariah Haber

* Corresponding author.
E-mail address: nirsa@tauex.tau.ac.il (N. Sade).

https://doi.org/10.1016/j.plantsci.2024.112021
Received 14 November 2023; Received in revised form 25 January 2024; Accepted 31 January 2024
Available online 3 February 2024

base changes. Ongoing research is actively exploring ways to enhance the latter by inhibiting the former, as reviewed in Yeh et al., 2019.

The original function of the CRISPR/Cas9 system involving cleaving DNA out of the genome *via* DSB has a narrow spectrum of application. In order to make specific changes to the sequence without the risks associated with DSB, important improvements have been made. This includes fusing a catalytically nonfunctional Cas9 (dead Cas9, dCas9; which has lost its nuclease activity) with a deaminase, allowing base conversion without DSB (referred to as base editing; Komor et al., 2016). Alternatively, another approach is the fusion of dCas9 with an engineered reverse transcriptase, which is guided by a prime editing guide RNA (pegRNA), which not only targets the sequence but also dictates the desired sequence change (referred to as prime editing; Anzalone et al., 2019). Other variations in CRISPR technologies include genetic and epigenetic CRISPR activation or interference (CRISPRa or CRISPRi, respectively), *i.e.*, using a fusion of dCas9 to a transcription repressor (Qi et al., 2013) or activator (Gilbert et al., 2013) to repress or activate gene expression, respectively. Lastly, CRISPR is also used for gene screening, *i.e.*, targeting thousands of genes across the genome in individually silenced lines and functionally screening all lines (Shalem et al. 2014).

Nevertheless, it is important to acknowledge existing drawbacks in the CRISPR/Cas9 toolbox, mainly regarding the precision, accuracy and delivery (Wang and Doudna, 2023). Precision refers to achieving a 'perfect' sequence, *i.e.*, ensuring no unintended indels or editing within the editing window. Accuracy pertains to site-specificity, *i.e.*, ensuring no off-target activity, and imperfect accuracy and/or precision can cause undesired alteration of the gene-of-interest and/or off-target genes, an outcome deemed unacceptable in many cases. Delivery concerns overcoming interferences from the physical site of delivery and to the intended on-target site within the genome. While this is less an issue when dealing with plants, as genetic transformation protocols have been relatively established in many plant species, though transformation efficiency varies on the species and subspecies levels (Kausch et al., 2019).

Specifically, in plants, the potential of multiplexing in CRISPR applications involving the targeting multiple sites or genes simultaneously using multiple gRNA in a single fused sequence or targeting multiple sequences with a single gRNA is highlighted. This success is attributed to, *inter alia*, the redundancy of many plant genes, and the time- and labor-consuming generation of stable transgenic plant lines *via* crossing (Ling et al., 2014). There is a reported instance of over 100 targets successfully altered *via* CRISPR multiplexing (Najera et al., 2019). Another aspect of CRISPR in plants is the hurdles of Genetic Modified Organism (GMO) regulation and social intimidation. Different countries and/or multinational regulatory bodies have varying regulation regarding GMOs in general, and genome-edited crops in particular (Zhang et al., 2020). There are numerous methods exist for the development of transgene-free CRISPR crops such as exclusion of the transgene *via* Mendelian segregation using a ribonucleoprotein (RNP) complex, inducing transient expression of the CRISPR/Cas9 system, drug-induced elimination of transgenic lines, fluorescence marker elimination of transgenic lines or using self-destructive transformation, in which the already edited and still transgenic cells will commit programmed cell death (He and Zhao, 2019). Many proponents argue that the availability of these strategies is a compelling reason to develop a unique approach towards genome-edited crops, setting them apart from conventional GMOs (Huang et al., 2016). The social fear of GMOs (which would apply to CRISPR/Cas9 crops, if deemed as such by each respective regulatory body), provides another crucial hurdle which needs to be addressed soon, while we can still close the yield gap (Anders et al., 2021).

As mentioned before, many thorough reviews have been published regarding general CRISPR/Cas9 advancements, CRISPR/Cas9 in plants, and specifically in wheat. Here, we provide, to the best of our knowledge, the first multi-trait review analysis in bread wheat (*Triticum aestivum* L.), trying to depict a framework of creating a fully-fledged "super" crop, equipped to deal with multi-stress climate change and other yield constraints, an idea introduced by Li et al. (2021b). Is this possible and if so, how? We hope that this public discussion will encourage multi-trait research and implementation, in order to feed the growing human population sustainably in the near future. It is important to mention, that because of its relatively complex genome (size and polyploidy) and the challenging nature of its transformation, *T. aestivum* is much more scarcely researched using CRISPR/Cas9 than other common plants (*e.g.*, *Arabidopsis thaliana* and *Oryza sativa*; Kumar et al., 2019), though this is slowly changing recently. Hence, the amount of research papers we found, regarding using CRISPR/Cas9 on *T. aestivum* tackling specific traits is still relatively limited per trait.

2. High yield

Bread wheat contributes approximately 20% of the global human calorie consumption (Shewry and Hey, 2015). While a significant increase in demand for food is expected due to human population growth and due to the increase of the standard of living (Godfray and Garnett, 2014), supply is projected to critically decrease due to environmental stresses and international conflicts (Reynolds et al., 2012; Bentley et al., 2022). Despite the fact that a myriad of traits associated with increasing yield potential have been reported (*e.g.*, photosynthesis optimization, increasing source-sink grain filling and grain filling time period, improving water-use and nitrogen-use efficiencies, increasing grain size and number and decreasing plant height; Bailey-Serres et al., 2019; Gupta et al., 2023), global wheat production has only increased annually by no more than 1% (Dixon et al., 2009; Khadka et al., 2020). To our knowledge, no CRISPR/Cas9 system has been utilized yet to improve photosynthetic efficiency in wheat (though maize and rice have been tested; Wang et al., 2019a; Zheng et al., 2021b; Caddell et al., 2023), and here we will discuss the improvement of two other aspects of yield-related mechanisms *via* CRISPR/Cas9.

Gupta et al. (2023) generated CRISPR/Cas9 *T. aestivum* 'Fielder' lines, mutated in SQUAMOSA promoter-binding protein-like 13 (*TaSPL13*), the only gene in the *TaSPL* family in which the DSB would not occur in the coding region, rather in the 3'UTR. The mutation was generated in the miRNA156 Recognition Element (*M RE*), which, in turn, inhibited the miRNA156 suppression of *TaSPL13* transcription. The results in general showed that cleaving the MRE, while leaving the TaSPL13 protein intact, caused an increase of *TaSPL13-B* transcription (the majorly transcribed homeolog), a decrease in flowering time, tiller number and plant height and an increase in grain size and number. It is important to note that other genes have been targeted *via* CRISPR/Cas9 to increase seed size and weight (Wang et al., 2018; Wang et al., 2019b; Zhang et al., 2018; Zhang et al., 2019c), though we decided to focus on Gupta et al. (2023) as a case study regarding increasing seed size *via* CRISPR/Cas9.

Zhang et al. (2021) took a different approach to increase potential yield in wheat and generated CRISPR/Cas9 *T. aestivum* 'ZhengMai 7698' lines. These lines were mutated in abnormal cytokinin response1 repressor1 (*ARE1*), a repressor of ferredoxin-dependent glutamate 2-oxoglutarate aminotransferase (Fd-GOGAT), which is an enzyme directly involved in ammonium assimilation. Briefly, they have found that all mutant lines showed a higher tolerance to nitrogen (N) starvation, higher root-to-shoot ratio, higher chlorophyll content, delayed senescence (*i.e.*, exhibiting a prolonged 'stay green' phenotype compared to the wild type) and differential expression patterns for other genes involved in N assimilation and transport under N starvation. Specifically, the *AABBdd* and *aabbDD* mutants showed increased plant height, higher tiller number, higher spike length, higher spikelet number per spike, higher grain number per spike and higher 1000-grain weight.

3. Biofortification

Cereals, including wheat, have a slightly higher carbohydrate concentration albeit at the expense of protein concentration compared to

pulses (Bouchard et al., 2022), while also having a significantly higher yield per area (Joshi and Rao, 2017). These may be major factors as to why cereals still dominate globally at the expense of pulses (Singh, 2017). Besides their relatively lower protein content, cereals also contain antinutritional compounds, which cause malnutrition due to insufficient intake of micronutrients (Gupta et al., 2015). Such a compound is phytate, a chelator of micronutrients, specifically iron and zinc.

Ibrahim et al. (2022) created a *T. aestivum* L. 'Borlaug 2016' CRISPR/Cas9 mutant lines, mutated in inositol pentakisphosphate 2-kinase 1. A (*TaIPK1. A*) homoeolog, which showed lower phytate levels, higher iron and zinc levels, higher seed weight and length, though with a lower number of spikelets.

4. Lower gluten

Wheat is consumed mainly by grinding its seeds into flour and baking that flour into various products, *e.g.*, bread, pasta and cakes (Shewry, 2009). This is a unique characteristic of this crop due to the wheat storage proteins, *i.e.*, gluten, giving the dough viscoelasticity. Unfortunately, an approximation of 1% and 10% of the global population has celiac disease or gluten sensitivity, respectively (Sapone et al., 2011). The former entails an autoimmune reaction, which can result in diarrhea, abdominal distention, vomiting, anorexia, constipation, short stature, neurological symptoms, anemia and osteoporosis (Green and Cellier, 2007). The latter, which represents itself as distress subsequent to eating gluten-containing products, tends to be less severe with no intestinal damage (Sapone et al., 2011). Therefore, it is critical to generate wheat with low gluten content (both immunoreactive and non-immunoreactive), while retaining similar grain quality and product texture.

Sánchez-León et al. (2018) generated CRISPR/Cas9 *T. aestivum* 'BW208' and 'THA53' lines, mutated adjacent to a 33-amino acid peptide which is the immunodominant epitope in gluten reactivity (Tye-Din et al., 2010). They showed that α-, γ- and ω-gliadin (one of the two gluten protein families) levels were decreased in some of the lines, using A-PAGE and SDS-PAGE, while quantification *via* HPLC showed significant reduction in α- and γ-gliadin in most mutants. This caused a balancing effect with rising glutenin levels, specifically the high molecular weight fraction, which is associated with high quality flour (Rakszegi et al., 2005), while leaving the total protein levels unchanged. In a monoclonal ELISA test of R5 and G12 monoclonal antibodies (mAb; Valdés et al., 2003; Morón et al., 2008; respectively), they saw a strong reduction in gluten content, potentially signifying lower immunoreactivity. They also did not detect off-target mutations and confirmed stability and heritability of the low-gluten phenotype, along with full fertility and normal cytogenetics of the mutated lines. Finally, testing flour quality, they noted that in most cases the SDS levels were similar to those reported in 97% gluten-reduction RNAi lines, which showed high stability and tolerance to over-mixing, allowing production of bread similar to normal bread wheat (Gil-Humanes et al., 2010; Gil-Humanes et al., 2014a; Gil-Humanes et al., 2014b).

5. Drought tolerance

Drought, a water deficit on the whole-plant level, affects a plenitude of biological reactions, both plant-unique (*e.g.*, incapacitating photosynthetic machinery) and at the cell biology level (*e.g.*, loss of cellular turgor and impaired cell division; Farooq et al., 2009a; Farooq et al., 2009b). Crop yield loss was reported to be between approximately 30–90%, depending on the species tested (Hussain et al., 2019). This is especially concerning, due to climate change which is projected to increase drought occurrence across many global regions (Cook et al., 2018). Drought elicits a whole gene expression and hormone-receptor cascade, including ABA-dependent and ABA-independent pathways (including DREB [dehydration-responsive element-binding] and NAC [petunia *NAM* and Arabidopsis ATAFI, ATAF2, and CUC2] transcription factors; Shinozaki and Yamaguchi-Shinozaki, 2006). Main physiological plant responses to drought include active and passive downregulation of photosynthesis, fully or partially closing the stomata, "escaping" drought by shortening the plant's own life cycle, increasing root growth in order to increase water uptake, changing morphology (*e.g.*, producing smaller leaves), cellular osmotic adjustment and raised cellular antioxidation (Farooq et al., 2009b). Main transgenic approaches to instill drought tolerance include overexpression (OE) of drought-response-related transcription factors and phytohormone production genes, and finetuning physiological and morphological drought responses (*e.g.*, reducing stomata density, increasing root system length and density, increasing cellular antioxidant activity, raising soluble sugar content; Ilyas et al., 2021).

He et al. (2022) took a different approach by generating *T. aestivum* 'Fielder' CRISPR/Cas9 knockout (KO) lines, mutated in *T. aestivum* ECERIFERUM1–6A (*TaCER1–6A*) involved in wax alkane biosynthesis in wheat (as cuticular wax is known to protect the plant, *inter alia*, from water loss *via* involuntary transpiration; Ingram and Nawrath, 2017). They showed that the KO lines had significantly lower alkane content in seedling leaves and flag leaves (specifically C27-C33 alkanes, while OE lines showed the opposite trend). They also showed the induction of *TaCER1–6A* subsequent to drought, PEG, salinity and ABA applications. Subsequent to drought and salinity application, many other wax components values rose significantly, both in seedling leaves and flag leaves. Respectively, the OE lines showed lower chlorophyll leakage and water loss, and stayed greener than WT after 15 days of drought (while the KO lines showed the opposite results). They found two transcription factors (TaMYB96–2D and TaMYB96–5D; MYB stands for v-Myb myeloblastosis viral oncogene homolog), which plausibly bind to a specific motif in TaCER1–6A. They also noted that both the OE lines and WT lines under drought, showed no alteration to the total wax content, and they attribute this to the relatively low percentage of alkanes out of the total wax content in wheat, and to the hypothesis that specific components are designated for different roles, while the total wax content might not be as important, respectively.

6. Salinity tolerance

Salinity stress affects plants either by osmotic stress, inhibiting water uptake from the soil, or by ionic stress, causing cytotoxicity (Munns and Tester, 2008). Unfortunately, by 2050, 50% of arable land is projected to be salinized (Jamil et al., 2011), and even at moderate salinity, all agricultural glycophytes reduced their yield by over 50% (Zörb et al., 2019). Plant responses to salinity stress include sodium exclusion from leaf tissues, compartmentalization into vacuoles, and osmolyte accumulation (Munns and Tester, 2008). Besides physiological and morphological approaches, many genes and transcription factors are involved in salinity stress tolerance (*e.g.*, the sodium/hydrogen antiporter [NHX] for vacuole compartmentalization, high-affinity potassium transporter1 [HKT1] for cellular sodium uptake from the xylem and Salt Overly Sensitive 1 [SOS1] for sodium exclusion, and transcription factors including basic leucine zipper [bZIP], WRKY [named after the conserved WRKYGQK motif], basic helix–loop–helix [bHLH] and APETALA2/ ETHYLENE RESPONSE FACTOR [AP2/ERF]; Deinlein et al., 2014). Not much has been studied in wheat salinity stress tolerance using CRISPR/Cas9, as opposed to rice (Nazir et al., 2022), and we will discuss the sole relevant research published so far, to our knowledge.

Zheng et al. (2021a) generated *T. aestivum* 'Fielder' CRISPR/Cas9 KO lines, mutated in histone acetyltransferase of the GNAT family (GCN5-related N-terminal acetyltransferases) 1 in genomes A and B (*TaHAG1-KO-AB*), an acetyltransferase responsible for H3K9 and H3K14 acetylation in wheat. They reported that the KO line, compared with WT, showed lower shoot weight, lower spike length, lower number seeds per spike, higher Na^+ and lower K^+ in leaves under salinity stress. They further examined the role of TaHAG1 by comparing the bread wheat

progenitors (*T. turgidum* ['SCAUP'] and *Aegilops tauschii* ['SQ523']) with a synthetic allohexaploid wheat ['SCAUP/SQ523'] and comparing the WT 'Fielder' with TaHAG1 OE and *RNAi* KO lines. They revealed that SCAUP/SQ523 and SQ523 showed higher root and shoot growth, lower Na^+ and higher K^+ in leaves, higher expression of *TaHAG1*, higher levels of H_2O_2, and higher levels of superoxide dismutase (SOD), peroxidase (POD) and catalase (CAT) antioxidant activity under salinity stress, as compared to SCAUP. The OE lines showed higher root and shoot growth, lower Na^+, higher K^+, higher spike length, higher grain weight per spike, higher H_2O_2 levels, higher levels of H3K9 and H3K14 levels, and higher levels of SOD, POD and CAT activity under salinity stress, while the KO lines showed contrasting trends. They further found, *via* chromatin-immunoprecipitation (ChIP) analysis, that TaHAG1 plausibly binds under salinity stress as a transcription factor to the transcription starting sites (TSS) of *TraesCS4D02G324800*, *TraesCS1D02G284900*, and *TraesCS3D02G347900* (NADPH oxidases, involved in reactive oxygen species as signaling molecules under abiotic stress; Marino et al., 2012). These genes were also found to be upregulated in the OE lines and downregulated in the *RNAi* lines. Furthermore, the H3K9 and H3K14 acetylation at these TSS was significantly increased under salinity stress. All the results pointed, as they have concluded, towards the notion that *TaHAG1* activated, by epigenomic acetylation, ROS production under salinity stress, which caused tolerance to said stress.

7. Heat tolerance

Heat stress is a major contributor to yield uncertainties in the 21st century, due to climate change (for specifically wheat yields, see Asseng et al., 2013). Heat causes many cellular impairments, *e.g.*, protein dysfunction and misfolding and cellular and organellar membrane disruption (Richter et al., 2010), due to the lowering of the denaturation kinetic barrier (Bischof and He, 2006). The main currently known cellular response to heat stress is the activation of Heat Shock Proteins (HSPs), with functions including molecular chaperones, nucleic acid repair, metabolism reorganization and protein degradation (Richter et al., 2010), while physiological responses can include change in stomatal conductance (Marchin et al., 2022). As the temperature range for optimal growth of wheat during flowering and grain filling stages is quite narrow (Farooq et al., 2011), wheat yield is expected to decline significantly during the rise of the global temperature (Asseng et al., 2015). It is therefore crucial to use the most modern techniques to introduce heat-stress-tolerant wheat lines, to buffer this predicted strain on global food production.

Wen et al. (2023) generated *T. aestivum* 'Fielder' CRISPR/Cas9 KO lines, mutated in heat shock transcription factor subclass A6 'e' (*TaHSFA6e*; Kumar et al., 2018) and *T. aestivum* 'CB037' CRISPR/Cas9 KO lines, mutated in three groups of Heat Shock Protein 70 (*TaHSP70*) genes; the former being an upstream activator of the latter. They showed that in both lines, the survival rates were significantly much lower than WT, in response to heat stress, while showing no apparent vegetative negative effect under control conditions (though the TaHSP70 KO lines showed stunted plant height and a lower 1000-kernel weight, attributed to the putative additional involvement of TaHSP70 in agronomic traits). In order to explain the molecular mechanism of this phenotype, they showed that *TaHSFA6e* underwent alternative splicing (a known phenomenon specifically involved in heat shock response; reviewed for plants by Ling et al., 2021), resulting in one hypothetically-degraded protein (TaHSFA6e-I, due to a premature stop codon), and two functional proteins (TaHSFA6e-II and TaHSFA6e-III). While the former was overrepresented under moderate heat stress, the latter was upregulated only under high heat stress. Both bound to the mentioned *TaHSP70*s, though the latter activated the genes to a higher extent than the former, due to a 14 amino acid section, putatively upregulating transcription activation. Finally, they showed that the TaHSP70s co-localized with stress granules (complexes containing non-translating ribonucleoproteins, "frozen"for the duration of environmental stress; Protter and Parker, 2016), while the TaHSP70 mutants showed decreased stress granule disassociation, translational efficiency and translation re-initiation, during recovery from heat stress.

8. Cold tolerance

Even though climate change is typically associated with rising temperatures, it also entails unpredictable significantly lower-than-average temperatures, specifically in wheat-grown areas (Zhang et al., 2023). Cold stress causes cellular damage, mainly due to changing the permeability and material phase of the membrane, thus deactivating membranous enzymes crucial for cellular function, and allowing the unregulated influx and outflux of molecules (Zhang et al., 2019a). This is beside the fact that, similarly to heat stress (as mentioned above), cold stress shifts all enzymes from their optimal functional and structural temperature range, which affects all biological functions. Responses to cold stress include activating cold-induced genes, actively reducing growth, changing membrane composition and increasing antioxidant levels (Xin and Browse, 2000). All in all, this can cause major developmental and reproductive impediments, which can cause more than 75% loss of yield in wheat (Soualiou et al., 2022). It is therefore imperative to prepare for climate-change-driven yield loss due to cold stress, along with yields lost to expected drought and heat stresses.

Zhang et al. (2023) generated *T. aestivum* 'Fielder' CRISPR/Cas9 KO lines, mutated in phosphoglycerate kinase (PGK), a key enzyme in glycolysis, which was suggested to be positively upregulated under cold stress to provide more energy to deal with said stress (Perotti et al., 2015). The mutant lines showed lower TaPGK activity, pyruvate content and lower cold stress tolerance, *i.e.*, exhibiting dehydration and leaf droopiness and high levels of electrolyte leakage rate (REC), hydrogen peroxide (H_2O_2; a cytotoxic molecule generated during stress) and malondialdehyde (MDA; a biological marker of cellular fatty acid peroxidation; they showed similar results in *T. durum* 'Kronos' ethyl methanesulfonate (EMS)-mutagenized, mutated in the *T. durum* ortholog of *TaPGK*, and opposite trends in *T. aestivum* 'Fielder', *Agrobacterium*-transformed with the LGY-OE3-*TaPGK* vector for OE). In order to explain the 'bigger picture', they showed that TaPGK underwent crotonylation (an epigenomic upregulation by adding crotonyl to lysine, recently associated with plant cold stress response; Lin et al., 2021) under cold stress. They also showed that *T. aestivum* sirtuin-like gene 1 (TaSRT1; sirtuins were previously shown to perform decrotonylation; Lu et al., 2018) interacted with TaPGK, and overexpressing TaSRT1 (both *via Agrobacterium* -transformation of *T. aestivum* 'Fielder' and transient expression both in tobacco and in wheat protoplasts) showed lower levels of TaPGK and of its crotonylation, while *T. durum* 'Kronos' EMS plants, mutated in the ortholog of *TaSRT1*, showed the opposite results. The TaSRT1 Kronos 'EMS' mutants also showed higher TaPGK activity and pyruvate levels, along with less drooping, and less REC, H_2O_2 and MDA levels under cold stress, while *T. aestivum* 'Fielder' OE lines showed opposing results. Finally, they showed that cold stress upregulated four key glycolysis enzymes (*T. aestivum* glyceraldehyde 3-phosphate dehydrogenase (TaGAPC), phosphoglycerate mutase (TaPGM), enolase (TaENO) and pyruvate kinase (TaPK)), which were also differentially expressed under cold stress in TaPGK OE lines (upregulated relative to WT) and in CRISPR/Cas9 KO and 'Kronos' EMS lines (downregulated relative to WT), while pyruvate was shown to alleviate the cold stress in CRISPR/Cas9 KO and 'Kronos' EMS lines.

9. Heavy metal tolerance

Plants uptake micronutrients (*i.e.*, vitamins and minerals, including some metals) mainly from the soil, which mainly function as cofactors for a plenitude of enzymatic reactions (Merchant, 2010). Unfortunately, other metals, which can be abundant in the soil anthropogenically (*e.g.*, *via* the production of fertilizers and energy and from industrial waste), and which are commonly taken up by plants inadvertently, are toxic

even in small concentrations, while some beneficial micronutrients are also detrimental to plant growth at high concentrations (Ghori et al., 2019). This is compounded by the effect of consumption of metal-containing plants on human health (reviewed in Alengebawy et al., 2021). Heavy metals inactivate and/or denature crucial cellular enzymes, thus affecting major biological pathways, and main mechanisms of tolerance include avoidance by exclusion of heavy metals from uptake into the roots and tolerance by chelation and sequestration into metabolically regulated components (*e.g.*, the vacuole; Hossain et al., 2012). Due to increasing anthropogenic accumulation of heavy metals (Hassan et al., 2022), it is imperative to generate crops that are also tolerant of high concentrations of heavy metals in the soil.

Wang et al. (2023) have generated *T. aestivum* 'Fielder' CRISPR/Cas9 KO mutants, mutated in *T. aestivum* plant high-affinity phosphate transporter 9 (TaPHT1;9), which functions as a transporter of phosphate. They showed that the CRISPR/Cas9 mutants were not affected in root and shoot length and root and shoot weight under no arsenic (a highly toxic heavy metal; Smith et al., 2002) conditions, while under 15 μM arsenic acid, they exhibited higher root and shoot length and weight, relative to the wild type. They also showed that the mutants accumulated significantly less arsenic acid in the roots and shoots, relative to the wild type. They further demonstrated that TaPHT1;9 imported arsenic acid competitively with phosphate, and this depended on the phosphate concentration, as it exhibited higher affinity to phosphate. They finally showed that another related transporter (TaPHT1;3) did not import arsenic acid, and they attributed this to a hydrophilic loop between transmembrane segment 6 (TM6) and 7 (TM7), present in TaPHT1;3 and absent in TaPHT1;9. While silencing *TaPHT1;9* (*via* barley stripe mosaic virus (BSMV) vector for virus-induced gene silencing (VIGS)) resulted in lower shoot and root weight under control conditions, though showing higher growth and lower arsenic acid levels under high arsenic acid conditions, silencing *TaPHT1;3* resulted in lower shoot and root weight under both conditions and arsenic acid levels similar to wild type. Similarly, OE of *TaPHT1;9* in rice resulted in lower root and shoot length and weight, and higher arsenic acid levels in roots and shoots under high arsenic acid levels (though the OE lines showed higher shoot weight under low arsenic acid levels), and these results were alleviated partially by exogenous phosphate enrichment.

10. Powdery Mildew resistance

Biotic stresses are also a major factor in global yield losses (Savary et al., 2019), and this is suggested to be, in many cases, compounded by climate change (Shahzad et al., 2021). Pathogens affect plant cell function by indirectly increasing the energy spent by the plant cell due to defense mechanisms, by actively extracting phytonutrients, and by altering natural plant physiology and metabolism (*e.g.*, altering plant hormone levels) for biotrophs (van Dijk et al., 2021) or inducing cell death *via* toxin and cell wall degrading enzyme excretion for necrotrophs (Barna et al., 2012). Microorganismal biotic stresses are mainly managed *via* a successful, or unsuccessful, plant immune system, which involves pathogen-associated molecular pattern (PAMP)-triggered immunity (PTI), and effector-triggered immunity (ETI), as resistant plants recognize either generic microbial indicators (*e.g.*, flagellin), recognized by transmembrane pattern recognition receptors (PRRs), or special proteins exported by pathogens to enhance their virulence, recognized by resistance (R) genes (Jones and Dangl, 2006), respectively. Important phytohormones involved in plant biotic stress responses include salicylic acid (SA), jasmonic acid (JA) and ethylene (ET; Kunkel and Brooks, 2002), and other signaling molecules in basically all stresses include reactive oxygen species (ROS; Mittler et al., 2011) and calcium ions (Tuteja and Mahajan, 2007). Powdery mildew is a major biotic disease, caused by *Erysiphales* fungi (*Blumeria graminis* f. sp. *tritici* [*Bgt*] in wheat). This disease affects many plants, specifically cereals (Hückelhoven and Panstruga, 2011), causing up to 62% yield loss, depending, *inter alia*, on geography and climate (Singh et al., 2016). Therefore, it is essential to develop bread wheat lines resistant of powdery mildew.

Song et al. (2022) have generated *T. aestivum* 'Fielder' CRISPR/Cas9 KO mutants, mutated in *T. aestivum* histone acetyltransferase GCN5-related 1 (TaHAG1), an important epigenetic gene activator (Interestingly, this is the same gene discussed by the same research group in the 'Salinity tolerance' chapter). They showed that the KO lines exhibited higher susceptibility to *Bgt*, *i.e.*, harboring more spores with higher branching, with a higher micro-colony formation index (MI) and less accumulation of H_2O_2 and salicylic acid (while *TaHAG1* OE lines showed opposing trends). To further explain the molecular mechanism, they compared RNA-seq results between the wild type and OE lines, and found that two genes, namely *T. aestivum* phytoalexin deficient 4 (TaPAD4) and *T. aestivum* enhanced disease susceptibility 1 (TaEDS1), which are known to be involved in disease tolerance *via* salicylic acid and reactive oxygen species (ROS) biosynthesis (causing systemic acquired resistance), were upregulated significantly in OE lines, while being downregulated in the KO lines. Chromatin immunoprecipitation analysis showed that TaHAG1 bound to the promoter of *TaPAD4*, but not to that of *TaEDS1*. Furthermore, H3K9ac and H3K14ac levels highly increased in the wild type (and even more so in the OE lines), while being decreased in the KO lines. KO (*via* CRISPR/Cas9) and overexpressing TaPAD4 exhibited similar trends to KO and overexpressing TaHAG1. Finally, they showed that TaHAG1 formed a dimer with *T. aestivum* plant AT-rich zinc-binding protein 5 (TaPLATZ5) to increase activation of TaPAD4, allegedly causing more salicylic acid and H_2O_2 formation downstream and resistance to *Bgt*.

11. Stripe rust resistance

Another important biotic pathogen in wheat is stripe rust, caused by the fungus *Puccinia striiformis* f. sp. *tritici* (*Pst*), which can cause up to 100% yield loss (Bhardwaj et al., 2019). A specific issue with cereal rusts, is that new strains, which manage to evade the immunity response, develop more quickly than our ability to conventionally produce and regulate resistant cultivars. It is therefore utmostly important to quickly generate wheat cultivars resistant to *Pst*, *via* the most modern technologies (*e.g.*, the CRISPR/Cas9 system).

He et al. (2023) generated *T. aestivum* 'Fielder' KO mutants, mutated in *T. aestivum* calcineurin B-like interacting protein kinase 14 (*TaCIPK14*), an important component in calcium-signaling in response to endogenous or environmental cues, of which some homologs have been reported to serve as susceptibility genes (genes, which their gain-of-function facilitates biotic susceptibility, rather than resistance; see Ma et al., 2021; Sardar et al., 2017). They show that the KO lines exhibited significantly less *Pst* formation, in a variety of current virulent strains. These lines also showed higher expression of known resistance genes, namely, *T. aestivum* pathogenesis-related 1, 2 and 5 (*TaPR1*, *TaPR2* and *TaPR5*, respectively), higher spread of H_2O_2 and cell death, and lower levels of reactive oxygen species scavenger-related gene *T. aestivum* catalase 2 (*TaCAT2*). Agronomically, the KO lines did not differ from the wild type under control conditions, while retaining higher kernel area and weight than wild type post *Pst* infection. Silencing *TaCIPK14 via* barley stripe mosaic virus (BSMV)-induced gene silencing (VIGS) caused lower *Pst* formation and higher TaPR1, TaPR2 and TaPR5 levels, while OE of TaCIPK14 caused higher *Pst* formation and lower expression of *TaPR1, TaPR2* and *TaPR5*.

12. Multiplexing these traits into a 'super wheat'

As mentioned above, multiplexing is a promising advantage of CRISPR/Cas9 genome editing over other methods, especially conventional breeding. This is necessary for creating a 'super wheat', *i.e.*, a wheat cultivar that is also high yielding of quality grain, but also tolerant/resistant to many abiotic and biotic stresses. Transformation of multiple genes was discussed even before the introduction of CRISPR/Cas9 technologies (see Naqvi et al., 2010). Yet the application of

CRISPR/Cas9 multiplexing has mainly been reported as targeting similar sequences in gene families with one sgRNA (Najera et al., 2019; though a use of transcription activator-like effector nucleases (*TALENs*) genome editing on two unrelated genes has been reported; Li et al., 2016). The theoretical expression of CRISPR/Cas9 to target multiple genes with multiple sequences and one Cas protein (*e.g.*, raise yield potential, biofortify and lower gluten content, while also introducing tolerance to various stresses) has been suggested, though the obstacle for doing so is the necessity of using multiple guide RNAs (Abdelrahman et al., 2021). Doing this *via* multiple cloning into one binary vector is very burdensome, and this can be solved by using advanced multi-cloning techniques, such as one-step Golden Gate cloning (Engler et al., 2008). This can be done either *via* expression of multiple cassettes of single transcript each under a promoter, or *via* expression of a single cassette including a polycistronic mRNA under one promoter, which is cleaved post-transcriptionally. The latter being advantageous due to a lot less promoter sequence and hence a much smaller plasmid. Cas12a, a Cas protein variant, can further reduce the quantity of necessary sequences needed to be added to the binary vector (Abdelrahman et al., 2021).

It is important to note two points specific to plants. CRISPR/Cas9 multiplexing is specifically important for polyploid plants (*e.g.*, tetraploid *T. durum*, durum wheat, and hexaploid *T. aestivum*, bread wheat), as homoeologs often render each other redundant, and therefore necessitate KO all of them, in order to notice a phenotypic effect of even one gene (Kannan et al., 2018). Another point is that genome editing for resistance of multiple biotic stresses has already been demonstrated, as a change in a single gene can cause resistance to multiple strains or even species, and this is called 'broad spectrum resistance' (Oliva et al., 2019).

All-in-all, hypothetically it would seem rather easy to use multiplexing to affect multiple traits. However, it is needed to discuss a few important issues. First, as most published papers are only examples of genes targeted per these traits, and we can assume that many other genes can be targeted alternatively, some genes are positive regulators of these desired traits, while others are negative regulators. It is, therefore, important to tweak the system to fit these terms and conditions. For example, while overexpressing TaCER1–6A in 'Fielder' conferred drought tolerance (He et al., 2022), knocking out TaPHT1;9 in 'Fielder' conferred arsenic tolerance (Wang et al., 2023), and therefore necessitate different CRISPR/Cas9 systems (*e.g.*, CRISPR activation (CRISPRa) for the former, while the classic KO CRISPR/Cas9 system for the latter).

Next, it is important to discuss the biological intersections between stresses. While hypothetically we could just multiplex all ten traits and more into one 'super wheat', the question remains if this is relevant biologically for two reasons. First, it is possible that tolerance to one stress is antagonistic to the tolerance of the other stress. For instance, drought tolerance can demand closing stomata to reduce transpiration, while heat tolerance can demand opening stomata to reduce plant temperature, and introducing both tolerances can cause commotion between the two response cascades (Mittler, 2006). Furthermore, often plants do not experience one stress at a time, and the tolerance to the simultaneous combination of more than one stress (*e.g.*, the combination of drought with heat) may not overlap with the two individual introduced tolerances (*e.g.*, introducing a gene that confers higher tolerance to drought and introducing a gene that confers higher tolerance to heat; Mittler, 2006). This becomes even more complex by hypothetically creating a 'super wheat' that is tolerant not to one, not to two but to multiple stresses and to all their unique combinations. Is this possible?

Naturally, it would be very convenient if we were able to simply create a 'super wheat' that is tolerant to every abiotic and biotic stress, and which can be used in every geography and climate, along with beneficial yield- and nutrition-related traits. However, due to the problems raised above, *i.e.*, the technical complexity of designing the transformation and genomic editing systems of that many different genes/traits (due to the size of sequences required, the possibly differing systems required for various traits and the actual plausibility of off-targets and unprecise editing), along with the biological complexities of the likely counteractions between those genes and traits (and their various combinations), and due to the naturally diverging 'sets' of stresses encountered in each locality (*e.g.*, drought and heat stresses would naturally occur much more frequently in the Middle East, rather than in Canada and New Zealand, while cold and freezing stresses would most definitely show an opposing trend), we propose rejecting this highly ambitious notion of a "one-size-fits-all" 'super wheat'. Even when the technical difficulties will be overcome (and one can assume they will be in the future), the almost guaranteed combinatorial effect of mutually offsetting stress responses pushes us towards a more humble approach of using enhanced landraces.

Landraces typically mean locally grown or transported varieties, dynamically adapted to respective local conditions (Zeven, 1998). Modern agriculture majorly swapped historical landraces with elite cultivars, drastically diminishing genetic diversity, a crucial key to agro-environmental resilience (Raggi et al., 2022). In the past few decades, a huge spotlight is returning onto landraces, due to their genetic potential for stress tolerance (Dwivedi et al., 2016). Recently, there is a call to expand the definition of 'landrace' to include traditional selection along with using omics knowledge, in order to maximize landrace potential (Gesesse et al., 2023). Another approach presented by Casañas et al. (2017), is to expand the definition of 'landrace' to "plant materials consisting of cultivated varieties that have evolved and may continue evolving, using conventional or modern breeding techniques, in traditional or new agricultural environments within a defined ecogeographical area and under the influence of local human culture." We thus propose adopting this definition, *i.e.*, taking the already existing local landraces and further introducing novel tolerance or enhancing existing tolerance to the expected combination of stresses in the respective area of growth. For example, wheat grown in Arid areas, we can assume it will frequently encounter drought and heat stresses and may be even salinity stress (due to its location and climate), along with major biotic pathogens to wheat, *e.g.*, powdery mildew and rusts (while also testing their combinations). At the end of the day, modern agriculture lapses by using monoculture and eliminating genetic material crucial for dynamic natural evolution which bolsters plants against stresses (Dwivedi et al., 2016), and growing landraces should allow biodiversity to survive. However, instead of introducing genetic material from landraces into cultivars, as suggested by others, we propose (similar to Casañas et al., 2017) taking landraces and editing specific genes' *via* CRISPR/Cas9 systems from within, in order to alter a small bank of genes-of-interest, while maintaining the majority of the genetic heterogeneity.

Based on current published research, the usage of CRISPR/Cas9 for characterization of plant traits is still limited to a single trait in a single cultivar and is mostly oriented towards gene discovery and functionality rather than agronomical improvement *per se*. This is probably due to the abovementioned limitations (*i.e.*, complex plant genomes, gene redundancy, currently immature CRISPR/Cas9 systems, GMO regulation, and the complexity of testing commercial-scale field experiments with high throughput phenotyping). Also, while CRISPR/Cas9 systems are currently being used mainly for KO mutations, OE mutations are mainly introduced *via* traditional genetic transformation methods. We would advocate introducing stress tolerances *via* activation CRISPR/Cas9 systems (CRISPRa, as discussed above; this is slowly being canonized, as more and more CRISPR/Cas9 variations are maturing; Murovec et al., 2017).

Future research in CRISPR/Cas9 based wheat improvement should also focus in creating wheat lines with actual higher yield in field conditions, better nutritional value and tolerance to multiple stresses, both under control and stressful conditions. This obviously will not be achieved within the normal timeframe of a few years of experiments. Rather, this will take many years of multiplex CRISPR/Cas9 design, transformation, and commercial testing, while addressing the regulatory

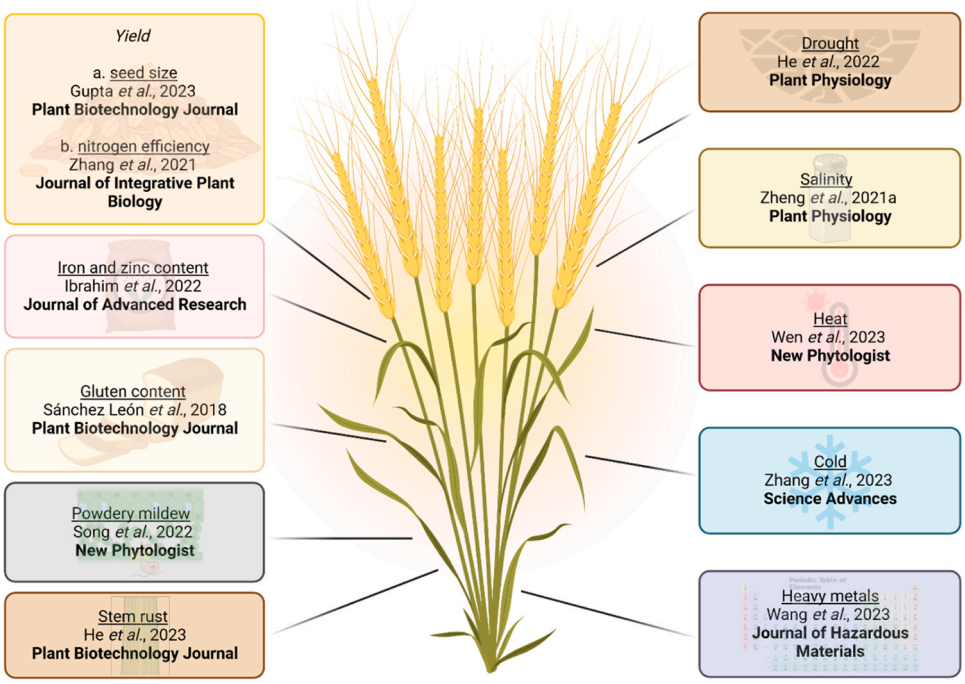

Fig. 1. A visual summary of the papers, genes and traits discussed in this review. This model was created with https://www.biorender.com.

and cultural issues regarding technologically altered crops.

We hope this paper encourages applicative CRISPR/Cas9 research in local varieties tolerant in the respective expected multi-stress combinations, along with tolerance to each individual stress. As opposed to dwarfed wheat which is highly prevalent globally (though geographically dependent; Pearch, 2021), we propose that the solution to the diversity of environmental stresses plants encounter, is local varieties with CRISPR/Cas9 genome editing for tolerance tailored to the specific 'cocktail' of stresses frequenting the relevant locality. Hopefully this will ensure diverse, yet robust wheat cultivars, able to sustain humanity throughout the century and beyond. This is not pertaining to the first three traits (*i.e.*, high yield, biofortification and minimal/mutated gluten content) and we would encourage incorporating these regardless of the respective 'cocktail of stresses' tolerance also introduced (though the prevalence of celiac and gluten intolerance might also depend on population genetics; Singh et al., 2018; Sallese et al., 2020).

13. Summary

In this paper we skimmed through 10 papers as a general example (for a visual summary, see Fig. 1), each demonstrating the use of CRISPR/Cas9 on an important single trait, either negatively or positively impacting wheat plants in that respective trait. This is very important, yet, frequently *in natura*, stresses occur in combination (Mittler, 2006). It is therefore imperative that research focuses on multiple stresses and tolerance towards them.

We would advocate the utilization of CRISPR/Cas9-edited local landraces that exhibit tolerance to specific stresses encountered in their respective locales. The success of this approach would be evaluated by comparing the yield per cultivated area and per unit of seed sown under both control and stressful conditions. Additionally, a comparison of metabolomic profiles would be conducted between the edited landrace, the original landrace and the common local cultivars. It would also compare the culinary and aesthetic characteristics of the flour and food products. We hope this serves as a clear callout to vigorous attempts to generate stress tolerant crops with higher yield before it is too late under climate change and population growth projections.

CRediT authorship contribution statement

Haber Zechariah: Conceptualization, Writing – original draft, Writing – review & editing. **Selvaraj K.S. Vijai:** Writing – review & editing. **Sharma Davinder:** Writing – review & editing. **Sade Nir:** Conceptualization, Writing – review & editing.

Declaration of Competing Interest

The authors declare that they have no known competing financial interests or personal relationships that could have appeared to influence the work reported in this paper.

Data Availability

No data was used for the research described in the article.

References

M. Abdelrahman, Z. Wei, J.S. Rohila, K. Zhao, Multiplex genome-editing technologies for revolutzionizing plant biology and crop improvement, Front. Plant Sci. 12 (2021) 721203.
A. Alengebawy, S.T. Abdelkhalek, S.R. Qureshi, M.Q. Wang, Heavy metals and pesticides toxicity in agricultural soil and plants: ecological risks and human health implications, Toxics 9 (2021) 42.
S. Anders, W. Cowling, A. Pareek, K.J. Gupta, S.L. Singla-Pareek, Gaining acceptance of novel plant breeding technologies, Trends Plant Sci. 26 (2021) 575–587.
A.V. Anzalone, P.B. Randolph, J.R. Davis, A.A. Sousa, L.W. Koblan, J.M. Levy, P.J. Chen, C. Wilson, G.A. Newby, A. Raguram, D.R. Liu, Search-and-replace genome editing without double-strand breaks or donor DNA, Nature 576 (2019) 149–157.
S. Asseng, F. Ewert, P. Martre, R.P. Rötter, D.B. Lobell, D. Cammarano, B.A. Kimball, M. J. Ottman, G.W. Wall, J.W. White, M.P. Reynolds, P.D. Alderman, P.V.V. Prasad, P. K. Aggarwal, J. Anothai, B. Basso, C. Biernath, A.J. Challinor, G. De Sanctis, J. Doltra, E. Fereres, M. Garcia-Vila, S. Gayler, G. Hoogenboom, L.A. Hunt, R. C. Izaurralde, M. Jabloun, C.D. Jones, K.C. Kersebaum, A.K. Koehler, C. Müller, S. N. Kumar, C. Nendel, G. O'Leary, J.E. Olesen, T. Palosuo, E. Priesack, E.E. Rezaei, A. C. Ruane, M.A. Semenov, I. Shcherbak, C. Stöckle, P. Stratonovitch, T. Streck, I. Supit, F. Tao, P.J. Thorburn, K. Waha, E. Wang, D. Wallach, J. Wolf, Z. Zhao, Y. Zhu, Rising temperatures reduce global wheat production, Nat. Clim. Change 5 (2015) 143–147.
S. Asseng, F. Ewert, C. Rosenzweig, J.W. Jones, J.L. Hatfield, A.C. Ruane, K.J. Boote, P. J. Thorburn, R.P. Rötter, D. Cammarano, N. Brisson, B. Basso, P. Martre, P. K. Aggarwal, C. Angulo, P. Bertuzzi, C. Biernath, J. Challinor, J. Doltra, S. Gayler, R. Goldberg, R. Grant, L. Heng, J. Hooker, L.A. Hunt, J. Ingwersen, R.C. Izaurralde,

K.C. Kersebaum, C. Müller, S.N. Kumar, C. Nendel, G. O'Leary, J.E. Olesen, T. M. Osborne, T. Palosuo, E. Priesack, D. Ripoche, M.A. Semenov, I. Shcherbak, P. Steduto, C. Stöckle, P. Stratonovitch, T. Streck, I. Supit, F. Tao, M. Travasso, K. Waha, D. Wallach, J.W. White, J.R. Williams, J. Wolf, Uncertainty in simulating wheat yields under climate change, Nat. Clim. Change 3 (2013) 827–832.

J. Bailey-Serres, J.E. Parker, E.A. Ainsworth, G.E.D. Oldroyd, J.I. Schroeder, Genetic strategies for improving crop yields, Nature 575 (2019) 109–118.

B. Barna, J. Fodor, B.D. Harrach, M. Pogány, Z. Király, The Janus face of reactive oxygen species in resistance and susceptibility of plants to necrotrophic and biotrophic pathogens, Plant Physiol. Biochem. 59 (2012) 37–43.

A.R. Bentley, J. Donovan, K. Sonder, F. Baudron, J.M. Lewis, R. Voss, P. Rutsaert, N. Poole, S. Kamoun, D.G.O. Saunders, D. Hodson, D.P. Hughes, C. Negra, M.I. Ibba, S. Snapp, T.S. Sida, M. Jaleta, K. Tesfaye, I. Becker-Reshef, B. Govaerts, Near-to long-term measures to stabilize global wheat supplies and food security, Nat. Food 3 (2022) 483–486.

S.C. Bhardwaj, G.P. Singh, O.P. Gangwar, P. Prasad, S. Kumar, Status of wheat rust research and progress in rust management- Indian context, Agronomy 9 (2019) 892.

J.C. Bischof, X. He, Thermal stability of proteins, Ann. N. Y. Acad. Sci. 1066 (2006) 12–33.

J. Bouchard, M. Malalgoda, J. Storsley, L. Malunga, T. Netticadan, S.J. Thandapilly, Health benefits of cereal grain- and pulse-derived proteins, Molecules 27 (2022) 3746.

D. Caddell, N.J. Langenfeld, M.J.H. Eckels, S. Zhen, R. Klaras, L. Mishra, B. Bugbee, D. Coleman-Derr, Photosynthesis in rice is increased by CRISPR/Cas9-mediated transformation of two truncated light-harvesting antenna, Front. Plant Sci. 14 (2023) 1050483.

T. Cardi, J. Murovec, A. Bakhsh, J. Boniecka, T. Bruegmann, S.E. Bull, T. Eeckhaut, M. Fladung, V. Galovic, A. Linkiewicz, T. Lukan, I. Mafra, K. Michalski, M. Kavas, A. Nicolia, J. Nowakowska, L. Sági, C. Sarmiento, K. Yıldırım, M. Zlatković, G. Hensel, K. Van Laere, CRISPR/Cas-mediated plant genome editing outstanding challenges a decade after implementation, Trends Plant Sci. (2023). DOI: https://doi.org/10.1016/j.tplants.2023.05.012.

F. Casañas, J. Simó, J. Casals, J. Prohens, Toward an evolved concept of landrace, Front. Plant Sci. 8:145 (2017).

L. Cong, F.A. Ran, D. Cox, S. Lin, R. Barretto, N. Habib, P.D. Hsu, X. Wu, W. Jiang, L. A. Marraffini, F. Zhang, Multiplex genome engineering using CRISPR/Cas systems, Science 339 (2013) 819–823.

B.I. Cook, J.S. Mankin, K.J. Anchukaitis, Climate change and drought: from past to future, Curr. Clim. Change Rep. 4 (2018) 164–179.

U. Deinlein, A.B. Stephan, T. Horie, W. Luo, G. Xu, J.I. Schroeder, Plant salt-tolerance mechanisms, Trends Plant Sci. 19 (2014) 371–379.

L.J.A. Van Dijk, J. Ehrlén, A.J.M. Tack, Direct and insect-mediated effects of pathogens on plant growth and fitness, J. Ecol. 109 (2021) 2769–2779.

J.A. Doudna, E. Charpentier, The new frontier of genome engineering with CRISPR-Cas9, Science 346 (2014) 1258096.

Dixon J., Braun H.J., Kosina P., Crouch J.H. (Eds.). 2009. Wheat facts and futures 2009. CIMMYT, Mexico City, Mexico.

S.L. Dwivedi, S. Ceccarelli, M.W. Blair, H.D. Upadhyaya, A.K. Are, R. Ortiz, Landrace germplasm for improving yield and abiotic stress adaptation, Trends Plant Sci. 21 (2016) 31–42.

C. Engler, R. Kandzia, S. Marillonnet, A one pot, one step, precision cloning method with high throughput capability, PLoS ONE 3 (2008) e3647.

M. Farooq, H. Bramley, J.A. Palta, K.H.M. Siddique, Heat stress in wheat during reproductive and grain-filling phases, Crit. Rev. Plant Sci. 30 (2011) 491–507.

M. Farooq, A. Wahid, S.M.A. Basra, Islam-ud-Din, Improving water relations and gas exchange with brassinosteroids in rice under drought stress, J. Agron. Crop Sci. 195 (2009a) 262–269.

M. Farooq, A. Wahid, N. Kobayashi, D. Fujita, S.M.A. Basra, Plant drought stress: effects, mechanisms and management, Agron. Sustain. Dev. 29 (2009b) 185–212.

C.A. Gesesse, B. Nigir, K. de Sousa, L. Gianfranceschi, G.R. Gallo, J. Poland, Y.G. Kidane, E. Abate Desta, C. Fadda, M.E. Pè, M. Dell'Acqua, Genomics-driven breeding for local adaptation of durum wheat is enhanced by farmers' traditional knowledge, Proc. Natl. Acad. Sci. U S A 120 (2023) e2205774119.

N.H. Ghori, T. Ghori, M.Q. Hayat, S.R. Imadi, A. Gul, V. Altay, M. Ozturk, Heavy metal stress and responses in plants, Int. J. Environ. Sci. Technol. 16 (2019) 1807–1828.

L.A. Gilbert, M.H. Larson, L. Morsut, Z. Liu, G.A. Brar, S.E. Torres, N. Stern-Ginossar, O. Brandman, E.H. Whitehead, J.A. Doudna, W.A. Lim, J.S. Weissman, L.S. Qi, CRISPR-mediated modular RNA-guided regulation of transcription in eukaryotes, Cell 154 (2013) 442–451.

J. Gil-Humanes, F. Pistón, R. Altamirano-Fortoul, A. Real, I. Comino, C. Sousa, C. M. Rosell, F. Barro, Reduced-gliadin wheat bread: an alternative to the gluten-free diet for consumers suffering gluten-related pathologies, PLoS ONE 9 (2014a) e90898.

J. Gil-Humanes, F. Pistón, F. Barro, C.M. Rosell, The shutdown of celiac diseae-related gliadin epitopes in bread wheat by RNAi provides flours with increased stability and better tolerance to over-mixing, PLoS ONE 9 (2014b) e91931.

J. Gil-Humanes, F. Pistón, S. Tollefsen, L.M. Sollid, F. Barro, Effective shutdown in the expression of celiac disease-related wheat gliadin T-cell epitopes by RNA interference, Proc. Natl. Acad. Sci. 107 (2010) 17023–17028.

H.C.J. Godfray, T. Garnett, Food security and sustainable intensification, Philos. Trans. R. Soc. B 369 (2014) 20120273.

A. Gupta, L. Hua, Z. Zhang, B. Yang, W. Li, CRISPR-induced miRNA156-recognition element mutations in TaSPL13 improve multiple agronomic traits in wheat, Plant Biotechnol. J. 21 (2023) 536–548.

R.K. Gupta, S.S. Gangoliya, N.K. Singh, Reduction of phytic acid and enhancement of bioavailable micronutrients in food grains, J. Food Sci. Technol. 52 (2015) 676–684.

P.H.R. Green, C. Cellier, Celiac disease, N. Engl. J. Med. 357 (2007) 1731–1743.

M.U. Hassan, M. Nawaz, A. Mahmood, A.A. Shah, A.N. Shah, F. Muhammad, M. Batool, A. Rasheed, M. Jaremko, N.R. Abdelsalam, M.E. Hasan, S.H. Qari, The role of zinc to mitigate heavy metals toxicity in crops, Front. Environ. Sci. 10 (2022) 990223.

F. He, C. Wang, H. Sun, S. Tian, G. Zhao, C. Liu, C. Wan, J. Guo, X. Huang, G. Zhan, X. Yu, Z. Kang, J. Guo, **Simultaneous editing of three homoeologues of *TaCIPK14* confers broad-spectrum resistance to stripe rust in wheat**, Plant Biotechnol. J. 21 (2023) 354–368.

J. He, C. Li, N. Hu, Y. Zhu, Z. He, Y. Sun, Z. Wang, Y. Wang, ***ECERIFERUM1-6A* is required for the synthesis of cuticular wax alkanes and promotes drought tolerance in wheat**, Plant Physiol. 190 (2022) 1640–1657.

Y. He, Y. Zhao, Technological breakthroughs in generating transgene-free and genetically stable CRISPR-edited plants, aBIOTECH 1 (2019) 88–96.

P. Horvath, R. Barrangou, CRISPR/Cas, the immune system of Bacteria and Archaea, Science 327 (2010) 167–170.

M.A. Hossain, P. Piyatida, J.A.T. da Silva, M. Fujita, Molecular mechanism of heavy metal toxicity and tolerance in plants: central role of glutathione in detoxification of reactive oxygen species and methylglyoxal and in heavy metal chelation, J. Bot. 2012 (2012) 872875.

S. Huang, D. Weigel, R.N. Beachy, J. Li, A proposed regulatory framework for genome-edited crops, Nat. Genet. 48 (2016) 109–111.

R. Hückelhoven, R. Panstruga, Cell biology of the plant-powdery mildew interaction, Curr. Opin. Plant Biol. 14 (2011) 738–746.

S. Hussain, S. Hussain, T. Qadir, A. Khaliq, U. Ashraf, A. Parveen, M. Saqib, M. Rafiq, Drought stress in plants: an overview on implications, tolerance mechanisms and agronomic mitigation strategies, Plant Sci. Today 6 (2019) 389–402.

S. Ibrahim, B. Saleem, N. Rehman, S.A. Zafar, M.K. Naeem, M.R. Khan, **CRISPR/Cas9 mediated disruption of *Inositol Pentakisphosphate 2-Kinase 1* (*TaIPK1*) reduces phytic acid and improves iron and zinc accumulation in wheat grains**, J. Adv. Res. 37 (2022) 33–41.

M. Ilyas, M. Nisar, N. Khan, A. Hazrat, A.H. Khan, K. Hayat, S. Fahad, A. Khan, A. Ullah, Drought tolerance strategies in plants: a mechanistic approach, J. Plant Growth Regul. 40 (2021) 926–944.

G. Ingram, C. Nawrath, The roles of the cuticle in plant development: organ adhesions and beyond, J. Exp. Bot. 68 (2017) 5307–5321.

A. Jamil, S. Riaz, M. Ashraf, M.R. Foolad, Gene expression profiling of plants under salt stress, Crit. Rev. Plant Sci. 30 (2011) 435–458.

M. Jinek, K. Chylinski, I. Fonfara, M. Hauer, J.A. Doudna, E. Charpentier, A programmable dual-RNA-guided DNA endonuclease in adaptive bacterial immunity, Science 337 (2012) 816–821.

M. Jinek, A. East, A. Cheng, S. Lin, E. Ma, J. Doudna, RNA-programmed genome editing in human cells, eLife 2 (2013) e00471.

J.D.G. Jones, J.L. Dangl, The plant immune system, Nature 444 (2006) 323–329.

P.K. Joshi, P.P. Rao, Global pulses scenario: status and outlook, Ann. N. Y. Acad. Sci. 1392 (2017) 6–17.

B. Kannan, J.H. Jung, G.W. Moxley, S.M. Lee, F. Altpeter, **TALEN-mediated targeted mutagenesis of more than 100 *COMT* copies/alleles in highly polyploid sugarcane improves saccharification efficiency without compromising biomass yield**, Plant Biotechnol. J. 16 (2018) 856–866.

A.P. Kausch, K. Nelson-Vasilchik, J. Hague, M. Mookan, H. Quemada, S. Dellaporta, C. Fragoso, Z.J. Zhang, Edit at will: genotype independent plant transformation in the era of advanced genomics and genome editing, Plant Sci. 281 (2019) 186–205.

K. Khadka, H.J. Earl, M.N. Raizada, A. Navabi, A physio-morphological trait-based approach for breeding drought tolerant wheat, Front. Plant Sci. 11 (2020) 715.

A.C. Komor, Y.B. Kim, M.S. Packer, J.A. Zuris, D.R. Liu, Programmable-editing of a target base in genomic DNA without double-stranded DNA cleavage, Nature 533 (2016) 420–424.

R. Kumar, A. Kaur, A. Pandey, H.M. Mamrutha, G.P. Singh, CRISPR-based genome editing in wheat: a comprehensive review and future prospects, Mol. Biol. Rep. 46 (2019) 3557–3569.

R.R. Kumar, S. Goswami, K. Singh, K. Dubey, G.K. Rai, B. Singh, S. Singh, M. Grover, D. Mishra, S. Kumar, S. Bakshi, A. Rai, H. Pathak, V. Chinnusamy, S. Praveen, Characterization of novel heat-responsive transcription factor (TaHSFA6e) gene involved in regulation of heat shock proteins (HSP) – A key member of heat stress-tolerance network of wheat, J. Biotechnol. 279 (2018) 1–12.

B.N. Kunkel, D.M. Brooks, Cross talk between signaling pathways in pathogen defense, Curr. Opin. Plant Biol. 5 (2002) 325–331.

J. Li, Y. Li, L. Ma, Recent advances in CRISPR/Cas9 and applications for wheat functional genomics and breeding, aBIOTECH 2 (2021a) 375–385.

J. Li, T.J. Stoddard, Z.L. Demorest, P.O. Lavoie, S. Luo, B.M. Clasen, F. Cedrone, E.E. Ray, A.P. Coffman, A. Daulhac, A. Yabandith, A.J. Retterath, L. Mathis, D.F. Voytas, M. A. D'Aoust, F. Zhang, **Multiplexed, targeted gene editing in *Nicotiana benthamiana* for glycol-engineering and monoclonal antibody production**. Plant Biotechnol. J. 14 (2016) 533–542.

S. Li, C. Zhang, J. Li, Y. Lei, N. Wang, L. Xia, Present and future prospects for wheat improvement through genome editing and advanced technologies, Plant Commun. 2 (2021b) 100211.

P. Lin, H.R. Bai, L. He, Q.X. Huang, Q.H. Zeng, Y.Z. Pan, B.B. Jiang, F. Zhang, L. Zhang, Q.L. Liu, **Proteome-wide and lysine crotonylation profiling reveals the importance of crotonylation in chrysanthemum (*Dendrathema grandiforum*) under low-temperature**, BMC Genom. 22 (2021) 51.

H.L. Ling, L. Dong, Z.P. Wang, H.Y. Zhang, C.Y. Han, B. Liu, X.C. Wang, Q.J. Chen, A CRISPR/Cas9 toolkit for multiplex genome editing in plants, BMC Plant Biol. 14 (2014) 327.

Y. Ling, M.M. Mahfouz, S. Zhou, Pre-mRNA alternative splicing as a modulator for heat stress response in plants, Trends Plant Sci. 26 (2021) 1153–1170.

G. Liu, Q. Lin, S. Jin, C. Gao, The CRISPR-Cas toolbox and gene editing technologies, Mol. Cell 82 (2022) 333–347.
Y. Lu, Q. Xu, Y. Liu, Y. Yu, Z.Y. Cheng, Y. Zhao, D.X. Zhou, Dynamics and functional interplay of histone lysine butyrylation, crotonylation, and acetylation in rice under starvation and submergence, Genome Biol. 19 (2018) 144.
Y. Ma, Q. Chen, J. He, J. Cao, Z. Liu, J. Wang, Y. Yang, **The kinase CIPK14 functions as a negative regulator of plant immune responses to *Pseudomonas syringae* in *Arabidopsis***, Plant Sci. 312 (2021) 111017.
P. Mali, L. Yang, K.M. Esvelt, J. Aach, M. Guell, J.E. Dicarlo, J.E. Norville, G.M. Church, RNA-guided human genome engineering via Cas9, Science 339 (2013) 823–826.
R.M. Marchin, D. Backes, A. Ossola, M.R. Leishman, M.G. Tjoelker, D.S. Ellsworth, Extreme heat increases stomatal conductance and drought-induced mortality risk in vulnerable plant species, Glob. Change Biol. 28 (2022) 1133–1146.
D. Marino, C. Dunand, A. Puppo, N. Pauly, A burst of plant NADPH oxidases, Trends Plant Sci. 17 (2012) 9–15.
S.S. Merchant, The elements of plant micronutrients, Plant Physiol. 154 (2010) 512–515.
R. Mittler, Abiotic stress, the field environment and stress combination, Trends Plant Sci. 11 (2006) 15–19.
R. Mittler, S. Vanderauwera, N. Suzuki, G. Miller, V.B. Tognetti, K. Vandepoele, M. Gollery, V. Shulaev, F. Van Breusegem, ROS signaling: the new wave? Trends Plant Sci. 16 (2011) 300–309.
B. Morón, Á. Cebolla, H. Manyani, M. Álvarez-Maqueda, M. Megías, M. del Carmen Thomas, M.C. López, C. Sousa, Sensitive detection of cereal fractions that are toxic to celiac disease patients by using monoclonal antibodies to a main immunogenic wheat peptide, Am. J. Clin. Nutr. 87 (2008) 405–414.
R. Munns, M. Tester, Mechanisms of salinity tolerance, Annu. Rev. Plant Biol. 59 (2008) 651–681.
J. Murovic, Ž. Pirc, B. Yang, New variants of CRISPR RNA-guided genome editing enzymes, Plant Biotechnol. J. 15 (2017) 917–926.
V.A. Najera, R.M. Twyman, P. Christou, C. Zhu, Applications of multiplex genome editing in higher plants, Curr. Opin. Biotechnol. 59 (2019) 93–102.
S. Naqvi, G. Farré, G. Sanahuja, T. Capell, C. Zhu, P. Christou, When more is better: multigene engineering in plants, Trends Plant Sci. 15 (2010) 48–56.
R. Nazir, S. Mandal, S. Mitra, M. Ghorai, N. Das, N.K. Jha, M. Majumder, D.K. Pandey, A. Dey, Clustered regularly interspaced short palindromic repeats (CRISPR)/CRISPR-associated genome-editing toolkit to enhance salt stress tolerance in rice and wheat, Physiol. Plant. 174 (2022) e13642.
R. Oliva, C. Ji, G. Atienza-Grande, J.C. Huguet-Tapia, A. Perez-Quintero, T. Li, J.S. Eom, C. Li, H. Nguyen, B. Liu, F. Auguy, C. Sciallano, V.T. Luu, G.S. Dossa, S. Cunnac, S. M. Schmidt, I.H. Slamet-Loedin, C.V. Cruz, B. Szurek, W.B. Frommer, F.F. White, B. Yang, Broad-spectrum resistance to bacterial blight in rice using genome editing, Nat. Biotechnol. 37 (2019) 1344–1350.
N. Tuteja, S. Mahajan, Calcium signaling network in plants, Plant Signal. Behav. 2 (2007) 79–85.
V.E. Perotti, A.S. Moreno, K.E.J. Trípodi, G. Meier, F. Bello, M. Cocco, D. Vázquez, C. Anderson, F.E. Podestá, Proteomic and metabolomic profiling of Valencia orange fruit after natural frost exposure, Physiol. Plant. 153 (2015) 337–354.
D.S.W. Protter, R. Parker, Principles and properties of stress granules, Trends Cell Biol. 26 (2016) 668–679.
L.S. Qi, M.H. Larson, L.A. Gilbert, J.A. Doudna, J.S. Weissman, A.P. Arkin, W.A. Lim, Repurposing CRISPR as an RNA-guided platform for sequence-specific control of gene expression, Cell 152 (2013) 1173–1183.
L. Raggi, L.C. Pacicco, L. Caproni, C. Álvarez-Muñiz, K. Annamaa, A.M. Barata, D. Batir-Rusu, M.J. Díez, M. Heinonen, V. Holubec, S. Kell, H. Kutnjak, H. Maierhofer, G. Poulsen, J. Prohens, P. Ralli, F. Rocha, M.L.R. Teso, D. Sandru, P. Santamaria, S. Sensen, O. Shoemark, S. Soler, S. Străjeru, I. Thormann, J. Weibull, N. Maxted, V. Negri, **Analysis of landrace cultivation in Europe: a means to support *in situ* conservation of crop diversity**, Biol. Conserv. 267 (2022) 109460.
M. Rakszegi, F. Békés, L. Láng, L. Tamás, P.R. Shewry, Z. Bedő, Technological quality of transgenic wheat expressing an increased amount of a HMW glutenin subunit, J. Cereal Sci. 42 (2005) 15–23.
M. Reynolds, J. Foulkes, R. Furbank, S. Griffiths, J. King, E. Murchie, M. Parry, G. Slafer, Achieving yield gains in wheat, Plant Cell Environ. 35 (2012) 1799–1823.
K. Richter, M. Haslbeck, J. Buchner, The heat shock response: life on the verge of death, Mol. Cell 40 (2010) 253–266.
M. Sallese, L.R. Lopetuso, K. Efthymakis, M. Neri, Beyond the HLA genes in gluten-related disorders, Front. Nutr. 7 (2020) 575844.
S. Sánchez-León, J. Gil-Humanes, C.V. Ozuna, M.J. Giménez, C. Sousa, D.F. Voytas, F. Barro, Low-gluten, nontransgenic wheat engineered with CRISPR/Cas9, Plant Biotechnol. J. 16 (2018) 902–910.
A. Sapone, K.M. Lammers, V. Casolaro, M. Cammarota, M.T. Giuliano, M. De Rosa, R. Stefanile, G. Mazzarella, C. Tolone, M.I. Russo, P. Esposito, F. Ferraraccio, M. Cartenì, G. Riegler, L. de Magistris, A. Fasano, Divergence of gut permeability and mucosal immune gene expression in two gluten-associated conditions: celiac disease and gluten sensitivity, BMC Med. 9 (2011) 23.
A. Sardar, A.K. Nandi, D. Chattopadhyay, **CBL-interacting protein kinase 6 negatively regulates immune response to *Pseudomonas syringae* in Arabidopsis**, J. Exp. Bot. 68 (2017) 3573–3584.
S. Savary, L. Willocquet, S.J. Pethybridge, P. Esker, N. McRoberts, A. Nelson, The global burden of pathogens and pests on major food crops, Nat. Ecol. Evol. 3 (2019) 430–439.
A. Shahzad, S. Ullah, A.A. Dar, M.F. Sardar, T. Mehmood, M.A. Tufail, A. Shakoor, M. Haris, Nexus on climate change: agriculture and possible solution to cope future climate change stresses, Environ. Sci. Pollut. Res. 28 (2021) 14211–14232.
O. Shalem, N.E. Sanjana, E. Hartenian, X. Shi, D.A. Scott, T.S. Mikkelsen, D. Heckl, B. L. Ebert, D.E. Root, J.G. Doench, F. Zhang, Genome-scale CRISPR-Cas9 knockout screening in human cells, Science 343 (2014) 84–87.
P.R. Shewry, Wheat, J. Exp. Bot. 60 (2009) 1537–1553.
P.R. Shewry, S.J. Hey, The contribution of wheat to human diet and health, Food Energy Secur. 4 (2015) 178–202.
K. Shinozaki, K. Yamaguchi-Shinozaki, Gene networks involved in drought stress response and tolerance, J. Exp. Bot. 58 (2006) 221–227.
N. Singh, Pulses: an overview, J. Food Sci. Technol. 54 (2017) 853–857.
P. Singh, A. Arora, T.A. Strand, D.A. Leffler, C. Catassi, P.H. Green, C.P. Kelly, V. Ahuja, G.K. Makharia, Global prevalence of celiac disease: systematic review and meta-analysis, Clin. Gastroenterol. Hepatol. 16 (2018) 823–836.
R.P. Singh, P.K. Singh, J. Rutkoski, D.P. Hodson, X. He, L.N. Jørgensen, M.S. Hovmøller, J. Huerta-Espino, Disease impact on wheat yield potential and prospects of genetic control, Annu. Rev. Phytopathol. 54 (2016) 303–322.
A.H. Smith, P.A. Lopipero, M.N. Bates, C.M. Steinmaus, Arsenic epidemiology and drinking water standards, Science 296 (2002) 2145–2146.
N. Song, J. Lin, X. Liu, Z. Liu, D. Liu, W. Chu, J. Li, Y. Chen, S. Chang, Q. Yang, X. Liu, W. Guo, M. Xin, Y. Yao, H. Peng, Z. Ni, C. Xie, Q. Sun, Z. Hu, Histone acetyltransferase TaHAG1 interacts with TaPLATZ5 to activate TaPAD4 expression and positively contributes to powdery mildew resistance in wheat, N. Phytol. 236 (2022) 590–607.
S. Soualiou, F. Duan, X. Li, W. Zhou, Crop production under cold stress: an understanding of plant responses, acclimation processes, and management strategies, Plant Physiol. Biochem. 190 (2022) 47–61.
J.A. Tye-Din, J.A. Stewart, J.A. Dromey, T. Beissbarth, D.A. van Heel, A. Tatham, K. Henderson, S.I. Mannering, C. Gianfrani, D.P. Jewell, A.V.S. Hill, J. McCluskey, J. Rossjohn, R.P. Anderson, **Comprehensive, quantitative mapping of T cell epitopes in gluten in celiac disease**. Science Translational Medicine, 41ra51 2 (2010).
I. Valdés, E. García, L. Mercedes, E. Méndez, Innovative approach to low-level gluten determination in foods using a novel sandwich enzyme-linked immunosorbent assay protocol, Eur. J. Gastroenterol. Hepatol. 15 (2003) 465–747.
W. Wang, Q. Pan, B. Tian, F. He, Y. Chen, G. Bai, A. Akhunova, H.N. Trick, E. Akhunov, Gene editing of the wheat homologs of TONNEAU1-recruiting motif encoding gene affects grain shape and weight in wheat, Plant J. 100 (2019b) 251–264.
W. Wang, J. Simmonds, Q. Pan, D. Davidson, F. He, A. Battal, A. Akhunova, H.N. Trick, C. Uauy, E. Akhunov, **Gene editing and mutagenesis reveal inter-cultivar differences and additivity in the contribution of *TaGW2*** homoeologues to grain size and weight in wheat, Theor. Appl. Genet. 131 (2018) 2463–2475.
H. Wang, S. Yan, H. Xin, W. Huang, H. Zhang, S. Teng, Y.C. Yu, A.R. Fernie, X. Lu, P. Li, S. Li, C. Zhang, Y.L. Ruan, L.Q. Chen, Z. Lang, A subsidiary cell-localized glucose transporter promotes stomatal conductance and photosynthesis, Plant Cell 31 (2019a) 1328–1343.
J.Y. Wang, J.A. Doudna, CRISPR technology: a decade of genome editing is only the beginning, Science 379 (2023) eadd8643.
P. Wang, Z. Chen, Y. Meng, H. Shi, C. Lou, X. Zheng, G. Li, X. Li, W. Peng, G. Kang, Wheat PHT1;9 acts as one candidate arsenate absorption transporter for phytoremediation, J. Hazard. Mater. 452 (2023) 131219.
J. Wen, Z. Qin, L. Sun, Y. Zhang, D. Wang, H. Peng, Y. Yao, Z. Hu, Z. Ni, Q. Sun, M. Xin, Alternative splicing of TaHSFA6e modulates heat shock protein-mediated translational regulation in response to heat stress in wheat, N. Phytol. 239 (2023) 2235–2247.
Z. Xin, J. Browse, Cold comfort farm: the acclimation of plants to freezing temperatures, Plant, Cell Environ. 23 (2000) 893–902.
C.D. Yeh, C.D. Richardson, J.E. Corn, Advances in genome editing through control of DNA repair pathways, Nat. Cell Biol. 21 (2019) 1468–1478.
A.C. Zeven, Landraces: a review of definitions and classifications, Euphytica 104 (1998) 127–139.
H. Zhang, J. Dong, X. Zhao, Y. Zhang, J. Ren, L. Xing, C. Jiang, X. Wang, J. Wang, S. Zhao, H. Yu, Research progress in membrane lipid metabolism and molecular mechanism in peanut cold tolerance, Front. Plant Sci. 10 (2019a) 838.
J. Zhang, H. Zhang, S. Li, J. Li, L. Yan, L. Xia, **Increasing yield potential through manipulating of an *ARE1* ortholog related to nitrogen use efficiency in wheat by CRISPR/Cas9**, J. Integr. Plant Biol. 63 (2021) 1649–1663.
N. Zhang, S. Wang, S. Zhao, D. Chen, H. Tian, J. Li, L. Zhang, S. Li, L. Liu, C. Shi, X. Yu, Y. Ren, F. Chen, **Global crotonylatome and GWAS revealed a *TaSRT1-TaPGK* model regulating wheat cold tolerance through mediating pyruvate**, Sci. Adv. 9 (2023) eadg1012.
Y. Zhang, D. Li, D. Zhang, X. Zhao, X. Cao, L. Dong, J. Liu, K. Chen, H. Zhang, C. Gao, D. Wang, Analysis of the functions of TaGW2 homoeologs in wheat grain weight and protein content traits, Plant J. 94 (2018) 857–866.
Y. Zhang, A.A. Malzahn, S. Sretenovic, Y. Qi, The emerging and uncultivated potential of CRISPR technology in plant science, Nat. Plants 5 (2019b) 778–794.
Y. Zhang, M. Pribil, M. Palmgren, C. Gao, A CRISPR way for accelerating improvement of food crops, Nat. Food 1 (2020) 200–205.
Z. Zhang, L. Hua, A. Gupta, D. Tricoli, K.J. Edwards, B. Yang, W. Li, Development of an Agrobacterium-delivered CRISPR/Cas9 system for wheat genome editing, Plant Biotechnol. J. 17 (2019c) 1623–1635.
M. Zheng, J. Lin, X. Liu, W. Chu, J. Li, Y. Gao, K. An, W. Song, M. Xin, Y. Yao, H. Peng, Z. Ni, Q. Sun, Z. Hu, Histone acetyltransferase TaHAG1 acts as a crucial regulator to strengthen salt tolerance of hexaploid wheat, Plant Physiol. 186 (2021a) 1951–1969.
S. Zheng, C. Ye, J. Lu, J. Liufu, L. Lin, Z. Dong, J. Li, C. Zhuang, Improving the rice photosynthetic efficiency and yield by editing ***OsHXK1* via CRISPR/Cas9 system**, Int. J. Mol. Sci. 22 (2021b) 9554.
C. Zörb, C.M. Geilfus, K.J. Dietz, Salinity and crop yield, Plant Biol. 21 (2019) 31–38.

Sub- chapter 4.4

Results presented in this sub-chapter are unpublished and are presented in an MS format.

Title: Network analysis and machine learning identify important control points in metabolic pathway associated with abiotic stress in the bread wheat pan-genome collection

Network analysis and machine learning identify important control points in metabolic pathways associated with abiotic stress in the bread wheat pan-genome collection

Zechariah Haber[1#], Davinder Sharma[1#], David Toubiana[1#], Tomer Parpar[1], Dagan Sade[2], Weronika Jasinska[3], Ahan Dalal[1], Gilor Kelly[4], Felix Shaya[4], Mira Carmeli-Weissberg[4], Shahar Rezenman[2], Nir Carmi[4], Wei Chen[5,6], Yariv Brotman[1,3], Amir Sharon[1], Saleh Alseekh[7], Alisdair R Fernie[7] and Nir Sade[1*]

[1]School of Plant Sciences and Food Security, Tel Aviv University, Tel Aviv, 69978 Israel

[2]Department of Biomolecular Sciences, Weizmann Institute of Science, 7610001 Rehovot,

[3]Department of Life Sciences, Ben Gurion University of the Negev, Beer Sheva, Israel

[4] Institute of Plant Sciences, Agricultural Research Organization, The Volcani Center, Rishon LeZion 7505101, Israel

[5] National Key Laboratory of Crop Genetic Improvement and National Center of Plant Gene Research (Wuhan), Huazhong Agricultural University, Wuhan 430070, China

[6]Hubei Hongshan Laboratory, Wuhan 430070, China

[7]Max Planck Institute of Molecular Plant Physiology, Potsdam-Golm, Germany

[#]equal contribution

[*]**Corresponding author**: nirsa@tauex.tau.ac.il

Keywords

Triticum aestivum, multi-omics, pangenome, correlation network analysis, Pearson correlation, indole-3-acetic acid inactivation VIII, L-carnitine biosynthesis,

Significance statement

Here adopt both multi-omics and systems biology along with standard statistical correlation and prove the importance of this approach with respect to auxin inactivation and carnitine biosynthesis, under drought and salinity stress. In doing so we demonstrate the power of combining these approaches in attempts to mitigate against future climate change scenarios.

Abstract

Triticum aestivum is a major global crop, responsible for a fifth of global human calorie consumption. The gap between supply and demand in many global crops is expected to rise mainly due to the co-incidence of massive population growth and climate change. Recently, multi-omics have allowed the relatively cheap generation of high-throughput biological data, yet their Achilles' heel of these approach seems to be the inability to manually process the torrent of data that such methods produce. As a consequence, many researchers are turning to statistical and computational biology, *i.e.*, "systems biology", to mine the data . Here, we use a multi-omics-based approach to studythe *Triticum aestivum* pangenome. We combined physiolomes, metabolomess, transcriptomes and microbiomes and analyzed the combined datasets using state-of-the-art correlation-based network analysis and machine learning techniques. Our analysis identified two pathways (indole-3-acetic acid inactivation VIII and L-carnitine biosynthesis), predicted exclusively under drought and salinity treatments, which were highly correlated with the expression of five genes (TraesCS1B02G388700, TraesCS5A02G024900, TraesCS6B02G191900, TraesCS6D02G286900 and TraesCS3D02G246700), four microbial counts (the genus of *Hydrogenophaga*, the order of *Neisseriales*, the genus of *Phenylobacterium* and the genus of *Jahnella*) and two physiological parameters (nitrogen content and shoot allocation). To verify our results, we generated virus-induced silenced gene lines, knocking down TraesCS5A02G024900 and TraesCS6D02G286900, which resulted in altered shoot allocation, and a change in either carnitine or auxin content (respectively), and modified expression of the respective genes involved in their metabolism. These combined findings illustrate how pan-genomes can be exploited in order to predict which alleles can improve plant performance in the changing climatic situation on earth and as such will likely contribute to closing the gap between global food demand and supply.

Introduction

Bread wheat (*Triticum aestivum* L.) is a crop grown in many countries all over the world, contributing to approximately 20% of the global human calorie consumption (Shewry and Hey, 2015). Moreover, it is also a considerable source of feed for livestock (Shewry, 2009),

rendering it both a direct and indirect source of sustenance in the human diet. The expected near future supply-demand trajectory shows a significant growth of global demand due to the continuous human population surge and an increase of the standard of living (Godfray and Garnett, 2014). Simultaneously, production is projected to critically drop due to environmental stresses, such as drought and salinity and/or international conflicts as exemplified by the contemporary Ukraine-Russia war (Bentley *et al.*, 2022; Reynolds *et al.*, 2012). It is therefore of utmost importance that science rapidly identifies genes and biological mechanisms that can dramatically boost global crop production under stress to meet the surging demand for wheat and other species.

The complex heterogeneous nature of plant traits responding to abiotic stresses, *i.e.*, quantitative traits (Fan *et al.*, 2015; Gupta *et al.*, 2020; Yang *et al.*, 2020), complicates our ability to understand and discover genes to significantly ameliorate productivity under stress in the field. Despite the fact that a myriad of genes associated with yield, drought and salinity stress have been reported (Bailey-Serres *et al.*, 2019; Liang *et al.*, 2018; Mahmood *et al.*, 2020; Sallam *et al.*, 2019; Zhao *et al.*, 2021), global wheat production has only registered an annual increase of no more than 1% (Dixon *et al.*, 2009; Khadka *et al.*, 2020), hinting at a hampered ability to increase production using known methods and tools. It is our opinion that in the big data era machine learning approaches should be adopted, as they have for example in fruit taste research (Colantonio *et al.*, 2022), to facilitate the finding of novel genes pertinent to abiotic stress responses.

Systems biology is a scientific discipline that deals with big data and data-driven approaches (Kitano, 2002). Modern high-throughput technologies have enabled us to collect omics data (genomics, transcriptomics, proteomics, metabolomics, microbiomics *etc.*) at a relatively low cost (Loman *et al.*, 2012). Using two or more omics together to screen for a desired trait (manifesting itself on multiple levels, *e.g.*, RNA and metabolomics) is called multi-omics (Hasin *et al.*, 2017). However, data alone does not suffice to obtain valuable biological insights using a systems biology approach; it requires the combination of the right tools to sift through the multitude of data (Misra *et al.*, 2019) in order to identify biological features contributing or affected by abiotic stresses. Correlation-based network analysis (CNA) has become the go-to tool in systems biology, as it allows for the aggregation of heterogeneous data into a single coherent dataset. It uses correlation analysis between the values of measurements (such as metabolites and physiological parameters) to estimate correlations between them. Next, the correlations are transformed into network form, where the nodes correspond to the molecules

(*e.g.*, genes, proteins, metabolites) and/or physiological measurements, and the edges represent the correlations between them (Langfelder and Horvath, 2008; Toubiana *et al.*, 2013). Network properties from graph theory can then be used to dissect the topology of the network and gain valuable biological insights (Aittokallio and Schwikowski, 2006; Gligorijević and Pržulj, 2015; Van den Broeck *et al.*, 2020). To increase the information that can be obtained from correlation networks (CNs), CNA has been recently combined with machine learning (ML) techniques, where the computer is trained to identify patterns within the network that reflect the conditions under which the samples were collected (Toubiana *et al.*, 2019b). In the current paper, we applied a systems biology approach to analyze eight *Triticum aestivum* pangenome lines (representing the majority of the global bread wheat genetic variation; Walkowiak *et al.*, 2020), allowing us to capture the full genetic potential of bread wheat whole-plant stress responses. We sampled wheat leaves and collected data on the physiolome, transcriptome, metabolome and microbiome respectively (Fig. 1). We then performed state-of-the-art CNA combined with ML techniques (Toubiana *et al.*, 2019b), in order to study complex quantitative traits in response to abiotic stresses. Our findings highlighted two metabolic pathways namely L-carnitine biosynthesis (from https://metacyc.org) and indole-3-acetic acid (IAA; the plant hormone auxin) inactivation VIII (from https://pmn.plantcyc.org), to be intimately involved in the plant drought and salinity stress responses, as well as genes corresponding to each pathway. Overall, our results unravel novel biological insights into the bread wheat pangenome, uncovering uncharted biological stress responses.

Results

Principal component analysis confirms representative characteristics of pangenome core set

As the basis for testing the effects of abiotic stresses (drought and salinity) on *Triticum aestivum*, we used a subpopulation of a recently assembled wheat pangenome (Bayer *et al.*, 2022). The lines used were chosen to sufficiently representing the separation of lines presented in Walkowiak *et al.* (2020). The subpopulation was composed of eight lines: Chinese Spring (CS), Claire, Jagger, Julius, Lancer, Landmark, Mace and Stanley. From here on we will refer to this set of wheat lines as the core set. To test for the genetic relationship of the core set in respect to the remaining pangenome lines, we recreated the principal component analysis (PCA) as performed by Walkowiak *et al.* (2020) and highlighted the core set within it in Fig.

2A. Polymorphisms captured from exomes were used to perform PCA. The analysis showed a homogeneous distribution of the core set within the distribution of the whole pangenomeFig. 2A, confirming that it is representative of the entire population.

Greenhouse experiment revealed significant differences between the physiological groups

To assess the effects of abiotic stresses on the physiology of *T. aestivum*, a greenhouse experiment was conducted, in which the core set was grown under control, drought and salinity conditions (see Fig. 2B and C and we refer the reader to the Materials and Methods section for a full description of the experiment). Across a time window of 60 days, vapor pressure deficit (VPD) was measured, exemplifying varying environmental conditions, simulating a field growth cycle as experienced by the plant *in natura* (Fig. 2D). To ensure consistent treatment application, soil volumetric water content (VWC) of drought-treated plants was monitored and lowered under controlled conditions, relative to the control-treated plants which were irrigated until saturation (Fig. 2E). Average transpiration rate (TR) during the treatment phase was calculated from the lysimeters weighing the plants at set intervals. From the onset of the treatments' application and till day 36, the TR rate of drought plants showed similar patterns to the TR rate control rate, while the TR rate of salinity was consistently lower. From day 37 the TR rate of drought plants dropped significantly and from day 39 was lower than the TR rate of control and salinity-treated plants (Fig. 2F). The fact that the treatments resulted in different transpiration patterns is suggestive of adaptive physiological behavior.

Weighing the plants at the beginning and the end of the experiment, we calculated the final dry weight (FDW), relative growth rate (RGR) and shoot allocation (SA; Supp. Fig. 1). All three measures showed differential responses. While drought-treated plants showed significantly lower RGR and FDW (and salinity-treated showed an intermediate change), salinity-treated plants showed higher SA, relative to the other two groups.

In addition, a lysimeter system was used to measure instantaneous and total transpiration, from which we estimated agronomic water use efficiency (AWUE), average transpiration rate (TR), average normalized transpiration rate (E), and response to daily midday VPD increase (dVPD; Supp. Fig. 1). Briefly, AWUE behaved like SA, while TR and E showed higher values for control-treated plants (though salinity-treated plants showed higher TR than drought-treated plants) and dVPD showed lower values for drought-treated plants. The different patterns were implicative of differential biological responses (physiological and others) to the treatments.

Last, leaf sampling was used to measure osmotic potential at full hydration (π_{100}) and CNH concentrations (C (%), N (%) and H (%); Supp. Fig. 1). In summation, both, drought- and salinity-treated plants, showed a decrease in transpiration, yet their response differed in the following physiological parameters: drought-treated plants showed impaired growth and lower nitrogen concentration but exhibited similar levels of SA in comparison to plants grown under controlled conditions. Salinity-treated plants, on the other hand, exerted higher SA, osmolytes, nitrogen concentration, and AWUE levels. Our findings are indicative for different long-term whole-plant physiological responses of drought-treated versus salinity-treated plants.

Metabolomic profiling highlights contrasting metabolic trends under drought and salinity

To understand the metabolic changes in response to strss, leaves were sampled from all plants and analyzed for relative content of central metabolites. While 13 metabolites did not significantly differ amongst the treatments (Supp. Fig. 2), 73 metabolites did; for instance, glycine and succinate were found to be lowest in drought-treated plants, followed by control plants, and highest in salinity-treated plants. Glycine and succinate have shown to be putatively involved in osmoregulation and reactive-oxygen-species-dependent stress responses, respectively (Ashraf and Foolad, 2007; Jardim-Messeder *et al.*, 2015). Moreover, serine and threonine were amongst the metabolites showing differential values decreasing in the following order: drought-treated, control-treated and salinity-treated plants. Pertinently, serine and threonine arebe precursors for osmoregulants (Ho and Saito, 2001; Joshi *et al.*, 2010; respectively). Furthermore, glutamine, of which values were highest under salinity, was shown to induce expression of salinity stress response transcription factors (Kan *et al.*, 2015). Other metabolites displayed a different trend, as both drought-treated and salinity-treated plants accumulated higher values than their control-treated counterparts, *e.g.*, γ-Aminobutyric Acid (GABA), which is known to be a major indicator of the activation of the GABA shunt in stress induced plants (Bouché *et al.*, 2003; Bouché and Fromm, 2004; Bown *et al.*, 2006). By contrast, drought-treated plants showed higher levels of soluble sugars (glucose, xylose, trehalose and fructose). Drought causes sugar accumulation and breakdown from storage sugars to soluble sugar (Kaur *et al.*, 2021).

Microbiomes show moderate differences between treatments

To understand the interaction between the leaf and its surrounding microbiome, all plants were sampled for their leaf microbiome, where phylum abundance was measured (Supp. Fig. 3A)

and further analyzed for alpha (Supp. Fig. 3B), beta (Supp. Fig. 3C), and gamma (Supp. Fig. 3D) diversities. While control-treated plants showed the highest richness per sample (alpha diversity), followed by drought-treated and salinity-treated plants (though the significance varies by diversity parameter; Supp. Fig. 3B), the accumulative species richness was significantly higher in drought- and salinity-treated plants (gamma diversity; Supp. Fig. 3D), which was implicative for reduction of the plant microbiome diversity under drought and salinity stress per plant, while maintaining higher species diversity per treatment, compared with control plants. Our analysis showed mild differences in community composition between treatments (beta-diversity; Supp. Fig. 3C). This finding highlighted that species unique to drought- and salinity-treated plants were dispersed amongst samples (*i.e.,* each sample employs few unique species, rendering the overall difference per sample small).

Multi-omics Integration of genetic and microbiome features reveals five stress-associated genes

To analyze the interplay of the different components (physiological traits, metabolites and microbiome) collected in the current study, we employed CNA which has shown time and again to be the go-to tool for systems biology studies (*e.g.* Badia-i-Mompel *et al.*, 2023, for transcriptomics; Hall *et al.,* 2022, for metabolomics; Layeghifard *et al.*, 2017, for microbiomics; Yan *et al.*, 2017, for multi-omics). First, metabolite CNs were constructed for the control-, drought- and salinity-treated plants as described in Toubiana *et al.* (2013), of which the corresponding visualizations of the networks are depicted in Fig. 3A-C. The CNA showed that drought and salinity treatments caused an increase in the number of edges and degree of connectivity, resulting in a higher edge density (Supp. Table 1), similar to what was reported for stress networks in Hochberg *et al.* (2013) and Rosental *et al.*, (2016).

Next, to study metabolic pathway activity of the different treatments, we implemented a method established by Toubiana *et al.* (2019b) that can identify pathways within CNs (Toubiana *et al.*, 2019b, Toubiana *et al.*, 2020), where CNA is combined with machine learning techniques. Specifically, L-carnitine biosynthesis and indole-3-acetic acid (IAA; a form of the phytohormone auxin) inactivation VIII were predicted for drought- and salinity-treated plants but not for control plants (Fig. 3D and Supp. Table 5; control-exclusively predicted pathways are in Supp. Table 2, drought-exclusively predicted pathways are in Supp. Table 3 and salinity-exclusively predicted pathways are in Supp. Table 4; the sensitivity analysis is shown in Fig. 3E-F, respectively). We next took the metabolomic data of the metabolites participating in the

indole-3-acetic acid inactivation VIII and L-carnitine biosynthesis pathways, respectively, and performed orthogonal partial least squares (OPLS) analysis, using the projections of the metabolites of each pathway onto PC1 (patAUX and patCAR, respectively).

In order to identify genes that could potentially be associated with the identified pathways, we sequenced the transcriptome of all plants, using the MARS-seq protocol (Jaitlin *et al.*, 2014). Weighted gene co-expression network analysis (WGCNA) is a well-known tool that highlights relationships between clusters of genes and traits of interest (here metabolic pathways; Langfelder and Horvath, 2008). To do so, it first applies hierarchical clustering of all genes and divides them accordingly into modules. To establish association between modules and traits of interest, eigenvectors, termed module eigengenes, are computed generating one-dimensional representations of groups of genes. Then, module eigengenes are correlated to the traits. Strong correlations are suggestive for an nondirectional causal relationship between a trait and a group of genes. The WGCNA produced 105 modules for the MARS-seq transcriptomics dataset. Here, we chose the cyan and black modules (with 468 and 871 genes, respectively), as their correlation coefficients (r) with patAUX were -0.86 and 0.76, respectively, and their correlation coefficients with patCAR were -0.71 and 0.74, respectively (being the modules with the strongest negative and strongest positive correlations with both patAUX and patCAR, respectively; the complete tables of correlation coefficients and p-values between the module eigengenes and patAUX and patCAR can be found in Supp. Table 6 and Supp. Table 11. Genes of the cyan and black modules, along with their per-gene correlation with patAUX and patCAR can be viewed in Supp. Table 7-8 and Supp. Table 12-13, respectively. The complete RNA-Seq data is available in Supp. Table 21). Modules generated by WGCNA often contain hundreds or even thousands of genes, making it difficult to pinpoint specific candidate genes with the greatest impact on the trait of interest. A genetic algorithm (GA) was recently developed by Toubiana *et al.* (2019a) to remedy this situation, which sifts through all genes of a module and highlights genes with the strongest correlation to a trait. We used named GA to identify strongly correlated genes within modules cyan and black to the indole-3-acetic acid inactivation VIII pathway (patAUX; producing 55 and 36 genes, respectively; with correlation coefficients of -0.863 and -0.773, respectively; the remaining genes after the GA in the cyan and black modules are in Supp. Table 9-10) and the L-carnitine biosynthesis pathway (patCAR; producing 17 and 59 genes, respectively; with correlation coefficients of -0.788 and -0.764, respectively; the remaining genes after the GA in the cyan and black modules are in Supp. Table 14-15). The GA analysis discovered five biologically pertinent genes overlapping

between the two pathways, which were strongly correlated with several parameters aselaborated below. These genes and their correlations with the most highly correlated parameters are presented in Fig. 4, while their respective correlation p-values are presented in Supp. Fig. 4. Four genes (TraesCS1B02G388700, a methyltransferase, TraesCS5A02G024900, a methionine synthase, TraesCS6B02G191900, an MLO-like protein, and TraesCS6D02G286900, a geranylgeranyl diphosphate reductase) were positively correlated with patAUX and patCAR, along with nitrogen composition, shoot allocation and *Hydrogenophaga* (Genus) counts, and were negatively correlated with *Neisseriales* (Order), *Phenylobacterium* (Genus) and *Jahnella* (Genus) counts. Interestingly, TraesCS3D02G246700 (Tryptophan aminotransferase related) showed a contrasting trend.

Virus-Induced Gene Silencing

We generated Virus Induced Gene Silencing (VIGS) *Triticum aestivum* 'Chinese Spring' lines for each of the five genes discussed above and due to statistical analysis of the expression levels (Supp. Fig. 5) and of tested metabolite levels (Supp. Table 16), we decided to further study the functionality of two of the GA-resulted genes under salinity conditions (*i.e.*, TraesCS5A02G024900 and TraesCS6D02G286900; Fig. 5-6, respectively). The silenced plants showed the anticipated gene silencing. Interestingly, TraesCS5A02G024900-silenced plants showed significantly higher levels of carnitine and slightly higher shoot allocation, while also showing a higher expression of an endogenic carnitine transporter (TraesCS3A02G136700; Fig. 4). Furthermore, TraesCS6D02G286900-silenced plants showed lower levels of indole-3-acetic acid (IAA), slightly lower shoot allocation, and differential expression levels in *Triticum aestivum* orthologs of *Arabidopsis thaliana* genes participating in indole-3-acetic acid inactivation VIII, according to https://www.plantcyc.org (higher expression levels of TraesCS3B02G335300 and TraesCS3B02G353200, though unchanged levels of TraesCS2B02G600800 and TraesCS1B02G332400; Fig. 5).

Discussion

The gap between the global supply and demand of food is expected to increase over time due to a decrease in supply from plateauing crop yields (Ray *et al.*, 2013) and climate change (Jägermeyr *et al.*, 2021; for most crops), and due to a rise in demand from the increasing human population and a concomitant rise in the average standard of living (Ray *et al.*, 2013). Therefore, it is imperative to increase global yields significantly. Many agrotechnological and

genomic tools have been implemented (reviewed in Stewart, and Hickey *et al.*, 2019; respectively), yet global crop yields are not increasing sufficiently (Ray *et al.*, 2012). Scientifically-driven global yield breakthroughs include the Haber-Bosch process (industrial ammonia fixation; Erisman *et al.*, 2008) and the green revolution (Hedden, 2003). While the need for a second green revolution is clear, the means to reach that end are not. We can only assume this will require some vertically disruptive technologies, such as multi-omics and computational tools (Liu *et al.*, 2013; Tian *et al.*, 2020).

Multi-omics have been used recently in a plethora of plant studies, such as nitrogen fertilization (Ichihashi *et al.*, 2020), microbiomes (reviewed in Trivedi *et al.*, 2021), hormones (Zander *et al.*, 2020), biotic stress response (Wang *et al.*, 2021b), metal stress response (Wang *et al.*, 2021a), drought stress response and senescence (Jiang *et al.*, 2020; Wang *et al.*, 2022; Großkinky *et al.*, 2018), salinity stress response (Singhal *et al.*, 2021), metabolite diversity and mapping (Shang and Huang, 2019; Zhan *et al.*, 2022), plant disease ecology (Crandall *et al.*, 2020) and even general crop improvement (reviewed in Scossa *et al.*, 2021). Specifically, wheat species have been studied using multi-omics, *e.g.* with regard to Head Blight disease (Wu *et al.*, 2022), sawfly feeding response (Biyiklioglu *et al.*, 2018), heavy metal stress (Saeed *et al.*, 2021; Zhou and Zheng, 2022; Hua *et al.*, 2022), potassium stress (Zhao *et al.*, 2020) and salinity stress responses (Yang *et al.*, 2022). To facilitate future wheat functional genomics studies, a wheat multi-omics database has been established (Ma *et al.*, 2021). Transitioning to using systems biology in conjuncture with multi-omics analyses in molecular biological research, and the unique insights it provides, is inevitable. For this reason, a multi-omics approach to analyze *Triticum aestivum* L. response to drought and salinity stresses has been implemented in the current study.

Computational methods, such as machine learning and correlation-based network analysis (CNA), facilitate the ability to mine the vast amount of data from multi-omics experimental setups (Misra *et al.*, 2019). Weighted gene co-expression network analysis (WGCNA) has established itself as one of the standard pipelines for transcriptomics analysis (Langfelder and Horvath, 2008), while the use of a genetic algorithm (GA) was suggested as an add-on to WGCNA to optimize the identification of candidate genes (Toubiana *et al.*, 2019a). DADA2 and the Ribosomal Database Project (RDP) classification have been substantiated for the analysis of microbiomics (Callahan *et al.*, 2016; Wang *et al.*, 2007). A combination of CNA with machine learning was demonstrated for the analysis of metabolomics, revealing biological

insights that have not been shown before such as the identification of a metabolic pathway that had previously not been reported in tomatoes (Toubiana *et al.*, 2019b).

Here, we applied a systems-biology in conjuncture with multi-omics approaches to analyze *Triticum aestivum*. We sampled wheat leaves obtaining information at the physiolome, transcriptome, metabolome and microbiome levels, respectively (Fig. 1) and applied all aforementioned analytical computational tools. Our approach was carried out on a representative subset of the published *Triticum aestivum* pangenome (representing the global bread wheat diversity; taken from Walkowiak *et al.*, 2020, Fig. 1A), a hexaploid major global crop with a large genome consisting of three relatively overlapping subgenomes, rendering genomics (and therefore transcriptomics) a considerable challenge (Walkowiak *et al.*, 2020).

Our physiolomics analysis revealed that the plant fresh dry weight (FDW) and relative growth weight (RGR) decreased under drought and salinity conditions (Supp. Fig. 1), as even successful stress resistance is costly in energy (Laureano *et al.*, 2008). However, the water use efficiency (WUE), shoot allocation (SA) and nitrogen content (N (%)) increased under salinity conditions, contrasting with results reported earlier (Lea-Cox and Syvertsen, 1993; Cheeseman, 1988; Van Hoorn *et al.*, 2001). Indeed, conflicting results in water use efficiency and shoot-to-root allocationhave been reported for various species (Katerji *et al.*, 2008; Franco *et al.*, 2011), and the effect on nitrogen uptake is not always unidirectional (Hu and Schmidhalter, 2005). This might be due to a stress response unique to wheat or due to the fact that mature plants might be less susceptible to salinity stress than young plants (Kütük *et al.*, 2004). We believe that considerably more research is needed to elucidate the exact reasons underlying this phenomenon.

To understand underlying molecular composition and mechanisms, a metabolomics analysis was performed. Our analysis highlighted metabolites with differential statistical patterns for the different stress regimes used in the current study (Supp. Fig. 2). Plants respond to biotic and abiotic stresses by reconfiguring their metabolic networks (Obata and Fernie, 2012; Tenenboim and Brotman, 2016; Choudry *et al.*, 2021). It has therefore been suggested to study the dynamics of the complete metabolic network rather than its single features (Alseekh and Fernie, 2018). Consequently, we opted to analyze the inter and intra relationships of metabolites using CNA as discussed below.

We also performed 16S microbiome sequencing and used the Swift Biosciences 16S-SNAPP-py3 pipeline to analyze the microbiomics data. Our findings revealed that control-treated plants

showed higher species richness but lower accumulative species diversity, relative to the stress-treated groups (though with varying significance, depending on the diversity parameter). This indicated that, under drought and salinity stress, wheat plants employed more species per treatment, but less species per plant. These trends were moderate and thus neccesitated integration into a multiomic network.

To fully understand the interplay of all physiological and molecular components in response to drought and salinity stress and also to overcome the ambiguousness of the findings obtained from the physiolome, metabolome, and microbiome analyses, we decided to integrate all data components into one coherent data network. To this end, we first constructed CNs using metabolomics data as described in Toubiana *et al.* (2019b), creating a metabolite network for each treatment (Fig. 3A-C). The networks displayed different topologies, specifically highlighted by an increase of edge numbers and degree of connectivity under stress (Supp. Table 1). Next, we combined CNA with machine learning techniques to identify metabolic pathways within CNs (Toubiana *et al.*, 2019b). while several pathways were predicted to occur in plants under different intersections of treatments (Fig. 3D and Supp. Table 2-5). The analysis predicted that L-carnitine biosynthesis and indole-3-acetic acid inactivation VIII were present exclusively under drought and salinity stress conditions (Fig. 2E-F).

The genetic connection between auxin and abiotic stress responses has been recently reviewed (Verma *et al.*, 2022), with DNA-binding AUXIN RESPONSE FACTORS (ARFs) being documented to affect root growth, chlorophyll content, stomatal conductance and sugar metabolism under drought and salinity conditions. Intriguingly, although auxin inactivation was shown to be negatively correlated with drought and salinity stress tolerance in *Oryza sativa* and *Arabidopsis thaliana* (Du *et al.*, 2012; Casanova-Sáez *et al.*, 2022), it was also shown to be positively correlated with drought and salinity stress tolerance in *Gossypium hisutum* (Kirungu *et al.*, 2019). Thus, it is important to bear in mind that different plants (especially during varying developmental stages) employ different mechanisms in response to stress.

L-Carnitine, has been shown to be an essential component of fatty acid metabolism, as well as serving as an antioxidant and osmolyte in animals and in microorganisms; the role of carnitine in plants, on the other hand, has not yet been elucidated (Jacques *et al.*, 2018). Nevertheless, applying exogenous L-carnitine was reported to induce salt stress resistance in barley (Oney-Birol, 2019), which supports our hypothesis that an increase of carnitine can cause salinity and drought stress resistance. In conclusion, our pathway analysis emphasizes the function of the

phytohormone auxin in relation to stress response but also suggests a novel role, in plants, of the lesser-known amino acid carnitine.

Next, we performed MARS-seq, followed by WGCNAs and a genetic algorithm in order to sift through the transcriptomics data, and to identify potential candidate genes associated with the highlighted pathways. The analysis showed that four genes from the cyan and black gene modules were highly correlated with both L-carnitine biosynthesis and indole-3-acetic acid inactivation VII, along with nitrogen content, shoot allocation and *Hydrogenophaga* counts, while showing inverse correlation with *Neisseriales*, *Phenylobacterium* and *Jahnella* counts, from the physiolome and microbiome data. Integrating multi-omics in plants via standard statistical correlation has scarcely been implemented (Jamil *et al.*, 2020), and this integration of physiolome, metabolome, transcriptome and microbiome data has not, to our knowledge, yet been undertaken, especially in a genomically complex organism such as *Triticum aestivum*. In order to associate results obtained from the metabolomics analysis to the remaining omics data, we performed OPLS on the metabolites participating in each respective pathway and used the respective OPLS analysis' first principal component to correlate them with the remaining physiolome, metabolome, transcriptomeand microbiome data.

The genes that were detected using this approach included TraesCS1B02G388700, TraesCS3D02G246700, TraesCS5A02G024900, TraesCS6B02G191900 and TraesCS6D02G286900 (Fig. 4 and Supp. Fig. 4). *Arabidopsis thaliana* orthologs of TraesCS1B02G388700 (AT1G48600, AT1G73600 and AT3G18000), a methyltransferase (according to https://plant.ensembl.org), were shown to be associated with auxin-mediated cell differentiation (Zou *et al.*, 2019). The expression of the rubber tree (*Hevea brasiliensis*) *HbMlo1*, a Mildew Resistance Locus O gene (MLO) similar in sequence to the *Arabidopsis thaliana* ortholog of TraesCS6B02G191900 (AT4G24250), was shown to be induced by indole-3-acetic acid (Qin *et al.*, 2015). Furthermore, chlorophyll biosynthesis, for which geranylgeranyl diphosphate reductase provides phytol as a precursor (Tanaka *et al.*, 1999; TraesCS6D02G286900 in *Triticum aestivum*), was shown to be intertwined with auxin regulation (reviewed in Tognetti *et al.*, 2011). Next, a *Triticum aestivum* Tryptophan aminotransferase related 2 (TraesCS3D02G246700), was suggested to be involved in auxin biosynthesis (Shao *et al.*, 2017). Contrarily, an *Arabidopsis thaliana* ortholog of TraesCS5A02G024900 (AT5G17920; a methionine synthetase), was shown to be involved in the S-adenosyl methionine (SAM) cycle (González and Vera, 2019), producing a substrate in

synthesizing trimethyllysine, an intermediate in L-carnitine biosynthesis (Maas *et al.*, 2020; though the pathway's existence in plants has not yet been proven; Jacques *et al.*, 2020).

The four directly correlated genes showed positive correlations with nitrogen content (N%), shoot allocation and *Hydrogenophaga* counts, while showing negative correlation with *Jahnella*, *Phenylobacterium* and *Neisseriales* counts (Fig. 4). Particularly nitrogen has been studied extensively regarding plant drought and salinity stress effects and responses (reviewed in Cui *et al.* (2019), Ding *et al.* (2018) and Ashraf *et al.* (2018)), and as the majority of nitrogen in plant leaves is chloroplastic, retention of nitrogen in leaves was associated with drought and salt tolerance (Sade *et al.*, 2017; Mansour, 2000). Furthermore, *Portulaca oleracea*, a halophyte, shows increased shoot allocation under salt stress (Franco *et al.*, 2011). As a *Hydrogenophaga* species was depicted as beneficial for soybean under salt stress (Ilangumaran *et al.*, 2021), and another *Hydrogenophaga* species was associated with increasing plant growth (Chanway and Holl, 1993), we hypothesize that both L-carnitine biosynthesis and indole-3-acetic acid inactivation VIII (along with nitrogen content, shoot allocation, and *Hydrogenophaga* abundance) are responses to salinity stress in *Triticum aestivum*.

Phenylobacterium abundance was juxtaposed to the more saline-tolerant species of the *Fictibacillus* genus (Kalwasińska *et al.*, 2017), while a subgenus species (*Phenylobacterium* sp. RIFCSPHIGHO2_01_FULL_69_31) was negatively correlated with shoot and root growth (Fernández-Baca *et al.*, 2021). *Neisseriales* species are known for their reduced tolerance to salinity and high temperature stresses (Klann *et al.*, 2016), while the genus *Jahnella* is part of the *Polyangiaceae* family, which is not known for its salinity tolerance (Garcia and Müller, 2014); these findings support our results, as the counts of these bacteria are negatively correlated with nitrogen content, shoot allocation, and *Hydrogenophaga* abundance (Fig. 4). Nevertheless, *Phenylobacterium* was classified as nitrogen-fixating (Yang *et al.*, 2017) and was shown to be positively correlated with nitrogen content (Liu *et al.*, 2021), although this was reported for bacteria in soil only.

We proceeded to test two of these genes using virus-induced gene silencing (VIGS) under salinity conditions. Interestingly, the silenced plants (*i.e.*, silencing TraesCS5A02G024900, which is correlated with L-carnitine biosynthesis and shoot allocation; Fig. 4), showed a slightly higher shoot allocation and higher levels of carnitine (Fig. 5), further supporting the notion of a positive correlation between carnitine levels and shoot allocation. This may further be explained by the fact that in the silenced plants, an endogenous carnitine transporter was

upregulated (TraesCS3A02G136700). On the other hand, in silencing the auxin-related gene (*i.e.*, silencing TraesCS6D02G286900, which is correlated with indole-3-acetic acid inactivation VIII and shoot allocation; Fig. 4), the auxin levels did decrease (Fig. 6). This silencing coincided with an increase in the gene expression of two auxin inactivation genes (TraesCS3B02G335300 and TraesCS3B02G353200) and an insignificant decrease in shoot allocation was observed. The fact that the alterations in shoot allocation were insignificant for both VIGS experiments can be explained as a result of examining the effect of silencing one gene at a time, while significant alteration of shoot allocation under salinity stress is achieved as a result of changes in multiple genes simultaneously, as a quantitatively additive effect.

In summation, in the current study we applied an unbiased top-down based approach to study the complex molecular and physiological relationships of *T. aestivum* grown under different stress conditions. We started from a broad whole-plant physiological experiment and through multi-omics and systems biology we uncovered two metabolic pathways and associated genes which showed clear phenotypic responses under prominent abiotic stresses. This method revealed genes that would not be detected using targeted methods (*i.e.*, focusing specifically on genes related to auxin and carnitine in established genomic, transcriptomic and metabolomic databases). Furthermore, receiving relatively high correlations (as in our results) between biological factors should not be automatically assumed, as demonstrated specifically for microbiome data (Weiss *et al.*, 2016) and for genome-wide association studies (Tam *et al.*, 2019). The fact that we demonstrated relatively high correlation coefficients with microbial counts could also be a result of using a coverage method for microbiome amplification that was much more thorough than usually implemented (see methods). We did not delve further into the function of these pertinent altered genes, rather we showed the interconnectivity of our *in silico* and *in vivo* results, both in a well-known pathway, *i.e.*, indole-3-acetic acid inactivation VIII, and a novel pathway in plants, *i.e.*, L-carnitine biosynthesis. We believe that our results can make significant contributions towards sustainable crop productivity in the future. We additionally emphasize that the current analysis was performed on the painstakingly generated hexaploid *Triticum aestivum* pangenome (published in Walkowiak *et al.*, 2020), and we therefore deem this highly relevant to all sequenced global bread wheat cultivars.

Materials and Methods

Greenhouse experiment

The experiment was conducted in a semi-commercial greenhouse at the Faculty of Agriculture, Food and Environment (Rehovot) of the Hebrew University of Jerusalem during February-March 2020. *Triticum aestivum* 'Chinese Spring', 'Claire', 'Jagger', 'Julius', 'Lancer', 'Landmark', 'Mace' and 'Stanley' plants were germinated and planted into 3.9L pots (containing Negev Sand soil) on lysimeters (the pot, irrigation and computer software setup is elaborately explained in Halperin *et al.* (2017)), and were subjected to control, drought and salinity treatments (3 plants per line per treatment, *i.e.*, $3_{(\text{replicates})} * 3_{(\text{treatments})} * 8_{(\text{lines})} = 72$ plants). Treatments started 3.5 weeks from the beginning of the experiment and the drought was intensified 1.5 weeks afterwards. The plants were sampled a week later for osmotic potential at full hydration, transcriptomics, microbiomics and metabolomics, and were subjected to recovery treatment 3 days later for the duration of 3-4 days. The drought treatment was changed dynamically to keep the soil volumetric content uniform amongst all drought-treated plants. The salinity treatment was kept at 130mM NaCl throughout the experiment. Both control and salinity treatments included nightly flushing of the pots with the respective irrigation in order to ensure full hydration. Throughout the experiment, Vapor-Pressure Deficit (VPD; Fig. 2D) and Volumetric Water Content (VWC) for the drought-treated plants (Fig. 2E) were measured.

Sampling and Initial Analyses

The lysimeter system allows for many physiological parameters to be calculated for each plant from the respective momentary and terminal recorded weight. Relative Growth Rate (RGR) was calculated as follows: $RGR = \frac{W_{end} - W_{beginning}}{Days\ of\ experiment}$ (W signifying dry weight, *i.e.* W_{end} signifying final dry weight and $W_{beginning}$ signifying initial dry weight). Agronomic Water Use Efficiency (AWUE) was calculated as follows: $AWUE = \frac{W_{end} - W_{beginning}}{Total\ Transpiration}$. For each plant, final shoot and root, wet and dry weight were measured, and shoot allocation (SA) was calculated as follows: $SA = \frac{W_{shoot}}{W_{shoot} + W_{root}}$. Average transpiration rate (TR; grams of water per minute) was taken for each plant for the day before sampling during 09:54-11:54 (according to the VPD peak). Average E was calculated using the respective TR and FDW as follows: $E = \frac{TR}{FDW}$. Finally, change in TR in response to the daily rise in VPD (ΔVPD) was calculated for that day by taking the average TR during 07:15-08:15 and average TR during 10:30-11:30 (according to the VPD fluctuation pattern that day) as follows: $\Delta VPD = \frac{TR_{10:30-11:30} - TR_{07:15-08:15}}{TR_{07:15-08:15}} * 100\%$.

Samples of the dry biomass were also sampled and analyzed for Carbon-Nitrogen-Hydrogen (CNH) composition (in percentages). Shoots and roots were separated, cleaned and dried in an oven (70°C, over a few days) and crushed using a standard kitchen electric blender. The CNH content of each sample was quantified by combustion (via the Dumas method, as discussed in Krotz *et al.*, 2016), using 5 mg of powder and an elemental analyzer (FlashSmart™ Elemental Analyzer; Thermo Fisher, MA, USA). All plants were sampled (leaves) for osmotic potential at full hydration (π_{100}) and were immersed in dH_20 for approximately 4h. The samples were cut and stuffed into 2mL spin column micro centrifuge tubes with a pad at their bottom. After storing at -80°C for 24h the samples were centrifuged (9000 RPM, 25°C) in order to extract the sap, which was measured using a vapor pressure osmometer (Vapro Wescor 5600, South Logan, UT, USA), in units of mmol/kg.

Each plant was sampled for metabolomics using gas chromatography mass spectrometry (GC-MS). Metabolite extraction, derivatization, and relative content measurements via GC-MS from *T. aestivum* leaves were performed as described by Lisec *et al.* (2006). The GC–MS data was obtained using an Agilent 7683 series auto-sample (Agilent Technologies, http://www.home.agilent.com), coupled to an Agilent 6890 gas-chromatograph–Leco Pegasus two time-of-flight mass spectrometer (Leco; http://www.leco.com/). Data analysis were done as described in Zhu *et al.*,2022. Day-normalization and sample median-normalization were conducted; the resulting data matrix was used for further analysis.

For transcriptome analysis, RNA was extracted as described by Sharma *et al.* (2019) using 100mg of leaf and quantified using Qubit and TapeStation. RNA-Seq libraries were prepared, using the MARS-seq protocol (Jaitin *et al.*, 2014), at the Crown Genomics institute of the Nancy and Stephen Grand Israel National Center for Personalized Medicine, Weizmann Institute of Science. A bulk adaptation of the MARS-Seq protocol (Jaitin *et al.*, 2014; Keren-Shaul *et al.*, 2019) was used to generate RNA-Seq libraries for expression profiling. Briefly, 30 ng of input RNA from each sample was barcoded during reverse transcription and pooled. Following Agencourt® AMPure® XP beads cleanup (Beckman Coulter), the pooled samples underwent second strand synthesis and were linearly amplified by T7 *in vitro* transcription. The resulting RNA was fragmented and converted into a sequencing-ready library by tagging the samples with Illumina sequences during ligation, RT, and PCR. Libraries were quantified by Qubit and TapeStation as previously described (Jaitin *et al.*, 2014; Keren-Shaul *et al.*, 2019). Single-end reads were sequenced on 1 lane of an Illumina NovaSeq instrument. The output was ~13 million reads per sample. Poly-A/T stretches and Illumina adapters were trimmed from the

reads using cutadapt (Martin, 2011); resulting reads shorter than 30bp were discarded. Remaining reads were mapped onto 3' UTR regions (1000 bases) of the *Triticum aestivum*, IWGSC genome according to Refseq annotations, using STAR (Dobin *et al.*, 2013) with the End-To-End option and outFilterMismatchNoverLmax was set to 0.05. Deduplication was carried out by flagging all reads that were mapped to the same gene and had the same UMI. Counts for each gene were quantified using htseq-count (Anders *et al.*, 2015), using the gtf above and corrected for UMI saturation. Differentially expressed genes were identified using DESeq2 (Love *et al.*, 2014) with the betaPrior, cooksCutoff and independentFiltering parameters set to False. Raw P values were adjusted for multiple testing using the Benjamini and Hochberg correction (Benjamini and Hochberg, 1995). The pipeline was run using snakemake (Köster and Rahmann, 2012).

Leaf samples were also collected for microbiome analysis from each plant and kept in liquid nitrogen while transferred to the laboratory and kept at −80°C until extraction. Metagenomic DNA was extracted from 100 mg of the root sample using ZymoBIOMICS DNA Kit (Qiagen, Germany) based on the manufacturer's instructions. Libraries of the 16S rRNA gene and ITS's amplicons were amplified from the extracted DNA by using the Swift amplicon 16S plus an internal transcribed spacer panel kit (Swift Biosciences, USA) according to the manufacturer's instructions (now IDT, Coralville, Iowa, USA), using SWIFT AMPLICON^{TM} 16S+ITS PANEL, which amplifies the V1-V9 areas of the 16S gene (a much higher coverage than the common method, thus giving significantly more accurate bacterial identification than commonly produced). The library was sequenced on an Illumina Novaseq platform (2 × 150-bp paired ends) to achieve short, high-quality reads.

Metabolomics Analysis (Correlation Network Analysis and Machine Learning)

Using Correlation Network Analysis (CNA) and Machine Learning (ML) to predict which metabolic pathways are active in plants has been established and the general outline has been explained previously (Toubiana *et al.*, 2020; Toubiana *et al.*, 2019b). The metabolomic data was used to create a weighted correlation network for each of control, drought and salinity treatment groups using 'qvalue', 'e1071' and 'igraph' R packages. Each metabolite was represented as a node and each Pearson correlation between two metabolites was represented as an edge (the value of the correlation coefficient was represented as the edge weight). Spurious correlations were sifted out by taking only correlations with a q-value ≤ 0.05, and with an r-value ≥ 0.52 (calculated according to Toubiana and Maruenda (2021)). PlantCyc

version PMN 13.0 was used as a plant pathway reference, and MetaCyc version 20.0 was used as a general pathway reference. For the ML training set, the PlantCyc pathways were used as positive instances and the difference between MetaCyc pathways and PlantCyc pathways (*i.e.,* pathways that exist in MetaCyc but not in PlantCyc) were used as negative instances. Random sets of metabolites were additionally used as negative instances in a final composition of 50% positive pathways, 25% negative pathways and 25% random metabolite sets). In order to evaluate the ML model for each network, Receiver Operating Characteristic (ROC) plots and confusion matrices were produced for 10-fold cross-validated models using 'xgboost', 'DiagrammeR', 'Matrix' and 'ROCit' R packages (the ROC plots and confusion matrices for the 10-fold cross-validated ML models are in Supp. Fig. 6). The confusion matrices showed accuracies of 0.803, 0.851 and 0.789 for the 10-fold cross-validated ML models for the control-, drought- and salinity-treated plants, respectively. The ML-based pathway predictions were produced per each tested pathway per treatment group network. Finally, each prediction underwent a sensitivity test by bootstrapping the ML model 100-times using 80% of the pathways (*i.e.,* predicting each pathway using a ML based on 80% of the training set) and the average prediction value (out of the 100 reiterations) per pathway per network was used as the sensitivity value. Only pathways which resulted in an original prediction value ≥ 0.5 and sensitivity value ≥ 0.5 were considered positively predicted per network.

Transcriptomics and Microbiome Analysis

The transcriptomic data was first analyzed according to Langfelder and Horvath (2008), using the 'WGCNA' R package, to choose gene modules in highest correlation with the indole-3-acetic acid inactivation VIII and L-carnitine biosynthesis pathways. Following, the respective modules were narrowed down to specific genes (with the individual highest correlations with the mentioned pathway) using a genetic algorithm (GA), according to Toubiana *et al.* (2019a). The Microbiome data was analyzed using the Swift Biosciences 16S-SNAPP-py3 pipeline (available online at https://github.com/swiftbiosciences/16S-SNAPP-py3) for bacteria, to generate the most likely microbial composition and ratios of a given sample. The resulting raw data was rarefied using the 'phyloseq' R package for further analysis.

Multi-omics Integration

The metabolomic data of the metabolites participating in indole-3-acetic acid inactivation VIII L-carnitine biosynthesis was transformed using OPLS (in the 'ropls' R package) and the respective PC1s were used to represent the pathway (as PCA was too strict to show the already

known and predicted separation of the drought and salinity treatments from the control treatment; Worley and Powers, 2013). For each vector, we correlated (using Pearson correlation) the GA-chosen genes, the aforementioned physiological and biochemical parameters, and finally to all OTUs (of which four with the highest correlation values were chosen). This finetuned correlation network represented our multi-omics results.

Virus-Induced Gene Silencing

The BSMV vectors used for gene silencing in this study were based on the constructs described in Yuan *et al.* (2011). To facilitate direct cloning of the VIGS target sequences, the *pγ* vector was modified to include a ligation independent cloning (LIC) system. The *pγ:TaPDS* vector, which contained a fragment of the *Triticum aestivum phytoene desaturase* gene, served as the positive control, while the *pγ:null* vector without any insert served as the negative control. To identify target sequences with minimal or no similarity to off-target genes, the sequences of the *TraesCS6D02G286900.1* and *TraesCS5A02G024900.1* gene were analyzed using si-Fi (siRNA Finder) against the entire wheat cDNAs annotation IWGSC RefSeq v1.0.

Two regions, one comprising 226 base pairs from *TraesCS6D02G286900.1* and the other comprising 229 base pairs from *TraesCS5A02G024900.1*, were selected as the VIGS target sequences. These target sequences were synthesized by Rhenium (Modiin, Israel). The *pγ* vector was then linearized using the ApaI restriction enzyme at 25 °C for 2 hours, creating a LIC cloning site. Both the linearized pγ vector and the synthesized VIGS fragments were treated with T4 DNA polymerase to generate complementary sticky ends. The treated PCR products and the treated pγ vector were mixed and ligated together. The resulting mixture was transformed into competent *Neb Stable E. coli* cells. Plasmids were purified from PCR-verified bacteria and subjected to Sanger sequencing for verification.

The verified plasmids were then introduced into *A. tumefaciens strain GV3101* through electroporation and plated on LB agar supplemented with kanamycin (50 μg/ml) and rifampicin (10 μg/ml). Single colonies were propagated overnight, diluted, and grown at 28°C overnight. The cultures were spun down, and the cells were re-suspended in infiltration medium. The OD_{600} of the suspension was adjusted to 1.0, and the mixture was incubated at RT without shaking for 3 hours or longer.

Equal volumes of *A. tumefaciens* strains carrying the pγ:VIGS1, pγ:VIGS2, pγ:TaPDS, or pγ:null constructs, along with pα and pβ, were combined and infiltrated into the adaxial side of 4-week-old *Nicotiana benthamiana* leaves using a 1 mL syringe. After 5 days, the infiltrated

N. benthamiana leaves were harvested and ground in a pre-chilled mortar and pestle using a potassium phosphate buffer containing Celite® 545 AW abrasive. The extracted sap was then used to rub-inoculate the second leaf of two-leaf stage wheat seedlings.

Concurrently *Triticum aestivum* cv. Chinese Spring plants were grown under salinity conditions. Pre-germinated seeds, which were nearly uniform in size, were planted in plastic pots with a diameter of 12 cm and a capacity of 1 liter. These pots were filled with 1.5 kg of thoroughly washed sand. The seedlings were grown in a controlled growth room with a 14/10 light/dark regime at 22 °C and an irradiance of 500 μmol m^{-2} s^{-1}. Initially, all pots were irrigated with a 1:500 dilution of "Or 4-2-6" fertilizer solution (GAT ISP, Kiryat Gat, Israel) for a period of two weeks, following which the NaCl treatment in the nutrient solution was introduced. To avoid salt shock, the salinity concentration was raised by 50 mM increments each day until reaching a final concentration of 150 mM NaCl in the nutrient solution. In order to maintain a consistent salinity level in the sand, 200 ml of 150 mM NaCl in the nutrient solution was applied to each pot on alternate days. After three weeks of growth, the plants were infected with the BSMV virus.

After two weeks from inoculation, fresh leaves that were different from the previously inoculated ones were harvested for further analysis. A fraction of the harvested leaves was employed for RNA extraction, following the protocol described in Sharma *et al.* (2019). This facilitated the evaluation of the downregulation of gene expression of the targeted genes. Concurrently, another fraction of the harvested leaves was dedicated to metabolite extraction, allowing for the exploration of specific metabolites alterations within the samples.

RNA was extracted using TRIzol (Invitrogen, Carlsbad, CA, USA) and was treated with DNAse and M-MLV reverse transcriptase (Promega, Madison, WI, USA). GOI expression levels were quantified via quantitative RT-PCR (with *Triticum aestivum* 18S rRNA used as an internal control). Carnitine and indole-3-acetic acid (IAA) were extracted and analyzed using LC-MS as explained by Kelly *et al.* (2021). Plants were cut, the roots were washed and all the plants were dried in 60℃ over a couple of days and were weighed separately for shoot and roots, and shoot allocation was calculated as explained above.

References

Aittokallio T and Schwikowski B. 2006. **Graph-based methods for analysing networks in cell biology**. Briefings in Bioinformatics 7:243-255.

Alseekh S and Fernie AR. 2018. **Metabolomics 20 years on: what have we learned and what hurdles remain?** The Plant Journal 94:933-942.

Anders S, Pyl PT, Huber W. 2015. **HTSeq – a python framework to work with high-throughput sequencing data**. Bioinformatics 31:166-169.

Ashraf M and Foolad MR. 2007. **Roles of glycine betaine and proline in improving plant abiotic stress resistance**. Environmental and Experimental Botany 59:206-216.

Ashraf M, Shahzad SM, Imtiaz M, Rizwan MS. 2018. **Salinity effects on nitrogen metabolism in plants – focusing on the activities of nitrogen metabolizing enzymes: a review**. Journal of Plant Nutrition 41:1065-1081.

Badia-i-Mompel P, Wessels L, Müller-Dott S, Trimbour R, Flores ROR, Argelaguet R, Saez-Rodriguez J. 2023. **Gene regulatory network inference in the era of single-cell multi-omics**. Nature Reviews Genetics. DOI: https://doi.org/10.1038/s41576-023-00618-5.

Bailey-Serres J, Parker JE, Ainsworth EA, Oldroyd GED, Schroeder JI. 2019. **Genetic strategies for improving crop yields**. Nature 575:109-118.

Bayer PE, Petereit J, Durant É, Monat C, Rouard M, Hu H, Chapman B, Li C, Cheng S, Batley J, Edwards D. 2022. **Wheat Panache: A pangenome graph database representing presence-absence variation across sixteen bread wheat genomes**. The Plant Genome 15:e20221.

Benjamini Y and Hochberg Y. 1995. **Controlling the false discovery rate: a practical and powerful approach to multiple testing**. Journal of the Royal Statistical Society. Series B (Methodological) 57:289-300.

Bentley AR, Donovan J, Sonder K, Baudron F, Lewis JM, Voss R, Rutsaert P, Poole N, Kamoun S, Saunders DGO, Hodson D, Hughes DP, Negra C, Ibba MI, Snapp S, Sida TS, Jaleta M, Tesfaye K, Becker-Reshef I, Govaerts B. 2022. **Near-to long-term measures to stabilize global wheat supplies and food security**. Nature Food 3:483-486.

Biyiklioglu S, Alptekin B, Akpinar BA, Varella AC, Hofland ML, Weaver DK, Bothner B, Budak H. 2018. **A large-scale multiomics analysis of wheat stem solidness and the wheat stem sawfly feeding response, and syntenic associations in barley, *Brachypodium*, and rice.** Functional & Integrative Genomics 18:241-259.

Bouché N and Fromm H. 2004. **GABA in plants: just a metabolite?** Trends in Plant Science 9:110-115.

Bouché N, Lacombe B, Fromm H. 2003. **GABA signaling: a conserved and ubiquitous mechanism**. Trends in Cell Biology 13:607-610.

Bown AW, MacGregor KB, Shelp BJ. 2006. **Gamma-aminobutyrate: defense against invertebrate pests?** Trends in Plant Science 11:424-427.

Caldana C, Degenkolbe T, Cuadros-Inostroza A, Klie S, Sulpice R, Leisse A, Steinhauser D, Fernie AR, Willmitzer L, Hannah MA. 2011. **High-density kinetic analysis of the metabolomic and transcriptomic response of *Arabidopsis* to eight environmental conditions**. The Plant Journal 67:869-884.

Callahan BJ, McMurdie PJ, Rosen MJ, Han AW, Johnson AJA, Holmes SP. 2016. **DADA2: high-resolution sample inference from Illumina amplicon data**. Nature methods, 13:581-583.

Casanova-Sáez R, Mateo-Bonmatí E, Šimura J, Pěnčík A, Novák O, Staswick P, Ljung K. 2022. **Inactivation of the entire *Arabidopsis* group II GH3s confers tolerance to salinity and water deficit**. New Phytologist 235:263-275.

Chanway CP and Holl FB. 1993. **First year field performance of spruce seedlings inoculated with plant growth promoting rhizobacteria**. Canadian Journal of Microbiology 39:1084-1088.

Cheeseman JM. 1988. **Mechanisms of salinity tolerance in plants**. Plant Physiology 87:547-550.

Choudry S, Sharma P, Moulick D, Mazumder MK. 2021. **Unrevealing metabolomics for abiotic stress adaptation and tolerance in plants**. Journal of Crop Science and Biotechnology 24:479-493.

Colantonio V, Ferrão LFV, Tieman DM, Bliznyuk N, Sims C, Klee HJ, Munoz P, Resende Jr. MFR. 2022. **Metabolomic selection for enhanced fruit flavor**. Proceedings of the National Academy of Sciences of the United States of America 119:e2115865119.

Cuadros-Inostroza Á, Caldana C, Redestig H, Kusano M, Lisec J, Peña-Cortés H, Willmitzer L, Hannah MA. 2009. **TargetSearch – a Bioconductor package for the efficient preprocessing of GC-MS metabolite profiling data**. BMC Bioinformatics 10:428.

Cui G, Zhang Y, Zhang W, Lang D, Zhang X, Li Z, Zhang X. 2019. **Response of carbon and nitrogen metabolism and secondary metabolites to drought stress and salt stress in plants**. Journal of Plant Biology 62:387-399.

Crandall SG, Gold KM, Jiménez-Gasco MdM, Filgueiras CC, Willett DS. 2020. **A multi-omics approach to solving problems in plant disease ecology**. PLOS ONE 15:e0237975.

Ding L, Lu Z, Gao L, Guo S, Shen Q. 2018. **Is nitrogen a key determinant of water transport and photosynthesis in higher plants upon drought stress**. Frontiers in Plant Science 9:1143.

Dixon J, Braun HJ, Kosina P, Crouch JH (Eds.). 2009. **Wheat facts and futures 2009**. CIMMYT, Mexico City, Mexico.

Dobin A, David CA, Schlesinger F, Drenkow J, Zaleski C, Jha S, Batut P, Chaisson M, Gingeras TR. 2013. **STAR: ultrafast universal RNA-seq aligner**. Bioinformatics 29:15-21.

Du H, Wu N, Fu J, Wang S, Li X, Xiao J, Xiong L. 2012. **A GH_3 family member, $OsGH_3$-2, modulates auxin and abscisic acid levels and differentially affects drought and cold tolerance in rice**. Journal of Experimental Botany 63:6467-6480.

Erisman JW, Sutton MA, Galloway J, Klimont Z, Winiwarter W. 2008. **How a century of ammonia synthesis changed the world**. Nature Geoscience 1:636-639.

Fan Y, Shabala S, Ma Y, Xu R, Zhou M. 2015. **Using QTL mapping to investigate the relationships between abiotic stress tolerance (drought and salinity) and agronomic and physiological traits**. BMC Genomics 16:43.

Fernández-Baca CP, Rivers AR, Maul JE, Kim W, Poudel R, McClung AM Roberts DP, Reddy VR, Barnaby JY. 2021. **Rice plant-soil microbiome interactions driven by root and shoot biomass**. Diversity 13:125.

Franco JA, Bañón S, Vicente MJ, Miralles J, Martínez-Sánchez JJ. 2011. **Root development in horticultural plants grown under abiotic stress conditions – a review**. Journal of horticultural science & biotechnology 86:543-556.

Garcia R and Müller R. 2014. **The Family *Polyangiaceae***. In: Rosenberg E, DeLong EF, Lory S, Stackebrandt E, Thompson F (Eds.), The Prokaryotes, pp. 247-279, Springer, Berlin, Heidelberg.

Gligorijević V and Pržulj N. 2015. **Methods for biological data integration: perspectives and challenges**. Journal of the Royal Society Interface 12:20150571.

Godfray HCJ and Garnett T. 2014. **Food security and sustainable intensification**. Philosophical Transactions of the Royal Society B 369:20120273.

González B and Vera P. 2019. **Folate metabolism interferes with plant immunity through 1C methionine synthase-directed genome-wide DNA methylation enhancement**. Molecular Plant 12:1227-1242.

Großkinky DK, Syaifullah SJ, Roitsch T. 2018. **Integration of multi-omics techniques and physiological phenotyping within a holistic phenomics approach to study senescence in model and crop plants**. Journal of Experimental Botany 69:825-844.

Gupta PK, Balyan HS, Sharma S, Kumar R. 2020. **Genetics of yield, abiotic stress tolerance and biofortification in wheat (Triticum aestivum L.)**. Theoretical and Applied Genetics 133:1569-1602.

Hall RD, D'Auria JC, Ferreira ACS, Gibon Y, Kruszka D, Mishra P, van de Zedde R. 2022. **High-throughput plant phenotyping: a role for metabolomics?** Trends in Plant Science 27:549-563.

Halperin O, Gebremedhin A, Wallach R, Moshelion M. 2017. **High-throughput physiological phenotyping and screening system for the characterization of plant-environment interactions**. The Plant Journal 89:839-850.

Hasin Y, Seldin M, Lusis A. 2017. **Multi-omics approaches to disease**. Genome Biology 18:83.

Hedden P. 2003. **The genes of the green revolution**. Trends in Genetics 19:5-9.

Hickey LT, Hafeez AN, Robinson H, Jackson SA, Leal-Bertioli SCM, Tester M, Gao C, Godwin ID, Hayes BJ, Wulff BBH. 2019. **Breeding crops to feed 10 billion**. Nature Biotechnology 37:744-754.

Ho CL and Saito K. 2001. **Molecular biology of the plastidic phosphorylated serine biosynthetic pathway in *Arabidopsis thaliana***. Amino Acids 20:243-259.

Hochberg U, Degu A, Toubiana D, Gendler T, Nikoloski Z, Rachmilevitch S, Fait A. 2013. **Metabolite profiling and network analysis reveal coordinated changes in grapevine water stress response**. BMC Plant Biology 13:184.

Hu Y and Schmidhalter U. 2005. **Drought and salinity: a comparison of their effects on mineral nutrition of plants**. Journal of Plant Nutrition and Soil Science 168:541-549.

Hua YP, Chen JF, Zhou T, Zhang TY, Shen DD, Feng YN, Guan PF, Huang SM, Zhou ZF, Huang JY, Yue CP. 2022. **Multiomics reveals an essential role of long-distance translocation in regulating plant cadmium resistance and grain accumulation in allohexaploid wheat (*Triticum aestivum*)**. Journal of Experimental Botany 73:7516-7537.

Ichihashi Y, Date Y, Shino A, Shimizu T, Shibata A, Kumaishi K, Funahashi F, Wakayama K, Yamazaki K, Umezawa A, Sato T, Kobayashi M, Kamimura M, Kusano M, Che FS, O'Brien M, Tanoi K, Hayashi M, Nakamura R, Shirasu K, Kikuchi J, Nihei N. 2020. **Multi-omics analysis on an agroecosystem reveals the significant role of organic nitrogen to increase agricultural crop yield**. Proceedings of the National Academy of Sciences 117:14552-14560.

Ilangumaran G, Schwinghamer TD, Smith DL. 2021. **Rhizobacteria from root nodules of an indigenous legume enhance salinity stress tolerance in soybean**. Frontiers in Sustainable Food Systems 4:617978.

Jacques F, Rippa S, Perrin Y. 2018. **Physiology of L-carnitine in plants in light of the knowledge in animals and microorganisms**. Plant Science 274:432-440.

Jacques F, Zhao Y, Kopečná M, Končitíková R, Kopečný D, Rippa S, Perrin Y. 2020. Roles for **ALDH10 enzymes in γ-butyrobetaine synthesis, seed development, germination, and salt tolerance in Arabidopsis**. Journal of Experimental Botany 71:7088-7102.

Jägermeyr J, Müller C, Ruane AC, Elliott J, Balkovic J, Castillo O, Faye B, Foster I, Folberth C, Franke JA, Fuchs K, Guarin JR, Heinke J, Hoogenboom G, Iizumi T, Jain AK, Kelly D, Khabarov N, Lange S, Lin TS, Liu W, Mialyk O, Minoli S, Moyer EJ, Okada M, Phillips M, Porter C, Rabin SS, Scheer C, Schneider JM, Schyns JF, Skalsky R, Smerald A, Stella T, Stephens H, Webber H, Zabel F, Rosenzweig C. 2021. **Climate impacts on global agriculture emerge earlier in new generation of climate and crop models**. Nature Food 2:873-885.

Jaitin DA, Kenigsberg E, Keren-Shaul H, Elefant N, Paul F, Zaretsky I, Mildner A, Cohen N, Jung S, Tanay A, Amit I. 2014. **Massively parallel single-cell RNA-Seq for marker-free decomposition of tissues into cell types**. Science 343:776-779.

Jamil IN, Remali J, Azizan KA, Muhammad NAN, Arita M, Goh HH, Aizat WM. 2020. **Systematic multi-omics integration (MOI) approach in plant systems biology**. Frontiers in Plant Science 11:944.

Jardim-Messeder D, Caverzan A, Rauber R, de Souza Ferreira E, Margis-Pinheiro M, Galina A. 2015. **Succinate dehydrogenase (mitochondrial complex II) is a source of reactive oxygen species in plants and regulates development and stress responses**. New Phytologist 208:776-789.

Jiang L, Yoshida T, Stiegert S, Jing Y, Alseekh S, Lenhard M, Pérez-Alfocea F, Fernie AR. 2020. **Multi-omics approach reveals the contribution of KLU to leaf longevity and drought tolerance**. Plant Physiology 185:352-368.

Joshi V, Joung JG, Fei Z, Jander G. 2010. **Interdependence of threonine, methionine and isoleucine metabolism in plants: accumulation and transcriptional regulation under abiotic stress**. Amino Acids 39:933-947.

Kalwasińska A, Felföldi T, Szabó A, Deja-Sikora E, Kosobucki P, Walczak M. 2017. **Microbial Communities associated with the anthropogenic, highly alkaline environment of a saline soda lime, Poland**. Antonie van Leeuwenhoek 110:945-962.

Kan CC, Chung TY, Juo YA, Hsieh MH. 2015. **Glutamine rapidly induces the expression of key transcription factor genes involved in nitrogen and stress responses in rice roots**. BMC Genomics 16:731.

Katerji N, Mastrorilli M, Rana G. 2008. **Water use efficiency of crops cultivated in the Mediterranean region: review and analysis**. European Journal of Agronomy 28:493-507.

Kaur H, Manna M, Thakur T, Gautam V, Salvi P. 2021. **Imperative role of sugar signaling and transport during drought stress responses in plants**. Physiologia Plantarum 171:833-848.

Kelly G, Brandsma D, Egbaria A, Stein O, Doron-Faigenboim A, Lugassi N, Belausov E, Zemach H, Shaya F, Carmi N, Sade N, Granot D. 2021. **Guard cells control hypocotyl elongation through HXK1, HY5, and PIF4**. Communications Biology 4:765.

Keren-Shaul H, Kenigsberg E, Jaitin DA, David E, Paul F, Tanay A, Amit I. 2019. **MARS-seq2.0: an experimental and analytical pipeline for indexed sorting combined with single-cell RNA sequencing**. Nature Protocols 14:1841-1862.

Khadka K, Earl HJ, Raizada MN, Navabi A. 2020. **A physio-morphological trait-based approach for breeding drought tolerant wheat**. Frontiers in Plant Science 11:715.

Kitano H. 2002. **Computational systems biology**. Nature 420:206-210.

Kirungu JN, Magwanga RO, Lu P, Cai X, Zhou Z, Wang X, Peng R, Wang K, Liu F. 2019. **Functional characterization of Gh_A08G1120 (GH$_{3.5}$) gene reveal their significant role in enhancing drought and salt stress tolerance in cotton**. BMC Genetics 20:62.

Klann J, McHenry A, Montelongo C, Goffredi SK. 2016. **Decomposition of plant-sourced carbon compounds by heterotrophic betaproteobacteria isolated from a tropical Costa Rican bromeliad**. MicrobiologyOpen 5:479-489.

Köster J and Rahmann S. 2012. **Snakemake – a scalable bioinformatics workflow engine**. Bioinformatics 28:2520-2522.

Krotz L, Leone F, Giazzi G. 2016. **Nitrogen/protein determination in food and animal feed by combustion method (Dumas) using the Thermo Scientific Flash*Smart* elemental analyzer**. *Thermo Fisher Application Note* AN42262-EN, 716.

Kütük C, Çaycı G, Heng LK. 2004. **Effects of increasing salinity and 15N-labelled urea levels on growth, N uptake, and water use efficiency of young tomato plants**. Australian Journal of Soil Research 42:345-351.

Langfelder P and Horvath S. 2008. **WGCNA: an R package for weighted correlation network analysis**. BMC Bioinformatics 9:559.

Laureano RG, Lazo YO, Linares JC, Luque A, Martínez F, Seco JI, Merino J. 2008. **The cost of stress resistance: construction and maintenance costs of leaves and roots in two populations of *Quercus ilex***. Tree Physiology 28:1721-1728.

Layeghifard M, Hwang DM, Guttman DS. 2017. **Disentangling interactions in the microbiome: a network perspective**. Trends in Microbiology 25:217-228.

Lea-Cox JD and Syvertsen JP. 1993. **Salinity reduces water use and nitrate-N-use efficiency of citrus**. Annals of Botany 72:47-54.

Liang W, Ma X, Wan P, Liu L. 2018. **Plant salt-tolerance mechanism: a review**. Biochemical and Biophysical Research Communications 495:286-291.

Lisec J, Schauer N, Kopka J, Willmitzer L, Fernie AR. 2006. **Gas chromatography mass spectrometry-based metabolite profiling in plants**. Nature Protocols 1:387-396.

Liu J, He X, Sun J, Ma Y. 2021. **A degeneration gradient of poplar trees contributes to the taxonomic, functional, and resistome diversity of bacterial communities in rhizosphere soils**. International Journal of Molecular Sciences 22:3438.

Liu W, Yuan JS, Stewart Jr CN. 2013. **Advanced genetic tools for plant biotechnology**. Nature Reviews Genetics 14:781-793.

Loman NJ, Constantinidou C, Chan JZM, Halachev M, Sergeant M, Penn CW, Robinson ER, Pallen MJ. 2012. **High-throughput bacterial genomes sequencing: an embarrassment of choice, a world of opportunity**. Nature Reviews Microbiology 10:599-606.

Love MI, Huber W, Anders S. 2014. **Moderated estimation of fold change and dispersion for RNA-seq data with DESeq2**. Genome Biology 15:550.

Ma S, Wang M, Wu J, Guo W, Chen Y, Li G, Wang Y, Shi W, Xia G, Fu D, Kang Z, Ni F. 2021. **WheatOmics: a platform combing multiple omics data to accelerate functional genomics studies in wheat**. Molecular Plant 14:1965-1968.

Maas MN, Hintzen JCJ, Porzberg MRB, Mecinović J. 2020. **Trimethyllysine: from carnitine biosynthesis to epigenetics**. International Journal of Molecular Sciences 21:9451.

Mahmood T, Khalid S, Abdullah M, Ahmed Z, Shah MKN, Ghafoor A, Du X. 2020. **Insights into drought stress signaling in plants and the molecular genetic basis of cotton drought tolerance**. Cells 9:105.

Mansour MMF. 2000. **Nitrogen containing compounds and adaptation of plants to salinity stress**. Biologia Plantarum 43:491-500.

Martin M. 2011. **Cutadapt removes adapter sequences from high-throughput sequencing reads.** EMBnet.journal17:10-12.

Misra BB, Langefeld C, Olivier M, Cox LA. 2019. **Integrated omics: tools, advances and future approaches**. Journal of Molecular Endocrinology 62:R21-R45.

Obata T and Fernie AR. 2012. **The use of metabolomics to dissect plant responses to abiotic stresses**. Cellular and Molecular Life Sciences 69:3225-3243.

Oney-Birol S. 2019. **Exogenous L-carnitine promotes plant growth and cell division by mitigating genotoxic damage of salt stress**. Scientific Reports 9:17229.

Pons P and Latapy M. 2005. **Computing communities in large networks using random walks**. In: Yolum P, Güngör T, Gürgen F, Özturan C. (eds.) Computer and Information Sciences - ISCIS 2005. Lecture Notes in Computer Science, vol 3733. Springer, Berlin, Heidelberg. DOI: https://doi.org/10.1007/11569596_31.

Qin B, Zheng F, Zhang Y. 2015. **Molecular cloning and characterization of a Mlo gene in rubber tree (*Hevea brasiliensis*)**. Journal of plant physiology 175:78-85.

Ray DK, Mueller ND, West PC, Foley JA. 2013. **Yield trends are insufficient to double global crop production by 2050**. PLOS ONE 8:e66428.

Ray DK, Ramankutty N, Mueller ND, West PC, Foley JA. 2012. **Recent patterns of crop yield growth and stagnation**. Nature Communications 3:1293.

Reynolds M, Foulkes J, Furbank R, Griffiths S, King J, Murchie E, Parry M, Slafer G. 2012. **Achieving yield gains in wheat**. Plant, Cell & Environment 35:1799-1823.

Rosental L, Perelman A, Nevo N, Toubiana D, Samani T, Batushansky A, Sikron N, Saranga Y, Fait A. 2016. **Environmental and genetic effects on tomato seed metabolic balance and its association with germination vigor**. BMC Genomics 17:1047.

Sade N, Umnajkitikorn K, Wilhelmi MdMR, Wright M, Wang S, Blumwald E. 2017. **Delaying chloroplast turnover increases water-deficit stress tolerance through the enhancement of nitrogen assimilation in rice**. Journal of Experimental Botany 69:867-878.

Saeed M, Quraishi UM, Malik RN. 2021. **Arsenic uptake and toxicity in wheat (*Triticum aestivum* L.): a review of multi-omics approaches to identify tolerance mechanisms**. Food Chemistry 355:129607.

Sallam A, Alqudah AM, Dawood MFA, Baenziger PS, Börner A. 2019. **Drought stress tolerance in wheat and barley: advances in physiology, breeding and genetics research**. International Journal of Molecular Sciences 20:3137.

Scossa F, Alseekh S, Fernie AR. 2021. **Integrating multi-omics data for crop improvement**. Journal of Plant Physiology 257:153352.

Shang Y and Huang S. 2019. **Multi-omics data-driven investigations of metabolic diversity of plant triterpenoids**. The Plant Journal 97:101-111.

Shao A, Ma W, Zhao X, Hu M, He X, Teng W, Li H, Tong Y. 2017. **The auxin biosynthetic *TRYPTOPHAN AMINOTRANSFERASE RELATED TaTAR2.1-3A* increases grain yield of wheat**. Plant Physiology 174:2274-2288.

Sharma D, Golla N, Singh S, Singh PK, Singh D, Onteru SK. 2019. **An efficient method for extracting next-generation sequencing quality RNA from liver tissue of recalcitrant animal species**. Journal of Cellular Physiology 234:14405-14412.

Shewry PR. 2009. **Wheat**. Journal of Experimental Botany 60:1537-1553.

Shewry PR and Hey SJ. 2015. **The contribution of wheat to human diet and health**. Food and Energy Security 4:178-202.

Singhal RK, Saha D, Skalicky M, Mishra UN, Chauhan J, Behera LP, Lenka D, Chand S. Kumar V, Dey P, Indu, Pandey S, Vachova P, Gupta A, Brestic M, Sabagh AE. 2021. **Crucial cell signalling compounds crosstalk and integrative multi-omics techniques for salinity stress tolerance in plants**. Frontiers in Plant Science 12:670369.

Stewart RE. "**Agricultural technology**". *Encyclopedia Britannica*, Invalid Date, https://www.britannica.com/technology/agricultural-technology. Accessed 13 April 2023.

Tam V, Patel N, Turcotte M, Bossé Y, Paré G, Meyre D. 2019. **Benefits and limitations of genome-wide association studies**. Nature Reviews Genetics 20:467-484.

Tanaka R, Oster U, Kruse E, Rüdiger W, Grimm B. 1999. **Reduced activity of geranylgeranyl reductase leads to loss of chlorophyll and tocopherol and to partially geranylgeranylated chlorophyll in transgenic tobacco plants expressing antisense RNA for geranylgeranyl reductase**. Plant Physiology 120:695-704.

Tenenboim H and Brotman Y. 2016. **Omic relief for the biotically stressed: metabolomics of plant biotic interactions**. Trends in Plant Science 21:781-791.

Tian Z, Wang JW, Li J, Han B. 2020. **Designing future crops: challenges and strategies for sustainable agriculture**. The Plant Journal 105:1165-1178.

Tognetti VB, Mühlenbock P, Van Breusegem F. 2011. **Stress homeostasis – the redox and auxin perspective**. Plant, Cell & Environment 35:321-333.

Toubiana D, Fernie AR, Nikoloski Z, Fait A. 2013. **Network analysis: tackling complex data to study plant metabolism**. Trends in Biotechnology 31:29-36.

Toubiana D and Maruenda H. 2021. **Guidelines for correlation coefficient threshold settings in metabolite correlation networks exemplified on a potato association panel**. BMC Bioinformatics 22:116.

Toubiana D, Puzis R, Sadka A, Blumwald E. 2019a. **A genetic algorithm to optimize weighted gene co-expression network analysis**. Journal of Computational Biology 26:1349-1366.

Toubiana D, Puzis R, Wen L, Sikron N, Kurmanbayeva A, Soltabayeva A, Wilhelmi MdMR, Sade N, Fait A, Sagi M, Blumwald E, Elovici Y. 2019b. **Combined network analysis and machine learning allows the prediction of metabolic pathways from tomato metabolomics data**. Communications Biology 2:214.

Toubiana D, Sade N, Liu L, Wilhelmi MdMR, Brotman Y, Luzarowska U, Vogel JP, Blumwald E. 2020. **Correlation-based network analysis combined with machine learning techniques highlight the role of the GABA shunt in *Brachypodium sylvaticum* freezing tolerance**. Scientific reports 10:4489.

Trivedi P, Mattupalli C, Eversole K, Leach JE. 2021. **Enabling sustainable agriculture through understanding and enhancement of microbiomes**. New Phytologist 230:2129-2147.

Van den Broeck L, Gordon M, Inzé D, Williams C, Sozzani R. 2020. **Gene regulatory network inference: connecting plant biology and mathematical modeling**. Frontiers in Genetics 11:457.

Van Hoorn JW, Katerji N, Hamdy A, Mastrorilli M. 2001. **Effect of salinity on yield and nitrogen uptake of four grain legumes and on biological nitrogen contribution from the soil**. Agricultural Water Management 51:87-98.

Verma S, Negi NP, Pareek S, Mudgal G, Kumar D. 2022. **Auxin response factors in plant adaptation to drought and salinity stress**. Physiologia Plantarum 174:e13714.

Walkowiak S, Gao L, Monat C, Haberer G, Kassa MT, Brinton J, Ramirez-Gonzalez RH, Kolodziej MC, Delorean E, Thambugala D, Klymiuk V, Byrns B, Gundlach H, Bandi V, Siri JN, Nilsen K, Aquino C, Himmelbach A, Copetti D, Ban T, Venturini L, Bevan M, Clavijo B, Koo DH, Ens J, Wiebe K, N'Diaye A, Fritz AK, Gutwin C, Fiebig A, Fosker C, Fu BX, Accinelli GG, Gardner KA, Fradgley N, Gutierrez-Gonzalez J, Halstead-Nussloch G, Hatakeyama M, Koj CS, Deek J, Costamagna AC, Fobert P, Heavens D, Kanamori H, Kawaura K, Kobayashi F, Krasileva K, Kuo T, McKenzie N, Murata K, Nabeka Y, Paape T, Padmarasu S, Percival-Alwyn L, Kagale S, Scholz U, Sese J, Juliana P, Singh R, Shimizu-Inatsugi R, Swarbreck D, Cockram J, Budak H, Tameshige T, Tanaka T, Tsuji H, Wright J, Wu J, Steuernagel B, Small I, Cloutier S, Keeble-Gagnère G, Muehlbauer G, Tibbets J, Nasuda S, Melonek J, Hucl PJ, Sharpe AG, Clark M, Legg E, Bharti A, Langridge P, Hall A, Uauy C, Mascher M, Krattinger SG, Handa H, Shimizu KK, Distelfeld A, Chalmers K, Keller B, Mayer KFX, Poland J, Stein N, McCartney CA, Spannagl M, Wicker T, Pozniak CJ. 2020. **Multiple wheat genomes reveal global variation in modern breeding**. Nature 588:277-283.

Wang G, DiTusa SF, Oh DH, Herrmann AD, Mendoza-Cozatl DG, O'Neill MA, Smith AP, Dassanayake M. 2021a. **Cross species multi-omics reveals cell wall sequestration and elevated global transcript abundance as mechanisms of boron tolerance in plants**. New Phytologist 230:1985-2000.

Wang J, Sidharth S, Zeng S, Jiang Y, Chan YO, Lyu Z, McCubbin T, Mertz R, Sharp RE, Joshi T. 2022. **Bioinformatics for plant and agricultural discoveries in the age of multiomics: a review and case study of maize nodal root growth under water deficit**. Physiologia Plantarum 174:e13672.

Wang Q, Garrity GM, Tiedje JM, Cole JR. 2007. **Naive Bayesian classifier for rapid assignment of rRNA sequences into the new bacterial taxonomy**. Applied and environmental microbiology, 73:5261-5267.

Wang S, Liu L, Mi X, Zhao S, An Y, Xia X, Guo R, Wei C. 2021b. **Multi-omics analysis to visualize the dynamic roles of defense genes in the response of tea plants to gray blight**. The Plant Journal 106:862-875.

Weiss S, Van Treuren W, Lozupone C, Faust K, Friedman J, Deng Y, Xia LC, Xu ZZ, Ursell L, Alm EJ, Birmingham A, Cram JA, Fuhrman JA, Raes J, Sun F, Zhou J, Knight R. 2016. **Correlation detection strategies in microbial data sets vary widely in sensitivity and precision**. The ISME Journal 10:1669-1681.

Worley B and Powers R. 2013. **Multivariate analysis in metabolomics**. Current Metabolomics 1:92-107.

Wu F, Zhou Y, Shen Y, Sun Z, Li L, Li T. 2022. **Linking multi-omics to wheat resistance types to Fusarium head blight to reveal the underlying mechanisms**. International Journal of Molecular Sciences 23:2280.

Yan J, Risacher SL, Shen L, Saykin AJ. 2017. **Network approaches to systems biology analysis of complex disease: integrative methods for multi-omics data**. Briefings in Bioinformatics 19:1370-1381.

Yang G, Pan W, Cao R, Guo Q, Cheng Y, Zhao Q, Cui L, Nie X. 2022. **Multi-omics reveals the key and specific miRNA-mRNA modules underlying salt tolerance in wild emmer wheat (*Triticum dicoccoides* L.)**. BMC Genomics 23:724.

Yang L, Lei L, Liu H, Wang J, Zheng H, Zou D. 2020. **Whole-genome mining of abiotic stress gene loci in rice**. Planta 252:85.

Yang Y, Wang N, Guo X, Zhang Y, Ye B. 2017. **Comparative analysis of bacterial community structure in the rhizosphere of maize by high-throughput pyrosequencing**. PLOS ONE 12:e0178425.

Yuan C, Li C, Yan L, Jackson AO, Liu Z, Han C, Yu J, Li D. 2011. **A high throughput *Barley Stripe Mosaic Virus* vector for virus induced gene silencing in monocots and dicots**. PLOS ONE 6:e26468.

Zander M, Lewsey MG, Clark NM, Yin L, Bartlett A, Guzmán JPS, Hann E, Langford AE, Jow B, Wise A, Nery JR, Chen H, Bar-Joseph Z, Walley JW, Solano R, Ecker JR. 2020. **Integrated multi-omics framework of the plant response to jasmonic acid**. Nature Plants 6:290-302.

Zhan C, Shen S, Yang C, Liu Z, Fernie AR, Graham IA, Luo J. 2022. **Plant metabolic gene clusters in the multi-omics era**. Trends in Plant Science 27:981-1001.

Zhao S, Zhang Q, Liu Zhou H, Ma C, Wang P. 2021. **Regulation of plant responses to salt stress**. International Journal of Molecular Sciences 22:4609.

Zhao Y, Sun R, Liu H, Liu X, Xu K, Xiao K, Zhang S, Yang X, Xue C. 2020. **Multi-omics analyses reveal the molecular mechanisms underlying the adaptation of wheat (*Triticum aestivum* L.) to potassium deprivation**. Frontiers in Plant Science 11:588994.

Zhou M and Zheng S. 2022. **Multi-omics uncover the mechanism of wheat under heavy metal stress**. International Journal of Molecular Sciences. 23:15968.

Zou Y, Zhang X, Tan Y, Huang JB, Zheng Z, Tao LZ. 2019. **Phosphoethanolamine N-methyltransferase 1 contributes to maintenance of root apical meristem by affecting ROS and auxin-regulated cell differentiation in Arabidopsis**. New Phytologist 224:258-273.

Funding and Acknowledgments

This research was supported by the Israeli Science Research Foundation grant 234/19 for NS.

ZH was supported by a scholarship from The ADAMA Center for Novel Delivery Systems in

Crop Protection, Tel-Aviv University. We acknowledge Prof. Assaf Distelfeld for suppling the seeds stock.

Conflict of interest

The authors declare that they have no conflict of interest.

Data Availability

All data supporting the findings of this study are available within the paper and the Supplementary data.

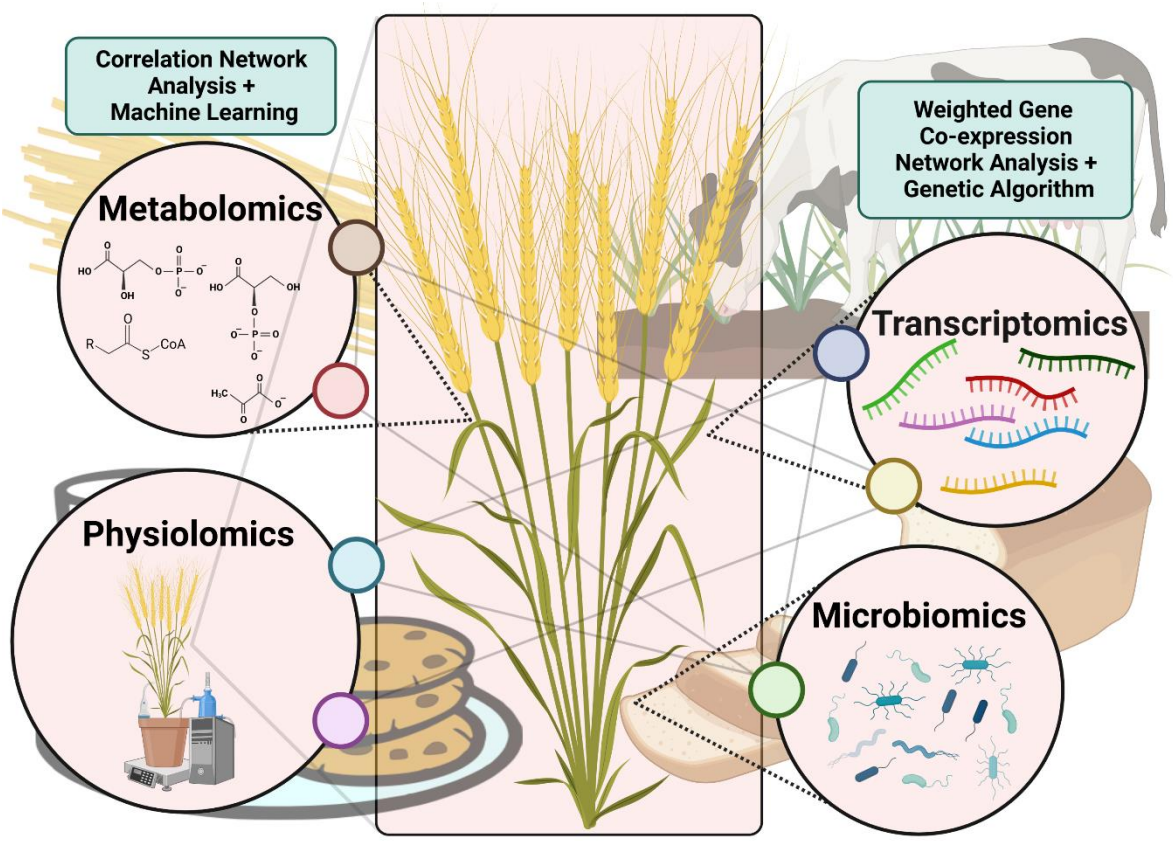

1065

1066 Fig. 1. **The biological model of the experiments and analyses performed in the**
1067 **current research.** Created with BioRender.com.

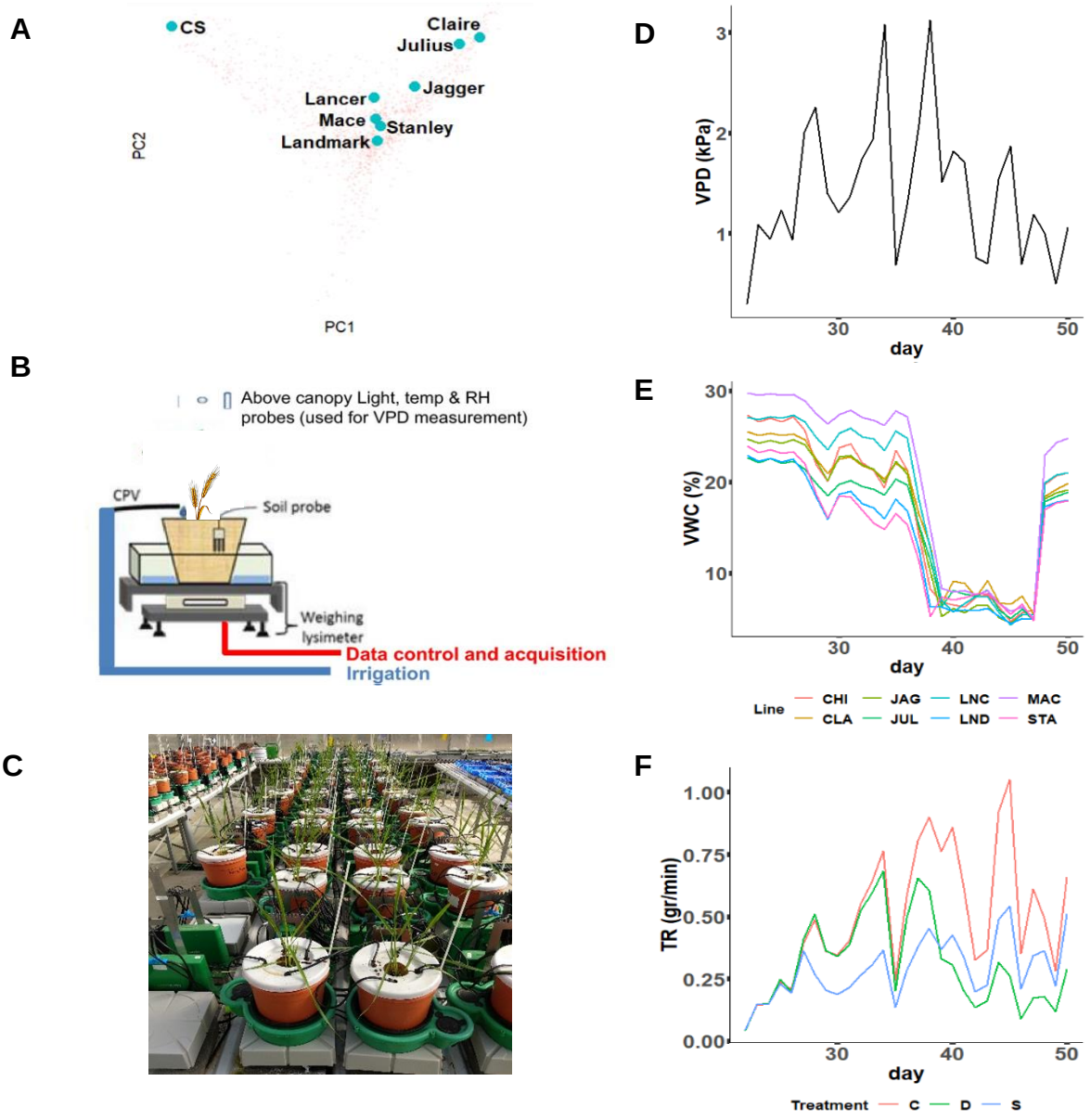

Fig. 2. **Experimental Setup. (A)** Principal component analysis of polymorphisms from exome-capture sequencing of approximately 1,200 lines (adapted from Walkowiak *et al.*, 2020, Fig. 1A). The blue dots represent lines used in this research. **(B)** An illustration of the experimental setup of one plant, generally consisting of a pot, automated irrigation, a lysimeter and environmental probes (adapted from Halperin *et al.*, 2017). Each plant was automatically irrigated and constantly weighed, and all plants were connected to a central system which collects and logs all the weight and environmental data. **(C)** Wheat plants on the mentioned lysimeter system. **(D-F)** Vapor Pressure Deficit (VPD) (D), average Volumetric Water Content (VWC) of drought plants by line (CHI - Chinese Spring, CLA - Claire, JAG - Jagger, JUL - Julius, LNC - Lancer, LND - Landmark, MAC - Mace, STA - Stanley) (E) and average Transpiration Rate by treatment (C- Control, D - Drought, S - Salinity) throughout the experiment (F).

1104

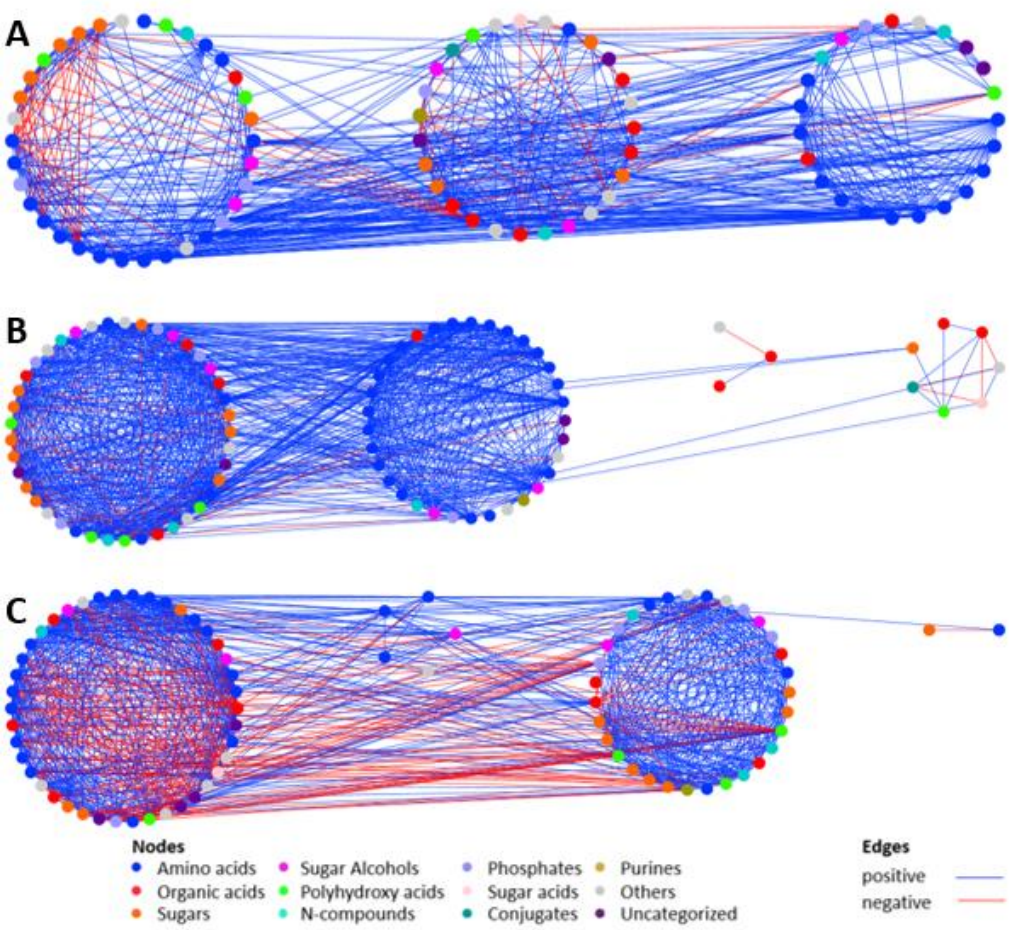

D

Pathway	Con Pred	Con Sens	Dro Pred	Dro Sens	Sal Pred	Sal Sens
L-carnitine biosynthesis	0.497	0.257	0.697	0.532	0.859	0.765
L-arginine biosynthesis I (via L-ornithine)	0.155	0.452	0.927	0.888	0.570	0.562
indole-3-acetate inactivation VIII	0.155	0.527	0.927	0.863	0.928	0.822
glycine biosynthesis III	0.497	0.374	0.697	0.586	0.859	0.764
nitric oxide biosynthesis II (mammals)	0.497	0.375	0.801	0.703	0.928	0.749

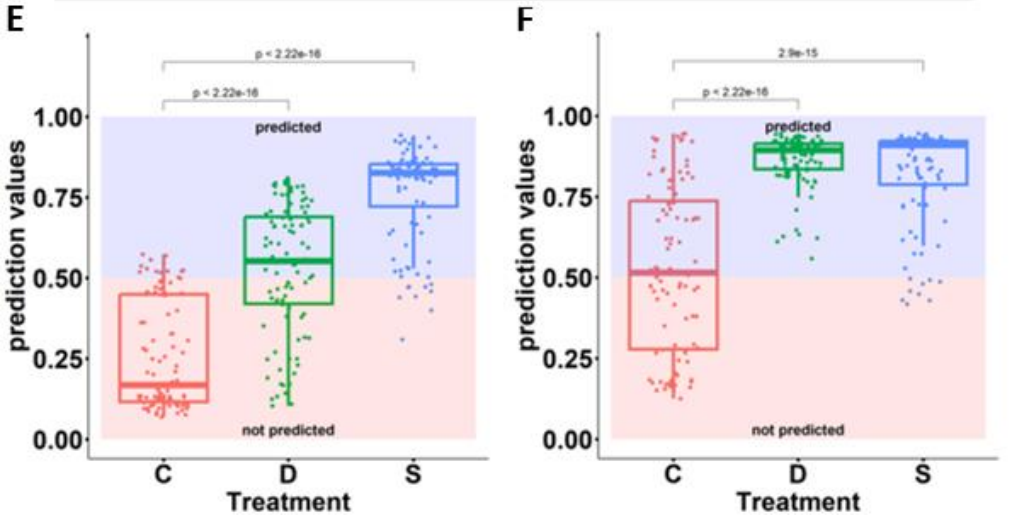

Fig. 3. **Unique pathways predicted for control-, drought- and salinity-treated plants.** A metabolic network was created for each treatment group, which was tested via machine learning (trained by positive and negative pathways) for pathway predictions. **(A-C)** The Cytoscape visualizations were presented for Control- (A), Drought- (B) and Salinity-treated plants (C) metabolic correlation networks. Each metabolite is represented as a node and each correlation between two metabolites is represented as an edge. Metabolites are color-coded according to their metabolic group (see key). Positive edges are color-coded as blue, and negative edges are color-coded as red. Metabolites were grouped into communities (*i.e.*, circle-formations) using the Walktrap algorithm (Pons and Latapy, 2005). (**D-F**) The MA models were also bootstrapped using a sensitivity test (100 times, 80% of positive and 80% negative pathways), and the average prediction result of each pathway was presented (Control – CON SENS, Drought – DRO SENS and Salinity – SAL SENS). Only pathways which received PRED and SENS values ≥ 0.5 (for each treatment respectively) were considered predicted for the respective treatment, as described by Toubiana *et al.* (2019b). (**D**) Pathways exclusively predicted for drought- and salinity-treated plants are presented. Pathways predicted exclusively for control-treated plants, drought-treated plants, salinity-treated plants and drought- and salinity-treated plants are presented in Supp. Table 2-5, respectively. (**E-F**) The sensitivity values were plotted by treatment (C – control, D – drought and S – salinity) for L-carnitine biosynthesis (E) and indole-3-acetate inactivation VIII (F).

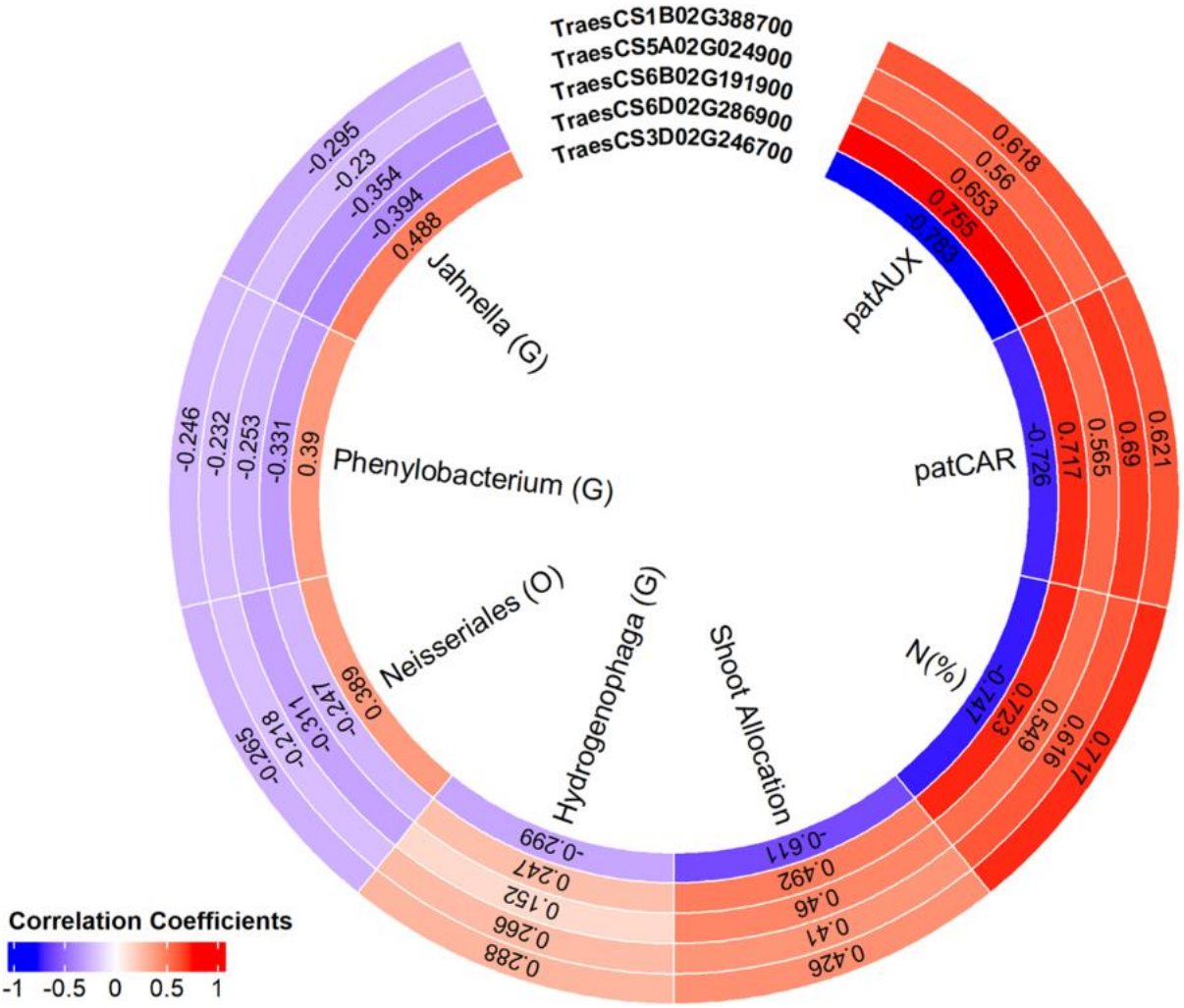

Fig. 4. **Correlation heatmap between post-GA genes' expression data and physiological, biochemical and microbiome parameters.** Following WGCNA and GA, genes with high Pearson correlation with the indole-3-acetate inactivation VIII (patAUX) and L-carnitine biosynthesis (patCAR) pathway OPLS-produced PC1s, and with biological pertinence, were selected. Their expression data were correlated with the indole-3-acetate inactivation VIII (patAUX) and L-carnitine biosynthesis (patCAR) pathway OPLS-produced PC1's, Nitrogen content (N(%)), shoot allocation (Shoot Allocation), *Hydrogenphaga* counts (Hydrogenphaga (G)), *Neisseriales* counts (Neisseriales (O)), *Phenylobacterium* counts (Phenylobacterium (G)), *Jahnella* counts (Jahnella (G)), and the correlation coefficients are shown in a false-color blue-white-red scale (low-high).

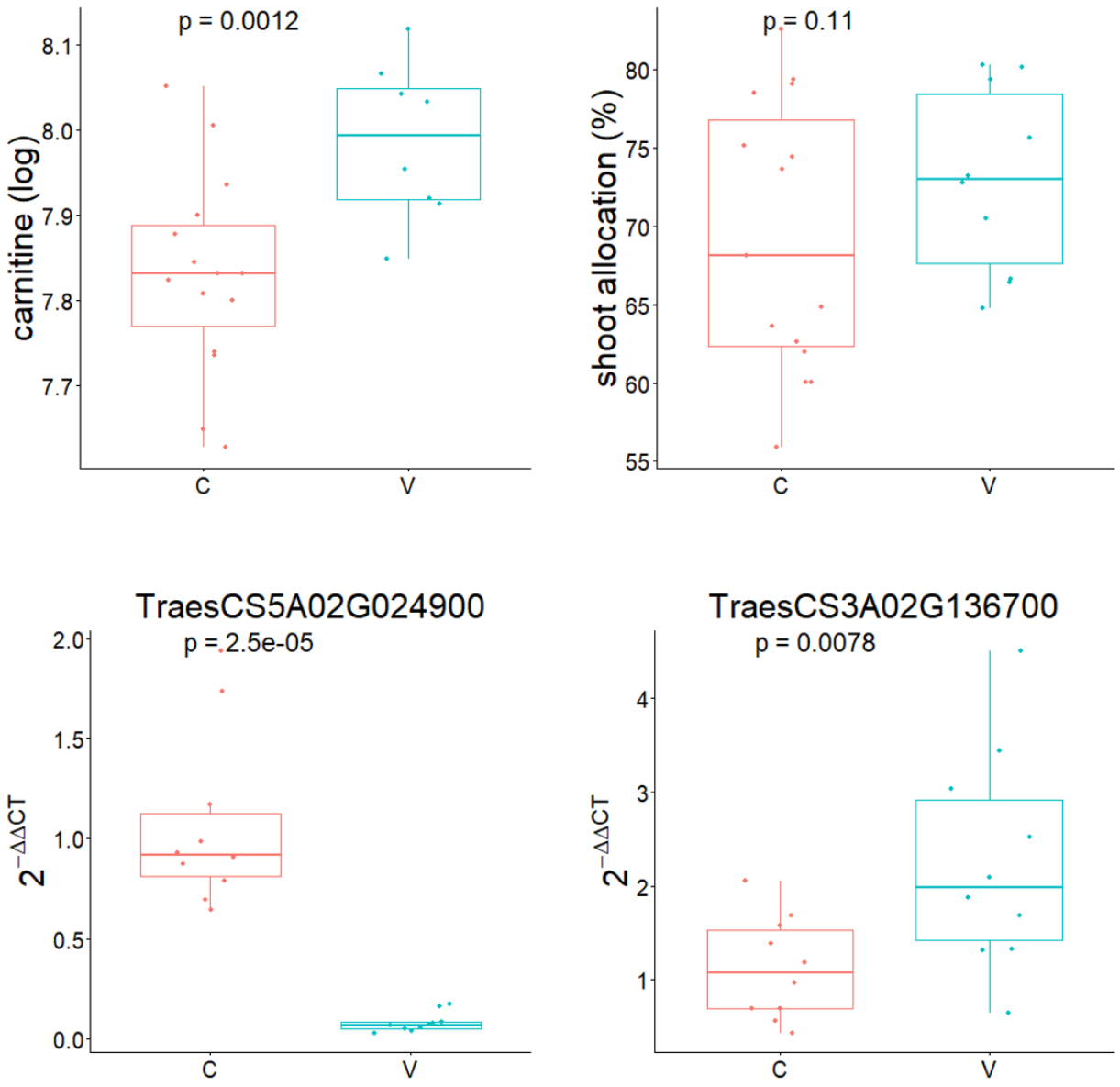

Fig. 5. **The effect of Virus-Induced Gene Silencing on L-carnitine biosynthesis under salinity conditions**. The boxplot representation of carnitine levels, shoot allocation, TraesCS5A02G024900 (a GA-chosen gene whose expression was directly correlated with the L-carnitine biosynthesis pathway PC1) expression levels and TraesCS3A02G136700 (a carnitine transporter) expression levels for control (C) and TraesCS5A02G024900-silenced (V). The results were tested using a student's t-test and the respective p-values are presented above each comparison.

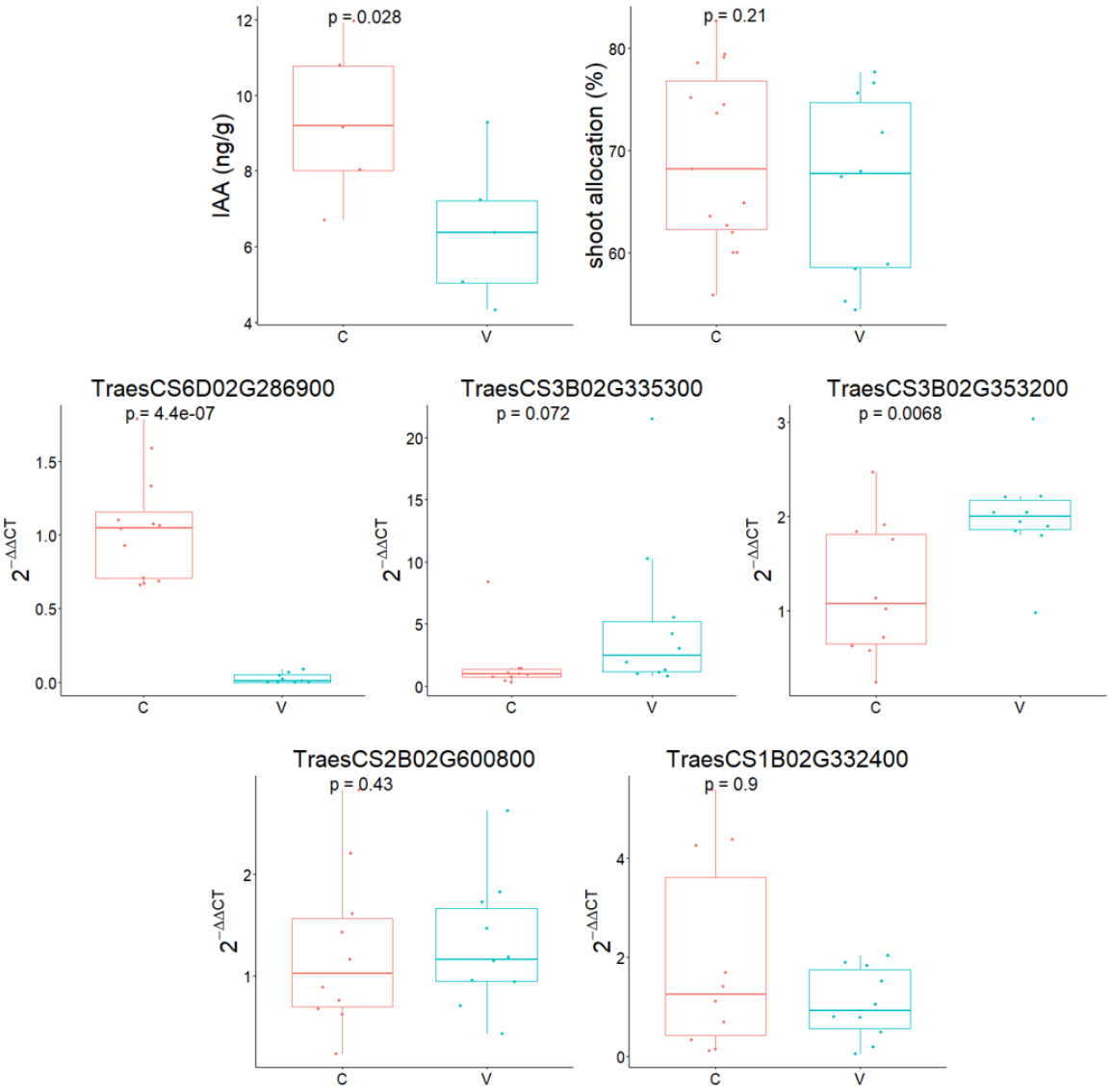

Fig. 6. **The effect of Virus-Induced Gene Silencing on indole-3-acetic acid Inactivation VIII under salinity conditions**. The boxplot representation of indole-3-acetic acid (IAA) levels, shoot allocation, TraesCS6D02G286900 (a GA-chosen gene whose expression was directly correlated with the indole-3-acetic acid inactivation VIII pathway PC1) expression levels, and TraesCS3B02G335300, TraesCS3B02G353200, TraesCS2B02G600800 and TraesCS1B02G332400 (Triticum aestivum orthologs of *Arabidopsis thaliana* genes participating in indole-3-acetic acid inactivation VIII, according to https://www.plantcyc.org) expression levels for control (C) and TraesCS5A02G024900-silenced (V). The results were tested using a student's t-test and the respective p-values are presented above each comparison.

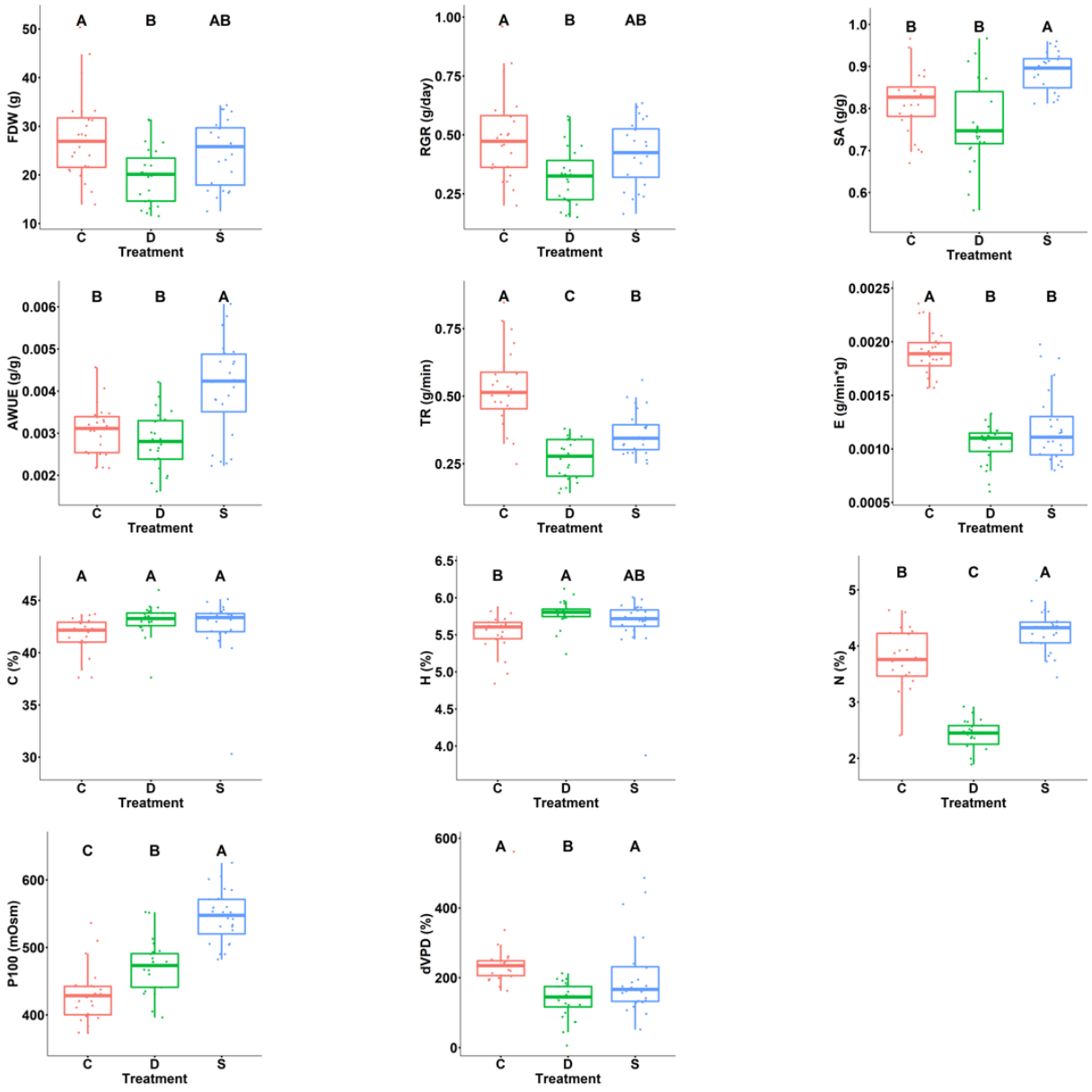

Supp. Fig. 1. **Physiological and Biochemical Parameters comparison between control-, drought- and salinity-treated plants.** Fresh Dry Weight (FDW), Relative Growth Rate (RGR), Shoot Allocation (SA), Agronomic Water Use Efficiency (AWUE), average Transpiration Rate (TR), E (E), Carbon (C), Hydrogen (H) and Nitrogen (N), Osmotic Potential at Full Hydration (π_{100}) and transpiration response to VPD increase (ΔVPD) are presented by treatment (C- Control, D - Drought, S - Salinity). Significant Differences were tested via the Tukey-Kramer test and the test values were denoted above each plot. The physiological raw data is in Supp. Table 17.

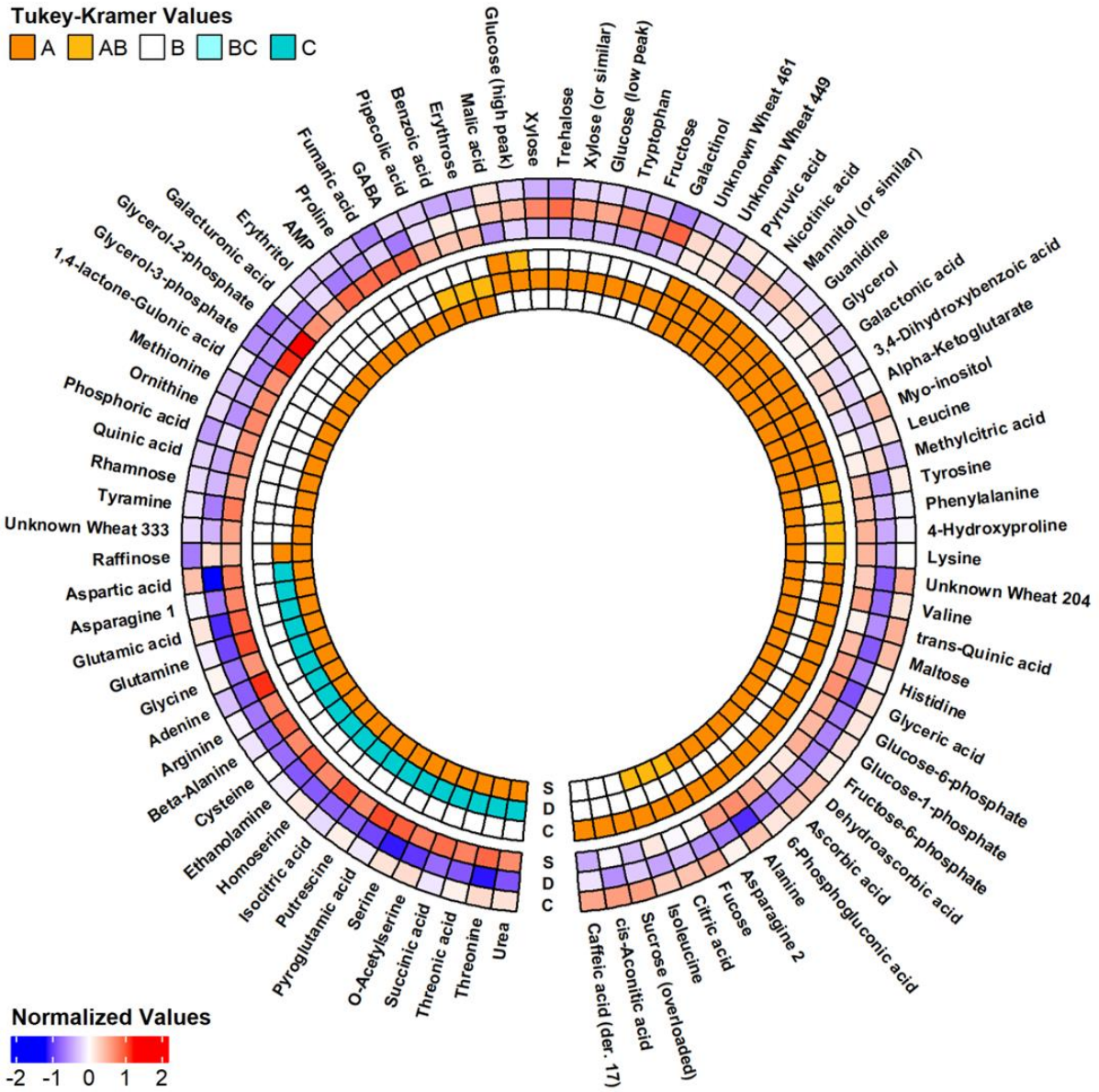

Supp. Fig. 2. **Metabolomics comparison between control-, drought- and salinity-treated plants.** Metabolite values were represented by their respective z-score and the average value by treatment (C- Control, D - Drought, S - Salinity) was represented in a false color blue-white-red scale. Significant differences between the transformed values were tested via the Tukey-Kramer test and the test values are presented in a false color blue-white-orange scale. The metabolomic raw data is in Supp. Table 18.

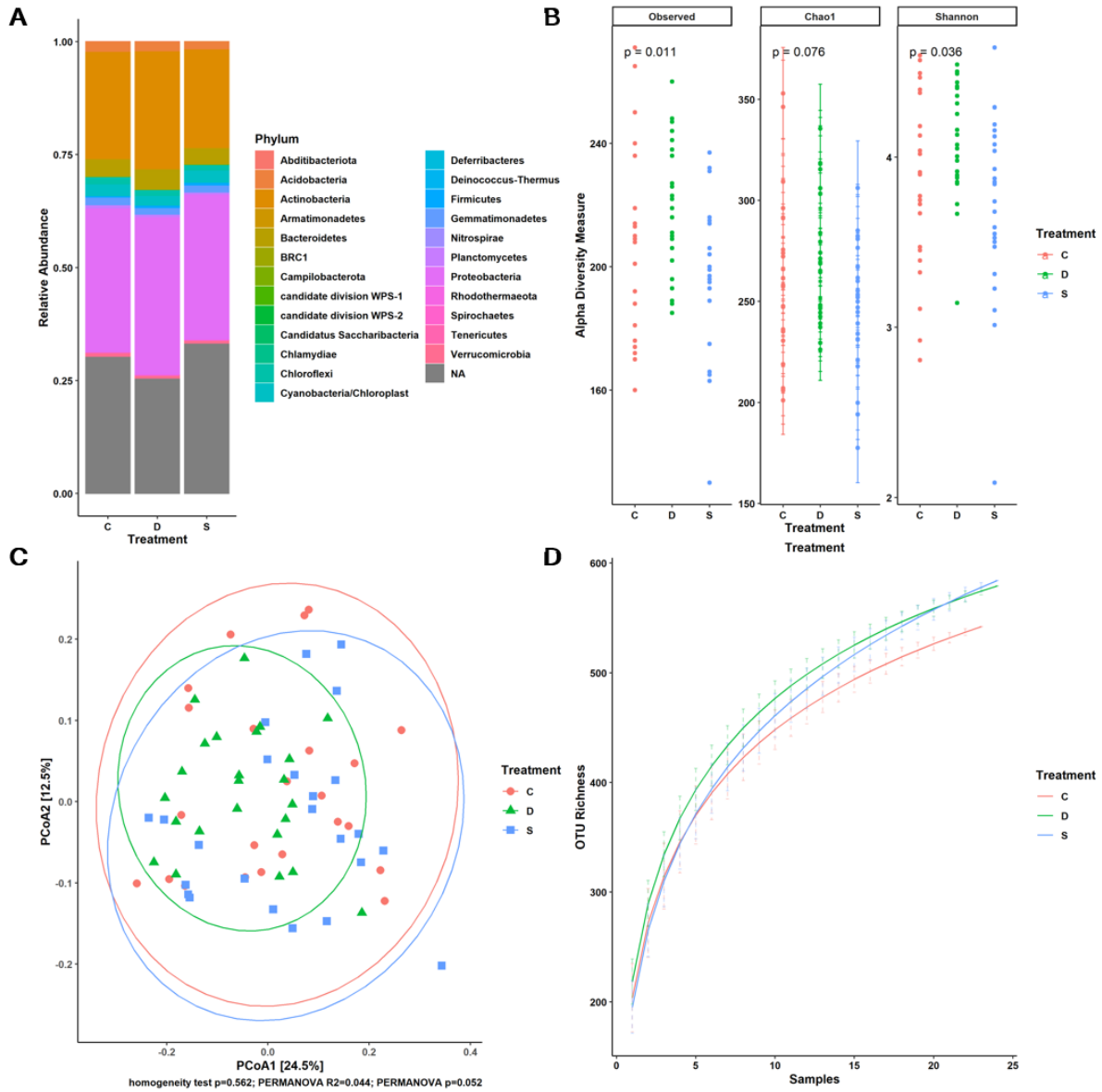

Supp. Fig. 3. **Microbiome diversity comparison between control-, drought- and salinity-treated plants.** OTU counts of control (C), drought (D) and salinity (S) treated plants (n=71) were rarefied. (A) A comparison of the relative abundance of taxa by phylum (n=23-24). (B) Alpha diversity analysis using observed species, Chao1 and Shannon indices along with their respective p-values. (C) Beta diversity analysis with Principal Coordinates Analysis (PCoA) using Bray-Curtis dissimilarity. (D) Gamma diversity analysis using geocluster accumulation curves for mean OTU richness from a random sampling of geoclusters ± SD. The microbiomic raw data is in Supp. Table 19 and the taxonomic file is in Supp. Table 20.

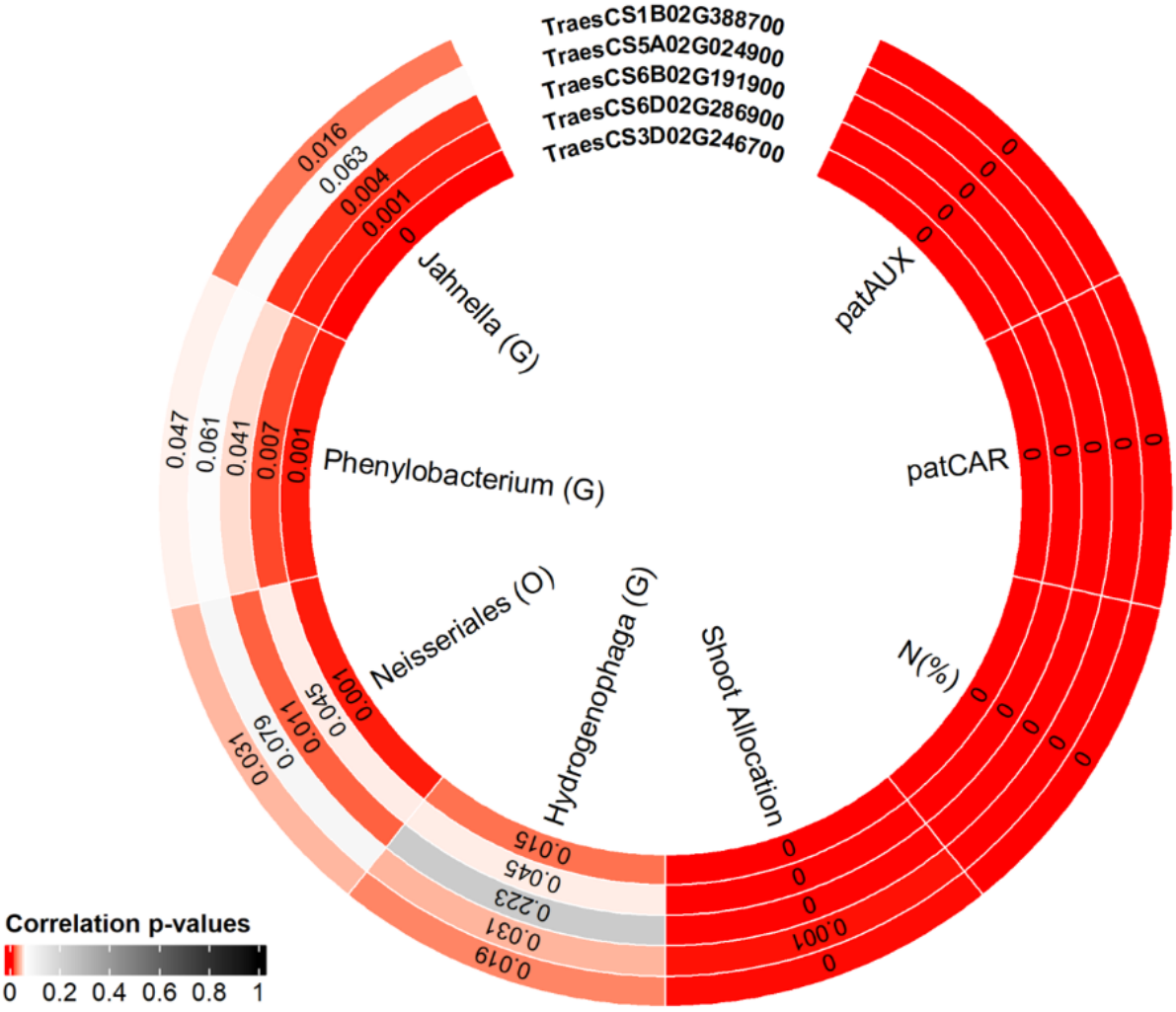

Supp. Fig. 4. **Correlation p-value heatmap between post-GA genes' expression data and physiological, biochemical and microbiome parameters.** Following WGCNA and GA, genes with high Pearson correlation with the indole-3-acetate inactivation VIII (patAUX) and L-carnitine biosynthesis (patCAR) pathway OPLS-produced PC1s, and with biological pertinence, were selected. Their expression data were correlated with the indole-3-acetate inactivation VIII (patAUX) and L-carnitine biosynthesis (patCAR) pathway OPLS-produced PC1s, Nitrogen content (N(%)), shoot allocation (Shoot Allocation), *Hydrogenphaga* counts (Hydrogenphaga (G)), *Neisseriales* counts (Neisseriales (O)), *Phenylobacterium* counts (Phenylobacterium (G)), *Jahnella* counts (Jahnella (G)), and the corresponding correlation p-values are shown in a false-color red-white-black scale (low-high).

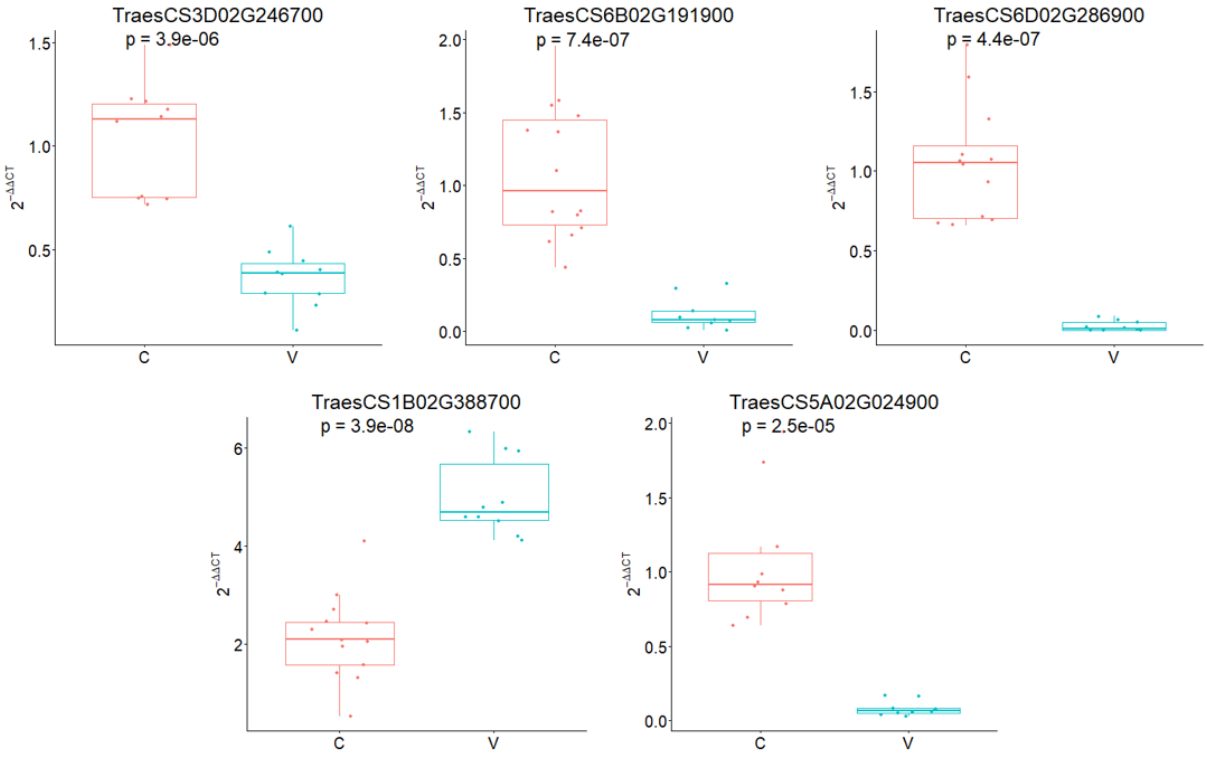

Supp. Fig. 5. **The effect of Virus-Induced Gene Silencing on gene expression under salinity conditions**. The boxplot representation of TraesCS3D02G246700, TraesCS6B02G191900, TraesCS6D02G286900, TraesCS1B02G388700 and TraesCS5A02G024900 (the GA-chosen genes whose expression was directly correlated with the indole-3-acetic acid inactivation VIII pathway PC1 and L-carnitine biosynthesis pathway PC1) expression levels for control (C) and silenced (V). The results were tested using a student's t-test and the respective p-values were presented above each comparison.

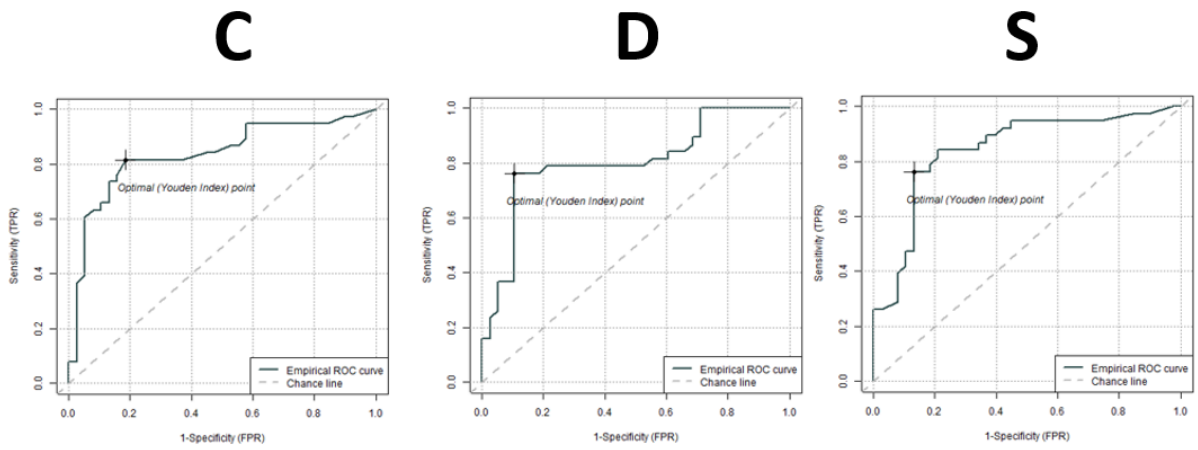

	REFERENCE	
PREDICTION	1	2
1	32	6
2	9	29

	REFERENCE	
PREDICTION	1	2
1	34	4
2	9	29

	REFERENCE	
PREDICTION	1	2
1	28	10
2	6	32

Supp. Fig. 6. **ROC curves (top) and confusion matrices (bottom) of 10-fold cross-validated ML models for the control- (C), drought- (D) and salinity-treated (S) plants**.

5. Discussion

Scientifically driven global yield breakthroughs include the Haber-Bosch process (industrial ammonia fixation; Erisman et al., 2008) and the green revolution (Hedden, 2003). While the need for a second green revolution is clear, the means to reach that end are not. We can only assume this will require some vertically disruptive technologies, such as multi-omics and computational tools (Liu et al., 2013; Tian et al., 2020).

In this thesis, we applied an unbiased top-down based approach to study the complex molecular and physiological relationships of crop plants grown under different stress conditions. We started from a broad whole-plant physiological experiments and through multi-omics and systems biology we uncovered clear phenotypic responses under prominent abiotic stresses that are associated with yet unknown metabolic pathways in the context of stress response.

The metabolome encompasses all metabolites present within a biological system and exhibits variability due to genetic differences, environmental fluctuations, and their interactions. Plant stress response is significantly influenced by changes in the metabolome, leading to detrimental effects like reduced energy supply and inhibition of metabolic enzyme activity. In response to stress, plants undergo metabolic reprogramming to better adapt to challenging environmental conditions, often by enhancing the production of "anti-stress" compounds (Obata & Fernie, 2012). The metabolome acts as a critical mediator linking genetic variation to complex traits such as stress tolerance in plants (Rinschen et al., 2019). Therefore, analyzing changes in metabolome pathways under stress, coupled with an examination of the plant's overall physiological response, can offer valuable insights into the genetic mechanisms underlying plant stress response.

Moreover, understanding the functioning of metabolic pathways within the intricate coordination of cellular metabolism is crucial for crop enhancement and stress tolerance. The conventional constraint-based method is widely used to propose metabolic pathways in organisms, organizing genes that regulate these pathways into comprehensive genome-scale networks. This approach involves enrichment analysis using expression data to identify significant metabolic processes (Karp et al.,2005; Kanehisa et al.,2014). However, it overlooks the post-regulatory mechanisms occurring across genetic, enzymatic, and metabolic levels within cells. The approach outlined and used in this thesis relies on quantitative metabolite measurements, providing a means to account for post-transcriptional and post-translational events without the need for a-priori rely on gene data integration. This thesis demonstrates that

metabolic correlation-based networks capture a wealth of information about cellular activity beyond their previous attribution in crop plants under different environmental conditions. To detect metabolic pathways within metabolic CNs, network analysis was combined with ML techniques.

Employing this innovative approach, we successfully unearthed novel metabolic pathways linked to stress tolerance in two prominent crop species, wheat and tomato. These pathways include L-Glutamine biosynthesis, L-arginine biosynthesis, L-carnitine biosynthesis, and indole-3-acetic acid inactivation. Furthermore, by integrating high-throughput physiological, transcriptional, and microbiome data, we established connections between metabolic profiles and various plant stress indicators such as nitrogen content, shoot allocation, photosynthesis, and microbiome composition (e.g., Hydrogenophaga, Neisseriales, Phenylobacterium, Jahnella). Additionally, we identified potential novel regulators of plant stress response and metabolic pathways, exemplified by genes like TraesCS5A02G024900 and Solyc08G067630. Although this thesis did not explore the specific functions of these altered genes, it underscored the interconnectedness between in silico predictions and in vivo observations, underscoring the efficacy and significance of our "system biology" approach for enhancing stress tolerance in crop plants. Moreover, this approach revealed genes and metabolic pathways that would not be detected using targeted methods (i.e., focusing specifically on genes related to metabolic pathways in established genomic, transcriptomic and metabolomic databases).

Finally, this thesis also discusses and emphasizes the importance of function validation of computational studies as a part of the “systems biology” approach. This is typically accomplished using reverse genetic methodologies such as CRISPR and VIGS for gene knockout, as demonstrated in this thesis for plant crops. However, to achieve sufficient and feasible progress in crop plant breeding, enhancement of multiple traits in parallel is required, including biotic and abiotic stress tolerance, high yield, and nutritional values, thereby generating "super crops" (Li et al.,2021). Due to the complexity of technical difficulties in generating multi-target CRISPR lines and the interactions between stress responses, we propose in this thesis enhancing already commercially available local landraces with higher yield traits, along with stress tolerances specific to the respective localities, instead of generating a general 'super crop'. We hope this conclusion will serve as a sustainable solution to commercially enhancing crop yields under both stable and challenging environmental conditions.

6. References

Alotaibi F, Alharbi S, Alotaibi M, Al Mosallam M, Motawei M, Alrajhi A (2021) Wheat omics: Classical breeding to new breeding technologies. Saudi Journal of Biological Sciences **28:** 1433-1444

AGI (The Arabidopsis Genome Initiative). 2000. Analysis of the genome sequence of the flowering plant Arabidopsis thaliana. Nature 408:796-815.

Bagati S, Mahajan R, Nazir M, Dar AA, Zargar SM. 2018. "Omics": a gateway towards abiotic stress tolerance. In: Zargar SM and Zargar MY (Eds.) Abiotic stress-mediated sensing and signaling in plants: an Omics perspective (pp. 1-45). Springer, Singapore.

Ben-Amar A, Daldoul S, Reustle GM, Krczal G, Mliki A (2016) Reverse Genetics and High Throughput Sequencing Methodologies for Plant Functional Genomics. Current Genomics **17:** 460-475

Berger B, Peng J, Singh M (2013) Computational solutions for omics data. Nature Reviews Genetics **14:** 333-346

Brenchley R, Spannagl M, Pfeifer M, Barker GLA, D'Amore R, Allen AM, McKenzie N, Kramer M, Kerhornou A, Bolser D, Kay S, Waite D, Trick M, Bancroft I, Gu Y, Huo N, Luo MC, Sehgal S, Gill B, Kianian S, Anderson O, Kersey P, Dvorak J, McCombie WR, Hall A, Mayer KFX, Edwards KJ, Bevan MW, Hall N (2012) Analysis of the breadwheat genome using whole-genome shotgun sequencing. Nature 491: 705-710

Erisman JW, Sutton MA, Galloway J, Klimont Z, Winiwarter W (2008) How a century of ammonia synthesis changed the world. Nature Geoscience **1:** 636-639

Feng ZY, Mao YF, Xu NF, Zhang BT, Wei PL, Yang DL, Wang Z, Zhang ZJ, Zheng R, Yang L, Zeng L, Liu XD, Zhu JK (2014) Multigeneration analysis reveals the inheritance, specificity, and patterns of CRISPR/Cas-induced gene modifications in Arabidopsis. Proceedings of the National Academy of Sciences of the United States of America **111:** 4632-4637

Fiehn O, Barupal DK, Kind T (2011) Extending biochemical databases by metabolomic surveys. (vol 286, pg 23637, 2011). Journal of Biological Chemistry **286:** 30244-30244

Gastinel LN. 2012. Principal component analysis in the era of «Omics» data. In: Sanguansat P (Ed.) Principal component analysis: multidisciplinary applications (pp. 21-42). InTech, Rijeka.

Goel S, Singh K, Grewal S, Nath M (2020) Impact of "Omics" in Improving Drought Tolerance in Wheat. Critical Reviews in Plant Sciences **39:** 222-235

Hedden P (2003) The genes of the Green Revolution. Trends in Genetics **19:** 5-9

Hochberg U, Degu A, Toubiana D, Gendler T, Nikoloski Z, Rachmilevitch S, Fait A (2013) Metabolite profiling and network analysis reveal coordinated changes in grapevine water stress response. Bmc Plant Biology **13**

Ivanova O, Richards LB, Vijverberg SJ, Neerincx AH, Sinha A, Sterk PJ, Maitland-van der Zee AH. (2019) What did we learn from multiple omics studies in asthma? Allergy 74:2129-2145.

IWGSC (The International Wheat Genome Sequencing Consortium). 2014. A chromosome-based draft sequence of the hexaploidy bread wheat (Triticum aestivum) genome. Science 345:1251788.

IWGSC (The International Wheat Genome Sequencing Consortium). 2018. Shifting the limits in wheat research and breeding using a fully annotated reference genome. Science 361:eaar7191

Joyce AR, Palsson BO (2006) The model organism as a system: integrating 'omics' data sets. Nature Reviews Molecular Cell Biology **7:** 198-210

Kanehisa M, Goto S, Sato Y, Kawashima M, Furumichi M, Tanabe M (2014) Data, information, knowledge and principle: back to metabolism in KEGG. Nucleic Acids Research **42:** D199-D205

Karp PD, Ouzounis CA, Moore-Kochlacs C, Goldovsky L, Kaipa P, Ahrén D, Tsoka S, Darzentas N, Kunin V, López-Bigas N (2005) Expansion of the BioCyc collection of pathway/genome databases to 160 genomes. Nucleic Acids Research **33:** 6083-6089

Kumar A, Pathak RK, Gupta SM, Gaur VS, Pandey D (2015) Systems Biology for Smart Crops and Agricultural Innovation: Filling the Gaps between Genotype and Phenotype for Complex Traits Linked with Robust Agricultural Productivity and Sustainability. Omics-a Journal of Integrative Biology **19:** 581-601

Li SY, Zhang C, Li JY, Yan L, Wang N, Xia LQ (2021) Present and future prospects for wheat improvement through genome editing and advanced technologies. Plant Communications **2**

Liu WS, Yuan JS, Stewart CN (2013) Advanced genetic tools for plant biotechnology. Nature Reviews Genetics **14:** 781-793

Lu R, Martin-Hernandez AM, Peart JR, Malcuit I, Baulcombe DC (2003) Virus-induced gene silencing in plants. Methods **30:** 296-303

Misra BB, Langefeld C, Olivier M, Cox LA. (2019). Integrated omics: tools, advances and future approaches. Journal of Molecular Endocrinology. **62**, R21–R45

Monk J, Nogales J, Palsson BO (2014) Optimizing genome-scale network reconstructions. Nature Biotechnology **32:** 447-452

Obata T, Fernie AR (2012) The use of metabolomics to dissect plant responses to abiotic stresses. Cellular and Molecular Life Sciences **69:** 3225-3243

Rinschen MM, Ivanisevic J, Giera M, Siuzdak G (2019) Identification of bioactive metabolites using activity metabolomics. Nature Reviews Molecular Cell Biology **20:** 353-367

Shah T, Xu JS, Zou XL, Cheng Y, Nasir M, Zhang XK (2018) Omics Approaches for Engineering Wheat Production under Abiotic Stresses. International Journal of Molecular Sciences **19**

Shah ZH, Rehman HM, Akhtar T, Daur I, Nawaz MA, Ahmad MQ, Rana IA, Atif RM, Yang SH, Chung G (2017) Redox and Ionic Homeostasis Regulations against Oxidative, Salinity and Drought Stress in Wheat (A Systems Biology Approach). Frontiers in Genetics **8**

Tian ZX, Wang JW, Li JY, Han B (2021) Designing future crops: challenges and strategies for sustainable agriculture. Plant Journal **105:** 1165-1178

Toubiana D, Cabrera R, Salas E, Maccera C, dos Santos GF, Cevallos D, Lindqvist-Kreuze H, Lopez JM, Maruenda H (2020) Morphological and metabolic profiling of a tropical-adapted potato association panel subjected to water recovery treatment reveals new insights into plant vigor. Plant Journal **103:** 2193-2210

Toubiana D, Fernie AR, Nikoloski Z, Fait A (2013) Network analysis: tackling complex data to study plant metabolism. Trends in Biotechnology **31:** 29-36

Toubiana D, Maruenda H (2021) Guidelines for correlation coefficient threshold settings in metabolite correlation networks exemplified on a potato association panel. Bmc Bioinformatics **22**

Toubiana D, Puzis R, Sadka A, Blumwald E (2019) A Genetic Algorithm to Optimize Weighted Gene Co-Expression Network Analysis. Journal of Computational Biology **26:** 1349-1366

Toubiana D, Puzis R, Wen LL, Sikron N, Kurmanbayeva A, Soltabayeva A, Wilhelmi MDR, Sade N, Fait A, Sagi M, Blumwald E, Elovici Y (2019) Combined network analysis and machine learning allows the prediction of metabolic pathways from tomato metabolomics data. Communications Biology **2**

Toubiana D, Sade N, Liu LF, Wilhelmi MDR, Brotman Y, Luzarowska U, Vogel JP, Blumwald E (2020) Correlation-based network analysis combined with machine learning techniques highlight the role of the GABA shunt in Brachypodium sylvaticum freezing tolerance. Scientific Reports **10**

van Dijk ADJ, Kootstra G, Kruijer W, de Ridder D (2021) Machine learning in plant science and plant breeding. Iscience **24**

Walkowiak S, Gao LL, Monat C, Haberer G, Kassa MT, Brinton J, Ramirez-Gonzalez RH, Kolodziej MC, Delorean E, Thambugala D, Klymiuk V, Byrns B, Gundlach H, Bandi V, Siri JN, Nilsen K, Aquino C, Himmelbach A, Copetti D, Ban T, Venturini L, Bevan M, Clavijo B, Koo DH, Ens J, Wiebe K, N'Diaye A, Fritz AK, Gutwin C, Fiebig A, Fosker C, Fu BX, Accinelli GG, Gardner KA, Fradgley N, Gutierrez-Gonzalez J, Halstead-Nussloch G, Hatakeyama M, Koh CS, Deek J, Costamagna AC, Fobert P, Heavens D, Kanamori H, Kawaura K, Kobayashi F, Krasileva K, Kuo T, McKenzie N, Murata K, Nabeka Y, Paape T, Padmarasu S, Percival-Alwyn L, Kagale S, Scholz U, Sese J, Juliana P, Singh R, Shimizu-Inatsugi R, Swarbreck D, Cockram J, Budak H, Tameshige T, Tanaka T, Tsuji H, Wright J, Wu JZ, Steuernagel B, Small I, Cloutier S, Keeble-Gagnère G, Muehlbauer G, Tibbets J, Nasuda S, Melonek J, Hucl PJ, Sharpe AG, Clark M, Legg E, Bharti A, Langridge P, Hall A, Uauy C, Mascher M, Krattinger SG, Handa H, Shimizu KK, Distelfeld A, Chalmers K, Keller B, Mayer KFX, Poland J, Stein N, McCartney CA, Spannagl M, Wicker T, Pozniak CJ (2020) Multiple wheat genomes reveal global variation in modern breeding. Nature **588**

תקציר

שיפור פרודוקטיביות היבול במיוחד תחת תנאי עקה סביבתית הינה תכונה העומדת היום בראש סדר העדיפויות של חוקרי צמחים בעולם. עמידות לעקות סביבתיות טופחה באופן מסורתי על ידי בחירת הצמחים המתאימים ביותר מהשדה. בעשורים האחרונים התקדמות במחקר ושיטות מתקדמות של טיפוח, טרנספורמציה גנטית ועריכה גנומית נכנסו לשימוש תדיר במחקר צמחים תחת תנאי עקה אך לאלה הייתה השפעה יחסית שולית על גילוי גנים וגורמים חשובים לעמידות לעקות. לאחרונה, שיפור ביכולות איסוף מידע מהיר אפשרו לייצר מסדי נתונים ביולוגיים זולים יחסית בתפוקה גבוהה מצמחים תחת תנאי עקה, אך עקב האכילס שלהם הוא חוסר היכולת לעבד באופן ידני את כמות הנתונים. לכן, רבים פונים לסטטיסטיקה ולביולוגיה חישובית כדי לגשר על הפער והשילוב הזה מכונה גם "ביולוגיה רב מערכתית".

בפרקי התזה, ישמנו גם בצמחי חיטה וגם בצמחי עגבניה גישה של ביולוגיה רב מערכתית תוך שימוש במדידות פיזיולוגיות, ביוכימיות, מטבולומיות ומיקרוביומיות תחת תנאי סביבה אופטימליים ותנאי עקה סביבתית (מליחות, יובש ותנאי עקה של מחסור בחנקן). על מנת לפענח נתונים אלה, כמו גם לבאר באופן ספציפי את הנתונים בהקשר המטבולי שלהם, השתמשנו בטכניקות ביולוגיה חישובית, כגון ניתוח רשתות מתאם ולמידת מכונה על מנת לזהות מסלולים מטבוליים חדשים וגני מטרה המעורבים בתגובת הגידולים לעקות. יתרה מכך, גילוי הגנים החדשים הללו מאומת בצמח השלם באמצעות טכניקות הנדסה גנטית, כולל Clustered Regularly Interspaced Short Palindromic Repeats (CRISPR) והשתקת גנים הנגרמת על ידי וירוסים (VIGS).

בעזרת שימוש בביולוגיה מערכתית, הראנו שפרקטיקת השימוש בפסולת עגבניות כחומר תוספת למצע הגידול הינו בעל השפעה חיובית על גידולי עגבניות תחת מליחות גבוהה וחנקן עם שיפור בצמיחת הצמח, התפוקה והביצועים הפיזיולוגיים וזאת תוך שינויים של המטבולומיקה ואוכלוסיית החיידקים של הצמח.

עוד חקרנו בעזרת ביולוגיה רב מערכתית את ייצוב הכלורופלסט כתכונה להגביר את היכולת של עלי מקור העגבניות לשמור על קצב פוטוסינטזה גבוה וגם להאריך את משך ההטמעה הכולל ובכך להשפיע על חילוף החומרים של הפרי. ניתוח רב מערכתי של רנ"א ומטבולומיקה על צמחי עגבניה מוטנטים תחת עקת מלח ויובש בשילוב למידת מכונה חשפה את מסלולי הביוסינתזה של חומצות אמינו חשובות כמו גלוטמין וארגינין כקשורים לתגובת הצמח לעקה ולאיכות הפרי.

בנוסף, חקרנו את ההשפעה של עקת יובש ומלח על אוסף חיטת הלחם העולמי תוך שימוש בגישה ביולוגית רב מערכתית וטכניקות אנליטיות מתקדמות כמו ניתוח רשת ולמידת מכונה. זאת על מנת לזהות מסלולים וגנים ספציפיים המעורבים בתגובת חיטה לעקה. בעזרת גישה זו, זיהינו שני מסלולים (סינטזה של אוקסין וסינטזה של חומצה אמינית קרניטין) והגנים הקשורים להם כקשורים לתגובת חיטה לעקות סביבתיות.

לבסוף, אנו דנים ביישום טכנולוגיות עריכת גנומית לשיפור צמחי חיטה עם דגש על עקות סביבתיות. אנו מדגישים את החשיבות של שיפור עמידות במספר תכונות בו-זמנית. אנו מספקים דוגמאות למניפולציה מוצלחת של תכונות חיטה שונות באמצעות עריכה גנטית. אנחנו מדגישים את הפוטנציאל החקלאי ביצירת זן חיטה עמיד להשפעות של שינויי האקלים. סקירתנו מציעה לשפר זנים מקומיים עם עמידות ספציפית במקום לנסות לייצר "סופר חיטה", כפתרון יותר בר-קיימא לשיפור תנובת היבול בתנאי סביבה מגוונים.

GEORGE S. WISE FACULTY OF LIFE SCIENCES
GRADUATE SCHOOL

חיבור לשם קבלת תואר

דוקטור בפילוסופיה

״גישה ביולוגית רב מערכתית לזיהוי ואפיון תכונות צמחי יבול התורמות לעמידות לעקות סביבתיות״

מאת

זכריה הבר

המחקר נערך בביה"ס למדעי הצמח

תחת הדרכתו של

ד"ר ניר שדה

אפריל 2024